"Development of Spectroscopic Methods for Drug Analysis"

A Thesis Submitted to
The Maharaja Sayajirao University of Baroda
for the Award of the Degree of
Doctor of Philosophy in Chemistry

By

Sibaprasad Sahoo

Research Supervisor

Prof. B. V. Kamath

DEPARTMENT OF CHEMISTRY
FACULTY OF SCIENCE
THE MAHARAJA SAYAJIRAO UNIVERSITY OF BARODA
VADODARA – 390 002, GUJARAT

January 2013

सत्यं शिवं सुन्दरम्

Department of Chemistry
DST-FIST Sponsored Department
The Maharaja Sayajirao University of Baroda
Faculty of Science, Vadodara – 390 002, INDIA
Phone: (+91–0265) 2795552

No. :CHL/ 624/Ph.D. **Date:** 12 JAN 2013

CERTIFICATE

This is to certify that the work presented in the thesis entitled **"Development of Spectroscopic Methods for Drug Analysis"** submitted by **Mr. Sibaprasad Sahoo** for the award of the degree of **Doctor of Philosophy in Chemistry** is the authentic and original research work carried out by him under my guidance and supervision in the Department of Chemistry, Faculty of Science, The Maharaja Sayajirao University of Baroda, Vadodara – 390 002, India.

12.1.2013

Prof. B. V. Kamath
Research Supervisor

12.1.2013

Prof. Neelima D. Kulkarni
I/C Head
Department of Chemistry

HEAD,
CHEMISTRY DEPARTMENT
FACULTY OF SCIENCE
M. S. UNIVERSITY OF BARODA
VADODARA - 390 002.

Prof. A. C. Sharma
I/C Dean
Faculty of Science

DEAN,
FACULTY OF SCIENCE
M S. UNIVERSITY OF BARODA
VADODARA - 390 002

DECLARATION

I hereby declare that all the information in the thesis entitled **"Development of Spectroscopic Methods for Drug Analysis"** has been obtained and presented in accordance with the academic rules and ethical conduct. To the best of my knowledge no part of this thesis has been submitted for any Degree or Diploma to this University or any other University or Institute. Any errors in fact or interpretation in the thesis are purely the fault of the researcher.

12-01-13

Sibaprasad Sahoo

Dedicated to My Family

Acknowledgements

There are many people at The Maharaja Sayajirao University of Baroda and Sun Pharma Advanced Research Company Ltd, Baroda, Gujarat that I would like to thank. First of all, I would like to express my deep gratitude to my supervisor, Prof. B. V. Kamath, for his enthusiastic guidance and friendly encouragement. I really appreciate his care and efforts to ensure my professional development and my successful integration. I consider myself very fortunate that he taught me critical scientific thinking and excellent editing of manuscript and thesis. His hard-working spirit impressed and stimulated me all the time.

I am thankful to the Department of Chemistry, The Maharaja Sayajirao University of Baroda for providing me the necessary facilities available for my research work.

I am thankful to Shri. Dilipbhai, Sun Pharmaceutical Industries Ltd, Vadodara, Gujarat, India for the permission to pursue the research work with all type of research facilities.

I express my sincere thanks to Dr. T. Rajamannar and Dr. K. Shivram, SPARCL, Vadodara, for their continuous help as well as friendly encouragement.

My sincere thanks to Prof. N. D. Kulkarni, Head, Department as well as all respected faculties and non-teaching staff of chemistry department for supporting me throughout the research work.

I would like to thank Prof. S. R. Shah and Dr. A. V. Bedekar, Dr. Prakash Samnani, Dr. Sanjeev Kumar and Mr. Harish Talele, Department of Chemistry, M. S. University of Baroda for their encouragement, guidance and support throughout my research work.

I thank Dr. C. T. Rao, Dr. Nishith Chaturvedi, Dr. Kanaksingh Jadhav, Mr. Arun Kumar Yadav, Mr. Vipul Patel, Manish Gandhi, Kunal Pandya, Kamlesh Borkhataria, Kirit Joshi, Jigar Joshi, Organic Synthesis Department, SPARCL for helping in performing the freeze drying, centrifuge and autoclave of my samples.

I thank Dr. S. Bhowmick, Dilip Dash, B. Mahant, Vashmang Hora, Mr. Muralidhar Zope, Mr. Chandan Awaiti, Keyur Doshi, Sachin Taumbe, Prashant Gandhi, NDDS, SPARCL for helping SEM, TEM, microsphere in vitro release study, DLS and Zeta potential study of my samples.

I wish to thank to all the research colleagues especially Nisarg, Niral, Soumik, Khushbu, Kushal, Devesh, Debashish Rout, Ashish Jaishwal, Anil Bhatt, Hiren Shah, Kishor, Nilesh Motka, Narendrabhai, Ketanbhai, Yuvraj, Dushyant, Sasanka Baidya, Prahlad, Dr. Ravi, Dr. Ashok, Dr. Amol Rana, Dr. Tejas Patel, Mehul Bhatt, Jigar Gajjar, Payal Prajapati, Hiren Rana, Jashmin, Varshesh Patel, Aditya, Nilesh, Hemant and Shyamsundar for their moral support and pleasant company.

Above all, I am very much grateful to my mother, my family members for their constant support and blessings.

Finally, I must thank all research scholars and my colleagues those who cooperated with me directly or indirectly during the pursuance of the research work.

Sibaprasad Sahoo

Contents

List of Abbreviations and Symbols

WFI	Water for injection
CD	Circular dichroism
cm	Centimeter
CPL	Circularly polarized luminescence
DMA	N,N-Dimethylamine
DMF	N,N-Dimethylformamide
EDTA	Ethylenediaminetetraacetic acid
DSC	Differential Scanning Calorimetry
MDSC	Modulated Differential Scanning Calorimetry
DTA	Differential Thermal Analysis
TGA	Thermal Gravimetry Analysis
PSD	Particle Size Distribution
ATR	Attenuated Total Reflectance
NIR	Near Infra Red
SAXS	Small Angle X-ray Scattering
DVS	Dynamic Vapour Sorption
API	Active Pharmaceutical Ingredient
ESI-MS	Electro Spray Ionization Mass Spectrometry
UPLC	Ultra Performance Liquid Chromatography
NDA	New Drug Application
ANDA	Abbreviated New Drug Application
FID	Free Induction Decay
SW	Sweep Width
FTIR	Fourier transform infrared spectroscopy
T_1	Spin-Lattice relaxation time
T_2	Spin-Spin relaxation time
T_c	Crystallization temperature
T_g	Glass transition temperature
T_m	Melting temperature
HRMS	High-resolution mass spectrometry
NOE	Nuclear Overhauser Effect
α	Flip Angle

M.P	Melting Point
h	Hour
s	Second
min	Minute
γ	Gyromagnetic ratio
J	Coupling constant
DOSY	Diffusion Ordered Spectroscopy
CP-MAS	Cross Polarization Magic Angle Spinning
NMR	Nuclear magnetic resonance
LOD	Limit of Detection
LOQ	Limit of Quantification
EE	Entrapment Efficiency or Encapsulation Efficiency
RT	Room temperature
WHO	World Health Organization
USFDA	United States Food Drug Administration
RLD	Reference Listed Drug
BCS	Bio-pharmaceutics Classification System
TMS	Tetramethyl Silane
TLC	Thin Layer Chromatography
CNS	Central Nervous System
IM	Intramuscular
QbD	Quality by Design
PCA	Principal Component Analysis
PCR+	Principal Component Regression Plus
PLS	Partial Least Square
CP-ANN	Counter Propagation-Artificial Neural Network
UV-Vis	Ultraviolet–Visible spectroscopy
HPLC	High Performance Liquid Chromatography
GC	Gas Chromatography
FNDB	1-Fluro-2-4-dinitro benzene
TEA	Triethylamine
CHN	Elemental analyzer
m/z	Mass-to-charge ratio

PXRD	Powder X-Ray Diffraction
M	Mole
mL	Milliliters
w/v	Mass concentration/ Weight to volume ratio
C	Concentration
α	Alpha
β	Beta
δ	Delta
°	Degree
ppm	parts per million
mHz	Mega hertz
θ	Theta
Å	Angstrom
nm	Nanometer
°C	Degree Celsius
K	Kelvin
mg	Milligrams
g	Grams
kHz	Kilo Hertz
D	Diffusion Co-efficient
G	Amplitude of the applied gradient
L	Correlation for finite gradient length.
Ω	omega
ν	Nu
ψ	psi
Φ	phi
μ	mu
Δ	Diffusion time
D_0	Intrinsic diffusion coefficient
δ	Correlation for finite gradient length
K	Boltzman Constant
η	Viscosity of dispersion medium
R_h	Hydrodynamic radius

ICH	International Compendia of Harmonization
BP	British Pharmacopeia
RSD	Relative Standard Deviation
PLA	Poly Lactic Acid
PLGA	Poly Lactic co-Glycolic Acid
Ilo	Iloperidone
CSS	Cholesteryl sulfate sodium
sCT	Salmon Calcitonin
TFE	Trifluoroethanol
BTC	Benzethonium chloride
CBT	Chlorobutanol
BKC	Benzalkonium chloride
FLB	Flurbiprofen
MF·HCl	Metformin hydrochloride
DMA·HCl	Dimethyl amine hydrochloride
δ	Chemical shift in ppm
ν	Nu
PDE	Permitted Daily Exposure
DMSO-d_6	Dimethylsulphoxie-d_6
D_2O	Deuterium Oxide
CD_3OD	Methanol-d_4
CSA	Chemical Shift Anisotropy
t_{aq}	Acquisition time
TSP-d_4	3-(Trimethylsilyl)propionic acid-d_4

Chapter 1

Introduction

Since the Second World War a rapid development of biologically active molecules in general, and pharmaceuticals in particular, have made a quantum progress. Through these molecules synthetic Organic chemists, Pharmacologists, Biochemists, Analytical chemists, Microbiologists and Medical professionals have worked together to minimize the suffering of human beings and improve the quality of life. In this new century, there is a concerted effort to internationalize research and development of life saving molecules to achieve the common objective 'better drugs for a better world'.

According to the definition of WHO, a drug is any substance or product that is used to modify or explore physiological systems or pathological states for the benefit of the recipient. In the context of medicine, it means a chemical used in the prevention, diagnosis or treatment of diseases.

In spite of all targeted successes of synthetic drug research achieved in the last four decades to combat over 80,000 different aliments, only about one third can be treated with drugs, most of them only symptomatically. There are many life-threatening diseases which have eluded effective ways treatment. The challenge therefore is to discover better, effective and safer drugs to fight the causes of dreadful diseases like cancer, acquired-immuno-deficiency-syndrome (AIDS), cardio-vascular diseases, disorders of the central nervous system (CNS) such as Alzheimer's disease and other vital infectious and metabolic disorder like rheumatoid arthritis.

Once a molecule is synthesized that exhibits desirable biological activity, the efforts are directed towards creating a pharmaceutical drug product from this molecule. This involves a long sequence of activities like toxicology and efficacy studies, development of methods for manufacture of the active molecule and its formulation which includes mode of delivery of the drug in therapeutic doses at the targeted site. New drug development also involves detailed chemical studies of raw materials, synthetic intermediates, drug substance and the final formulated product. At this stage finding a form of the active molecule which exhibits appropriate physical

properties is critical. The form ultimately selected is called the active pharmaceutical ingredient (API), or drug substance. The API must be stable and should have desirable bioavailability so that it can be formulated into a drug product. The important properties that are crucial in the developmental protocol are listed in Table 1.1.

Bioavailability	Physico-chemical stability	Processability
a) Dissolution rate b) Solubility c) Toxicity	a) Excipient compatibility b) Hygroscopicity c) Oxidative stability d) Photostability e) Thermodynamic stability f) Crystal form	a) Colour b) Compatibility c) Density d) Ease of drying e) Filterability f) Flow ability g) Hardness h) Melting point i) Particle size

Table 1.1: Important properties of drug substance

An important component of the drug development research is the development of efficient analytical methods to identify and quantify the API and the degradation products, to determine the degradation rates and to ascertain level of impurities. Therefore, the role of analyst vis-a-vis the drug development process has become extremely important and crucial.

1.1: Pharmaceutical analysis:

Modern pharmaceutical analysis involves much more than analysis of active pharmaceutical ingredients (APIs), inert ingredients (excipients), or formulated drug product. Though the primary goal of pharmaceutical analysis is to help build and assure quality of drug products, it is well known that quality cannot be tested into a product. However, well planned testing with suitable methodology and reliable instrumentation, assure quality into a drug product. A thorough understanding of interactions of drug substances with excipients is necessary, especially when residual solvents (including moisture) are present. Recognition of these principles has encouraged the Food and Drug Administration (FDA) to issue the new initiative

protocol "Quality by Design" (QbD) outlined in their report as "Pharmaceutical Quality for the 21st Century: A Risk-Based Approach."

The focus of this concept is that quality should be built into a product by means of thorough understanding of the product and the process by which it is developed and manufactured, along with knowledge of the risks involved in product improvement.

Various analytical techniques have been widely used in pharmaceutical sciences to obtain both fundamental and applied information of a product from synthesis of the molecule to the final formulation. During the development of any drug candidate – both synthetic and natural - spectroscopy is used extensively to establish the structure of the compound and understand its interaction with other constituents. Different spectroscopic methods used for structural elucidation are UV-Visible, IR, Raman, NMR and Mass. Further information on the molecular and crystal structure of solid substances is obtained by using single crystal and powder XRD techniques.

Thermal methods such as DTA, TGA and DSC give stability related information of these substances individually as well as in the presence of excipients. Microscopic evidences from both SEM and TEM are also gathered to provide additional information on these issues.

Chromatographic methods coupled with various spectroscopic methods are used for isolation, separation, purification and quantitative determination of drug and other related substances like impurities, excipients, degradation products and metabolites.

1.2: UV-Vis spectroscopy:

UV-Vis spectroscopy involves the absorption of electromagnetic radiation from the 200-800 nm range and the subsequent excitation of electrons to higher energy states. The absorption of ultraviolet-visible light by organic molecules is restricted to certain groups (chromophores) that contain valence electrons of low excitation energy. The UV-Vis spectrum is complex with broad absorption bands because the superimposition of rotational and vibrational transitions with the

electronic transitions gives a combination of overlapping lines. UV-Vis spectroscopy is used more often for quantitative determination rather than to obtain structural information.[1,2]

Pharmaceutical applications of UV-Vis spectroscopy:

The analysis of pharmaceuticals is an integral and increasingly important part of an overall drug development of numerous synthetic drugs.

Direct UV-Vis spectrophotometric method is not suitable for simultaneous determination of drugs with spectral overlapping.[3] Application of this spectrophotometry in derivative mode offers a better option for quantitative analysis of multi-component mixtures. Over the years, this technique has rapidly gained application in the field of pharmaceutical analysis to overcome the problem of interference, due to the presence of excipients such as placebo, colors and preservatives other than analytes commonly present in pharmaceutical formulations or for combination of two or more drug substances. The derivative technique has now been used in single and multi-component quantitative analysis of pharmaceutical drug substances, especially in UV-absorbing matrices.[4]

Kaur *et al* reviewed the UV-Vis spectrophotometric and its derivative spectrophotometric methods used for pharmaceutical analysis,[5] like individual determination of Atorvastatin,[6] Citalopram,[7] Ezetimibe,[8] Gemcitabine,[9] Prednisolone,[10] Repaglinide.[11] Similarly, the derivative stability-indicating procedures used for the analysis of drug products such as Disopyramide,[12] Fluoroquinolones,[13] Lansoprazole have also been reported.[14]

Simultaneous determination of pharmaceutical compounds such as Aceclofenac and Paracetamol,[15] Amlodipine besylate and Atorvastatin,[16] Ibuprofen and Paracetamol,[17] Metformin and Pioglitazone,[18] Metropolol tartrate and Ramipril,[19] Paracetamol with Aceclofenac or Tramadol have been achieved by using the derivative technique.[20]

Pescitelli *et al* studied cyclodextrins as carriers for kavalactones in aqueous media and characterized (S) 7,8-dihydrokavain and beta-cyclodextrin inclusion complex by using normal UV spectroscopy.[21]

1.3: Vibrational spectroscopy:

A molecular vibration occurs when all the atoms in a molecule are in a periodic motion at their mean position, while the molecule as a whole has constant translational and rotational motion. The frequency of the periodic motion is known as vibrational frequency and the energy absorption phenomenon dealing with the vibrational frequency leads to vibrational spectroscopy.

Infrared spectroscopy:

IR spectroscopy is one of the most important and widely used analytical techniques in pharmaceutical applications. The IR is commonly obtained by passing infrared electromagnetic radiation through a sample that possesses a permanent or induced dipole moment and determining what fraction of the incident radiation is absorbed at a particular energy level. The energy of each peak in an absorption spectrum corresponds to the frequency of the vibration of a molecular part, thus allowing qualitative identification of certain bond types in the sample.

Application of FT-IR in pharmaceuticals:

Bertacche and coworkers developed a quantification method to detect the amount of amorphous cyclosporine (cyclosporine-A) by using FT-IR spectroscopy. It was quantified and characterized by using linearity curve with partial least square (PLS) method of different standard percentages of synthetic mixture of crystalline cyclosporine with amorphous cyclosporine over the frequency range from bending (450 cm^{-1} to 1125 cm^{-1}) and stretching regions (1515 cm^{-1} to 3200 cm^{-1}).[22]

Carbamazepine API exists in three polymorphic forms *viz* Form-I, Form-III (P-monoclinic) and IV (C-monoclinic) having very poor water solubility coupled with known bioavailability problems related to its polymorphism. The pharmaceutically undesirable Form-IV may be formed, which has very low solublity in water, under various conditions during drug formulation. A non destructive quantitative method has been developed by Kipouros *et al* to quantify Form IV present in Form III.[23]

Bartolomei *et al* studied the easy differentiation and characterization of the conversion of anhydrous Diclofenac sodium to tetrahydrate Form in standard relative humidity even below 60 % RH at 25ºC by FTIR spectroscopy along with XRD and

DSC.[24] Bunaciu *et al* developed FTIR spectroscopic method for the rapid, direct measurement of dehydroepiandrosterone (DHEA) drug in microcrystalline cellulose (MCC) with KBr matrix by using chemometric approaches like PLS and principal component regression plus (PCR+).[25]

A novel analytical technique was developed by Khanmohammadi *et al* by ATR-FTIR spectrometry for quantitative determination of Levodopa and Carbidopa in aqueous binary solutions acidified by HCl and without any other sample pretreatment.[26] Similarly, by using PLS technique with mid-IR spectral region Khanmohammadi and his group have developed a quantitative determination of Naltrexone in aqueous solutions.[27]

A simple, rapid and convenient analytical method without any special sample handling procedures has been reported by Boyer *et al* for the determination of Niflumic acid in a pharmaceutical gel with ATR/FT-IR spectroscopy.[28]

Kovela *et al* developed a quantitative FT-IR and Raman spectroscopic approach for determination of Phenacetin and Salophen in binary solid mixtures of Caffeine, such as Phenacetin/Caffeine and Salophen/Caffeine where the Raman data showed slightly higher confidence limit in comparison with FT-IR for both the systems.[29] Nemet *et al* quantified low levels of polymorphic impurity in Clopidogrel bisulphate Form II in Form I by IR and Raman spectroscopy with chemometric and model building techniques.[30]

1.4: Raman spectroscopy:

Raman spectroscopy is a powerful instrumental technique which provides specific information on the identification of analyte, characterization of sample matrices and molecular spectroscopic information useful for the structural identification of drugs and unknowns in dosage forms.[31,32] The technique also provides fundamental spectroscopic information on the API as well as excipients used in the specific pharmaceutical formulations. This technique is rapid with respect to sample preparation, methodologies, and the extent of information obtained from pharmaceutical products.[33]

Application of Raman spectroscopy in pharmaceuticals:

Raman spectroscopy is used to study various pharmaceutical forms of the drug products, in ß-blockers like[34] acebutolol, alprenolol, arternol, antifungals like amphotericin,[35] fluconazole,[36] Non-steroidal anti-inflammatory drugs like Aspirin,[37] Ibuprofen,[38] Diclofenac,[39] H_2 blockers like Cimetidine,[40] Opoid analgesics like Cocaine,[41] Sulphonamides like[42] Sulfamerazine, Sulfadiazine, Triamterene[43] and antidiuretics like Spironolactone.[44]

Strachan *et al* reviewed the use of Raman spectroscopy as a potential tool for qualitative and quantitative analysis of tables for their pharmaceutical solid forms, their drug content and also to monitor polymorphic transitions. The advanced Raman spectroscopy techniques has now been extended to complex pharmaceutical formulations like microsphere, suspensions, in-situ granulation and batch crystallisation.[45]

Eliasson *et al* reported that Raman spectroscopy can also be used for quantitative, non-invasive probing of the bulk content in production line with specific pharmaceutical drug substance contained within the capsules and also through packaging.[46]

Niemczyk *et al* reported that Raman spectroscopy using NIR excitation has significant potential for nondestructive quality control method for pharmaceutical samples in which the spectral data are collected directly from drug formulations in gel capsules as well as present inside blister pack containing 0-100 mg of a Bucindolol API.[47]

Andrew *et al* exploited Raman spectroscopy for imaging the complex multi-component, multi-phase emulsion systems by inter phasing with con-focal Raman microscope through fiber optics with an automated stage for observing high-resolution three dimensional image and microstructure of heterogeneous and multi-phase materials of different chemical composition.[48]

Similarly Breitenbach *et al* used confocal Raman spectroscopy to investigate the physiochemical stability of the formulation under the stress temperature range from -90 ºC to 90 ºC along with the content uniformity of Ibuprofen in the

formulation matrix. This technique was also applied for the analysis of layers coatings on a tablet, areas and the quality of mixing in a manufacturing process.[49]

Wikstrom *et al* and Vergote *et al* reported that Raman spectroscopic techniques can used as an on-line method to monitor drug hydration, solvation state in drying process, hydrate formation during high shear wet granulation, blending of drug substance with wax beads, and kinetics of polymorphism.[50,51]

The beta form of mannitol which is widely used in many pharmaceutical products contains other polymorphs (alpha and delta) as contaminants. Campbell *et al* used FT-Raman spectroscopy method for identification and quantification of the polymeric impurity of delta and alpha form in mannitol by using binary mixture method.[52]

1.5: NMR spectroscopy:

It was in the mid-1950s that chemists began to take an interest in NMR spectroscopy after the publication of the high-resolution spectrum of ethanol obtained by Arnold, Dharmatti and Packard,[53] Followed by the remarkable thesis work of Arnold[54] and Anderson,[55] who convincingly demonstrated the enormous potential of this technique. NMR spectroscopy is a powerful, non-destructive technique that gives a comprehensive structural and conformational analysis of simple and now of complex molecules after the introduction of high resolution NMR spectrometers.

NMR is uniquely capable of revealing the structure and dynamics of molecules. This has caused NMR spectrometers to penetrate as standard tool of prime importance in laboratories whose main interest is not NMR but chemistry and biochemistry.

NMR spectroscopy has traditionally been limited in quantitative application due to its relative lack of sensitivity compared to other methods; however, advances in technology, such as the introduction of High-field Super-Conducting magnets, FT-spectroscopy and Pulse Field Gradient methods have overcome this problem to a large extent.[56] NMR has thus become a feasible option for quantitative methods in some specific cases such as analysis of drugs and drug mixtures in dosage forms, polymers, bio-molecules and polymorphism study.

Basics of NMR spectroscopy:

Nuclear Magnetic Resonance (NMR) spectroscopy is another form of absorption spectroscopy akin to IR or UV spectroscopy. Under the influence of an external magnetic field, a nucleus can absorb electromagnetic radiations in the radiofrequency regions at frequencies governed by the characteristics of the nuclei. The half spin nucleus generates a magnetic dipole along the axis which behaves as a spinning magnet having a certain precessional frequency that can align or oppose an external magnetic field. The precessional frequency of any particular nuclei is in the range of megahertz depending upon the strength of the external magnetic field. The disturbances and detection of the nuclear magnetic interaction occurs at radio frequencies region.

The displacement of the magnetization from equilibrium or excitation is produced by a second magnetic field which is known as a radio frequency impulse or simply RF pulses having a particular shape and specified width (duration). This is nothing else than an oscillator or transmitter with the Larmor frequency of a particular nucleus.[57,58]

$$\text{Pulse angle (flip angle) } \alpha = \gamma B_1 p_1 \qquad (1\text{-}1)$$

where, γB_1 is the power or amplitude of the pulse and p_1 is the length or width of the pulse.

The time dependent alternating voltage in a coil which is perpendicular to B_0 is induced and detected by the receiver coil at a specific axis which exponentially decays to zero after completion of relaxation phenomena spin-lattice (T_1) and spin-spin (T_2) relaxation which is known as Free Induction Decay (FID). Further, this FID or time domain signal is subjected to Fourier transformation (FT) to extract the frequencies from the data. Hence FT is nothing but a mathematical operation which converts the information in the FID (i.e. time domain) into the more familiar NMR spectrum (i.e. frequency domain).

A number of analytical techniques are commonly used for pharmaceutical analysis but with NMR methods, it is particularly important to ensure that the magnetic field is reproducible or that any fluctuations are compensated for by the use of appropriate standards. Full qualitative and, where necessary, quantitative characterization of any reference standard is required.

For the development of a new quantitative chemical analysis method of any pharmaceutical product by using NMR, the desirable nuclear properties, apart from nuclear spin I = 1/2, include:

- *A high natural abundance,*
- *A large gyromagnetic ratio*
- *A relatively short spin-lattice relaxation time*

When all the above parameters are considered, only ^{1}H, ^{19}F and ^{31}P turn out to be suitable nuclei for quantitative determination.

The specificity of qNMR means the ability to assess uniquely the signal of analyte in the presence of other components. The superiority of NMR[59] reveals the fact that many nuclei are NMR active and have a characteristic gyromagnetic ratio (γ), precessional frequency (ν) and magnetic strength (B_0 in Tesla) dependent upon following Equation (1-2) and the detail values are shown in Table 1.2.

$$\nu = \frac{\gamma B_0}{2\pi} \qquad (1\text{-}2)$$

Nuclei	Unpaired Protons	Unpaired Neutrons	Net Spin	Gyromagnetic ratio γ (MHz/T)	Frequency (ν) (MHz)
^{1}H	1	0	½	42.58	500.13
^{2}H	1	1	1	6.54	76.77
^{13}C	0	1	½	10.71	125.75
^{19}F	0	1	½	40.08	470.59
^{31}P	0	1	½	17.25	202.45

Table 1.2: Different NMR-active nuclei and its properties

The NMR signal used for quantification is called monitor signal of the analyte and must be assigned to one of the specific groups of the substance. These signals are singlets, doublets or simple multiplets due to scalar coupling (*J*) which consist of one or a few Lorentzian lines of a typical Full Width Half Height (FWHH).

In some cases, the monitor signals may consist of multiplets due to coupling with other nuclei in the molecule or of superconductions with other signal within the same spectrum.

The ^{13}C NMR spectra are generally measured using composite pulse techniques to enhance sensitivity by ^{1}H decoupling for nuclear overhauser enhancement (NOE) or by polarization-transfer methods.[60] So to obtain quantitative results, ^{13}C NMR spectra must be measured using inverse gated proton decoupling experiments. In Solid State ^{13}C-NMR spectroscopy with a combination of MAS (Magic Angle Spinning) and a high-power decoupling to remove their dipolar interactions with ^{1}H nucleus and good signal-to-noise ratio can be achieved with cross-polarization sequence.[61]

Acquisition parameters

The pulse excitation must be uniform for the entire spectral width (SW) of interest, which requires optimum pulse length for complete relaxation. In ^{1}H qNMR, spectra can be acquired quantitatively with optimum number of scans and ideal phase correction. The NMR spectrum of heavier nuclei such as ^{19}F and ^{31}P which are having larger chemical shift ranges and therefore may suffer intensity distortion, particularly if measured at different magnetic field strength.[62]

The repetition time τ (or recycling time) depends on the longest longitudinal relaxation (spin-lattice relaxation) time T_1 of all signals of interest. The T_1 relaxation is described by the Equation (1-3),

$$M_z = M_0 \left(1 - e^{-(\tau/T_1)}\right) \qquad (1\text{-}3)$$

where, M_Z and M_0 being the magnetization along the axis (response factor) after waiting time τ and at thermal equilibrium, respectively. Routinely, measurements are done by choosing recycle delay (τ) = $5T_1$.

Heteronuclear NMR experiments of X nuclei (^{31}P, ^{19}F etc.) with simultaneous ^{1}H broadband decoupling cause inherent intensity distortions by the NOE. This NOE effect on the spectrometer constant (K_S) can be calculated by using the Equation (1-4).[63]

$$K_s = K_0\,(1 + E_n)\left(\frac{1-e^{-(\tau/T_1)}}{1-cos\alpha.e^{-(\tau/T_1)}}\right)sin\alpha \qquad (1\text{-}4)$$

where, K_0 is a constant instrumental factor, E_n is the nuclear overhauser enhancement factor and α is the flip angle of the excitation pulse. Intensity distortions can be decreased below 1% by using the pulse techniques having the sequence; (i) ^{1}H decoupling is applied only during the signal acquisition time (inverse gated technique) to minimize the NOE factor (E_n), (ii) the repetition time must be five to seven times of its spin-lattice relaxation (T_1),[64] and (iii) 90° pulse length should be used for the excitation with highest intensity.

The acquisition time t_{aq} depends on the smallest line width in the spectrum, and truncation of the FID signal in the time domain must be avoided and process upto zero filling. Otherwise "wiggles" will appear in the spectra if the FID is truncated, wrong relative intensities will result after zero order or first order baseline correction.[65] Henceforth the signal should decay completely halfway through the acquisition period and also contain enough data points to completely describe the NMR lines with minimum five data points above the half-height, in such a way that the integration procedure does not cause artificial distortions. (Intensity error < 1%).[66-68]

Processing parameters

The optimum window functions are used to enhance the signal-to-noise ratio at the cost of the resolution of the spectrum prior to the Fourier transformation. For qNMR measurements, exponential multiplication (em) is best with a larger line broadening factor (lb) as the em function improves the signal-to-noise ratio, but the simultaneous line broadening of the signal sometimes complicates the integration. Gunther describes the best compromise is to use a small line broadening with an optimum number of scans to increase the signal to noise ratio.[57] Prior to the fourier transformation, the zero filling process in the time domain data leads to the addition of data points with zero value to increase the digital resolution.

Spectra integration procedure

The operator is the main source of error in qNMR measurements for various reasons because baseline and phase correction must be performed with very high precision to ensure accurate results.[65,69] Frequency dependent phase errors of larger than 10° resulting from improper spectra processing cannot be corrected with the BIAS and SLOPE functions of the integration and results in significant deviations of the calculated areas of larger than 1%. The signal integration of a line shape fit can be used to determine the signal areas of interest. A unique profile for the line shape does not exist in qNMR method because it depends on the shimming (field homogeneity) of the magnets along with the probe head and some of parameters shown in Table 1.3.

Parameter	Bruker nomenclature	Value
90º pulse strength	pl_1	Instrument specific
90º pulse length	p_1	Instrument specific
Spin rotation	ro	20
Measurement temperature	te	295 K
Frequency of excitation	o_1	Middle of spectrum
Pulse angle	α	90^0
Pre acquisition delay	de	6μs
Acquisition time	aq	5.9 s
Relaxation delay	τ	≥ (7/3) x longest T_1
Sweep width	sw	14ppm
Filter width	fw	≥ 20ppm
Number of FID points	td	64 k
Number of scans	ns	Multiple of eight
Signal-to-noise ratio	S/N	≥ 150:1
Line broadening (em)	lb	0.5 Hz
Number of frequency points	si	64 k

Table 1.3: Key parameters for qNMR

Detailed validations of qNMR using single pulse excitation of ^{1}H NMR and ^{1}H inverse-gated ^{31}P NMR spectra proved that the qNMR is robust and hence the length of acquisition times, repetition times, and the signal to noise ratios collected are as per the validation data.[70, 71]

1.5.1: Quantitative NMR (qNMR) spectroscopy:

Quantitative NMR (qNMR) is an important but underutilised area till now due to its sensitivity issue though it was first applied in 1963 by Jungnickel, Forbes[72] and Hollis.[73] In 1970, the second generation NMR spectrometers were introduced with superconducting cryomagnets and pulsed Fourier Transformation capability. Since then due to accessibility for manipulation of the sample's magnetisation and spin physics, the growth of NMR spectroscopy has been explosive in solution NMR,[74] Solid-State NMR and MRI.[75-78]

Further development in NMR instrumentation has increased the versatility and the sensitivity of the technique allowing samples of microgram size to be analysed, and with the recent release of the 1000 MHz (23.5 T magnet), sample size limitation is greatly diminished. As a matter of fact, there has never been as short a delay between an initial discovery and such a wide spread application and acceptance. Subsequently, several areas in NMR have progressed utilising the dramatic enhancement in the quality of the acquired NMR spectrum.

NMR spectroscopy has been used as a quantitative technique since its invention, but has only been seriously investigated for quantitative analysis since the late 1970s with an emphasis on its application in pharmaceutical research.[79-81] Other areas of applications include natural products, metabolism, synthetic and combinatorial chemistry, foods and beverages, petrochemicals, agriculture etc.

Jancke concluded that high field ^{1}H NMR spectroscopic method is eminently suitable for quantitative analysis because of its high frequency and sensitivity, relatively short spin-lattice relaxation times, no NOE (nuclear overhausser effect) impediments and nearly 100 % natural abundance of ^{1}H. The signal area which is directly proportional to quantity of the measured nucleus, has reinforced the discussions of qNMR being a primary ratio analytical method which does not need authentic standard reference of the material under investigation.[82]

Proton (^{1}H) NMR has been widely used for the analysis of bulk drug formulations, because little sample preparation is required; analysis times are often shorter than those of the official pharmacopeia procedures.[83] The development of

quantitative NMR methodology and its validation protocol as a primary ratio and absolute assay analytical method in pharmaceutical analysis was first reported by Malz and Jancke.[70] The applications of qNMR kept on growing and in the late 1980's, the quantification of many drug products by using an internal standard have been published.

NMR spectroscopy as an absolute analytical technique

Quantitative analysis by NMR is based on the proportionality of the NMR peak area to the number of nuclei contributing to the peak. In the presence of spin-spin splitting, the area under the entire multiplet is also proportional to the number of nuclei generating the corresponding resonance line presented in Equation (1-5). In such consequence NMR is an absolute analytical technique

$$I_x = K_s \, . N_x \qquad (1\text{-}5)$$

where, I_x = Integral area, N_x = Nuclei evoking signal, K_s = Spectrometer constant

The precision of the integrals determines the accuracy of quantification depending on the (a) noise level, (b) line shape, (c) shimming, (d) window function, (e) phase, base line and the drift corrections.[84]

Relative mole ratio method

When two components are present, determining ratios is the easiest way to obtain quantitative results by NMR. The molar ratio n_x / n_y of two compounds "*x*" and "*y*" can be calculated straight forward by using the Equation (1-6)

$$\frac{n_x}{n_y} = \frac{I_x}{I_y} \frac{N_y}{N_x} \qquad (1\text{-}6)$$

Similarly, the amount fraction of a compound "*x*" in a mixture of "*m*" components can be calculated by using Equation (1-7) irrespective of the solvent signal used for sample preparation.

$$\frac{n_x}{\sum_{i=1}^{m} n_i} = \frac{I_x/N_x}{\sum_{i=1}^{m} I_i/N_i} \times 100\ \% \qquad (1\text{-}7)$$

The qNMR is the most important method for quantifying the mole ratios of isomers, diastereomers, and enantiomers,[85] due to excellent qNMR method selectivity for structural characterization and rapid quantification. By using chiral solvents or complexing agent, enantiomers can also be differentiated and quantified by qNMR.[86,87]

Absolute method

The qNMR spectra include only information about the ratio of intensities but by adding an internal standard having following special requirements for the mixture,[88] absolute results of assays, contents, or concentrations can also be determined.

- Most stable, inexpensive, inert and simple NMR signal well separated from the analyte.
- Easily available in pure form and non hygroscopic in nature and soluble in most of NMR solvents

A number of possible internal standard compounds were used by Pauli *et al* for the ^{1}H qNMR[89] and Martino *et al* for ^{19}F and ^{31}P qNMR.[90]

Assay calculation of drug substance:

Assay determination of analyte "P_x" with an internal standard of known assay "P_{std}" and known amount "W_{std}" is needed gravimetrically.[70] The requirement of such internal standard for qNMR is suitable for calculating the assay using following Equation (1-8) and (1-9).

$$P_x = \frac{I_x}{I_{std}} \times \frac{N_{std}}{N_x} \times \frac{M_x}{M_{std}} \times \frac{m_{std}}{m} \times P_{std} \qquad (1\text{-}8)$$

$$W_x = \frac{I_x}{I_{std}} \times \frac{N_{std}}{N_x} \times \frac{M_x}{M_{std}} \times W_{std} \qquad (1\text{-}9)$$

where, P_x = Assay of the analyte

I_x = Mean integral value of the analyte

I_{std} = Integral value of the standard

N_{std} = Number of nuclei for the standard

N_x = Number of of nuclei for the analyte in drug

M_x = Molar mass of the analyte

M_{std} = Molar mass of the standard

W_{std} = Weight of the standard

W = Weight of the analyte drug

P_{std} = Known assay of the standard

In the qNMR method that uses external standard the spectra are recorded either in a concentric tube[91] (capillary, filled with the dissolved standard, inside the analyte NMR tube) or in a separate precision tube (two NMR tubes filled with the analyte and standard solutions) for the non contamination of the analyte.[92,93] In both cases analyte and standard should be dissolved in the same solvent and the volumes of the tubes perfectly calibrated before use.

In 1998 Akoka *et al* introduced a new NMR spectroscopic technique called ERETIC (electronic reference to access in vivo concentrations) for the quantification purpose without using any internal standard. In ERETIC technique an electronic reference signal was fed in the resonance circuit of the probe, during the acquisition time, fixed NMR scale of amplitude observed by using a free coil in the multinuclear probe head.[94,95] This technique is suitable for ^{1}H qNMR, ^{13}C qNMR,[60] two-dimensional (2D) NMR,[56,96] Solid-State NMR[61,97] and Magnetic Resonance Imaging (MRI)[98] due to the feasibility of shifting reference electronic signal from the analytes.

1.5.2: qNMR method validation:

As mentioned earlier NMR is a quantitative spectroscopic tool because the intensity of a resonance line is directly proportional to the number of resonant nuclei (spins) which enables a precise determination of the amount of analyte in solids as well as liquids. With the increase of sensitivity due to stronger and stronger static magnetic fields coupled with improved electronics, the detection limits have been pushed down significantly. However, the lack of a precise protocol that considers and controls the aspects of the measurement procedure as well as the spectra processing and evaluation may be responsible for the fact that quantitative investigations of identical samples in various laboratories differ drastically.

Method validation defines the analytical procedure and its conditions in which it is capable to perform consistently within application requirements. Analytical method validation is the "confirmation by examination and the provision of objective evidences of method suitability and performance and the parameters and other factors are within specifications and it provides the boundaries." As a straightforward conclusion, nonstandard methods like NMR must be validated. The validation process requires the testing of linearity, robustness, and parameters of accuracy (repeatability, comparability and measurement uncertainty), specificity and selectivity shown in Figure 1.1.[99]

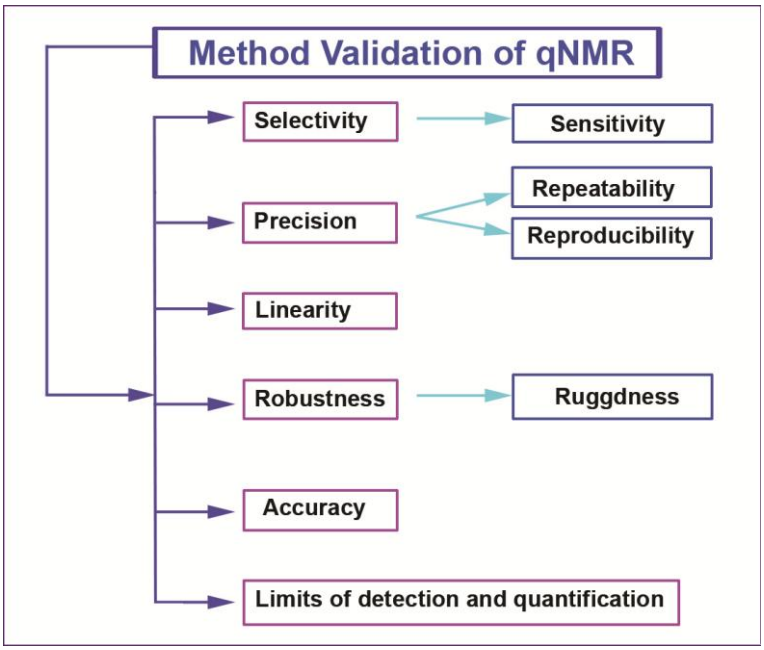

Figure 1.1: Schematic diagram of validation components in qNMR

System suitability

System suitability test is performed to show that the control measures required have been complied for a particular analysis on a particular day. The performance of the spectrometer and proposed method used for quantification must evaluate and ensure that the expected specificity and sensitivity should be achieved as per the guide line.[59] The advantages of the use of NMR technique as a quantification method is that the sample itself also provide such system suitability test, by making use of line-width or S/N ratio value from the sample spectrum. Because of the high precision and intrinsic accuracy, system precision for NMR is not required. However, in the present

study, system precision was performed for every parameter by replicate acquisition of standard preparation, hence this is nothing but the system suitability test and it will check the compliance of specific acceptance criteria.

Selectivity

The selectivity of a method is given by the ability to determine analytes of interest in a mixture without any interference from the other components.[100] Different qNMR experimental protocols are required to check the specificity and selectivity as listed below:

- Due to higher intensity of analyte, an internal signal integration of several analytes can identify hidden impurity signals.
- Spectral resolution is enhanced by higher magnetic field.
- Comparison of signals intensities of the specific group signal for two different samples prepared by different route.
- Homo and Heteronuclear correlation spectra (H-H, H-X, Correlated Spectroscopy (COSY), Heteronuclear Multiple Quantum Coherence (HMQC), Heteronuclear Multiple-Bond Correlation (HMBC), Heteronuclear Single Quantum Coherence (HSQC) and Nuclear Overhauser Effect Spectroscopy (NOESY) show signal correlations of hidden impurities signal with resolved resonance lines.
- Variable temperature experiments lead to simplification of any spectrum
- Homo-nuclear decoupling experiments also produce simpler spectra.
- NMR with high-performance liquid chromatography (LC-NMR) can be obtained separately (offline or online).

The selectivity of the qNMR method can be achieved by (i) change in the temperature, (ii) change the solution pH, (iii) shift reagents, and (iv) use other solvents with different concentration to separate complex signals.

Sensitivity

In comparison to other spectroscopic and chromatographic techniques the main disadvantage of qNMR is its poor sensitivity. The spins of NMR active nucleus gets splitted in two energy levels α and β, when kept in a static magnetic field B_0. The

Boltzmann relationship describes the population ratio N_α/N_β between these two energy levels given by the following Equation (1-10).

$$\frac{N_\alpha}{N_\beta} = e^{-(\gamma h B_0/2\pi kT)} \qquad (1\text{-}10)$$

where, γ is the gyromagnetic ratio of the observed nucleus, h = Planck's constant, 6.6 x 10^{-34} joules/sec and k is the Boltzmann constant. The population difference is inherently small, but it also increases with the increasing field strength.[57]

Szantay *et al* discussed four ways in which the sensitivity (or better S/N) can be increased (i) increasing the field strength, (ii) increasing the sensitivity of detection of the RF coil, (iii) number of spins within the active volume and (iv) decreasing the noise by using Cryoprobes.[84]

Precision

The method precision of qNMR procedure expresses the closeness of agreement between a series of measurements obtained from multiple sampling of the same homogenous sample. Method precision can be considered at two levels such as repeatability and comparability.[101]

The precision of the integration procedure depends on the signal to noise ratio of the signals of interest which should be necessarily at least 150 : 1 for every resonance line with proper tuning and matching of the resonating frequency. The calculated content of drug in percentage assay for each preparation and also the statistical parameters should fulfill the ICH guidelines.[59] All influences of the inhomogeneity of the magnetic field (shimming) as well as by the acquisition, processing, and evaluation parameters are taken into account for the calculations.

Repeatability and comparability (Intermediate precision)

As per the ICH (International Conference on Harmonization) guidelines the precision of repeatability was acquired by six repeated determinations. In contrast, the precision of comparability (or intermediate precision) was evaluated by a second analyst and/or a second NMR spectrometer with a different magnetic field strength.[102] Integration of peaks as well as phase and baseline correction are the most subjective

parts of the method. Therefore, intermediate precision was determined by performing measurements on above mentioned occasions.

Linearity

For any quantitative method it is necessary to determine the range of analyte concentration over which the method is applied. The linearity of an analytical procedure or method is defined as the ability of test results that are directly proportional to the amount of analyte. The qNMR method is linear as the intensity of the response signal is directly proportional to the amount of nuclei contributing to this signal and no calibration is necessary for the determination of molar ratios in the mixtures. In qNMR assays or potency determinations, the linearity data can be evaluated by varying the contents of the substance within a range of 70-130 % of label claim according to the content of analyte in the test sample with a linear regression coefficient ($r^2 > 0.999$) is achievable.[103]

Robustness

The robustness of an analytical method involves variation of all important parameters of data acquisition, processing and evaluation. Further it is also a measure of its capacity to remain unaffected by small but deliberate variations in procedural parameters listed in the procedure documentation and provide an indication of its suitability during normal usage.

The parameter sets required for accurate and precise measurements must be found and fixed as otherwise it will definitely yield wrong measuring results. By varying the spectrometer parameter sets, three different effects can be distinguished such as no significant influence (robust), significant influence on the signal-to-noise ratio and systematic change or correct signal intensity. Most of the qNMR parameters should not have significant effects on the accuracy or precision of the method within their evaluated ranges.[10]

Accuracy

The International Union of Pure and Applied Chemistry Compendium of Chemical Technology, 1985 has defined accuracy as “a quantity referring to the

differences between the mean of a set of results or an individual result and the value which is accepted as conventionally true or correct value for the quantity measured". The term accuracy when applied to a set of results involves a combination of random and systematic components.

The direct proportionality between signal intensity and the amount of nuclei of a resonance line in qNMR method combined with ability to be a potential primary ratio method.[105] A standard which is certified or whose assay can be back calculated by using a certified reference material must be used as a standard for assay or content determinations. The accuracy of qNMR method must be checked by any substance with at least two measurable signal intensities which satisfy the stoichiometry and structure.

The accuracy of an analytical procedure should be established across its range. The ICH documents recommend that accuracy should be assessed using a minimum of nine determinations over a minimum of three concentration levels, covering the specified range (*i.e*. three concentrations and three replicates of each concentration).

The Limit of detection (LOD) and Limit of Quantification (LOQ) can be calculated from Equation (1-11) and (1-12) respectively by using the standard deviation of the response 'σ' and the slope '*s'* of a calibration curve in the case of NMR with Lorentzian lines as response signals,:

$$\text{LOD} = 3.3\,\frac{\sigma}{s} \qquad (1\text{-}11)$$

$$\text{and} \quad \text{LOQ} = 10\,\frac{\sigma}{s} \qquad (1\text{-}12)$$

1.5.3: qNMR spectroscopy in pharmaceutical analysis:

NMR spectroscopy can be considered as the most important tool used for the identification of a drug substance, the identification and quantification of impurities arising from the synthetic pathway and degradation or residual solvents. Its usefulness has now been extended for the determination of the drug content in API or a formulation. NMR spectroscopy being a primary ratio method of measurement is also

suitable to evaluate the quality of drugs. Holzgrabe *et al* have given an overview of application of quantitative NMR spectroscopy in international pharmacopoeias.[106]

Elizabeth *et al* have reported the usefulness of Nuclear Quadrupole Resonance (NQR), a related noninvasive technique, in pharmaceutical analysis due to linear response. The NQR can be used *in situ* within a formulation and its packaging, lending itself to the "black-box" deployment of the technology.[107]

Nigel *et al* developed the concept of ultrahigh-throughput method for acquiring ^{1}H NMR spectra by utilizing capillary flow NMR technology for the efficient analysis of compound libraries and large collections of compound.[108]

Dumas *et al* reported the NMR spectra of biofluids combined with multivariate pattern recognition. This is a robust and precise approach for metabonomics and such findings make metabonomics suitable for high-throughput long-term epidemiological research.[109]

Conventional NMR spectroscopy is unable to distinguish between enantiomers of a chiral drug molecule because the spectral pattern is determined by the chemical shifts (δ) and spin-spin coupling constants (J). Buckingham *et al.* reported the computations of the precessing electric polarisation followed by a $\pi/2$ pulse. The application of an electrostatic field induces a chirally sensitive magnetisation in the direction of the magnetic field of spectrometer.[110]

Quantitative ^{13}C-NMR isotopic profiling is a well-established technique to obtain information about the chemical history of a given compound. The complementary methodology of isotope ratio mass spectrometry (IRMS) can only determine the intramolecular ^{13}C content. Silvestre *et al* developed a quantitative isotopic ^{13}C NMR spectrometry at natural abundance to assess internal site specific isotopic profile of Aspirin and Paracetamol API and also used for detection of counterfeiting and patent infringement in the pharmaceutical industry.[111] Webster *et al*. developed a NMR spectroscopic method to calculate the relative response factors for chromatographic investigations to normalize peak area response by mass yield values.[112]

Forshed and his group developed the algorithms and methods for peak alignment of first order NMR data of complex biological samples which exhibit variations in signal position (δ) and line width due to variations of sample matrix, shimming and instrumental parameters. The peak alignment methods produce better results than classical bucketing or raw data considering the measure of class separation of scores from PCA or PLS-DA.[113]

Christopher Jones reported that antibodies against the cell surface carbohydrates of many microbial pathogens protect against infection which was initially exploited by the development of purified polysaccharide vaccines for which NMR spectroscopy proved to be efficient tool for identification and quality control testing. Quantification of polysaccharide purity and polysaccharide-protein ratios in the final conjugate are easily possible by qNMR spectroscopy.[114] Rizzo *et al* reported a quantitative NMR method that is rapid and generic method for determining concentration, purity, reaction yield, and mixture composition in synthetic and combinatorial chemistry.[115]

Wawer *et al* proposed that ^{1}H, ^{13}C and ^{15}N NMR spectroscopy can be used effectively for identification and quantification of Sildenafil citrate (Viagra) in solution and solid state pharmaceutical formulations.[116]

In comparison with other analytical spectroscopic techniques, NMR has an intrinsically low sensitivity and many potential applications are therefore precluded by the limited available quantity of certain types of sample. After the miniaturization of the receiver coil which increases the mass sensitivity, the microcoils technology has become very useful for NMR detection with micro separation. Webb *et al.* demonstrated the application of microprobes and cryoprobes which have comparable mass sensitivities that play complementary roles in NMR studies.[117] Similarly Price *et al* also proposed metabolic profiling of tissue targeted metabonomics by microdialysis sampling with microcoil NMR detection.[118] Putzbach *et al* reported the hyphenation of capillary high-performance liquid chromatography separation and solenoidal-micro-probe NMR detection of various Carotenoids in a small sized spinach sample.[119] Gu *et al* studied the effects of sample contamination with folate-deficient food in the metabolomic analysis of mouse urine and fecal particles by ^{1}H NMR using

principal component analysis.[120] The metabolic profile of urine mixed with folate-deficient food was found different than that of clear urine.

Xu *et al* proposed a novel molecular imprinting process with the selective adsorption of Norfloxacin in aqueous media by a polymer based on hydrophobic and electrostatic interactions by NMR spectroscopy.[121] Wang *et al* isolated and characterised the structure of related impurities in Etimicin sulphate by LC/ESI-MS^n and NMR.[122]

Martino *et al* reviewed different applications of in vitro ^{19}F or ^{31}P NMR to the quantitative metabolic studies of some fluoropyrimidines or oxazaphosphorine drugs in clinical use which is applicable in Pharmacy, Biochemistry and Medicine.[123]

Diffusion Ordered Spectroscopy (DOSY) experiments are also suitable for identification of different ingredients and preservatives in formulations. Holzgrabe *et al* have reviewed the quantitative NMR spectroscopy and DOSY NMR in anti-counterfeiting of drug substances in formulation.[124]

1.5.4: Solid State-NMR (SS-NMR) spectroscopy in pharmaceuticals:

As approximately 80 % of all pharmaceutical products are solid state formulations, and traditionally, polymorphism has been investigated by powder X-ray diffraction and various thermo analytical techniques. Since the advent of SS-NMR in the 1970s an increasing number of applications of SS-NMR have been published and use of SS-NMR relatively new and most popular in the pharmaceutical analysis.[97]

In the case of pharmaceutical solids which are dominated by carbon and proton nuclei, hetero-nuclear dipolar interaction was removed by high power proton decoupling with magic angle spinning (MAS). The magnitude of chemical shift anisotropy (CSA) was removed by high spinning of sample and enhancement of signal intensity was achieved through cross polarization (CP) from proton to carbon nucleus.[125]

Recently, the use of SS-NMR to solid pharmaceutical samples has gradually shifted from exclusive use of the basic ^{13}C NMR with CP-MAS experiments to heteronuclear two dimensional solid state NMR (2D SS-NMR), and spin lattice

relaxation time measurement. This shift has coincided with advances in instrumentation, including more robust and flexible probe designs, higher mass spinning rates, higher static field strengths, and electronic device to pulsing of rapid frequency, phase, and amplitude switching at high radiofrequency powers.[61] SS-NMR has been applied in a number of pharmaceutical applications including studies of polymorphism, solvation, salts, co-crystals and various types of formulations,[126]

- Polymorphic drug identification
- Differentiation of crystalline and amorphous phase
- Identification and characterization of excipients and non polymorphic impurities
- Identification of crystal bound solvents and co-crystals
- Characterization of drug-drug, drug-placebo interaction
- Physical and chemical stability and solid state reactivity studies

Saindon *et al* studied SS-NMR spectra of tablets and/or capsules of Prednisolone, Enalapril maleate, Lovastatin, Simvastatin, Ibuprofen, Flubriprofen, Mefenamic acid, Indomethacin, Diflunisal, Sulindac, and Piroxicam.[127] Gao *et al* proposed a method to unambiguously identify and quantify the relative composition of Delavirdine mesylate polymorph and pseudopolymorph mixtures of Form VIII, XI and XII using ^{13}C CP-MAS NMR.[128]

Booy *et al* developed the use of ^{13}C labeling to enhance the sensitivity of ^{13}C solid state CP-MAS NMR to study the effect of tabletting on the polymorphism in low dose solid formulations.[129] Offerdahl *et al* reported the quantification of multiple crystalline and amorphous forms of artificial sweetener of anhydrous Neotame by using ^{13}C CP-MAS NMR spectroscopy.[130]

Aso *et al* developed a method with varying drug contents of amorphous Nifedipine-PVP (poly vinylpyrrolidone) and Phenobarbital-PVP solid dispersions by using ^{13}C-CP/MAS NMR spin lattice relaxation times and chemical shift of PVP carbonyl carbon to elucidate drug-PVP interactions and molecular mobility of drug and PVP in solid dispersions.[131] Bauer *et al* proposed methods for identification, preparation and characterization of seven crystal polymorphs and solvates of Terazosin monohydrochloride, an antihypertensive drug by SS-NMR.[132]

Sotthivirat *et al* developed a method for characterization of Prednisolone in controlled porosity osmotic pump pellets under different formulation and processing conditions by using SS-NMR spectroscopy.[133] Sanchez *et al* proposed an improved SS-NMR protocol for quantitative measurement of active principles in pharmaceutical formulations with optimal sensitivity, excellent precision and accuracy.[134] Gonnella *et al* studied and characterized the crystalline hydrate/polymorph forms of 5,11-dihydro-11-ethyl-5-methyl-8-(2-(1-oxido-4-quinolinyl)ethyl-6H-dipyrido(3,2-B:2',3'-E)(1,4)diazepin-6-one by ^{13}C SS-NMR and solution NMR with spectral editing techniques for chemical shift assignment and number of molecules per asymmetric unit cell.[135]

1.6: Powder X-Ray Diffraction (PXRD):

Application of powder X-ray diffraction in pharmaceuticals:

Malpezzi *et al* studied the single crystal and powder X-ray diffraction characterization of three polymorphic forms of Acitretin. He concluded that PXRD is not only useful for qualitative analysis but also for quantitative phase analysis of Acitretin Form II and Form III.[136]

Yamada *et al* demonstrated the potential of synchrotron powder X-ray diffractometry for detection and quantification of small amounts of Fenoprofen calcium crystalline drug substances in pharmaceutical tablets and also studied the dehydrate detection in intact film-coated tablets.[137]

Bansal *et al* developed a quantitative X-ray powder diffraction method to determine the amount of polymorphic drug substance of Olanzapine Form I present in Form II.[138] The above method was found to give good linearity from 0-100% (w/w), with LOD upto 0.40% and LOQ of 1.22%.

Bergstorm *et al* reported the crystal structure and relative stabilities of two polymorphs of anhydrous Ropivacaine HCl based on PXRD studies and used it to rationalize their physical behavior.[139]

1.7: Mass spectroscopy:

Application of mass spectroscopy in pharmaceuticals:

Hopfgartner *et al* demonstrated Desorption Electro Spray Ionization (DESI) technique to analyze more than twenty commercial drugs and a large number of counterfeit tablets. The consistency of quantitative results so obtained were comparable with the result obtained from GC-MS and LC-MS techniques.[140]

Cooks *et al* applied positive and negative ion DESI technique for on-line high-throughput monitoring of pharmaceutical samples *viz* tablets, ointments and liquids without prior sample preparation at ambient environment and reported that sampling rate, specificity and the high potential carryover effects are minimized in high-throughput on-line analysis with adequate sensitivity.[141]

Williams *et al* demonstrated the application of DESI, Direct Analysis in Real Time (DART) and Desorption Atmospheric Pressure Chemical Ionization (DAPCI) techniques for different types of drug molecules and observed that for weakly polar gaseous samples the ionization efficiency of DART was higher than DESI and the sensitivity of majority of drug molecules with DAPCI was also better than DESI techniques.[142]

Ding *et al* examined tooth paste samples with extremely high viscosity by using Natural Desorption Extractive Electro Spray Ionization (ND-EESI) techniques and showed that the detection limit of diethylene glycol as low as 0.2 ppm.[143]

Chen *et al* demonstrated that the active ingredients of powdered drugs were rapidly detected by using Desorption Atmospheric Pressure Chemical Ionization Mass Spectroscopy (DAPCI-MS) techniques, which is probably most sensitive for *in situ* analysis of powdered drug preparation.[144]

Zhou *et al* investigated the thermal decomposition of three common pharmaceuticals, Acetaminophen, Indomethacin and Mefenamic acid by using ESI-Mass Spectrometric techniques. The usefulness of ESI-MS is rapid for determining the relative stability and identifying thermal decomposition products comparative measurements with HPLC techniques.[145]

Morrison *et al* evaluated that a four-channel multiplexed electrospray inlet system (MUX) coupled to a triple quadrupole mass spectrometer as a higher throughput approach to quantitative analysis of drugs in biological media for DMPK screening procedures.[146]

Advantage of qNMR and Raman spectroscopic methods:

NMR is a reliable, precise and accurate quantitative analytical technique which has several advantages over other chromatographic techniques used for the purity assessment of organic compounds. In NMR, sample preparation is minimal which is achieved by dissolving the analyte and the reference material in the deuterated solvent. In NMR, spectra are routinely run on 10-60 mg of material and no further dilution is required whereas chromatographic methods are tedious with multi-step and may have the chance of manual errors and also involve an extensive sample preparation involving weighing of sample and an internal standard, followed by a series of dilutions to bring the analytical solution into the linear range of the detector or to accommodate the capacity factor of the analytical column. Sometimes derivatizaton, degassing etc. are also used or needed. NMR is a non-destructive technique which allows an intact retrieving of the sample and it offers a solution for many representatives that are not feasible for direct HPLC or GC determination due to lack of a suitable UV chromophore or are highly polar. Also in contrast to chromatographic methods, there is no need for the use of standard reference materials for each constituent in the analyte; instead one internal standard of known purity, unrelated to the target sample is enough. Finally a highly reproducible measurement with a precision and accuracy better than 0.1% is achievable using NMR.

Methods based on Raman spectroscopy are excellent for identifying the samples in the range of 10-3600 cm^{-1} (mid to far-IR) and do not require much sample preparation and can be applied to any optically accessible sample. Raman spectra are barely affected by sampling parameters and thereby provide best technique for accurate quantitative analysis of tablets, powders and liquids and quantitative polymorph assay in drug formulations.

1.8: Objectives:

The objective of the thesis is mainly to develop new and/or alternative methods of analysis which are rapid, highly specific and selective for the identification and quantification of drugs in their different dosage forms, based on FT-NMR (^{1}H, ^{19}F, ^{31}P) and FT-Raman spectroscopy. The other objectives are to use these and other sophisticated instruments to investigate the possible interaction of the drug with the excipients and also to develop methods to quantify polymorphic impurities in the case of some model drugs and their formulations.

The work presented in the thesis consists of five chapters. In Chapter 1, a brief introduction to the various sophisticated instrumental techniques that are now becoming popular in pharmaceutical science has been presented. Literature survey of the applications of these analytical techniques to identify and quantify the active pharmaceutical (API) and to investigate various other aspects of pharmaceutical science has also been presented.

In Chapter 2, the development of methods based on NMR spectroscopy has been presented. This involves optimization of condtions related to pulse sequence, delay time and relaxation time to generate the NMR data for the simulataneous identification and quantification of the drug substances. In each case appropriate internal standard has been identified and used. Section I, this chapter deals with method development for the quantitative determination of N,N-dimethylamine hydrochloride content in Metformin hydrochloride by using ^{1}H qNMR spectroscopy in which glycine has been used as an internal stanadard. ^{1}H qNMR method by using maleic acid as an internal standard has also been developed for the quantification of Sitagliptin phosphate in its tablet formulations which is presented in Section II of Chapter 2.

Similarly, a ^{19}F qNMR quantitative method has been developed for the assay of Flurbiprofen in drug products as well as for its recovery and stability study in human plasma. The internal standard used in this experiment is 4-fluorobenzoic acid. This also necessitated detailed cross correlation study of ^{19}F and ^{1}H involving Flurbiprofen and three other structurally related compounds. These results are presented in Section III of Chapter 2.

In Section IV, a ^{31}P qNMR method that is developed to identify and quantify Amifostine trihydrate and in its drug products has been presented.

In the case of determination of DMA·HCl content in Metformin hydrochloride and Amifostine assay, new and alternative HPLC methods have also been developed and a comparision of the qNMR and HPLC method has been made.

All ther above methods have been validated based on the performance criteria such as linearity, precision and accuracy.

Chapter 3, describes a detailed interaction study between Salmon Calcitonin (sCT) with Benzethonium chloride as preservative by using various NMR spectroscopic techniques, which is further extended to Benzalkonium chloride and Chlorobutanol for getting an insight into the extent of interaction, stability and preservative efficacy of the drug product. Therapeutic peptides such as Salmon Calcitonin which are short proteins consisting between about 10 to 50 amino acid residues have therapeutic activity. In solution drug products or nasal spray of any therapeutic peptide there is always a need to add suitable preservatives. The interaction study of peptides and preservatives in their liquid formulations is a major factor and it can modify the molecular properties such as secondary structure, stability, biological activity or toxicity. In the present case of sCT and preservatives, specific identification in terms of mole ratio and existence of molecular or ionic moieties in a given system are studied by using various analytical techniques such as CD, DLS, ITC, Fluorescence etc. Actual conformation of the sCT in the drug product has been determined by using various NMR spectroscopic techniques.

In Chapter 4, preparation of an improved hydrophobic drug complex, also called co-crystals, of Iloperidone with Cholesteryl sulfate sodium using various techniques has been reported. Complete characterization of these co-crystals has been carried out by using spectroscopic techniques. Co-crystals so prepared have been incorporated into the microspheres of DL-Copoly Lactic glycolic acid (PLGA) to get sustained release product using the optimum solvent evaporation method. Accelerated *in vitro* dissolution profile of the prepared microspheres has been studied by bottle rotating apparatus with chromatographic monitering. These results have also been presented.

The accurate identification and quantification of crystalline or amorphous polymorphic forms of drug materials is becoming increasingly important, due to stringent requirements set by various regulatory bodies. Sertraline hydrochloride, an antidepressant and anorectic drug exists in various polymorphic modifications. The synthesis and physicochemical characterization of various polymorphic forms (Form I, III, V) of this drug and their identification in drug substances has been carried out by using various analytical techniques. Again by using highly selective and sensitive Raman spectroscopic technique a quantitative determination method of its polymorphic impurities, Form I and Form III, present in Form V of Sertraline hydrochloride in its solid oral formulations has been developed. The results of this study are presented in Chapter 5.

Conclusions drawn from the investigations carried out have been presented at the end of each chapter and/or section.

References

1. Hollas, J. M. *Modern Spectroscopy*, **1996,** 3rd ed. J. Wiley and Sons, Chichester, UK.
2. Foster, H. *UV-Vis Spectroscopy*, **2004,** *4*, p.337, Springer, Berlin/Heidelberg, Germany.
3. Sanchez, R. F.; Ojeda, C. B.; Cano Pavon, J. M. *Talanta*, **1995**, *42*, 1195.
4. Ojeda, C. B.; Sanchez, R. F. *Anal. Chim. Acta*, **2004**, *518*, 1.
5. Kaur, K.; Kumar, A.; Malik, A. K.; Singh, B.; Rao, A. L. J. *Crit. Rev. Anal. Chem.* **2008**, *38*, 2.
6. Staniz, B.; Rafa, W. *Chem. Anal.* **2008**, *53*, 417.
7. Skibinski, R.; Misztal, G. *Acta. Polym. Pharm.* **2005**, *62*, 331.
8. Sharma, M.; Mhaske, D.; Mahadik, M.; Kadam, S.; Dhaneshwar, S. *Indian J. Pharm. Sci.* **2008**, *70*, 258.
9. Yilmaz, B.; Kadioglu, Y. *Farmaco,* **2004**, *59*, 425.
10. Singh, D. K.; Verma, R. *Anal. Sci.* **2007**, *23*, 1241.
11. Alkhalidi, B. A.; Shtaiwi, M.; Alkhatib, H. S.; Mohammad, M.; Bustanji, Y. *J. AOAC Int.* **2008**, *91*, 530.
12. Salem, M. Y.; Ramadan, N. K.; Moustafa, A. A.; El-Bardicy, M. G. *J. AOAC Int.* **2006**, *89*, 976.
13. Salem, M. Y.; EI-Guindi, N. M.; Mikael, H. K.; Abd-EL-Fattah, L. E. S. *Chem. Pharm. Bull.* **2006**, *54*, 1625.
14. EL-Sherif, Z. A.; Mohamed, A. O.; EL-Bardeicy, M. G.; EL-Tarras, M. F. *Spectrosc. Lett.* **2005**, *38*, 77.
15. Nikam, A. D.; Pawar, S. S.; Gandhi, S. V. *Asian J. Chem.* **2007**, *19*, 5075.
16. Riahi, S.; Ganjali, M. R.; Pourbasheer, E.; Norouzi, P. *Curr. Pharm. Anal.* **2007**, *3*, 268.
17. Hassan, W. S. *Am. J. Applied Sci.* **2008**, *5*, 1005.
18. Shankar, M. B.; Modi, V. D.; Shah, D. A.; Bhatt, K. K.; Mehta, R. S.; Geetha, M.; Patel, B. J. *J. AOAC Int.* **2005**, *88*, 1167.
19. Garg, G.; Saraf, S. *J. Indian Chem. Soc.* **2007**, *84*, 609.
20. Shrinivasan, K.; Alex, J.; Shirwaikar, A.; Jacob, S.; Sunilkkumar, M.; Prabhu, S. *Indian J. Pharm. Sci.* **2007**, *69*, 540.

21. Pescitelli, G.; Bilia, A.; Bergonzi, M.; Vincieri, F.; Bari, L.; *J. Pharm. Biomed. Anal.* **2010**, *52*, 479.
22. Bertacche, V.; Pini, E.; Stradi, R.; Stratta, F. *J. Pharm. Sci.* **2006**, *95*, 159.
23. Kipouros, K.; Kachrimanis, K.; Nikolakakis, I.; Malamataris, S. *Anal. Chim. Acta*, ***2005***,*550*,191
24. Bartolomei, M.; Bertocchi, P.; Antoniella, E.; Rodomonte, A. *J.Pharm.Biomed. Anal.* **2006**, *40*,1105.
25. Bunaciu, A. A.; Aboul-Enein, H. Y.; Fleschin, S. *II Farmaco,* **2005**, *60*, 33.
26. Khanmohammadi, M.; Mobedi, E.; Garmarudi, A.B.; Mobedi, H.; Kargosha, K. *Pharma. Dev. Tech.* **2007**, *12*, 573.
27. Khanmohammadi, M.; Mobedi, H.; Mobedi, E.; Kargosha, K; Garmarudi, A. B.; Ghasemi, K. *Spectroscopy*, **2009**, *23*, 113.
28. Boyer, C.; Bregere, B.; Crouchet, S.; Gaudin, K.; Dubost, J.P. *J. Pharm. Biomed. Anal.* **2006**, *40*, 433.
29. Kovela, B. B.; Kolev, T. M.; Tsalev, D. L.; Spiteller, M. *J. Pharm. Biomed. Anal.* **2008**, *46*, 267.
30. Nemet, Z.; Demeter, A.; Pokol, G. *J. Pharm. Biomed. Anal.* **2009**, *49*, 32.
31. McCreery, R. L. *Raman Spectroscopy for Chemical Analysis*, **2000**, John-Wiley and Sons, New York.
32. Grasselli, J. G.; Bulkin, B. J. *Analytical Raman Spectroscopy. Chemical Analysis*, **1991,** Vol. *114*, John-Wiley and Sons, New York.
33. Vankeirsbilck, T.; Vercauteren, A.; Baeyens, W.; Van der Weken, G.; Verpoort, F.; Vergote, G.; Remon, J. P. *Trends Anal. Chem.* **2002**, *21*, 869.
34. Ruperez, A.; Laserna, J. J. *Anal. Chim. Acta*, **1996**, *335*, 87.
35. Lewis, E. N.; Kalasinsky, V. F.; Levin, I. W. *Anal. Chem*. **1988**, *60*, 2306.
36. Cyr, T. D.; Dawson, B. A.; Neville, G. A.; Shurvell, H. F. *J. Pharm. Biomed. Anal*. **1996**, *14*, 247.
37. Wang, C.; Vickers, T. J.; Mann, C. K. *J. Pharm. Biomed. Anal*. **1997**, *16*, 87.
38. Breitenbach, J.; Schrof, W.; Neuman, J. *J. Pharm. Res.*, **1999**, *16*, 1109.
39. Davies, M. C.; Binns, J. S.; Melia, C. D.; Hendra, P. J.; Bourgeois, D.; Church, S. P.; Stephenson, P.J. *Int. J. Pharm*. **1990**, *66*, 223.
40. Jalsovszky, G.; Egyed, O.; Holly, S.; Hegedus, B. *Appl. Spectrosc.* **1995**, *49*, 1142.
41. Ryder, A. G.; Connor, G. M.; Glynn, T. J. *J. Raman Spectrosc.* **2000**, *31*, 221.

42. Sutherland, W. S.; Laserna, J. J.; Angebranndt, M. J.; Winefordner, J. D. *Anal. Chem*. **1990**, 62,689.
43. Ruperez, A.; Laserna, J. J. *Talanta,* **1997**, *44*, 213.
44. Neville, G. A.; Beckstead, H. D.; Shurvell, H. F. *J. Pharm. Sci.* **1992**, *81*, 114.
45. Strachan, C. J.; Rades, T.; Gordan, K. C.; Rantanen.J. *J .Pharm. Pharmacol.* **2007**, 59, 179.
46. Eliasson, C.; Macleod, N. A.; Jayes, L. C.; Clarke, F. C. *J. Pharm. Biomed. Anal*. **2008**, *47*, 221.
47. Niemczyk, T. M.; Delgado-Lopez, M. M.; Allen, F. S. *Anal. Chem.* **1998**, *70*, 2762.
48. Andrew, J. J.; Browne, M. A.; Clark, I. E.; Hancewicz, T. M.; Millichope, A. *J. Appl. Spectrosc*. **1998**, *52*, 790.
49. Breitenbach, J.; Schrof, W.; Neumann, J. *Pharm. Res*. **1999**, *16*, 1109.
50. Wikstrom, H.; Marsac, P. J.; Taylor, L. S. *J. Pharm. Sci*. **2005,** *94*, 209.
51. Vergote, G. J.; Beer, de, T. R. M.; Vervaet, C.; Remon, J. P.; Baeyens, W. R. G.; Diericx, N.; Vorpoort, F. *Eur. J. Pharm. Sci*. **2004,** *21*, 479.
52. Campbell, R. S. N.; Williams, A. C.; Grimsey, I. M.; Booth, S. W. *J. Pharm. Biomed. Anal*. **2002,** *28*, 1135.
53. Atrnold, J. T.; Dharmatti S. S.; Packard, M. E. *J. Chem. Phys.* **1951**, *19*, 507.
54. Arnold, J. T. *Phys. Rev*. **1956**, *102*, 136.
55. Anderson, W. A. *Phys. Rev*. **1956**, *102*, 151.
56. Ernst, R. R.; Anderson, W. A. *Rev. Sci. Instrum*. **1966**, *37*, 93.
57. Gunther, H. *NMR Spectroscopy*, **1995**, Wiley, Chichester.
58. Farrar, T. C.; Becker, E. D. *Pulse and Fourier Transform NMR,* **1971**, Academic Press, New York.
59. EURACHEM/ ICH Q2A, **1998**, CPMP/ICH/381/95.
60. Caytan, E.G.R.; Tenailleau, E.; Akoka, S. *Talanta*, **2007**, *71*, 214.
61. Ziarelli, F. *Solid State Nucl. Magn. Reson.* **2006**, *29*, 214.
62. Freeman, R. *Handbook of Nuclear Magnetic Resonance*, 2nd ed. **1997,** Addison Wesley Longman, Edinburgh.
63. El-Shahed, F.; Doerffel, K.; Radeglia, R. *J. Prakt. Chem.* **1979**, *321*, 859.
64. Mooney, J. R. in *Analytical NMR*, (Ed.), Field, L. D.; Sternhell, S. **1989,** John-Wiley and Sons, Chichester.
65. Rabenstein, D. L.; Millis, K. K.; Strauss, E. J. *Anal. Chem.* **1988**, *60*, 1380A.

66. Herring, F. G.; Philips, P. S. *J. Magn. Reson.* **1985**, *62*, 19.
67. Grivet, J. P. *Signal Treatment and Signal Analysis in NMR*, **1996,** Elsevier, Amsterdam, The Netherlands.
68. McLeod, K.; Comisarow, M. B. *J. Magn. Reson.* **1989**, *84*, 490.
69. Rabenstein, D. L.; Keire, D. A. *Pract. Spectrosc.* **1991**, *11*, 323.
70. Malz, F.; Jancke, H. *J. Pharm. Biomed. Anal.* **2005**, *38*, 813.
71. Maniara, G.; Rajamoorthi, K.; Srinivasan, R.; Stockton, G. W. *Anal. Chem.* **1998**, *70*, 4921.
72. Jungnickel, J. L.; Forbes, J. W. *Anal. Chem.* **1963**, *35*, 938.
73. Hollis, D. P. *Anal. Chem.* **1963**, *35*, 1682.
74. Ernst, R. R.; Bodenhausen, G.; Wokaun, A. *Principles of Nuclear Magnetic Resonance in one and two dimensions, Oxford University Press*, **1991,** Oxford.
75. Waugh, J. S. *Anal. Chem.* **1993**, *65*, 725A.
76. Freeman, R. *Anal. Chem.* **1993**, *65*, 743A.
77. Noble, D. *Anal. Chem*. **1994**, *66*, 658A.
78. Komoroski, R. A. *Anal. Chem.* **1994**, *66*, 1024A.
79. Rackham, D. M. *Talanta*, **1976**, *23*, 269.
80. Shoolery, J. N. *Progress in NMR Spectroscopy*, **1977**, *11*, 79.
81. Greenhalgh, R.; Shoolery, J. N. *Anal. Chem.* **1978**, *50*, 2039.
82. Jancke, H. *NMR Spectroscopy as a Primary Analytical Method,* CCQM Report, **1998**, *98*, 1.
83. Holzgrabe, U.; Diehl, B.; Wawer, I. *NMR Spectroscopy in Pharmaceutical Analysis,* **2008,** Elsevier, Oxford, UK.
84. Szantay Jr, C.; Beni, Z.; Balogh, G.; Gati, T. *Trends Anal. Chem.* **2006**, *25*, 806.
85. Deubner, R.; Holzgrabe, U. *Magn. Reson. Chem.* **2002**, *40*, 762.
86. Hanna, G. M. *Enantiomer*, **2000**, *5*, 303.
87. Salsbury, J. S.; Isbester, P. K. *Magn. Reson. Chem.* **2005**, *43*, 910.
88. Larive, C. K.; Jayawickrama, D.; Orfi, L. *Appl. Spectrosc.* **1997**, *51*, 1531.
89. Pauli, G. F.; Jaki, B. U.; Lankin, D. C. *J. Nat. Prod.* **2005**, *68*, 133.
90. Martino, R.; Gilard, V.; Desmoulin, F.; Malet-Martino, M. *J. Pharm. Biomed. Anal.* **2005**, *38*, 871.
91. Fulton, D. B.; Sayer, B. G.; Bain, A. D.; Malle, H. V. *Anal. Chem*. **1992**, *64*, 349.
92. Laycock, M. V.; Thibault, P.; Ayer, S. W.; Walter, J. A. *Nat. Toxin*, **1994**, *2*, 175.

93. Ramsey, U. P.; Douglas, D. J.; Walter, J. A.; Wright, J. L. C. *Nat. Toxin*, **1996**, *6*, 137.
94. Akoka, S.; Barantin, L.; Trierweiler, M. *Anal. Chem.* **1991**, *71*, 2554.
95. Remaud, G. S.; Silvestrs, V.; Akoka, S. *Accred. Qual. Assur.* **2005**, *10*, 415.
96. Michel, N. S. A. *J. Magn. Reson.* **2004**, *168*, 118.
97. Haleblian, J.; Mc Crone. W. *J. Pharma. Sci*. **1969**, *58*, 911.
98. Franconi, F. C. C.; Lemaire, L.; Lehmann, V.; Barantin, L.; Akoka, A. *Magn. Reson. Imaging*, **2002**, *20*, 587.
99. Kromidas, S. *Nachr. Chem. Tech. Lab.* **1998**, *46*, 28.
100. EURACHEM/NATA, **1998**, Tech Note # 13.
101. EURACHEM Guide, "*The Fitness for Purpose of Analytical Methods*", A Laboratory Guide to Method Validation and Related Topics, 1st ed. **1998**.
102. EURACHEM/ISO 3534-1, **1998.**
103. Branch, S. K. *J. Pharm. Biomed. Anal.* **2005**, *38*, 798.
104. EURACHEM/AOAC-PVMC, **1998.**
105. Jancke, H.; Malz, F.; Hasselbarth, W. *Accred. Qual. Assur.* **2005**, *10*, 421.
106. Holzgrabe, U.; Deubner, R.; Schollmayer, C.; Waibel, B. *J. Pharm. Biomed. Anal.* **2005**, *38*, 806.
107. Balchin, E.; Malcolme-Lawes, D. J.; Poplett, I. J. F.; Rowe, M. D.; Smith, J. A. S.; Pearce, G. E. S.; Wren, S. A. C. *Anal. Chem.* **2005**, *77*, 3925.
108. Bailey, N. J. C.; Marshall, I. R. *Anal. Chem.* **2005**, *77*, 3947.
109. Dumas, M. E.; Maibaum, E. C.; Teague, C.; Ueshima, H.; Zhou, B.; Lindon, J. C.; Stamler, J.; Elliott, P.; Chan, Q.; Holmes, E. *Anal. Chem.* **2006**, *78*, 2199.
110. Buckingham, A. D.; Fischer, P. *Chem. Phys.* **2006**, *324*, 111.
111. Silverstre, V.; Mobula, V. M.; Jouitteau, C.; Akoka, S.; Robins, R. J.; Remauds, G. S. *J. Pharm. Biomed. Anal.* **2009**, *50*, 336.
112. Webster, G. K.; Marsden, I.; Pmmerening, C. A.; Tyrakowsky, C. M.; Tobias, B. *J. Pharm. Biomed. Anal.* **2009**, *49*, 1261.
113. Forshed, J.; Torgrip, R. J. O.; Aberg, K. M.; Karlberg, B.; Lindberg, J.; Jacobsson, S. P. *J. Pharm. Biomed. Anal.* **2005**, *38*, 824.
114. Jones, C. *J. Pharm. Biomed. Anal.* **2005**, *38*, 840.
115. Rizzo, V.; Pinciroli, V. *J. Pharm. Biomed. Anal.* **2005**, *38*, 851.
116. Wawer, I.; Pisklak, M.; Chilmonczyk, Z. *J. Pharm. Biomed. Anal.* **2005**, *38*, 865.
117. Webb, A. G. *J. Pharm. Biomed. Anal.* **2005**, *38*, 892.

118. Price, K. E.; Vandaveer, S. S.; Lunte, C. E.; Larive, C. K. *J. Pharm. Biomed. Anal.* **2005**, *38*, 904.

119. Putzbach, K.; Krucker, M.; Grynbaum, D.; Hentschel, P.; Webb, A. G.; Albert, K. *J. Pharm. Biomed. Anal.* **2005**, *38*, 910.

120. Gu, H.; Pan, Z.; Duda.; Mann, D.; Kissinger, C.; Rohde, C.; Raftery, D. *J. Pharm. Biomed. Anal.* **2007**, *45*, 134.

121. Xu, Z.; Kuang, D.; Liu, L.; Deng, Q. *J. Pharm. Biomed. Anal.* **2007**, *45*, 54.

122. Wang, H.; Zhang, Z.; Xiong, F.; Wu, L.; Li, P.; Ye, W. *J. Pharm. Biomed. Anal.* **2011**, *55*, 902.

123. Malet-Martino, M.; Holzgrabe, U. *J. Pharm. Biomed. Anal.* **2011**, *55*, 1.

124. Holzgrabe, U.; Malet-Martino, M. *J. Pharm. Biomed. Anal.* **2011**, *55*, 679.

125. Bugay, D. E. *Pharm. Res.* **1993**, *10*, 317.

126. Burn, S. R.; Pfeiffer, R. R.; Stowell, J. C. *Solid State Chemistry of Drug,* **1999**, 2nd ed. SSCI, Inc.

127. Saindon, P.; Cauchon, N.; Sutton, P.; Chang, C.; Peck, G.; Byrn, S. *Pharm. Res.* **1992**, *10*, 197.

128. Gao, P. *Pharm. Res*. **1996**, *13*, 1095.

129. Booy, K.; Wiegernick, P.; Vader, J.; Kaspersen, F.; Lambregts, D.; Vromans, H.; Kellenbach, E. *J. Pharm. Sci.* **2004**, *94*, 458.

130. Offerdahl, T.; Salsbury, J.; Dong, Z.; Grant, D.; Schroeder, S.; Prakash, I.; Gorman, E.; Barich, D.; Munson, E. *J. Pharm. Sci*. **2005**, *94*, 2591.

131. Aso, Y.; Yoshioka, S. *J. Pharm. Sci*. **2006**, *95*, 318.

132. Bauer, J.; Morley, J.; Spanton, S.; Leusen, F. J. J.; Henry, R.; Hollis, S.; Heitmann, W.; Mannino, A.; Quick, J.; Dziki, W. *J. Pharm. Sci.* **2006**, *95*, 917.

133. Sotthivirat, S.; Lubach, J.; Haslam, J.; Munson, E.; Stella, V. *J. Pharm. Sci.* **2007**, *96*, 1008.

134. Sanchez, S.; Ziarelli, F.; Viel, S.; Delaurent, C.; Caldarelli, S. *J. Pharm. Biomed. Anal.* **2008**, *47*, 683.

135. Gonnella, N.; Smoliga, J.; Campbell, S.; Busacca, C.; Cerreta, M.; Varsolona, R.; Norwood, D. *J. Pharm. Biomed. Anal.* **2010**, *51*, 1047.

136. Malpezzi, L.; Magnone, G.; Masciocchi, N.; Sironi, A. *J. Pharm. Sci.* **2005**, *94*, 1067.

137. Yamada, H.; Masuda, K.; Ishige, T.; Fujii, K.; Uekusa, H.; Miura, K.; Yonemochi, E.; Terada, K. *J. Pharm. Biomed. Anal.* **2011**, *56*, 448.

138. Bansal, A. K.; Tiwari, M.; Chawla, G. *J. Pharm. Biomed. Anal.* **2006**, *43*, 865.
139. Bergstrom, P.; Fischer, A.; Kloo, L.; Sebhatu, T. *J. Pharm. Sci.* **2006**, *95*, 680.
140. Leuthold, L. A.; Mandscheff, J. F.; Fathi, M.; Giroud, C.; Augsburger, M.; Varesio, E.; Hopfgartner, G. *Rapid Commun. Mass Spectrom.* **2006**, *20*, 103.
141. Chen, H. W.; Talaty, N.; Takats, Z.; Cooks, R. G. *Anal. Chem.* **2005**, *77*, 6915.
142. Williams, J. P.; Patel, V. J.; Holland, R.; Scrivens, J. H. *Rapid Commun. Mass Spectrom.* **2006**, *20*, 1447.
143. Ding, J.; Gu, H.; Yang. S.; Li, M.; Li. J.; Chen, H. *Anal. Chem.* **2009**, *81*, 8632.
144. Chen, H. W.; Lai, J. H.; Zhou, Y. F.; Li, J. Q.; Zhang, X.; Luo, M. B.; Wang, Z. C. *Chin. J. Anal. Chem.* **2007**, *35*, 1233.
145. Zhou, W.; Gilpin, R. K. *J. Pharm. Sci.* **2004**, *93*, 1545.
146. Morrison, D.; Davies, A. E.; Watt, A. P. *Anal. Chem.* **2002**, *74*, 1896.

Chapter 2

Quantitative Nuclear Magnetic Resonance (qNMR): Methodology and its Application

Introduction:

The qNMR methodology and its validation as a primary ratio and independent assay determination method and the measurement of uncertainty associated with this analysis depend upon the key NMR aspects involved in quantification.

This chapter reports the usefulness of ^{1}H, ^{31}P and ^{19}F, the most frequently used nuclei, for extending the qNMR methodology to and its quantitative applications method and its comparison with the chromatography.

Proton (^{1}H) is the most popular nucleus in quantitative NMR analysis, because it is the most abundant element, has high NMR frequency and sensitivity with excellent accuracy and reproducibility, and has widened its acceptance, and also become the most reliable quantitative NMR method.

^{1}H qNMR technique is considered as an important method for the analysis of drugs and pharmaceuticals because it has huge potential to be used as an ultimate method for the quantification of active ingredients.

In 1970, Rackham introduced ^{1}H qNMR as an alternative, quicker and more accurate technique for the quantitative analysis of pharmaceutical materials with error of less than 2 %. The author deals with the development in quantitative NMR measurements with special regard to the choice of internal standard materials.[1a] The common internal standards used for the qNMR analysis are, 1,3,5-benzenetricarboxylic acid, 1, 3, 5- trimethoxybenzene, 1,3,5- trioxane, 1,4-bis (TMS)-benzene, 1,4- dinitrobenzene, Anthracene, Benzyl benzoate, Biphenyl, Dimethyl isophthalate, Dimethylformamide, Dimethylsulfone, Formic acid, Hexamethyl-cyclotrisiloxane, Maleic acid, Methenamine, Phloroglucinol, Sodium acetate, Tert-butanol, Tetramethylpyrazine, 3-(Trimethylsilyl)propionic acid-d_4 (TSP-d_4), Etacrynic acid, 2,5-dimethylfuran etc.

Abdel Fattah and group in 1980 carried out quantification of diclofenac sodium in bulk drug and tablets using anhydrous sodium acetate as an internal standard. They showed that ^{1}H qNMR provides a rapid, accurate and reproducible method for the analysis of the authentic drug and its tablets.[1b] Hassan *et al* developed an equally efficient method for methimazole in its pure form as well as in tablet formulations by using benzoic acid as internal standard on 60 MHz spectrometer.[2]

Commercial ophthalmic solution was analysed by George *et al* for the assay of Carbachol (cholineegic agent which is used in the ocular surgery) with minimum steps and reagents and with a high degree of accuracy using proton magnetic resonance spectroscopy. The developed method precludes interferences by synthetic celluloses that are added to carbachol ophthalmic solutions to both prolong and increase pharmacological effects.[3]

Abu, J. Ferdous *et al* investigated ^{1}H NMR as an analytical tool for the determination of rate of hydrolysis of drugs with ester groups. This will make it a precise method for the rapid evaluation of the shelf-life of aqueous solutions of such drugs.[4]

In 1991, George and Cesar developed a simple, accurate and specific ^{1}H NMR assay method for the quantification of Metoclopramide hydrochloride in tablets and injections by using acetamide as an internal standard in D_2O.[5]

Fardella and coworkers proposed a simple, rapid, precise and accurate ^{1}H and ^{19}F-NMR method for quantitative analysis of fluoroquinolones, like pefloxacin, norfloxacin and ofloxacin in their pharmaceutical dosage forms, which are oral synthetic anti bacterial agents.[6]

The analysis of various organic chemicals in the field of pharmaceutical, analytical standards and agricultural chemicals was carried out by Maniara and coworkers in 1998, for the quantitative analysis by ^{1}H and ^{31}P by qNMR spectroscopy.[7]

Ozden *et al* developed a rapid, specific and simple assay method involving the application of ^{1}H qNMR spectroscopy,[8] for the determination of Methocarbamol, a skeletal muscle relaxant, in solid dosage forms by using maleic acid as an internal

standard in DMSO-d_6 as a solvent. The proposed method can be easily adapted to various pharmaceuticals for their quantification.

Goger *et al* proposed a method for the determination of Azathiprine, an antileukaemic and immunosuppressive drug, again based on quantitative ^{1}H NMR method.[9]

Harris and coworkers have reported the quantification of Bambuterol hydrochloride in a formulated product using solid-state Qnmr.[10]

The first report of the quantitative analysis for the enantiomeric purity of acetyl-L-carnitine was proposed by Kagawa, using qNMR spectroscopy on 500 MHz instrument. This method takes advantage of the fast interaction of the diasteriomers with chiral lanthanide-camphorato and chiral samarium-pdta shift reagents. The separation of the signals of the enantiomers was used for the successful quantitative analysis of DL-acetyl-carnitine.[11]

Michaleas *et al* developed a new approach to quantitative NMR for fluoroquinolones analysis by evaluating the chemical shift displacements. In this method, Ciprofloxacin solution was scanned over a wide range of concentrations and evaluated data was of acceptable characteristics regarding accuracy, precision and robustness.[12]

The usefulness of *p*-toluene sulfonic acid as a reference substance was reported by Gang Shao and coworkers to calibrate a water-soluble standard by NMR for quantitative analysis.[13]

In 2009 McEwen *et al* investigated the effect of Ca^{2+} on the ^{1}H NMR chemical shift of the methyl signal of over sulphated chondroitin sulphate, a contaminant in heparin.[14a-14b] Also Peter and coworkers developed an improved impurity finger printing of heparin by high resolution ^{1}H NMR spectroscopy.[15]

In the same year, Webster and group reported relative response factors of Fluoxetine hydrochloride for chromatographic investigations using NMR spectroscopy.[16] These values generated using NMR to normalize peak area responses by mass yield are not significantly different from the traditional mass detectors, chemical luminescence detectors (CLND) and charge aerosol detector (CAD).

Nageswara and coworkers isolated and characterized a potential process related impurity of Phenazopyridine hydrochloride (API) by routine HPLC method. By using MS-MS and 2D-NMR ^{1}H-^{1}H correlation COSY and NOESY NMR spectroscopy, the trace level of impurity was unambiguously identified. [17]

Orgovan and coworkers studied the kinetics of Tolperisone, a classical muscle relaxant and its decomposition products by qNMR spectroscopy. The acid base properties, kinetic constants including activation parameters and mechanism of decomposition were also studied by qNMR spectroscopy.[18]

Beyer *et al* investigated the influence of the nature of solvent on the signal separation of decisive resonances in the NMR spectra of codergocrine mesilate and flupentixol dihydrochloride.[19]

Keire *et al* developed a new assay method to detect the presence of economically motivated additives (EMAs) and poor manufacturing processes in heparin. In order to determine this, selected oversulfated glycosaminoglycans that are possible EMAs to heparin were synthesized and usefulness of ^{1}H NMR, SAX-HPLC or anticoagulation time protocols were demonstrated for the detection of native impurities like chondriotin sulphate A or B or heparin sulphate or synthetic contaminants spiked into heparin sodium active pharmaceutical ingredients.[20]

Recently, Staneva's group introduced quantitative analysis of sesquiterpene lactones in extract of *Arnica montana* L by ^{1}H qNMR spectroscopy.[21] They demonstrated the two different approaches for determination of lactones present in *Arnica Montana. T*his method complied well with the reported analysis.

Iqbal and coworkers characterized and determined relative response factor of process related impurity in Naproxen by NMR spectroscopy.[22] This method can be used as an alternative method to conventional HPLC method when the availability of the impurity standard is not likely during the early stage of drug development process.

Hanna *et al* optimized a method for enantiomeric separation and quantitative determination of the chiral drug propranolol by ^{1}H NMR spectroscopy utilizing a chiral solvating agent.[23]

Malz and Jancke described a validated protocol for quantitative high resolution ^{1}H NMR using single pulse excitation which has been confirmed by

national and international round robin test that considers all issues regarding linearity, robustness, specificity, selectivity and accuracy as well as influences of instrument specific parameters and the data processing and evaluation routines.[24]

Lavertu *et al* introduced the liquid phase proton NMR of chitosan for the determination of the degree of deacetylation (DDA) of chitosan, a natural polysaccharide obtained by partial deacetylation of chitin.[25] They found that the technique is precise, fast, reproducible, rugged, robust, stable and requires only a small amount of chitosan.

Li and coworkers analyzed the commercially available Praziquantel tablets by a high-performance liquid chromatography and a nuclear magnetic resonance spectroscopy methods.[26] The composition profiling of these tablets by NMR spectroscopy proved useful for comparing products from different manufacturers and also assessing batch-to-batch variation from a single manufacture.

Mazumdar and coworkers developed a quantitative NMR protocol for the simultaneous analysis of Atropine and Obidoxime chloride in parenteral injection devices.[27] The drug cartridges can be determined by ^{1}H NMR with the use of 4,4-dimethyl 4-silapentane sodium carboxylate (DSS) as internal standard which is compared to the reported LC-UV and LC-UV-GLC methods of analysis.

This work makes an attempt to overcome difficulty in determining assay by qNMR over conventional techniques such as titrimetry and relative chromatographic techniques.

Section – I

Quantification of DMA·HCl in Metformin hydrochloride by ^{1}H qNMR and HPLC derivatization method

2.I.1: Drug:

Metformin hydrochloride (MF·HCl),[28] 1,1-Dimethylbiguanide hydrochloride is a biguanide hypoglycaemic agent[29] commonly used for the treatment of type II diabetes.[30] Although MF·HCl was developed decades ago it is still widely used for the treatment of diabetes either alone or in combination with other drugs. Several techniques[31a-31d] such as HPLC,[32a,32b] Capillary Electrophoresis,[33] Near Infra Red (NIR)[34] and LC-MS-MS[35] have been reported for its determination in dosage form and biological fluids.[36]

N,N-Dimethylamine hydrochloride (DMA·HCl) is a non volatile, colourless, crystalline secondary amine which is a low melting solid, highly hygroscopic in nature and also a precursor to several industrially significant compounds.[37] The solvents *viz*. dimethyl formamide (DMF) and dimethyl acetamide are derived from N,N-dimethyl amine hydrochloride. It is also a raw material for the production of several agrochemicals, pharmaceutical intermediates and finished products. Zhang *et al* reported that the German cockroach utilizes dimethylamine as a pheromone for communication and DMA undergoes nitration under weak acid conditions to give dimethyl nitrosoamine. This animal carcinogen has been detected and quantified in human urine samples.[38]

The manufacturing process of Metformin hydrochloride (MF·HCl), by using different routes of synthesis always has a non volatile, UV-Visible inactive residual organic impurity,[39] in the form of DMA·HCl (Fig. 2.I.1). This is a residual solvent having specific higher limit by batch analysis data and the maximum daily dose capacity of MF·HCl pharmaceutical products. As the toxicity limit of DMA·HCl was not reported in ICH guidelines, it was considered as an equivalent toxic solvent with organic residual impurity such as. The permitted daily exposure (PDE) of triethylamine is 3.2 mg/day giving a limit of 320 ppm (for 10 g daily dose) was calculated from repeated dose toxicity and reproductive toxicity data.[40] In order to

control the limit of DMA·HCl in Metformin hydrochloride below the PDE, there is a need for separate quantitative method which can directly identify and quantify it in ppm level. However, none of the reported methods for the determination of DMA·HCl in MF·HCl appear to be stability indicating. Therefore, it is considered important to develop a stability indicating method, which can be employed in routine in-process and quality control analysis.

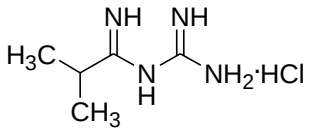

1

Metformin Hydrochloride

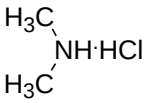

2

N,N-Dimethylamine Hydrochloride

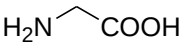

3

Glycine (Internal Standard)

Figure 2.I.1: Structure of Drug, Analyte and Internal standard

As highlighted in Chapter 1, Nuclear Magnetic Resonance (NMR) spectroscopy enables under favorable circumstances, accurate and precise determinations of pharmaceutical compounds in different matrices. Quantitative measurement by NMR spectroscopy (^{1}H qNMR) was first described by Hollis and Jungnickel *et al* in 1963 for the determination of drugs.[41,42] The lack of absorbing chromophores in DMA·HCl makes its detection practically impossible by any available chromatographic or other special detectors, further due to its non-volatile nature it is also not possible to quantify by GC.[43,44] The difficulties in establishing highly efficient solid or liquid phase extraction procedures have made NMR a suitable alternative techniques for biological sample analysis of many drug substances and drug products.[45,46] To the best of our knowledge, no official Pharmacopeial or no other monograph methods has been reported for the quantification of DMA·HCl by using ^{1}H qNMR, hence the present study has been undertaken.

The aim of this work is to develop an advantageous and competitive selective proton quantitative NMR spectroscopic (^{1}H qNMR) method for the determination of DMA·HCl in process, quality control, API and in formulation samples that complies well with the validation requirements in the pharmaceutical industry taking Metformin hydrochloride as a model drug. Apart from this, a new derivatization HPLC method[47-50] has also been developed. In ^{1}H qNMR method glycine has been used as internal standard (IS), by means of which simultaneously 1,1-dimethyl

hydrochloride (DMA·HCl) can be identified as well as quantified. Holzgrabe *et al* and Malet have reported the validation protocol and both the methods have been validated by assessing their specificity, linearity, range, precision, accuracy, limit of quantification, limit of detection, ruggedness and robustness.[51,52]

2.I.2: Experimental:

2.I.2.1: Materials and reagents:

High purity analytical and ICH grade materials were used throughout the study. Metformine·HCl BP was provided by Sun Pharmaceuticals Industries Ltd. (Vadodara, India). Glycine (99.9%) and Deuterium Oxide (99.96%D) were purchased from Merck Germany. N,N-dimethylamine hydrochloride (DMA·HCl) was purchased from Aldrich (99.9%). The following materials used in HPLC experiment, *viz* Acetonitrile and Triethylamine HPLC Grade, ortho phosphoric acid Analytical Grade and 1-Fluoro-2-4-dinitro benzene (FDNB) Analytical Grade were all purchased from Merck. MilliQ water was used in all the experiments.

2.I.2.2: ^{1}H qNMR experiment:

Diluent: Deuterium oxide (D_2O)

Stock solution (Internal Standard solution)

Glycine (IS), 125 mg was taken in a 250 mL volumetric flask and volume was made up with diluent.

Standard solution

DMA·HCl, 4 mg was dissolved in 1 mL of IS solution.

Sample preparation

100 mg of Metformin·HCl was accurately weighed and dissolved in 5 mL of IS.

All the ^{1}H NMR spectra were recorded on a Bruker BioSpin AV-III 500MHz (11.7 T) spectrometer operating at proton frequency 500.13 MHz using 5 mm Broad Band Observe probehead. All data were processed using Bruker`s Topspin 2.1 software. For all ^{1}H qNMR measurements carried out for method development, accurately 1 mL solution of 400 ppm concentration of DMA·HCl in pure D_2O solvent

was taken in a 5 mm NMR tube. For generating ^{1}H qNMR spectra, 16 scans were collected into 32 k data points over a spectral width of 9014.42 Hz with a transmitter offset in the centre of the spectrum. The acquisition time was 9.49 min followed by a relaxation delay of 35 s. All spectra were recorded at 295 K using a flip angle 90°. An exponential line broadening window function at 0.50 Hz was used in the data processing and baseline corrections were done automatically while phasing was always performed manually.

For accurate quantitative NMR analysis, the proper value of relaxation delay (d_1) was generally set at more than or equal to five times the value of the longest spin-lattice relaxation time (T_1) of the integrated resonance signals in order to ensure full relaxation of the corresponding protons. The T_1 relaxation time of MF·HCl, DMA·HCl and IS were measured by using NMR inversion-recovery pulse sequence and the maximum T_1 relaxation time values so obtained was found to be maximum with 6.80s for DMA·HCl protons at δ 2.6 ppm, where as MF·HCl having methyl and glycine having methylene protons, T_1 relaxation time was 2.96 s at δ 2.92 ppm and 3.90s at δ 3.43 ppm respectively.

2.I.2.3: HPLC Experiment:

The in-situ HPLC derivatization process for N,N-Dimethylamine hydrochloride

A solution of 1.0 g of 2,4-dinitrofluorobenzene and equimolar of N,N-dimethylamine hydrochloride in acetonitrile was heated at 60 °C for 30 min. The formed intermediate (mixture of N,N-dimethyl-2,4-dinitrobenzene was neutralized using triethylamine as base to form the N,N-dimethyl-2,4-dinitrobenzene (UV-Vis active), salt of triethylammonium chloride and triethylammonium fluoride.

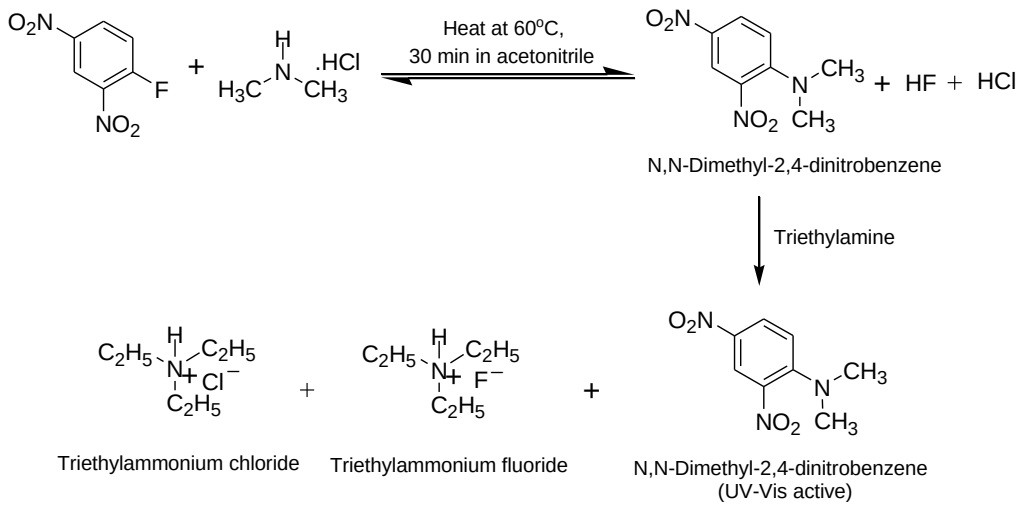

Scheme 2.I.1: Derivatization process for N, N-Dimethylamine hydrochloride (UV-Vis active)

1-Fluoro-2,4-Dinitro Benzene (FDNB) solution

FDNB solution was prepared by mixing 1 mL of 1-Fluoro-2,4-dinitro benzene (FDNB) and small amount of acetonitrile solution in a 100 mL volumetric flask. The solution was thoroughly mixed and made up to the mark with acetonitrile. This solution was prepared fresh just prior to use.

Standard preparation and system suitability preparation

Accurately weighed 36.2 mg of dimethylamine hydrochloride (Equivalent to 20 mg of dimethylamine) was dissoved in a small amount of diluent in 100 mL volumetric flask and diluted upto the mark with the diluent (solution-A).

Stock solution B of Dimethylamine

1.25 mL of the above solution-A was diluted to 50 mL with acetonitrile (stock solution-B).

Stock solution C of Dimethylamine

1.0 mL of above solution-A was diluted to 10 mL with acetonitrile (stock solution-C).

Further 2.5 mL of solution-A was diluted to 100 mL with the diluent. 1 mL of this solution was mixed thoroughly with 5 mL acetonitrile, 100 µL triethylamine and 1 mL of FDNB solution in 10 mL of volumetric flask. This solution was heated at 60 ºC for 30 min and allowed to cool to attain room temperature and then the volume was made upto the mark with acetonitrile to give 0.5 ppm solution of dimethylamine.

Sample preparation

A 1000 ppm solution of MF·HCl was prepared by weighing 10 mg of the sample and mixing it thoroughly with 5 mL acetonitrile, 100 µL triethyl amine and 1 mL of FDNB solution in 10 mL volumetric flask. This solution was heated at 60 ºC for 30 min and allowed to cool to attain room temperature and then made upto the mark with acetonitrile. This solution was centrifuged at 3000 rpm for 5 min in order to completely derivatize all DMA·HCl solvent present in MF·HCl.

2.I.2.4: Instrumental condition and gradient programme:

The quantitative derivatization gradient HPLC method for analysis of DMA·HCl in MF·HCl was performed on a Waters 2695 HPLC system with Dual Wavelength Detector 2487, using Empower software with a reverse phase column packed with octadecyl silane (C_{18}) chemically bonded phase particles (Inertsil ODS 3V : 150 mm x 4. 6 mm (5µm) , Make-GL Science, Japan).

Two mobile phases [Mobile phase A: 0.1% v/v orthophosphoric acid in water (buffer solution) and Moblile phase B: 100% Acetonitrile] were employed to run a gradient condition from 40 % B to 55 % B in 10 min, from 55 % B to 75 % B in 1 min, stay at 75 % B for 4 min, from 75 % B to 40 % B in 0.5 min and stay 40% B till 20 min as shown in Table 2.I.1.

Time (min)	Mobile phase A (% v/v)	Mobile phase B (% v/v)
0	60	40
10	45	55
11	25	75
15	25	75
15.5	60	40
20	60	40

Table 2.I.1: Gradient programme of HPLC method

2.I.3: Results and discussion:

2.I.3.1: ^{1}H qNMR method:

^{1}H qNMR spectrum of the sample is shown in Fig 2.I.2. The signals at (δ) 3.4 ppm and 2.6 ppm (calibrated with chemical shift (δ) of HOD signal from D_2O at 4.6 ppm) are due to IS (Glycine) and N,N-Dimethylamine·HCl. The integral values of both the ^{1}H signals are found to be directly and quantitatively proportional to the number of nuclei and weight of the sample.

The DMA content was calculated by using the Equation (2-1) given below,

$$W_x = \frac{I_x}{I_{std}} \times \frac{N_{std}}{N_x} \times \frac{M_x}{M_{std}} \times W_{std} \qquad (2\text{-}1)$$

where, W_x = weight of DMA·HCl, I_x = area of DMA·HCl methyl signal, I_{std} = area of IS N_{std} = number of nuclei involved in signal for standard, N_x = number of nuclei involved in signal for DMA·HCl, M_x is molecular weight of DMA·HCl, M_{std} is the molecular weight of IS and W_{std} weight of IS in sample solution.

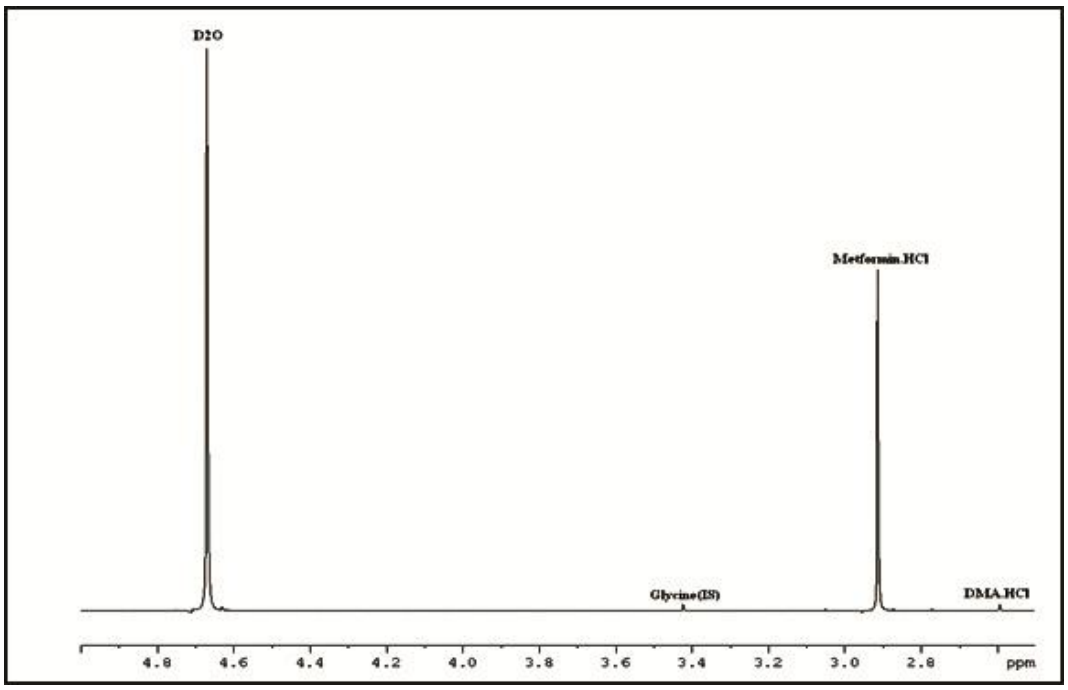

Figure 2.I.2: NMR spectrum of Metformin hydrochloride with N, N-Dimethylamine hydrochloride along with Internal Standard (IS) as Glycine in D_2O

The validity of the ^1H qNMR method was established through a study of linearity, method precision, LOD, LOQ, ruggedness, robustness, solution stability and recovery.

2.I.3.2: Linearity:

The linearity was evaluated and established by triplicate analysis of standard solution of DMA·HCl from the data presented in Table 2.I.2. The integrated NMR signal area obtained with respect to IS was plotted against the corresponding concentration to generate calibration curve (Fig 2.I.3). Good linearity was evident (r^2 = 0.9991) over the examined concentration range of 1 ppm to 1000 ppm with Equation y = 0.7524x ± 0.8303. The LOD and LOQ were calculated by the standard deviation of the response 'σ' and the slope 's' of the

calibration curve (Fig.2.I.3) obtained from the linearity results by using Equation (2-2) and (2-3) respectively.

$$\text{LOD} = \frac{3.3\,\sigma}{S} \qquad (2\text{-}2)$$

$$\text{LOQ} = \frac{10\,\sigma}{S} \qquad (2\text{-}3)$$

Sr. No.	Concentration of DMA in ppm	NMR signal area
1	1	0.53
2	10	7
3	50	38
4	100	79
5	125	95
6	250	185
7	500	374
8	750	584
9	1000	741

Table 2.I.2: Linearity data of DMA·HCl content by ^{1}H qNMR

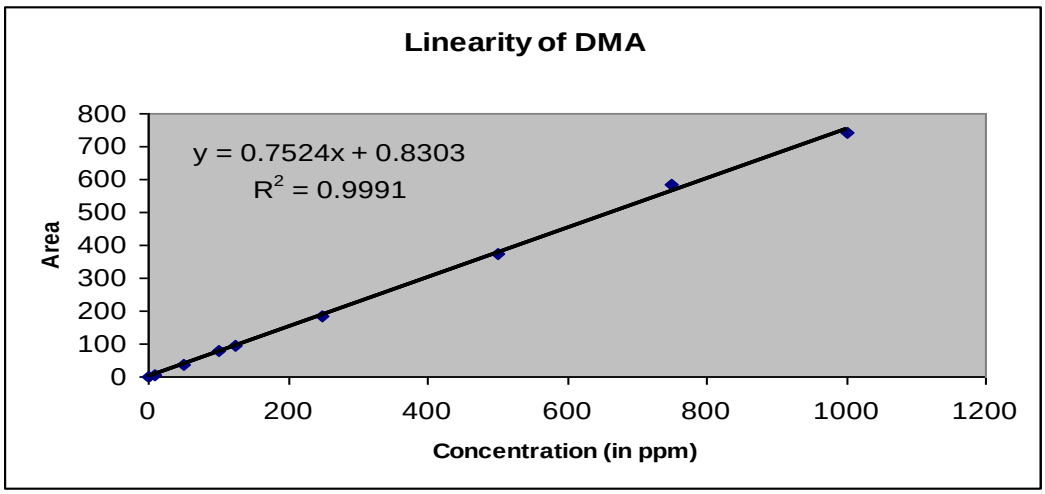

Figure 2.I.3: Linearity plot of DMA·HCl content by ^{1}H qNMR

2.I.3.3: Method precision:

The precision of the method, evaluated as the repeatability was established by calculating the relative standard deviation (% RSD) of the peak areas of DMA·HCl for six determinations made on the same day and under the same experimental conditions given in Table 2.I.3. The % RSD of DMA·HCl peak area obtained by ^{1}H

qNMR method is 1.68 %, which indicates that the proposed method is precise and within the acceptable limit of not more than 2 % deviation.

Sr. No.	I_x	W_x	Average	% RSD
1	362.33	3.28	3.24	1.68%
2	357.33	3.24		
3	361.00	3.27		
4	362.67	3.28		
5	356.67	3.23		
6	346.67	3.14		

Table 2.I.3: Method precision for DMA·HCl by ^{1}H qNMR

2.I.3.4: Ruggedness (Intermediate precision):

The precision of the method, evaluated as the repeatability was studied by calculating the relative standard deviation (% RSD) of the peak areas of DMA for six determinations made on a different frequency NMR instrument (400 MHz instead of 500 MHz) with different probe head (QNP-F), different analyst and sample depth variation under the same experimental conditions given in Table 2.I.4, 2.I.5 and 2.I.6 respectively. The % RSD of DMA·HCl peak area obtained by ^{1}H qNMR method is 2.02% and 2.20% respectively which is within acceptable limit of not more than 10% and the NMR tube should be filled with sample solution to at least 3.0 cm height.

Sr. No.	I_x	W_x	Average	% RSD
1	357.00	3.23	3.21	2.02%
2	358.33	3.25		
3	358.67	3.25		
4	359.67	3.26		
5	355.00	3.21		
6	340.67	3.09		

Table 2.I.4: Intermediate precision of DMA·HCl by ^{1}H qNMR on 400 MHz instrument (Instrument change)

Sr. No.	I_x	W_x	Average	% RSD
s	365.00	3.31	3.27	2.20%
2	370.00	3.37		
3	357.33	3.24		
4	351.00	3.18		
5	366.67	3.32		
6	355.33	3.22		

Table 2.I.5: Intermediate precision of DMA·HCl by ^{1}H qNMR (Different Analyst)

Study No.	Sample depth	W_x	Difference
1	1.5	0.00	-0.34
2	3.0	0.35	-0.01
3	4.5	0.35	-0.01
4	6.0	0.35	-0.01
5	7.5	0.34	N/A

Table 2.I.6: Sample depth variation study of DMA·HCl by ^{1}H qNMR

2.I.3.5: Robustness:

Method robustness was determined by analyzing the same sample at normal operating conditions and also by changing following operating analytical parameters of instrument like mode of shimming Table 2.I.7, pulse length Table 2.I.8 sweep width Table 2.I.9, offset Table 2.I.10, spinning rate Table 2.I.11, phase correction mode Table 2.I.12 and sample temperature variation Table 2.I.13. By changing only one operating parameter at a time while keeping all the other parameters fixed and using the same sample showed either no change and in some cases very close to the results obtained with normal instrumental conditions. Hence the robustness of the proposed method is established.

Sr. No.	Mode of shimming	W_x	Difference
1	Top Shim	0.35	N/A
2	Non shimming	0.35	0.00
3	Manual Shimming	0.35	0.00
4	Auto shim	0.35	0.00
5	Simplex Shim	0.35	0.00

Table 2.I.7: Mode of shimming variation of DMA·HCl by ^{1}H qNMR

Sr. No.	Pulse length (μs)	W_x	Difference
1	1.094	0.35	0.00
2	2.188	0.35	0.00
3	3.283	0.35	0.00
4	4.924	0.35	0.00
5	6.566	0.35	0.00
6	8.208	0.35	0.00
7	9.850	0.35	N/A

Table 2.I.8: Pulse length variation of DMA·HCl by ^{1}H qNMR

Sr. No.	Sweep width (ppm)	W_x	Difference
1	12	0.35	0.00
2	16	0.35	0.00
3	18	0.35	N/A
4	20	0.35	0.00
5	22	0.35	0.00
6	25	0.35	0.00

Table 2.I.9: Sweep width variation of DMA·HCl by ^{1}H qNMR

Sr. No.	Offset (ppm)	W_x	Difference
1	3.0	0.35	0.00
2	4.0	0.34	+0.01
3	5.0	0.35	0.00
4	7 .0	0.35	N/A
5	8.0	0.35	0.00
6	9.0	0.35	0.00

Table 2.I.10: Offset variation of DMA·HCl by ^{1}H qNMR

Sr. No.	Spinning rate	W_x	Difference
1	0 (non spin)	0.35	0.00
2	8	0.35	0.00
3	12	0.35	0.00
4	16	0.35	0.00
5	20	0.35	0.00
6	24	0.35	0.00
7	28	0.35	0.00
8	32	0.35	N/A

Table 2.I.11: Spinning rate variation of DMA·HCl by ^{1}H qNMR

Sr. No.	Mode of phase	W_x	Difference
1	abs	0.35	0.00
2	apk	0.35	0.00
3	manual phase	0.35	N/A

Table 2.I.12: Mode of phase correction of DMA·HCl by ^{1}H qNMR

Sr. No.	Sample temperature in	W_x	Difference
1	275	0.35	0.00
2	285	0.35	0.00
3	295	0.35	N/A
4	305	0.35	0.00
5	310	0.35	0.00
6	320	0.34	-0.01

Table 2.I.13: Temperature variation of DMA·HCl by ^{1}H qNMR

2.I.3.6: Solution stability:

Solution stability was studied upto 4 days (96 h) by ^{1}H qNMR method and the results are presented in Table 2.I.14. The observed results at different time intervals are very close to those at least of the freshly prepared sample. Hence, the solution can be considered stable upto 96 h.

Sr. No.	Time interval	W_x	Difference
1	0	3.25	N/A
2	12	3.24	0.01
3	24	3.23	0.02
4	48	3.24	0.01
5	72	3.22	0.03
6	96	3.21	0.04

Table 2.I.13: Solution stability of DMA·HCl by ^{1}H qNMR analysis

2.I.3.7: Accuracy (recovery):

According to ICH guidelines additional proof of accuracy (recovery) study was performed with three replicate determinations with solutions of three different concentrations of DMA·HCl in IS solution in presence of Metrformin·HCl API containing 200 ppm, 400 ppm and 600 ppm of DMA·HCl corresponding to 50 %,

100 % and 150 % of the analytical concentrations respectively. The observed results of concentration variation study are given in Table 2.I.15, 2.I.16 and 2.I.17, which show accuracies of 101.5 %, 107.9 % and 111.7 % for the concentrations 50 %, 100 % and 150 % respectively, with an average % RSD value 0.72, 2.51 and 0.80 respectively. The results of the present ^{1}H qNMR method are within acceptable limit of accuracy i.e. 80 % to 120 % and % RSD not more than 10.

Sr. No.	I_x	W_x	% recovery	Mean (%)	% RSD
1	215.00	1.95	100.82	101.5	0.72%
2	217.33	1.97	101.91		
3	217.00	1.97	101.74		

Table 2.I.15: Recovery at 50% level of DMA·HCl by ^{1}H qNMR

Sr. No.	I_x	W_x	% recovery	Mean (%)	% RSD
1	420.67	3.81	109.37	107.9	2.51%
2	420.67	3.81	109.37		
3	404.33	3.66	105.02		

Table 2.I.16: Recovery at 100% level of DMA·HCl by ^{1}H qNMR

Sr. No.	I_x	W_x	% recovery	Mean (%)	% RSD
1	618.00	5.60	110.80	111.7	0.80%
2	627.33	5.68	112.50		
3	623.33	5.64	111.77		

Table 2.I.17: Recovery at 150% level of DMA·HCl by ^{1}H qNMR

2.I.3.8: Derivatization HPLC method:

Derivatization and chromatographic run were carried out as per the procedures given in the experimental section. The chromatogram of blank solution was obtained with run time of 20 min as shown in Fig 2.I.4. The peaks eluted at approximate retention time of 6.0, 9.0, 12.0, 13.0 and 14.0 min are due to derivatized solutions, where as the peak with retention time of 7.4 min is due to DMA (Fig 2.I.5). The DMA content was determined from the Equation (2-4) given below.

$$DMA\ content = \frac{R_t - R_o}{R_s - R_o} \times \frac{C_s}{C_t} \times \frac{45.05}{81.55} \times P \qquad (2\text{-}4)$$

where, R_t, R_s and R_o = detector response for DMA in sample solution, standard solution and blank solution respectively, C_s = concentration(in ppm) of DMA·HCl in standard solution, C_t = concentration (in ppm) of sample solution, P = Potency of dimethyl amine hydrochloride, 45.05 and 81.55 are molecular weight of DMA and DMA·HCl respectively.

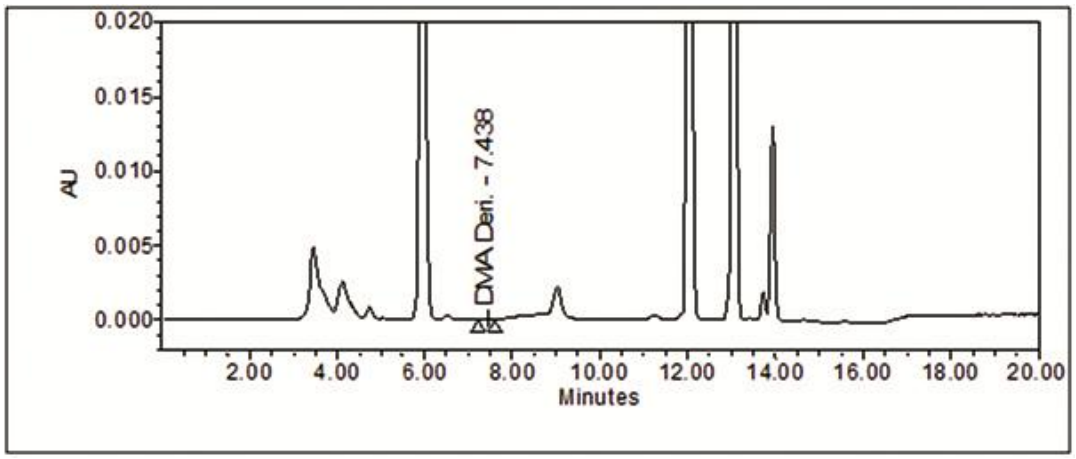

Figure 2.I.4: Blank Chromatogram of HPLC derivatization method

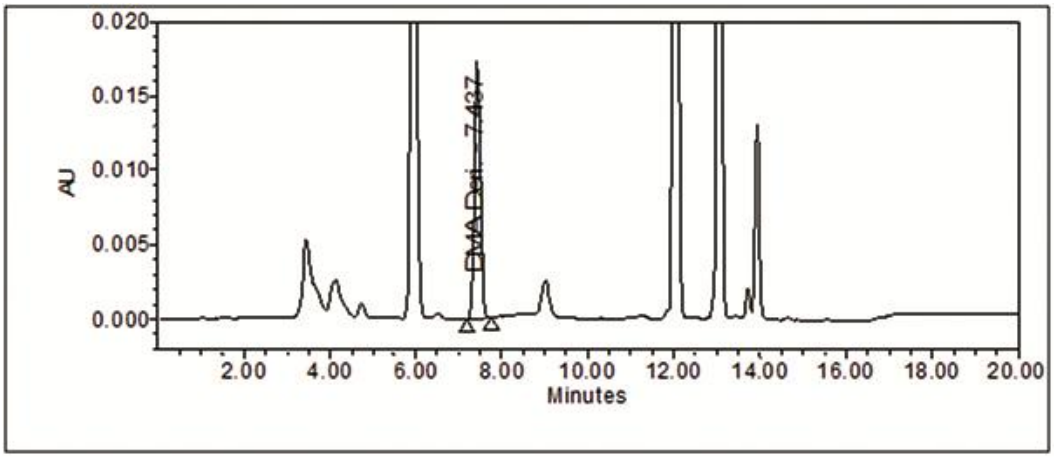

Figure 2.I.5: Typical Chromatogram of DMA·HCl by HPLC derivatization method

2.I.3.9: Linearity:

The linearity of detector response for dimethylamine was determined by using proposed derivatised HPLC method by preparing and injecting solutions of different concentrations as given in Table 2.I.18.

Set No.	Vol. of stock solution-B (µL)	Final dilution (mL)	Dimethyamine concentration (µg/mL)
1	1500	10	0.7499
2	1000	10	0.4999
3	500	10	0.2500
4	250	10	0.1250
5	125	10	0.0625
Dilution made from stock solution-C			
6	600	10	0.0300
7	300	10	0.0150
8	150	10	0.0075

Table 2.I.18: Dilution of stock solution for HPLC linearity study

20 µL of each of the above solutions were injected into the chromatographic system. Linearity was established by triplicate analysis of standard solution of DMA·HCl. The observed mean area counts calculated are given in Table 2.I.18. The peak areas are plotted against the corresponding concentration to generate calibration curve (Fig 2.I.6.) Good linearity has evident (r^2 = 0.9999) over the examined concentration range of 0.015 ppm to 0.75 ppm with equation y = 307998.47x ± 266.34.

Concentration of Dimethylamine (µg/mL)	Detector response (area counts)					Limit
	Inj. 1	Inj. 2	Inj. 3	Mean	Corrected	
0.7499	231016	231274	231769	231353	230917	
0.4999	153422	153362	152751	153178	152742	
0.2500	78404	78457	77131	77997	77561	
0.1250	40181	39775	40079	40012	39576	
0.0625	18769	18718	18815	18767	18331	
0.0300	9203	9295	9260	9253	8817	
0.0150 (LOQ)	3715	4050	4147	3971	3535	
0.0075 (LOD)	2536	2605	2906	2682	2246	
Blank	340	451	517	436	0	
Slope					307998.47	
Intercept					-266.34	
Coefficient of correlation (r^2)					0.99995	NLT 0.99

Table 2.I.19: Linearity data of DMA·HCl by HPLC method

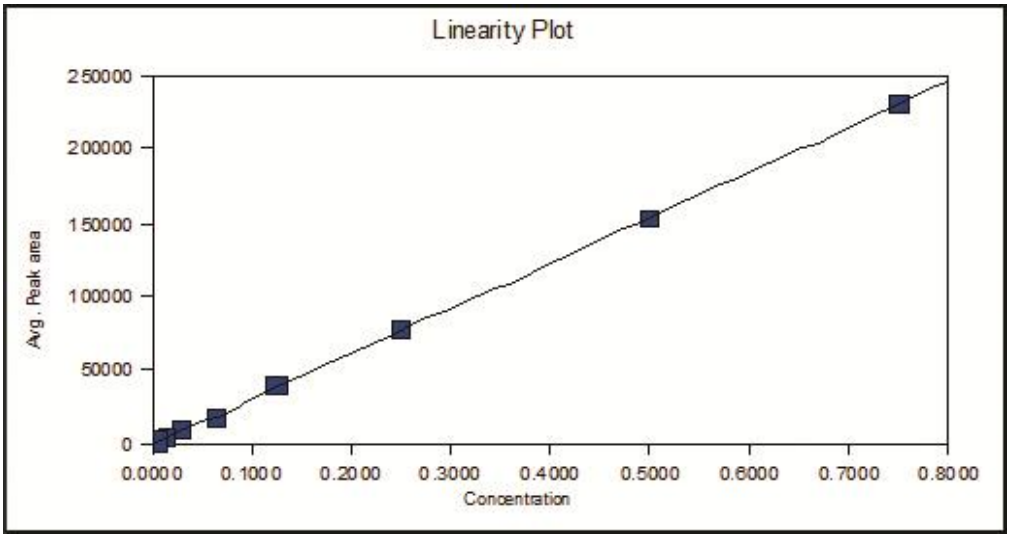

Figure 2.I.6: Linearity plot of DMA·HCl by HPLC method

2.I.3.10: Method precision:

The precision of the method, checked as the repeatability was determined by calculating the relative standard deviation (% RSD) of the peak areas of DMA·HCl for six determinations presented in Table 2.I.20 and observed on the same day and under the same experimental conditions. The calculated % RSD of DMA·HCl peak area obtained by the present HPLC method is 0.99 which is within the acceptable limit of not more than 2%.

Sample No.	Observed results of Dimethylamine (%)	Limit
1	0.0503	
2	0.0505	
3	0.0515	
4	0.0511	
5	0.0504	
6	0.0503	
Mean	0.0507	
SD	0.0005	
% RSD	0.99	NMT 2 %

Table 2.I.20: Precision of DMA·HCl content by HPLC method

2.I.3.11: Accuracy (recovery study):

Recovery study of the developed HPLC derivatization method was performed with three replicate determinations at three different levels of concentrations *viz* 50 %, 100 % and 150 % respectively and the results obtained are given in Table 2.I.21. When compared to the nominal values, the average recovery results of triplicate analysis was 100.61 %, 101.52 % and 100.12 % for the concentrations 50 %, 100 % and 150 % respectively with an average % RSD value 0.20, 0.27 and 0.53. The results of the method are within acceptable limit of accuracy of 80 % to 120 % and % RSD not more than 10.

Level	Percentage of recovery	Mean percentage of recovery	% RSD
50%	100.40	100.61	0.20
	100.81		
	100.61		
100%	101.38	101.52	0.27
	101.39		
	101.83		
150%	100.05	100.12	0.53
	100.68		
	99.63		

Table 2.I.21: Recovery of DMA·HCl by HPLC method

2.I.3.12: Limit of Detection and Limit of Quantification (LOD and LOQ):

Limit of detection is the lowest concentration of the component, where detector response is detected and limit of quantification is the lowest concentration of the component where the % RSD of three replicate injections is not more than 10 %. For determination of LOD and LOQ by derivatization HPLC method, the stock solutions A and B were sequentially diluted to give the final concentrations as mentioned in Table 2.I.22.

Sr. No.	Volume of stock solution-B (µL)	Final dilution (mL)	Concentration (µg/mL)
1	250	10	0.1250
2	125	10	0.0625
Dilution made from stock solution-C			
3	600	10	0.0300
4	300	10	0.0150
5	150	10	0.0075
6	75	10	0.0037

Table 2.I.22: Dilution of stock solution for LOD and LOQ by HPLC method

20 µL of each of the above solutions was injected in triplicate into chromatographic system and the observed mean area counts are given in Table 2.I.23 and % RSD was calculated at each concentration level. The calculated values of LOD and LOQ are 0.0037 µg/mL and 0.0075µg/mL respectively (Table 2.I.24).

Sr. No.	Conc. of Dimethylamine (µg/mL)	Detector response (area counts)					
		Inj-1	Inj-2	Inj-3	Mean	Corrected area	% RSD
1	0.1250	40181	39775	40079	40012	39576	0.53
2	0.0625	18769	18718	18815	18767	18331	0.26
3	0.0300	9203	9295	9260	9253	8817	0.50
4	0.0150	3715	4050	4147	3971	3535	5.71
5	0.0075	2536	2605	2906	2682	2246	7.34
6	0.0037	1042	1168	921	1044	608	11.83
7	Blank	340	451	517	436	0	20.52

Table 2.I.23: Results of LOD and LOQ by HPLC method

Component	Limit of Detection (LOD)		Limit of Quantification	
	Absolute (µg/mL)	w.r.t. sample conc. (%)	Absolute (µg/mL)	w.r.t. sample conc. (%)
Dimethylamine	0.0037	0.00037	0.0075	0.00075

Table 2.I.24: Summary of LOD and LOQ by HPLC method

2.I.3.13: Solution stability in derivatization HPLC method:

Standard preparation

The solution stability of derivatization HPLC method was checked upto 42 h with standard stock solution (Table 2.I.25) and the observed results at different time intervals are very close to that of the freshly prepared sample without any significant change in dimethylamine peak. Hence the solution can be considered stable upto 42 h.

Sr. No.	Time (h)	Mean area counts	% deviation	Limit
1	Initial	168150	0.00	NMT $\pm$ 10.0%
2	7	171047	1.72	
3	28	172052	2.32	
4	42	174955	4.05	

Table 2.I.25: Solution stability data of HPLC method

2.I.3.14: Comparison data of both techniques:

The validation and performance characteristics of quantification of DMA·HCl obtained by ^{1}H qNMR were also compared with derivatization HPLC technique (Table 2.I.26). The results of HPLC method are not much different from those of ^{1}H qNMR method.

Sr. No.	Study parameter	^{1}H q-NMR	HPLC
1	Correlation coefficient (r^2)	0.9991	0.9999
2	Slope	0.7524	307998.47
3	Intercept	0.8303	-266.34
4	Limit of Detection (LOD)	4 ppm	0.0037 ppm
5	Limit of Quantification (LOQ)	11 ppm	0.0075 ppm

Table 2.I.26: Performance characteristics of ^{1}H qNMR and HPLC method

Comparison with GC method

N,N-Dimethylamine (DMA) is a secondary amine basic in nature with highly available of loan pair of electrons due to presence of dimethyl group, hence it interacts with the stationary phase of non-polar GC column which causes peak broadening, affecting the sensitivity. The conversion of DMA·HCl to DMA which is volatile in nature in presence of base for GC analysis can be considered but it degrades the active pharmaceutical ingredient MF·HCl which also generates DMA. So it is very difficult to quantify the DMA·HCl content in MF·HCl matrix by using GC technique as it shows much higher percentage of recovery than expected. Also quantification by GC is laborious and time consuming which can be overcome by the proposed ^{1}H qNMR and derivatization HPLC techniques.

Significant advancement of HPLC and ^{1}H qNMR method

The proposed new derivatization HPLC method for DMA·HCl quantification in MF·HCl active pharmaceutical ingredient is very simple involving in-situ heating at 60°C for 30 min with FDNB. There is no specific instrumental requirement, nor any special reagents and catalyst. It is very specific method because all the related impurities generated during the derivatization process along with MF·HCl get well resolved by these methods. This method is highly sensitive because the derivatization product generated with DMA·HCl is UV active due to presence of two nitro groups (auxochromic) at *ortho* and *para* position with the conjugated system.

2.I.3.15: Commercial sample analysis:

In order to test the suitability of the method in industry three commercial samples were analyzed. Accurately weighed 100 mg MF·HCl was transferred to 10 mL volumetric flask and diluted with IS solution. Exactly 1 mL of the solution was taken in a 5 mm NMR tube and scanned 16 times, the acquired data was processed as per the proposed NMR method.

Similarly, 10 mg of MF·HCl sample was accurately weighed and transferred to a 10 mL volumetric flask, 5 mL of HPLC grade acetonitrile was added and the solution was sonicated for 5 min. Exactly 100 µL of triethylamine and 1 mL of 1-fluoro-2-4-dinitro benzene (FDNB) solutions were added for derivatization process. The solution mixture was mixed well and heated at 60°C for 30 min and cooled to

achieve room temperature and made up the volume with acetonitrile. This solution was then centrifuged at 3000 rpm for 5 min in order to completely derivatize all DMA·HCl solvent present in MF·HCl .

Samples from three different production batches (two batches, S-1 and S-2 form Sun Pharmaceutical Industries Limited, Vadodara, India, and one batch, W-1 from Wanbury Limited, Hyderabad, India) of MF·HCl were analyzed for the estimation of DMA·HCl by the proposed derivatization HPLC and ^{1}H qNMR methods and the observed results are given in Table 2.I.27. The results show that both the methods are equivalent. Among the two, NMR method is more simple and quicker than HPLC method which can be easily adapted for the estimation of organic residual solvent DMA·HCl in MF·HCl for quality control and in-process.

Sample No.	Batch No.	^{1}H qNMR (ppm)	HPLC method (ppm)
1	S-1	72	65
2	S-2	24	19
3	W-1	60	52

Table 2.I.27: Analysis results of commercial samples of DMA·HCl content in MF·HCl by ^{1}H qNMR and HPLC method

Conclusion

The ^{1}H qNMR method developed for the quantification of DMA·HCl in Metformin here in proved to be rapid as well as easy to perform. The method satisfies various performance criteria such as linearity, precision and accuracy. It offers an attractive choice over previously described procedures and can be used for in-process, routine quality control for API and formulation analysis of Metformin hydrochloride tablets. Analysis can be carried out on any modern NMR equipment operating at a field of 400 MHz or more, equipped with suitable software for processing of data as per the protocol developed. Assay results obtained by ^{1}H qNMR have been confirmed by comparing them with a newly developed derivatization HPLC method, which has also been validated.

^{1}H qNMR method has a high potential in analysis of pharmaceutical products due to the simplicity, reliability, simultaneous identification and quantification, and the fact that there is no need of reference compound.

Section II

Quantification of Sitagliptin phosphate by ^{1}H qNMR

2.II.1:Drug:

Sitagliptin phosphate [(2*R*)-1-(2,4,5-trifluorophenyl)-4-oxo-4-[3-(trifluoro ethyl)-5,6-dihydro[1,2,4]triazolo[4,3-a]pyrazin-7(8*H*)-yl]butan-2 amine is a relatively new oral antihyperglycemic drug used to treat type II diabetes. Sitagliptin competitively inhibits dipeptydyl peptidase IV (DPPIV), an enzyme involved in the breakdown of incretins, such as Glucagon like particle-I [GLP-I] which potentiates insulin secretion in vivo. Inhibition of DPPIV reduces the breakdown of GLP-I and increases insulin secretion, which suppresses the release of glucagon from pancreas and drives down blood sugar levels.[53-55]

This section describes the development of a rapid, accurate, specific and simple method for the assay of Sitagliptin, based on the application of ^{1}H qNMR spectroscopy. The method involves addition of an internal standard to the sample and subsequent dilution with D_2O. The appropriate analytical peaks are integrated after the ^{1}H NMR spectrum has been recorded and the amount of Sitagliptin phosphate calculated.

2.II.2: Experimental:

2.II.2.1: Materials and reagents:

High purity analytical and ICH grade substances were used throughout the study. Sitagliptin phosphate was provided by Sun Pharmaceuticals Industries Ltd. India. Maleic acid (> 99 %) and Deuterium oxide (99.96 % D) was purchased from Merck, Germany. Januvia and Instavel tablets of 100 mg label claim, of Sitagliptin phosphate manufactured by Merck, were purchased from local market.

2.II.2.2: Instrumentation:

Bruker Biospin AV-III 500 FT-NMR spectrometer operating at frequency 500.13 MHz (11.74 Tesla) for protons, equipped with a 5 mm multinuclear Broad Band Observed (BBO) probe head, yielding a 90° proton pulse length of 9.85 µs, with software Topspin 2.1 was used. The relaxation delay along with acquisition time was 30 s and all weighing were performed on a Mettler Toledo analytical (Model-XS205) and micro (Model-UMX2) balance.

2.II.2.3: Preparation of standard and test solution:

Stock solution of maleic acid IS (5.00 mg /0.6 mL)

Accurately weighed 416.83 mg of maleic acid was transferred into 50 mL volumetric flask. About 10 mL of D_2O was added, and made up to the mark with the same diluent and mixed well.

Standard preparation

Accurately weighed 9.34 mg of Sitagliptin phosphate drug standard was transferred to a glass tube and 0.6 mL of stock solution of maleic acid IS was added. Solution was thoroughly mixed till complete dissolution.

Sitagliptin phosphate standard preparation for specificity

Accurately weighed 9.85 mg Sitagliptin phosphate standard was transferred to a glass tube and 0.6 mL of D_2O was added. Solution was thoroughly mixed till complete dissolution.

Maleic acid (IS) preparation for specificity

0.6 mL of stock solution of maleic acid IS was used directly.

Placebo solution preparation for specificity

Placebo (30 mg of excipients without drug) was accurately weighed and transferred to glass tube and 0.6 mL of D_2O was added. Solution was thoroughly mixed till complete dissolution and supernatant liquid was taken for analysis.

Standard preparation for robustness study (IS variation: 5.0 ± 2 mg)

10.36 mg and 10.34 mg of Sitagliptin phosphate drug standard was accurately weighed and transferred into two different glass tubes and 3.63 mg and 6.25 mg of maleic acid IS was added to both tubes respectively. Then 0.6 mL of D_2O was added. Solutions were thoroughly mixed till complete dissolution.

2.II.2.4: Sample preparation (tablets):

Ten tablets of 100 mg strength Januvia were weighed, crushed and thoroughly ground to fine powder. Portion equivalent to 10 mg Sitagliptin phosphate drug was weighed accurately and transferred into a stopper tube. Then 0.6 mL of stock solution of maleic acid IS was added. Solution was thoroughly mixed till complete dissolution and supernatant liquid was taken for analysis.

Sample preparation for robustness study (IS variation: 5.0 ± 2 mg)

Accurately weighed 39.83 mg and 40.42 mg ground sample (equivalent to 10.00 mg Sitagliptin phosphate drug) were transferred into two different glass tubes and 3.53 mg and 6.54 mg of maleic acid IS were added to the tubes respectively. Then 0.6 mL each of D_2O was added to the tubes. Solutions were thoroughly mixed till complete dissolution and supernatant liquid from each tube was taken for analysis.

2.II.2.5: ^{1}H qNMR method:

Determination of relaxation time (T_1)

For accurate quantification, proper value of relaxation delay is very important. The relaxation delay depends on the longest longitudinal relaxation time T_1 of all signals of interest and was calculated by inversion recovery experiments. The present method was developed in D_2O due to very good solubility of the drug in D_2O and therefore T_1 value in this solvent has been considered. The longest relaxation time 5.23 s was found for the maleic acid IS and 2.32 s for the proton of interest of drug. A delay of five T_1's means 30 s delay time between pulses was enough to fully ensure T_1 relaxation of all protons.

^{1}H qNMR spectra of the authentic drug and tablet samples were recorded (Bruker Biospin AV-III 500 MHz). Typically, 16 scans were collected for each sample

into 32,768 data points using a 90 degree pulse length; spectral width 10,000 Hz, digital resolution 0.305176 Hz/points; pre-acquisition delay 9.85 µs and acquisition time 8.36 m. A delay time of 30 s between pulses was used to fully ensure T_1 relaxation of protons.

The FIDs were apodized with 0.5 Hz exponential line broadening function before Fourier transformation. Manual two parameter phase correction was used to obtain high quality absorption line shape followed by baseline correction. This manual mode was also used for the signal integration. Chemical shifts were referenced internally to residual water signal (HOD) obtained at δ = 4.67 ppm.

The ^{1}H qNMR experiments were performed for the standard preparation in replicate (n = 6) and sample preparations were done in triplicate. The ^{1}H qNMR spectra were recorded under the above experimental conditions and with given scanning parameters. The analyte ^{1}H signals from aromatic ring (multiplet due to ^{19}F) were observed at 6.9 ppm and 7.2 ppm with respect to ^{1}H signal (singlet) of maleic acid IS at 6.25 ppm and integrated for quantification.

^{1}H qNMR assay and purity calculations

For purity determination of the substance, an internal standard with known purity is needed which is soluble in the solvent used and which does not interfere with the analyte. The analyte weight as well as assay can be calculated by using the Equation (2-5) and (2-6) respectively.

$$W_x = \frac{I_x}{I_{std}} \times \frac{N_{std}}{N_x} \times \frac{M_x}{M_{std}} \times W_{std} \qquad (2\text{-}5)$$

$$P_x = \frac{I_x}{I_{std}} \times \frac{N_{std}}{N_x} \times \frac{M_x}{M_{std}} \times \frac{W_{std}}{W} \times P_{std} \qquad (2\text{-}6)$$

where, W_x = Weight of the Sitagliptin phosphate drug (mg)

P_x = Assay of the Sitagliptin phosphate (in % w/w) on as is basis

I_x = Mean integral value of the analyte ^{1}H signal obtained at 6.96 ppm

I_{std} = Integral value of the ^{1}H signal of maleic acid IS obtained at 6.25 ppm

N_{std} = Number of protons for the maleic acid IS (2.0)

N_x = Number of protons for the analyte ^{1}H in drug (1.0)

M_x = Molar mass of the Sitagliptin phosphate drug (505.31 g / mole)

M_{std} = Molar mass of the maleic acid IS (116.07 g / mole)

W_{std} = Weight of the maleic acid IS (mg)

W = Taken weight of the analyte drug (mg)

P_{std} = Potency of the maleic acid IS (99.3 %)

2.II.3: Results and discussion:

2.II.3.1: NMR experiments for confirmation of structure and characterization:

The structure of Sitagliptin phosphate (analyte drug) and maleic acid (IS) is shown in following Figure 2.II.1. The ^{1}H NMR, ^{13}C NMR and DEPT experiments in D_2O were performed for confirmation of structure of Sitagliptin phosphate drug. The signals due to exchangeable protons present in -NH_2 moiety and H_3PO_4 present in Sitagliptin phosphate disappeared when analysis was performed in D_2O solvent. ^{1}H NMR spectra was also recorded by using DMSO-d_6 solvent for correct structure assignment of all protons (Fig. 2.II.2), but for NMR quantification D_2O was used as it was found to be most suited solvent. The ^{1}H NMR of maleic acid used as an IS was also recorded in D_2O for confirmation of its structure.

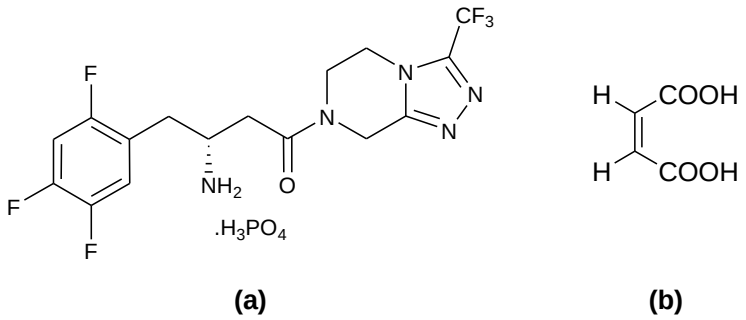

Figure 2.II.1: Structure of (a) Sitagliptin phosphate and (b) Maleic acid

2.II.3.2: Characterization of Sitagliptin phosphate:

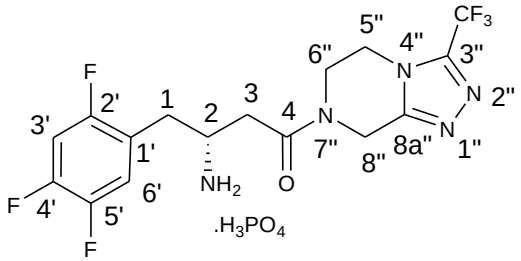

Figure 2.II.2: Structure of Sitagliptin phosphate and it's numbering

Chemical Name: *7-[(3R)-3-Amino-1-oxo-4-(2,4,5-trifluorophenyl)butyl]-5,6,7,8-tetrahydro-3-(trifluoromethyl)-1,2,4-triazolo[4,3-a]pyrazine phosphate*

Molecular Formula = $C_{16}H_{18}F_6N_5O_5P$

Molecular Weight = 505.31

^{1}H NMR (D_2O, 500.13 MHz): δ 7.22-7.11 (m, 1H), 7.09-6.97 (m, 1H), 4.93-4.76 (dd, 2H), 4.28-4.08 (m, 2H), 4.02-3.83 (m, 3H), 3.08-2.72 (m, 4H).

^{13}C NMR (D_2O, 125.7 MHz): δ 170.30 (s), 157.55 (s), 152.00 (s), 150.40 (s), 147.70 (s), 145.00 (s), 120.40 (s), 118.90 (s), 119.80 (d), 107.00 (d), 49.50 (d), 44.50 (t), 42.70 (t), 39.60 (t), 35.00 (t), 32.20 (t).

^{19}F NMR (D_2O, 470.6 MHz): δ -140.91 to -140.27 (ddd), -132.18 to -132.06 (dt), -116.37 to -116.13 (ddd), -61.00 (d).

OR used $\underline{C}H_3$, $\underline{C}H_2$, $\underline{C}H$ and $\underline{C}_q$ for quaternary carbon

MS (ESI): *m/z*- 408.22 (100%) ($[M+1]^+$)

Elemental analysis data: $C_{16}H_{18}F_3N_5O$: **Calcd.(Found)** C 38.03 % (38.06%), H 3.59%(3.38%); N 13.86%(13.79%)

IR (KBr): 3327, 3049-2926, 1636 cm^{-1}

No.	δ in ppm	Multiplicity	No. of fluorines	'*J*' in Hz	Assignment of Fluorine (s)
1.	-61.00	d	3	5.42 Hz	$-CF_3$
2.	-116.13 to -116.37	ddd	1	70.79,15.5, 4.10	4'
3.	-132.06 to -132.18	dt	1	21.78, 5.44	2'
4.	-140.27 to -140.91	ddd	1	51.18, 15.06,14.95	5'
			6		
Remark	Calibration with external reference standard TFT (-62.6ppm)				

Table 2.II.1: ^{19}F NMR spectral assignments of Sitagliptin phosphate

The spectral interpretation from its chemical shift (δ) in ppm of ^{1}H NMR (Fig. 2.II.3),^{13}C NMR along with DEPT-135 (Fig. 2.II.5) and ^{19}F NMR (Fig. 2.II.6) along with other spectroscopic data such as FT-IR, MS (ESI) and elemental analysis results complies with the structure of Sitagliptin phosphate. Similarly ^{1}H NMR (Fig.2.II.4) spectrum of maleic acid (IS) also conforms to the structure.

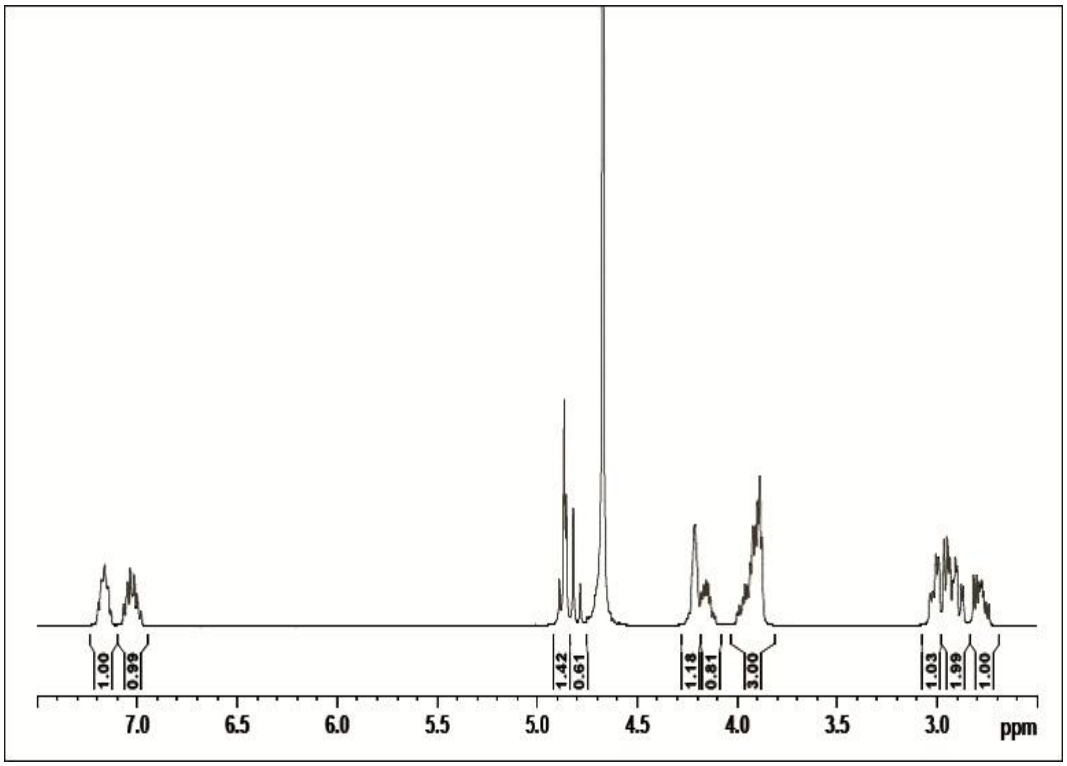

Figure 2.II.3: ^{1}H NMR spectrum of Sitagliptin phosphate in D_2O

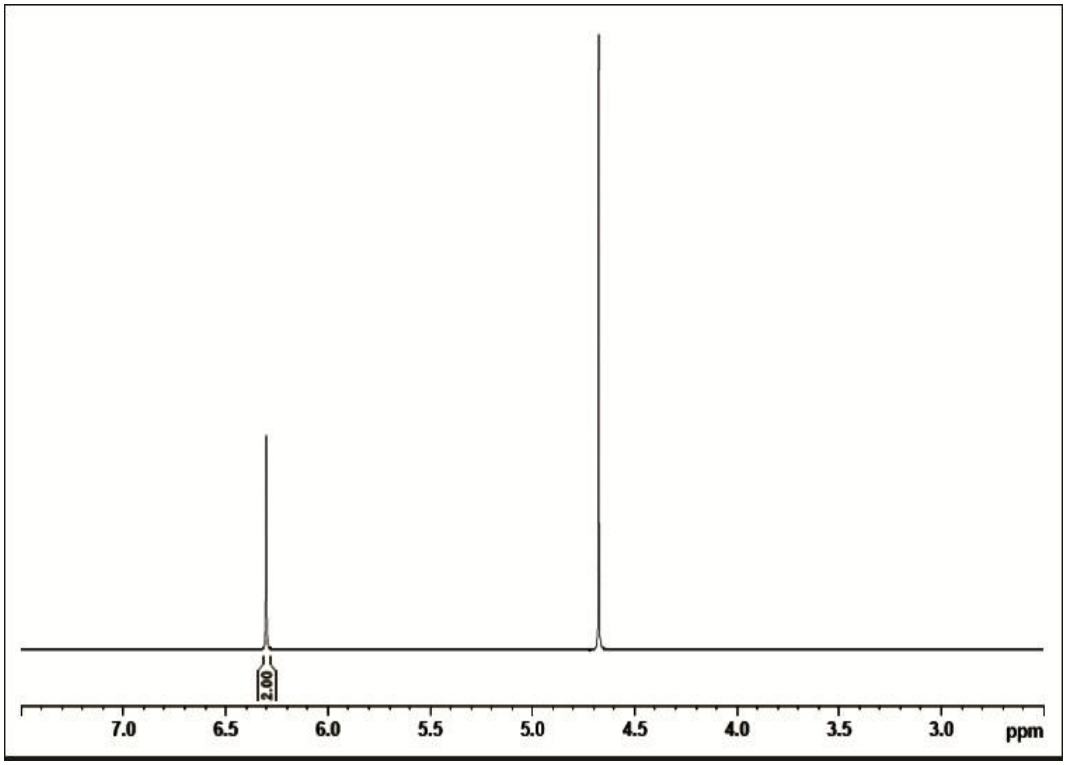

Figure 2.II.4: ^{1}H NMR spectrum of maleic acid as IS in D_2O

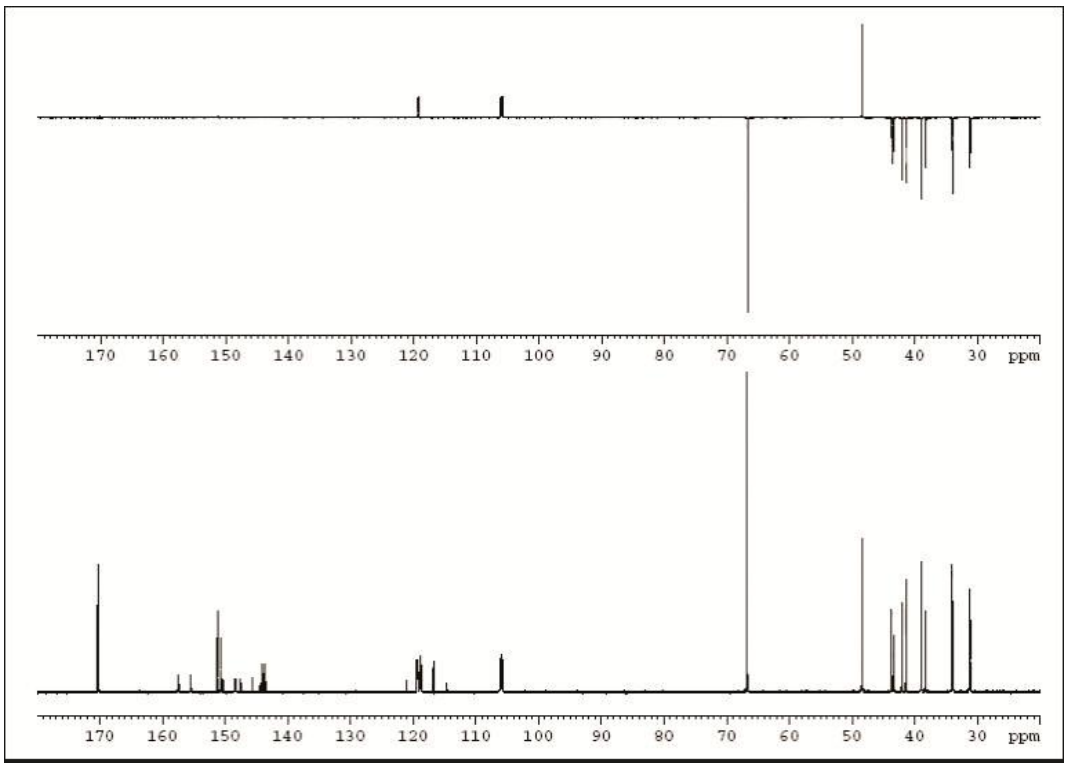

Figure 2.II.5: Proton decoupled ^{13}C-NMR with DEPT-135 of Sitagliptin phosphate

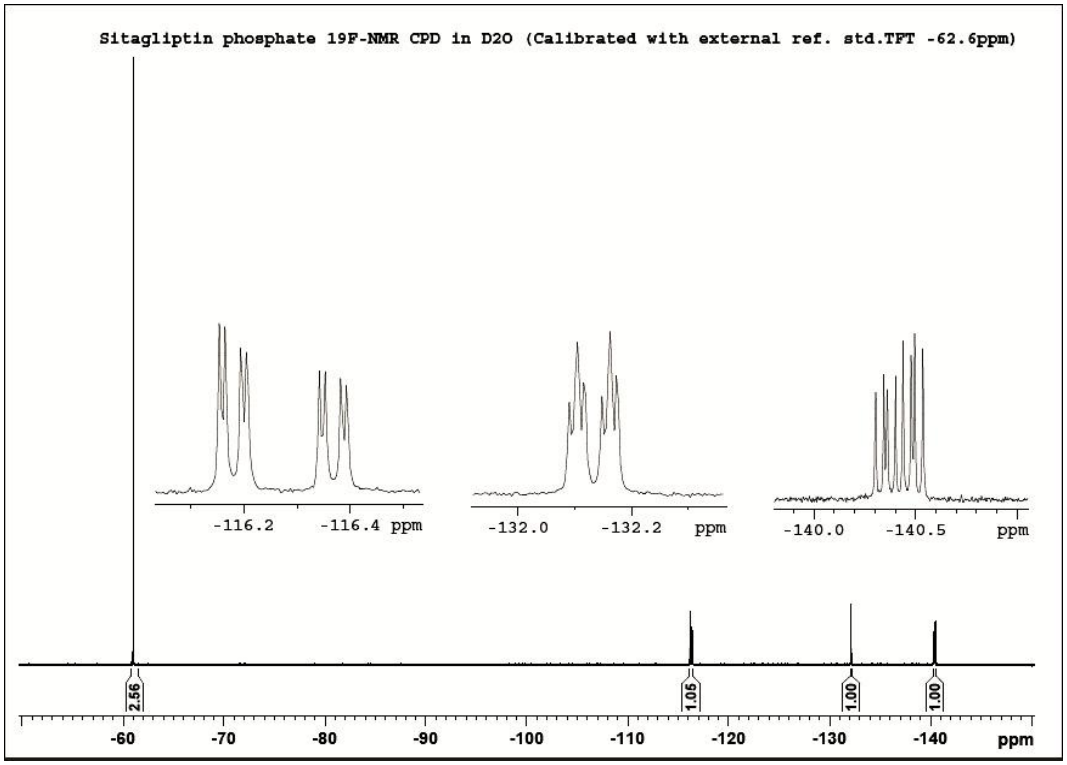

Figure 2.II.6: Proton decoupled ^{19}F NMR of Sitagliptin phosphate in D_2O

2.II.3.3: Quantitative NMR method:

The signal intensity of a known amount of IS was compared to the area of the peaks originating from the analyte. In the current study, the IS chosen is maleic acid, since it provides a well-separated signal without any interference from analyte drug signal in the integration region. Of all the common internal standards used in our laboratory, this was the most suitable with respect to both solubility and the chemical shifts of two ethylenic protons compared to the drug and placebo in the samples. The singlet of maleic acid chosen for quantification was assigned a value of 2.00 in each NMR spectrum. For Sitagliptin phosphate, the multiplet at 6.91 ppm, originating from one proton of the aromatic ring was used, since this signal appears well separated from other signals. The ^{1}H NMR spectra of both the sample and the standard in D_2O show a well-separated singlet of each analyte proton and the IS (Figure 2.II.7).

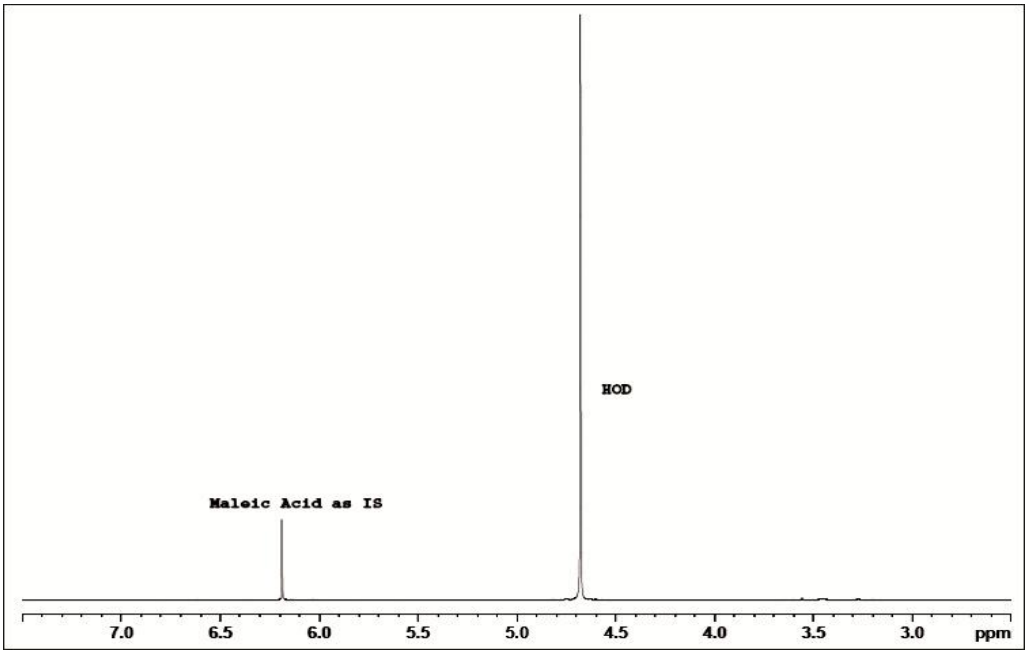

Figure 2.II.7: ^{1}H NMR spectra of placebo with Maleic acid as IS in D_2O

2. II.3.4: ^{1}H qNMR method validation:

The method was validated as per International Conference on Harmonization (ICH) Guidelines[39a] for following parameters like system suitability, specificity and selectivity, linearity, precision and intermediate precision, LOD and LOQ, range, accuracy and robustness.

System suitability

System suitability test is performed to show that the control measures have been complied for a particular analysis on a particular day. In the present study, system suitability test was performed for every parameter by replicate acquisition of standard mixture sample of analyte and IS. The system suitability test data confirms the compliance as per the acceptance criteria of % relative standard deviation (RSD) of the integral value of analyte and IS signal not more than 2.0%. The signal to noise ratio (S/N) of the analyte signal is 407 : 1 and difference between the chemical shift (δ) value of analyte signal with respect to IS was 0.71 ppm.

2.II.3.5: Specificity and selectivity:

The selectivity and specificity of the proposed method was evaluated through possible interference due to the presence of the excipients in the pharmaceutical formulations.

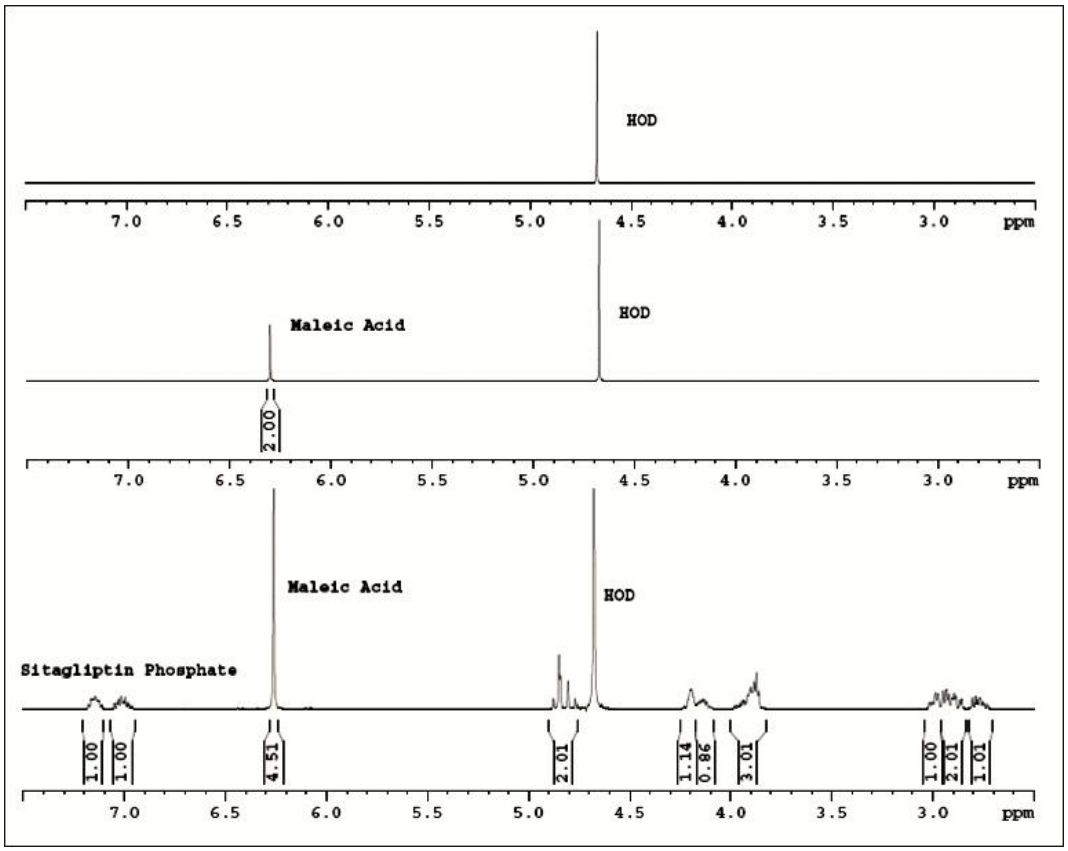

Figure 2.II.8: NMR spectral pattern overlay of Sitagliptin phosphate, Maleic acid and D_2O

Specificity study was performed by analyzing the diluent (D_2O), placebo solution preparation, Sitagliptin phosphate standard preparation, maleic acid IS preparation and sample (tablet) preparation. It was evident that there is no interference at the signals obtained at 7.2 ppm and 6.25 ppm for analyte proton and IS respectively due to diluent and placebo. Also the signals of the analyte protons and IS were well separated from each other in standard and sample preparations (Figure 2.II.8).

2.II.3.6: Linearity:

The linearity of the method was evaluated and established by preparing seven standard solutions of Sitagliptin phosphate having different concentrations ranging from approximately 17 % to 150 %, with respect to the content of analyte in the test

sample. Linearity curve of drug amount taken in mg (x-axis) was plotted against the drug amount found in mg (y-axis) to generate the calibration curve. The linearity Equation y = 0.9752x ± 0.200 was obtained from the data presented in Table 2.II.2 with a correlation coefficient of 0.9992 indicating good linearity as shown in Figure 2.II.9.

Sr. No.	m	I_x	W_x	P_x
1	1.71	4.76	1.67	97.76
2	3.61	9.95	3.50	96.80
3	6.28	17.75	6.24	99.28
4	7.77	22.02	7.74	99.51
5	10.45	29.64	10.42	99.58
6	11.87	34.05	11.97	100.73
7	14.06	39.73	13.97	99.27
8	15.89	44.38	15.60	98.10

Table 2.II.2: Linearity data of Sitagliptin phosphate by ^{1}H qNMR

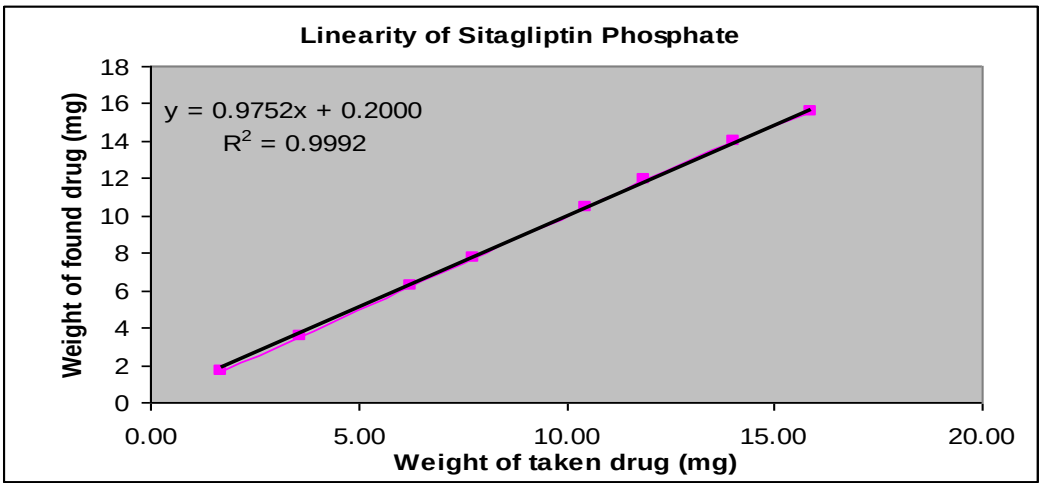

Figure 2.II.9: Linearity curve of Sitagliptin phosphate by ^{1}H qNMR

2.II.3.7: Precision and intermediate precision:

Six different sample preparations were made and analyzed on Bruker Biospin AV-III 500 MHz instrument with a 5 mm multinuclear BBO probe head by a different analyst on a different day with different instrument (400 MHz instead of 500 MHz) using 5 mm BBO-F probe head. The average of six replicates, and % RSD values were shown in Table 2.II.3. The precision and intermediate precision results obtained

due to instrument change and different analyst is presented in Table 2.II.4 and Table 2.II.4 respectively did not show any marked differences, hence the proposed method is precise and within the acceptable limit of not more than 2% deviation.

Sr. No.	m	I_x	W_x	P_x	Mean	% RSD
1	10.12	23.04	10.05	99.18	99.29	0.35
2	9.63	21.86	9.53	98.89		
3	8.81	20.18	8.80	99.79		
4	10.02	22.86	9.97	99.40		
5	10.01	22.73	9.92	98.95		
6	9.69	22.13	9.65	99.52		

Table 2.II.3: Method precision of Sitagliptin phosphate by ^{1}H qNMR

Sr. No.	m	I_x	W_x	P_x	Mean	% RSD
1	10.31	23.50	10.25	99.33	99.21	0.32
2	10.22	23.20	10.12	98.91		
3	10.11	22.95	10.01	98.91		
4	10.09	23.03	10.04	99.43		
5	9.95	22.61	9.86	98.99		
6	9.21	21.07	9.19	99.66		

Table 2.II.4: Intermediate precision of Sitagliptin phosphate by ^{1}H qNMR (Instrument change)

Sr. No	m	I_x	W_x	P_x	Mean	% RSD
1	9.32	21.24	9.26	99.30	99.02	0.61
2	10.07	22.88	9.98	98.98		
3	10.05	22.91	9.99	99.31		
4	10.15	22.99	10.03	98.68		
5	10.32	23.22	10.13	98.03		
6	10.31	23.61	10.30	99.79		

Table 2.II.5: Intermediate precision of Sitagliptin phosphate by ^{1}H qNMR (Different Analyst)

2.II.3.8: LOD and LOQ:

^{1}H NMR signal with Lorentzian lines as response signals, the LOD and LOQ were calculated by using the standard deviation of the response 'σ' and the slope 's' of the calibration curve (Fig.2.II.9) obtained from the linearity results. LOD and LOQ are calculated by using Equation (2-2) and (2-3) respectively and found to be 0.14 mg and 0.44 mg per 0.6 mL of diluent respectively.

2.II.3.9: Solubility range:

The solubility range study was performed by preparing solutions of drug up to saturated concentration in solution. Saturated solution was prepared by adding excess drug amount and analyzing supernatant solution for determining the dissolved concentration of drug. Saturation concentration was found to be approximately ~40 mg per 0.6 mL diluent, which therefore is the upper limit.

2.II.3.10: Accuracy:

The accuracy was performed with nine determinations over three concentration levels covering the specified range from 80 %, 100 % and 120 % levels with respect to the sample quantity label claim. The observed results of concentration variation study are shown in Table 2.II.6, Table 2.II.7 and Table 2.II.8. It is evident from the data that the method for assay content is accurate between the ranges of 80 % to 120 % level and % RSD at each level is 0.46, 0.22 and 0.64 which is well within the acceptable limit of not more than 2 %.

Level	m	I_x	W_x	P_x	Mean	% RSD
80 %	7.31	16.84	7.34	100.35	99.83	0.46
	8.01	18.29	7.98	99.47		
	8.39	19.19	8.37	99.68		

Table 2.II.6: Accuracy at 80% level of Sitagliptin phosphate by ^{1}H qNMR

Level	m	I_x	W_x	P_x	Mean	% RSD
100 %	9.32	21.24	9.26	99.30	99.2	0.22
	10.07	22.88	9.98	98.98		
	10.05	22.91	9.99	99.31		

Table 2.II.7: Accuracy at 100% level of Sitagliptin phosphate by ^{1}H qNMR

Level	m	I_x	W_x	P_x	Mean	% RSD
120 %	12.51	28.86	12.59	100.50	100.25	0.64
	11.78	26.91	11.74	99.52		
	13.42	31.02	13.53	100.71		

Table 2.II.8: Accuracy at 120% level of Sitagliptin phosphate by ^{1}H qNMR

2.II.3.11: Recovery:

The recovery was performed at 50 %, 100 % and 150 % levels within the specified range covered under ICH guidelines with respect to the sample quantity label claim by preparing the solutions in triplicate at each level. The observed results of recovery study are shown in Table 2.II.9, Table 2.II.10 and Table 2.II.11 the % RSD at each level is 0.22, 0.74 and 1.22 which is again well within acceptance limit of not more than 10 %.

Level	m	I_x	W_x	P_x	Mean	% RSD
50 %	5.30	12.29	5.36	101.01	101.07	0.22
	5.11	11.88	5.18	101.32		
	4.69	10.86	4.74	100.89		

Table 2.II.9: Recovery at 50 % level of Sitagliptin phosphate by ^{1}H qNMR

Level	m	I_x	W_x	P_x	Mean	% RSD
100 %	9.64	22.47	9.8	101.55	100.72	0.74
	10.19	23.51	10.25	100.53		
	10.33	23.73	10.35	100.09		

Table 2.II.10: Recovery at 100 % level of Sitagliptin phosphate by ^{1}H qNMR

Level	m	I_x	W_x	P_x	Mean	%RSD
150 %	14.58	33.15	14.46	99.08	99.28	1.22
	15.23	35.16	15.33	100.59		
	15.11	34.05	14.85	98.19		

Table 2.II.11: Recovery at 150 % level of Sitagliptin phosphate by ^{1}H qNMR

2.II.3.12: Stability of analyte in solution:

In this investigation, standard preparation and sample preparation were analyzed at ambient temperature (~25 °C) at 0 h (initial), 24 h, 36 h, 60 h, 90 h and 180 h time intervals and % assay for each interval was calculated. The difference in % assay at different time intervals as given in Table 2.II.12 is very close (less than 1.0 %) to that of the freshly prepared sample. The result shows no major change upto 180 h at ambient temperature, hence the solution can be considered stable at least upto 180 h.

Time interval (h)	m	W_x	P_x	Difference
0	9.66	9.60	99.32	N/A
24	9.66	9.60	99.28	0.04
36	9.66	9.60	99.23	0.09
60	9.66	9.61	99.41	0.09
90	9.66	9.60	99.28	0.04
180	9.66	9.64	99.68	0.36

Table 2.II.12: Solution stability of Sitagliptin phosphate by ^{1}H qNMR

2.II.3.13: Robustness:

The method robustness was determined by varying three parameters independently namely (i) number of scans, (ii) amount of internal standard up to 40 % variation (5.0 mg ± 2.0 mg) and (iii) different analyte proton signal (at δ = 7.2 ppm). The experimental results are given in Table 2.II.13. The results obtained at different number of scans i.e. from 16 to 128 were not much different. Similarly variation of amount of internal standard and a different signal of analyte at δ = 7.2 ppm (rather than δ = 6.9 ppm) also did not appreciably change the measured amount of drug. Therefore, this method is quite robust in terms of the above mentioned parameters.

Parameter	Change	I_x	m	W_x	P_x	Difference
No. of scan	16	22.04	9.66	9.61	99.41	N/A
	32	22.12	9.66	9.65	99.77	0.36
	64	22.15	9.66	9.66	99.91	0.50
	128	22.17	9.66	9.67	100	0.59
Analyte proton at ppm	6.9	22.02	9.66	9.6	99.32	N/A
	7.2	22.07	9.66	9.63	99.55	0.23
IS qty. with std.	5.00916	22.04	9.66	9.61	99.41	N/A
IS quantity with std.	3.63	33.24	10.36	10.51	101.31	1.90
	6.25	19.19	10.24	10.44	100.89	1.39

Table 2.II.13: Robustness study of Sitagliptin phosphate by ^{1}H qNMR

The robustness of the method was further evaluated by analyzing the same sample at normal operating conditions and also by changing following instrumental parameters independently, such as sample depth (Table 2.II.14), mode of shimming (Table 2.II.15), spinning rate (Table 2.II.16), sweep width (Table 2.II.17), offset (Table 2.II.18), pulse length (Table 2.II.19) and temperature in K (Table 2.II.20). The observed results indicate that the sample depth should be more than 6.0 cm, spinning rate less than 24 rps, sweep width not less than 12 ppm and temperature range within 12 °C to 37 °C by changing only one operating parameter at a time while keeping all the other parameters fixed and using the same sample showed either no change and in some cases very close to the results obtained with normal instrumental conditions. Hence the robustness of the proposed method is established.

Parameter	Change	I_x	m	W_x	P_x	Difference
Sample depth	1.5 cm	23.88	10.39	5.46	52.55	-45.50
	3.0 cm	22.64	10.39	9.92	95.35	2.71
	4.5 cm	22.84	10.39	10.00	96.17	1.89
	6.0 cm	23.18	10.39	10.15	97.60	0.46
	7.5 cm	23.29	10.39	10.20	98.06	N/A

Table 2.II.14: Sample depth variation of Sitagliptin phosphate by ^{1}H qNMR

Parameter	Change	I_x	m	W_x	P_x	Difference
Mode of shimming	Non-	23.06	10.39	10.10	97.09	0.51
	Manual	23.01	10.39	10.08	96.88	0.72
	Topshim	23.18	10.39	10.15	97.60	N/A
	Auto	23.14	10.39	10.13	97.43	0.17
	Simplex	23.11	10.39	10.12	97.33	0.27

Table 2.II.15: Shimming variation of Sitagliptin phosphate by ^{1}H qNMR

Parameter	Change	I_x	m	W_x	P_x	Difference
Spinning rate in rps	0	23.18	10.39	10.15	97.60	0.84
	8	23.18	10.39	10.15	97.60	0.84
	12	23.42	10.39	10.26	98.61	-0.17
	16	23.38	10.39	10.24	98.44	N/A
	20	23.50	10.39	10.29	98.94	-0.5
	24	23.18	10.39	10.15	97.63	0.81
	28	22.99	10.39	10.07	96.83	1.61
	32	23.04	10.39	10.09	97.02	1.42

Table 2.II.16: Spinning rate variation of Sitagliptin phosphate by ^{1}H qNMR

Parameter	Change	I_x	m	W_x	P_x	Difference
Sweep width in ppm	12	22.74	10.39	9.96	95.76	1.84
	15	23.10	10.39	10.12	97.29	0.31
	18	23.09	10.39	10.11	97.25	0.35
	20	23.18	10.39	10.15	97.60	N/A
	22	23.16	10.39	10.14	97.53	0.07
	25	23.05	10.39	10.10	97.06	0.54

Table 2.II.17: Sweep width variation of Sitagliptin phosphate by ^{1}H qNMR

Parameter	Change	I_x	m	W_x	P_x	Difference
Offset at ppm	3.5	23.25	10.39	10.18	97.91	-0.31
	5.5	23.11	10.39	10.12	97.33	0.27
	7.5	23.19	10.39	10.15	97.64	-0.04
	8.5	23.18	10.39	10.15	97.60	N/A
	9.5	23.16	10.39	10.14	97.51	0.09

Table 2.II.18: Offset variation of Sitagliptin phosphate by ^{1}H qNMR

Parameter	Change	I_x	m	W_x	P_x	Difference
Pulse length in µs	1.09	23.26	10.39	10.19	97.95	-0.62
	2.18	23.34	10.39	10.22	98.28	-0.95
	3.28	23.20	10.39	10.16	97.68	-0.35
	4.93	22.99	10.39	10.07	96.80	0.53
	6.57	23.10	10.39	10.12	97.26	0.07
	8.20	23.10	10.39	10.12	97.26	0.07
	9.85	23.11	10.39	10.12	97.33	N/A

Table 2.II.19: Pulse length variation of Sitagliptin phosphate by ^{1}H qNMR

Parameter	Change	I_x	m	W_x	P_x	Difference
Temperature in K	275	22.96	10.39	10.06	96.70	1.26
	285	23.35	10.39	10.22	98.31	-0.35
	295	23.26	10.39	10.19	97.96	N/A
	305	23.40	10.39	10.25	98.54	-0.58
	310	23.31	10.39	10.21	98.14	-0.18
	320	23.62	10.39	10.34	99.45	-1.49

Table 2.II.20: Sample temperature variation of Sitagliptin phosphate by ^{1}H qNMR

2.II.3.14: Commercial sample analysis:

In order to test the suitability of the method in industry one API and two solid oral tablets of Sitagliptin phosphate were analyzed. The % assay of the production batch of Sitagliptin phosphate API was determined by the proposed ^{1}H qNMR method and results of this analysis are shown in Table 2.II.21. For comparison HPLC results

based on an in-house method showed good agreement. Similarly, two different batches (Sitagliptin phosphate tablets of 100 mg label claim) such as Januvia (Merck, Germany) and Instavel (Sun Pharma, India) were analyzed by using the proposed ^{1}H qNMR method and the results are compared with that of in house HPLC method which shows very minor difference of less than 2.0 %.

Sr. No.	Sample name	% Assay by HPLC	% Assay by ^{1}H qNMR
1	Sitagliptin phosphate	99.15	99.05
2	Instavel (100 mg tablet)	99.16	99.13
3	Januvia (100 mg tablet)	99.56	100.77

Table 2.II.21: Comparative % assay of Sitagliptin phosphate by HPLC and ^{1}H qNMR

Conclusion

The ^{1}H qNMR method developed for quantification of Sitagliptin phosphate in this study offers an attractive choice over previously described procedures and can be used for routine quality control and stability analysis of Sitagliptin phosphate in different solid dosage forms. For this purpose, any modern NMR equipment operating at a field of 400 MHz or more may be used, provided that the software is suitable for data processing. ^{1}H qNMR technique has a huge potential in analysis of pharmaceutical products like the present one due to its simplicity, reliability, ability for simultaneous identification and quantification, and more importantly there is no requirement to have reference compound of drug.

Assay results obtained by the ^{1}H qNMR were confirmed by comparing it with a new in-house HPLC method for active pharmaceutical ingredient as well as its tablets.

References

1. (a) Rackham, D. M. *Talanta*, **1970**, *17*, 895. (b) Abdel Fattah, S. A.; El-Khateeb, S. Z.; Abdel Razeg, S. A.; Tawakkol, M. S. *Spectrosc. Lett.* **1988**, *21*, 533.
2. Hassan, Y.; Aboul-Enein. *J. Pharm. Pharmacol.* **1979**, *31*, 196.
3. George, M. H.; Lau-Cam, A. C. *Drug Dev. Ind. Pharm.* **1988** , *14*, 43.
4. Abu, J. F.; Noel, A. D.; Roger, D. W. *J. Pharm. Pharmacol.* **1991**, *43*, 860.
5. George, M. H.; Cesar, A. L. *Drug Develop. Ind. Pharm.* **1991**, *17*, 975.
6. Fardella, G.; Barbetti, P.; Chiappini, I.; Grandolini, G. *Int. J. Pharm.* **1995,** *121*, 123.
7. Manira, G.; Kannan, R.; Srinivasan, R.; Gerald, W. S. *Anal. Chem.* **1998**, *70*, 4921.
8. Ozden, T.; Hamide, S.; Inci, A. *J. Pharm. Biomed. Anal.* **1999**, *21*, 467.
9. Goger, N. G.; Parlatan, H. K.; Hasan, B.; Aysel, B.; Tuncel, O. *J. Pharm. Biomed. Anal.* **1999**, *21*, 685.
10. Harris, R. K.; Hodgkinson, P.; Thomas, L.; Muruganantham, A. *J. Pharm. Biomed. Anal.* **2005**, *38*, 858.
11. Kagawa, M.; Mochida, Y.; Nishi, H.; Haginaka, J. *J. Pharm. Biomed. Anal.* **2005**, *38*, 918.
12. Michaleas, S.; Antoniadou-Vyza, E. *J. Pharm. Biomed. Anal.* **2006**, *42*, 405.
13. Gang, S.; Roger, K.; Shiqi, P.; Guohui, C.; Roger, W. G. *J. Chromatogr.* A, **2007**, *1138*, 305.
14. (a) McEwen, I.; Torgny, R.; Marianne, E.; Birgit, H.; Gunnar, C.; Torbjorn, A. *J. Pharm. Biomed. Anal.* **2009**, *49*, 816. (b) McEwen, I.; Torgny, R.; Marianne, E.; Birgit, H.; Gunnar, C.; Torbjorn, A. *J. Pharm. Biomed. Anal.* **2009**, *49*, 1060.
15. Bigler, P.; Rudolf, B. *J. Pharm. Biomed. Anal.* **2009**, *49*, 1060.
16. Webster, G. K.; Marsden, I.; Pommerening, C. A.; Tyrakowski, C. M.; Tobias, B. *J. Pharm. Biomed. Anal.* **2009**, *49*, 1261.
17. Rao, R. N.; Pawan, K. M.; Narasa Raju, A. *J. Pharm. Biomed. Anal.* **2009**, *49*, 1287.
18. Orovan, G.; Tihanyi, K.; Noszal, B. *J. Pharm. Biomed. Anal.* **2009**, *50*, 718.

19. Beyer, T.; Schollmayer, C.; Holzgrabe, U. *J. Pharm. Biomed. Anal.* **2010**, *52*, 51.
20. Keire, D. A.; Daniel, J. M.; Hongping, Ye. *J. Pharm. Biomed. Anal.* **2010**, *52*, 656.
21. Staneva, J.; Pavletta, D.; Milka, T.; Ljuba, E. *J. Pharm. Biomed. Anal.* **2011**, *54*, 94.
22. Iqbal, Md. Y.; Rao, K. M. V. N.; Sridhar, G.; Padmanabha Raju, P.; Deshpande, G. R. *J. Pharm. Biomed. Anal.* **2011**, *56*, 484.
23. Hanna, G. M.; Frederick, E. E. *J. Pharm. Biomed. Anal.* **2000**, *24*, 189.
24. Malz, F.; Jancke, H. *J. Pharm. Biomed. Anal.* **2005**, *38*, 813.
25. Lavertu, I.; Xia, Z.; Serreqi, A. N.; Berrada, M.; Rodrigues, A.; Wang, D.; Buschmann, M. D.; Gupta, A. *J. Pharm. Biomed. Anal.* **2003**, *32*, 1149.
26. Li, J.; Yulan, W.; Alan, F.; Cryptan, T. A.; Yu, Y.; Lau, K.; Quigley, C. L.; John, C. L.; Jurg, U.; Elaaine, H. *J. Pharm. Biomed. Anal.* **2007**, *45*, 263.
27. Sharma, R.; Gupta, P. K.; Mazumder, A.; Dubey, D. K.; Kumaran, G.; Vijayaraghavan, R. *J. Pharm. Biomed. Anal.* **2009**, *49*, 1092.
28. *Medicines and Healthcare products Regulatory British Pharmacopoeia*, **2012**, Agency (MHRA), 5th Floor,151, Buckingham Palace Road, London, SW1W9SZ. Volume-II, 1414.
29. Hamdan, I. I.; Jaber, A. K.; Abushoffa, A. M. *J. Pharm. Biomed. Anal.* **2010**, *53*, 1254.
30. Bailey, C. J.; Path, M. R. C.; Turner, R. C. *N. Engl. J. Med.* **1996**, *334*, 574.
31. (a) Al-Rimawi, F. *Talanta*, **2009**, *79*, 1368. (b) Onal, A. *Eur. J. Med. Chem.* **2009**, *44*, 4998. (c) Huttunen, K. M.; Rautio, J.; Leppanen, J.; Vepsalainen, J.; Keski-Rahkonen, P. *J. Pharm. Biomed. Anal.* **2009**, *50*, 469. (d) Ali, A. R.; Duraidi, I. I.; Saket, M. M.; Abu-Nameh, E. S. *J. AOAC Int.* **2009**, *92*, 119.
32. (a) Jain, D.; Jain, S.; Jain, D.; Amin, M. *J. Chromatogr. Sci.* **2008**, *46*, 501. (b) Porta, V.; Schramm, S. G.; Kano, E. K.; Koono, E. E.; Armando, Y. P.; Fukuda, K.; Serra, C. H. *J. Pharm. Biomed. Anal.* **2008**, *46*, 143.
33. Song, J. Z.; Chen, H. F.; Tian, S. J.; Sun, Z. P. *J. Chromatogr., B: Anal. Technol. Biomed. Life Sci.* **1998**, *708*, 277.
34. Habib, I. H. I.; Kamel, M. S. *Talanta*, **2003**, *60*, 185.

35. Marques, M. A.; Soares, Ade. S.; Pinto, O. W.; Barroso, P. T.; Pinto, D. P.; Ferreira-Filho, M.; Werneck-Barroso, E. *J. Chromatogr., B: Anal. Technol. Biomed. Life Sci.* **2007**, *852*, 308.
36. Mistri, H. N.; Jangid, A. G.; Shrivastav, P. S. *J. Pharm. Biomed. Anal.* **2007**, *45*, 97.
37. Van Gysel, A. B.; Musin, W. *Encyclopedia of Industrial Chemistry,* **2012**, DOI: 10.1002/14356007.a16_535.pub3.
38. Zhang, A. Q.; Mitschell, S. C.; Smith, R. L. *Food Chem. Toxicol.* **1998**, *36,* 923.
39. (a) *ICH Harmonized Tripartite Guidelines. Validation of Analytical Procedures:* Text and Methodology Q2 (R1), **2005**. (b) *United States Pharmacopoeia 32*, NF 27, Rockville, Maryland, USA, **2009**.
40. Public document, PA/PH/CEP (04) 1 4R, *Content of the dossier for chemical purity and microbiological quality*, February **2007**, EDQM.
41. Hollis, D. P. *Anal. Chem.* **1963,** *35*, 1682.
42. Jungnickel, J. L.; Forbes, J. W. *Anal. Chem.* **1963**, *35*, 938.
43. Holzgrabe, U.; Diehl, B.; Wawer, I. *NMR Spectroscopy in Pharmaceutical Analysis,* **2008,** 49-50,Elsevier Ltd., Oxford, UK.
44. Imbenotte, M.; Azaroual, N.; Cartigny, B.; Vermeersch, G.; Lhermitte, M. *Foren. Sci. Int.* **2003,** *133*, 132.
45. Salem, A. A.; Mossa, H. A.; Barsoum, B. N. *Spectrochim. Acta, Part A,* **2005**, *62*, 466.
46. Salem, A. A.; Mossa, H. A.; Barsoum, B. N. *J. Pharm. Biomed. Anal.* **2006**, *41*, 654.
47. Eirod L.; White L.B.; Wong. C. F. *J. Chroma.* **1981,** *208*, 357.
48. Barends, D. M.; Brouwers, J. C.; Hulshoff, A. M.; *J. Pharm. Biomed. Anal.* **1987**, *5*, 613.
49. Chen, Z.; Xu, G.; Specht, K.; Yang, R. *Anal. Chim. Acta.* **1994**, *296*, 249.
50. Wong, L.T.; Beaubian, A. R.; Pakuts, A. P. *Curr. Eye. Res.* **1996**, *15*, 501.
51. Holzgrabe, U.; Diehl, B. W.; Wawer, I. *J. Pharm. Biomed. Anal.* **1998**, *17*, 557.
52. Malet, M. M.; Holzgrabe, U. *J. Pharm. Biomed. Anal*. **2011**, *55*, 1.
53. Badyal, D. K.; Kaur, J. *J. Med. Edu. Res.* **2008**, *10*, 97.

54. Swales, J. G.; Gallagher, R. T.; Denn, M.; Peter, R. M.; *J. Pharm. Biomed. Anal.* **2011**, *55*, 544.
55. Malleshwararao, C. S. N.; Suryanarayana, M. V.; Mukkanti, K. *Sci. Pharm.* **2012**, *80*, 139.

Section III

Quantification of Flurbiprofen by ^{19}F qNMR and its recovery and stability study in human plasma

Introduction:

Fluorine chemistry is a large field that has attracted since 1960's. The power of ^{19}F NMR spectroscopy arises from the fact that fluorine nucleus in a molecule is surrounded by nine electrons as against one electron in the case of ^{1}H NMR. Hence, the range of fluorine chemical shifts is much higher than that of hydrogen, which leads to precise and accurate measurements. This fact has made Fluorine (^{19}F) as the second nucleus with spin ½ used for quantitative NMR applications after ^{1}H. Further ^{19}F has 100 % natural abundance.[1] This fact makes ^{19}F NMR as sensitive as ^{1}H NMR spectroscopy (83 % of ^{1}H) and makes it a suitable tool for the quantitative analysis, but it has much wider range (~ 450 ppm). Further it is neither affected by the huge water signal nor has much interfering signals. Some of the internal standards used in the ^{19}F NMR analysis are: *para*-fluorobenzoic acid sodium salt (FBEN), sodium fluoroacetate, trifluoroacetic acid, *para*-fluoro-D-phenylalanine etc.

The method precision and accuracy observed by ^{19}F NMR has led to ready acceptance of this technique for quantitative applications in fields such as pharmaceutical chemistry and medical science.[2a] In routine qualitative analysis ^{19}F NMR has been used for many years covering several other fields such as, material science, cosmetics, agrochemicals, pesticides, insecticides, dairy science etc. with many publications appearing in leading journals.[2b]

2.III.1: Applications of ^{19}F qNMR:

Pharmaceutical sciences

Recently, Navratilova quantified an enantiomeric impurity ranging from 0.2 - 1 % of "Paroxetine hydrochloride" by using relative peak areas of ^{19}F (of the enantiomer) and ^{13}C satellite signals that are deconvoluted using an automatic Lorentzian line fitting.[3]

In 1995, Fardella developed a rapid, precise, accurate and simple quantitative method for analysis of fluoroquinolones antibiotics (pefloxacin, norfloxacin and ofloxacin) by ^{1}H and ^{19}F NMR using an appropriate internal standard for quality control.[4]

A process to investigate the interaction between the fluoroquinolone fleroxacin and bacterial cells using non-selective (all resonances are excited), selective (observed resonance is excited) spin-lattice relaxation rates and spin-spin relaxation measurements with the help of ^{1}H and ^{19}F NMR has been developed by Waibel which gave an idea of binding behavior of fluoroquinoline to a macromolecule.[5] Determination of diffusion constants by NMR appears to be an additional method to estimate the binding ability of fluoroquinolines to macromolecules. NMR relaxation measurements have proved to be a very useful method to estimate complexation behavior of a ligand towards bacteria.

In 2007, Shamsipur and coworkers introduced advanced and powerful technique based on ^{19}F NMR for the assay of anti-psychotic drug haloperidol with trifluoroacetic acid as an internal standard, in human serum and its pharmaceutical formulations.[6] The authors found that their proposed method is rapid and facile, and affords manipulation of large samples not requiring any sample pretreatment and lengthy instrument time.

Malet-Martino reported a suitable analytical method for quantitative in vitro metabolic studies of fluorinated or phosphorylated drugs using ^{19}F NMR or ^{31}P NMR spectroscopy.[7]

Everett *et al* studied the metabolites of flucloxacillin in urine of a rat and quantified along with three metabolites easily, the results of which were confirmed by HPLC and high-field spin-echo ^{1}H NMR. The proposed ^{19}F NMR method involves minimal sample preparation and is free from endogenous interference of urine.[8]

Martino *et al* studied the high quantitative potential of in-vitro and in vivo ^{19}F NMR for quality analysis and were able to overcome the difficulties encountered in investigations on anticancer drug 5-fluorouracil metabolism.[9]

Medical sciences

^{19}F NMR has been used since the early 1980s for *in vivo* and *in vitro* studies of many fluoride-containing compounds, metabolic studies in biofluids and pharmaceutical formulation of therapeutic agents in clinical or animal trials.[10]

Corcoran *et al* developed an important method to investigate the biotransformation of three model drugs in forty-eight taxonomically diverse organisms by using ^{19}F NMR spectroscopy. This is a rapid method permitting simultaneous detection of twenty biotransformation products without sample pre-treatment. This success made ^{19}F qNMR method supersede the conventional methods based on LC-MS techniques.[11]

Pouremad *et al* quantified trifluorothymidine (TFT) metabolism products in micro molar level of fluoride ion by using ^{l9}F qNMR in brain, liver as well as blood and urine.[12]

Hoeltzli *et al* and Gerig, J. T. studied ^{1}H NMR spectrum of a protein which, being a large molecule, had a lot of overlapping signals, while fluorinated analogue of this protein showed well-resolved resonances.[13-16]

Wade and coworkers demonstrated the superiority of NMR method utilizing the signals of ^{19}F over ^{1}H in a crowded spectrum when both trifluoromethylaniline (TFMA) and N-acetyl-TFMA (NTFMA) are present in urine. ^{19}F NMR techniques are also found to be quicker for detecting TFMA metabolites in bio-fluids and superior to highly sensitive proton NMR spectroscopy due to negligible interferences in the former.[17]

Hull *et al* developed the quantitative determination of the chain-fluorinated polyamines in excised tumor tissue by *in vitro* ^{19}F NMR with 500 MHz instrument and results were similar to those of method of extraction by HPLC analysis.[18]

Meeh *et al* developed a method to study the degradation products or lipoproteins by enzyme and were able to quantify them by using differences in spin-spin relaxation times (T_2). This methodology offers promise for the noninvasive, sequential, and longitudinal evaluation of lipoprotein metabolites *in vivo* studies.[19]

Material sciences

Taylor *et al* prepared forty-nine fluorinated derivatives of (70)-fullerene, and their properties were elucidated by ^{19}F NMR. Further the (70)-fullerene and MnF_3 was isolated into forty-nine components which were analyzed by HPLC and identified by 1D and 2D ^{19}F NMR spectroscopic techniques.[20]

Stebbins *et al* studied the Na, K, Ca and their mixed silicates containing fluoride was quantified and confirmed the sites which are structurally similar to the corresponding metal fluoride.[21]

Cosmetic, Agrochemicals and Pesticides

Loewen *et al* have applied 1D NOE solution ^{19}F NMR experiment to quantify the tertiary structure in the cytoplasm domain and its assessment of different regions of the cytoplasmic face.[22] Mabury *et al* studied the photo degradation of fluorinated agrochemicals which were detected and quantified using ^{19}F qNMR.[23] Krebs *et al* examined the presence of fluoroacetic acid in Arrabidea bilabiata and Palicourea marcgravii and quantified fluoroacetic acid upto a level of 3µg/g by using ^{19}F NMR spectroscopic method.[24]

Dairy products

Charton *et al* developed a method for determination of trifluoroacetic acid in rat milk samples by ^{19}F NMR spectroscopy and the results were compared to those obtained by capillary gas chromatography.[25]

2.III.2: Cross correlation effects on ^{19}F NMR spectroscopy:

Cross correlations, or interference terms between two different relaxation pathways in a system of nuclear spins, have been a subject of theoretical and experimental studies of many years. It is well known that ortho-substituted benzenes are more complex systems than their *meta* and *para*-disubstituted counterparts because close proximity of the substituents can cause changes in bond angles, bond lengths, and planarity of the ring. This phenomenon is known as "ortho effect" and its extent is dependent on the properties of the substituent.[26]

The major contributions to the *ortho* effect are:

- **Electrical effects**
- **Steric effects**
- **Intermolecular forces**

Early evidence for the ortho effect in NMR was obtained from solid state NMR studies of the ^{19}F chemical shielding tensor in fluorobenzenes. Recently, it has also been seen in NMR in solution through cross correlated relaxation between the chemical shift anisotropy (CSA) tensor and dipolar coupling.[27] The use of fluorine NMR in this investigation is mainly due to two factors: i) the chemical shift dispersion of fluorine is large which means that the fluorine chemical shift is more sensitive to the local environment than proton because of high natural abundance and magnetogyric ratio of the naturally occurring isotope and ii) the favorable pharmacokinetic properties of fluorinated ligands which have established ^{19}F as a standard component in medicinal chemistry.[28]

The $^{19}F/^{1}H$ magnetization is inverted with a 180° pulse and detected at different relaxation intervals. The fluorine spectra at different recovery times and the evolution of the single and the two spin order molecules have been obtained with inversion of the fluorine and the proton nuclei separately. The unequal relaxation of different lines of the fluorine multiplet is an evidence of the emergence of multi-spin order and is a direct measure of cross correlations in the system.[29] Further, due to the cross correlation effect the variable delay time is always not equivalent to the five times of T_1. The cross correlation thereby provides a detailed description of molecular dynamics and anisotropic interactions at the molecular level. Hence quantification for ^{19}F qNMR requires optimum relaxation delays, specific solvent with specific temperature for a particular system.

There are many reports in the literature which discuss the application of ^{19}F NMR from quantitative point of view, some of them are given below. For accurate quantification the longitudinal relaxation (spin-lattice) time T_1 measurements calculated by inversion recovery experiments for the optimum relaxation delay (d_1) as well as cross correlation factors of ^{19}F nucleus by taking mono fluorinated drugs such as Flurbiprofen *(Anti-inflammatory)*[30] and its related compounds like 2-Fluoroaniline,

4-Bromo-2-fluoroacetamide and 4-Bromo-2-fluro-1,1'-biphenyl shown in Figure 2.III.1.

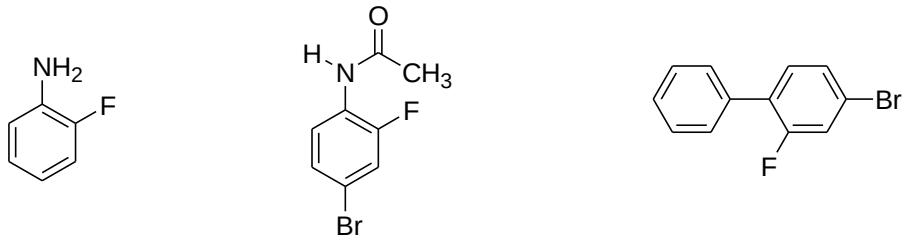

2-Fluoroaniline **4-Bromo-2-fluoroacetanilide** **4-Bromo-2-fluoro-1,1'-biphenyl**

Figure 2.III.1: Related compounds of Flurbiprofen

All the reported methods using an internal standard, have confirmed the reliability of ^{19}F qNMR methodology as an accurate and precise quantitative method in pharmaceutical areas, in which some have used it as an ultimate method for quantifying fluoro-containing drugs in human serum and pharmaceutical formulations.[31]

In this section, a quantitative method has been developed based on ^{19}F-NMR spectroscopy with an internal standard, 4-fluorobenzoic acid (PFBA) in methanol-d_4. This has been successfully applied for the human plasma linearity studies of Flurbiprofen as well as its stability study in human plasma at microgram level.

2.III.3: Experimental:

2.III.3.1: Drug:

Flurbiprofen was obtained as a gift sample from Sun Pharmaceutical Industries Limited, Vadodara, India. Flurbiprofen (Ocufen®) is a non-steroidal anti-inflammatory (NSAID), analgesic drug of the phenylalkanoic acid derivative family and is used for the treatment of arthritis pain management. Flurbiprofen is also used as an active ingredient in some kinds of throat lozenges. A single enantiomer of flurbiprofen, tarenflurbil [(*R*)-flurbiprofen)], is currently in clinical trials for the treatment of metastatic prostate cancer. Its chemical name is (*RS*) 2-Fluoro-α-methyl [1, 1′-biphenyl]-4-acetic acid, molecular formula is $C_{15}H_{13}FO_2$, (Fig.2.III.2) and molecular weight is 244.26. Flurbiprofen is a white crystalline powder practically insoluble in water and soluble in methanol, dichloromethane and it also dissolves in aqueous alkali and has a pK_a of 4.14.

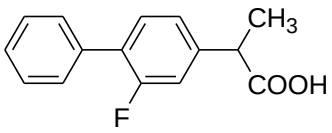

Flurbiprofen

Figure 2.III.2: Structure of Flurbiprofen

2.III.3.2: Materials and reagents:

High purity Analytical Grade substances were used throughout. Authentic sample of Flurbiprofen and its related compound 4-Bromo-2-fluoroacetamide and 4-Bromo-2-fluro-1,1'-biphenyl were obtained from Sun Pharmaceuticals Industries Ltd. India. Internal standard 4-fluoro benzoic acid (>99%), 2-fluoroaniline, and Deuterium Oxide (D_2O) (99.96% D) were purchased from Merck, Germany.

NMR sample preparation for cross correlation study

Similarly 10 mg of other related compounds were weighed accurately and the NMR sample solution tube was prepared by using different solvents and the tube was sealed properly after performing liquid nitrogen freeze and thaw process for three times in order to ensure complete removal of dissolved oxygen from the NMR solution.

For optimum relaxation delay with respect to spin-lattice (T_1) relaxations and other parameters such as structural change in the molecule which are 6 to 8 atoms apart from the fluorine nucleus, different viscosity solvents (such as $CDCl_3$, DMSO-d_6, CD_3OD, TCE-d_2) and temperature effect (from 10°C to 40°C) was studied for the 90° pulse calibration with maximum magnetization along z-axis after delay time and at thermal equilibrium.

Stock solution of 4-fluoro benzoicacid IS (2.5 mg /1.0 mL)

Accurately weighed 249.64 mg of 4-fluoro benzoic acid was transferred into 50 mL volumetric flask. About 10 mL of CD_3OD was added and made up to the mark with the same diluent and mixed well. 25 mL of solution was again diluted to 50 mL and used for further experiments.

Standard preparation

Accurately weighed 10.56 mg of Flurbiprofen drug (standard) was transferred to glass tube and 1.0 mL of stock solution of 4-fluoro benzoic acid IS was added. Solution was thoroughly mixed till complete dissolution.

Flurbiprofen standard preparation for specificity

10.19 mg Flurbiprofen standard was weighed accurately and transferred to glass tube and 1.0 mL of CD_3OD was added. Solution was thoroughly mixed till complete dissolution.

4-fluoro benzoicacid (IS) preparation for specificity

1.0 mL of stock solution of 4-fluoro benzoic acid IS was used directly.

2.III.3.3: Instrumentation:

Bruker Biospin AV-III 400 FT-NMR spectrometer operating at frequency 400.13 MHz (9.4 Tesla) for protons, equipped with a 5 mm Quadruple Nuclear Probe (QNP-F) probe-head, yielding a 90° fluorine pulse length of 19.0 µs, with software Topspin 3.0, the relaxation delay along with acquisition time was 20 s. All weighing were performed on a Mettler Toledo balance (Model-XS205 and XP2U).

^{19}F NMR instrumental method and processing

On a NMR Spectrometer with frequency 376.49MHz, typically, 32 scans of proton decoupled ^{19}F NMR spectra for each sample were collected into 131072 data points using a 90 degree pulse length; spectral width 37500.00 Hz; digital resolution 0.305176 Hz/points; pre-acquisition delay 19 µs and acquisition time 11.37 m. A delay time of 20 s between pulses was used to fully ensure T_1 relaxation of fluorine nucleus in Flurbiprofen and its internal standard 4-fluorobenzoic acid. The FIDs were apodized with 0.5 Hz exponential line broadening function before Fourier transformation. Manual two-parameter phase correction was used to obtain high quality absorption line shape followed by baseline correction. This manual mode was also used for the signal integration.

2.III.3.4: ^{19}F qNMR assay calculation:

For purity determination of Flurbiprofen, pure 4-fluoro benzoic acid of known purity was used as an internal standard.[32] The weight and assay were calculated using the following Equations (2-7) and (2-8).

$$W_x = \frac{I_x}{I_{std}} \times \frac{N_{std}}{N_x} \times \frac{M_x}{M_{std}} \times W_{std} \qquad (2\text{-}7)$$

$$P_x = \frac{I_x}{I_{std}} \times \frac{N_{std}}{N_x} \times \frac{M_x}{M_{std}} \times \frac{W_{std}}{W} \times P_{std} \qquad (2\text{-}8)$$

where, W_x = Weight of the Flurbiprofen drug (mg)

P_x = Assay of the Flurbiprofen (in % w / w) on as such basis

I_x, I_{std} = Mean integral value of the analyte ^{19}F signal obtained at δ = -117.35 ppm, and of 4-fluro benzoic acid IS obtained at δ = -105.96 ppm respectively, (Above chemical shift (δ) value was observed with the external calibration standard triflurotoluene at δ= -62.6 ppm)

N_{std}, N_x = Number of ^{19}F nuclei for the 4-fluoro benzoic acid IS (1.0) and ^{19}F nuclei for the analyte ^{19}F in drug respectively (1.0)

M_x, M_{std} = Molar mass of the Flurbiprofen drug (244.27g / mole) and molar mass of the 4-fluoro benzoic acid IS (140.11 g / mole) respectively

W_{std}, W= Weight of the 4-fluoro benzoic acid IS (mg), weight of the analyte Flurbiprofen drug (mg) respectively

P_{std} = Potency of the 4-fluoro benzoic acid IS (99.3%)

2.III.4: Results and discussion:

Cross correlation effect plays an important role in ^{19}F NMR spectroscopy and the variation of ^{19}F spin lattice relaxation time (T_1) was observed with same ^{19}F chemical environment with different type of solvents, variation of temperature and the neighboring coupling partner. The results of optimized experimental parameters for Flurbiprofen (FLB) and its related compounds such as 2-Fluoroaniline (A), 4-Bromo-2-fluoroacetanilide (B) and 4-Bromo-2-fluoro 1,1'-biphenyl are given below.

Variation of ^{19}F spin relaxation time with solvent

The cross correlation factor plays an important role by coupling with neighboring protons. The cross correlation factors were studied by using the inversion recovery experiments for multiplets of ^{19}F nucleus (Fig.2.III.5) and the spin lattice relaxation time was measured by using different deuterated solvents having different viscosity and variation of percentage of deuterium. The experiments were carried out using Flurbiprofen and related compounds like compound A, B, C by using ten point variable delays from 10 s to 0.01 s at room temperature. Table 2.III.1 and Figure 2.III.3 show that relaxation time varies with the solvent viscosity and the chemical environment of ^{19}F in the compounds.

Sr. No.	Solvent	Compound A	Compound B	Compound C	FLB
1	$CDCl_3$	7.387	2.938	2.908	1.254
2	DMSO-d_6	2.745	1.485	1.672	1.092
3	CD_3OD	7.498	3.891	4.280	2.443
4	TCE-D_2	3.313	1.306	1.465	0.793

Table 2.III.1: Spin lattice relaxation (T1) variations with solvent in ^{19}F-NMR

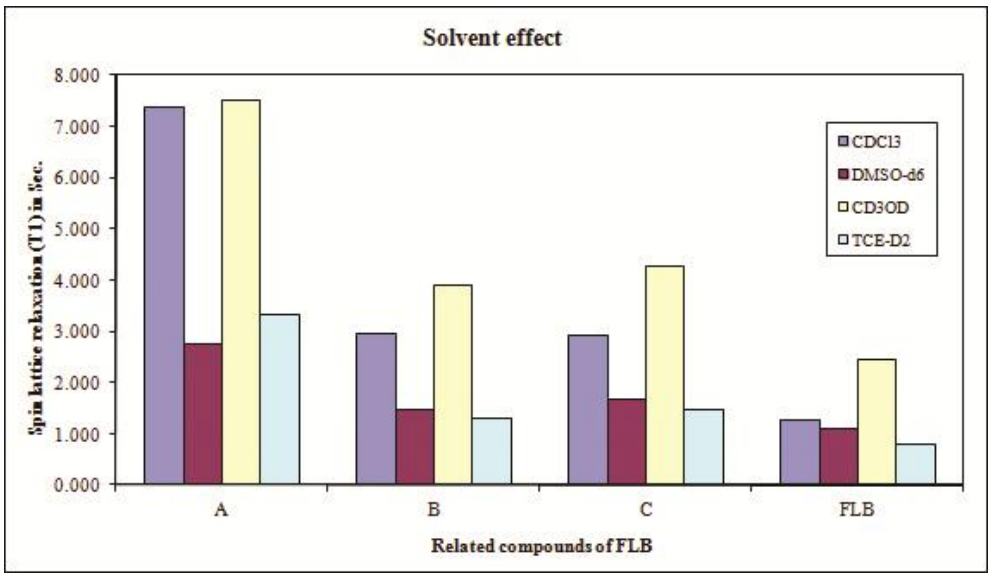

Figure 2.III.3: Variation of spin lattice relaxation time with solvents

Variation of ^{19}F spin relaxation time with temperature

Similarly, the temperature effect was studied from 10°C to 40°C by using above variable delay list for ^{19}F nucleus by using $CDCl_3$ as solvent. The spin lattice

relaxation time varies significantly with the variation in temperature for compound A, B and C whereas in the case of Flurbiprofen very small increase was observed especially between 20°C and 40°C as shown in Table 2.III.2 and Figure 2.III.4.

Sr. No.	Temperature	Compound A	Compound B	Compound C	FLB
1	10	3.760	1.833	1.986	0.924
2	20	7.387	2.938	2.908	1.254
3	30	8.722	2.825	2.725	1.377
4	40	3.643	1.342	2.261	1.412

Table 2.III.2: Temperature effect of spin lattice relaxation time (T_1) in $CDCl_3$ of ^{19}F-NMR

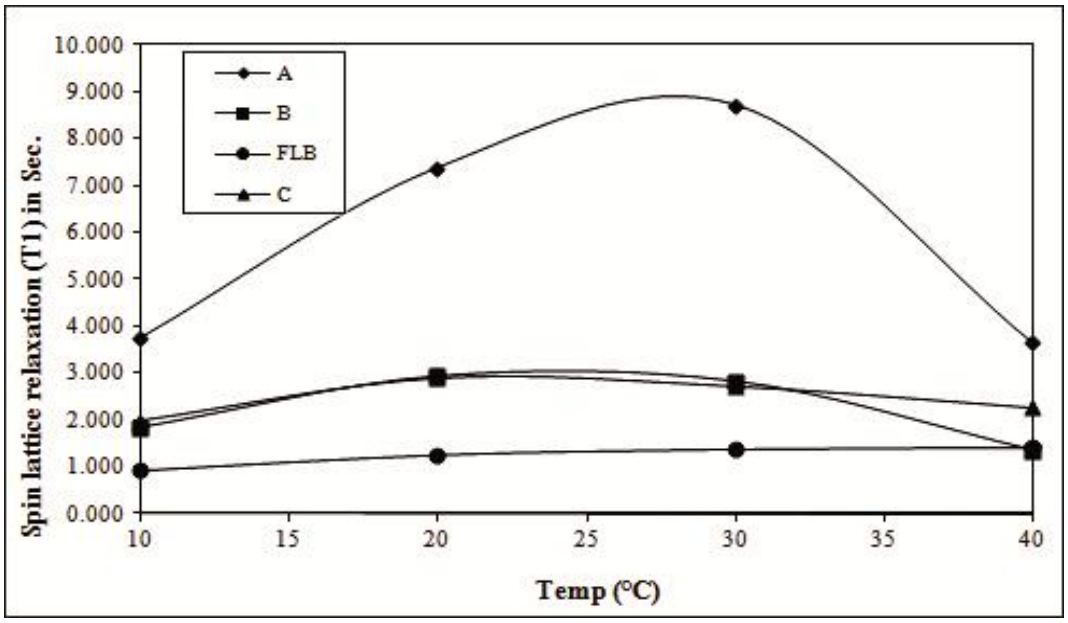

Figure 2.III.4: Variation of Temperature with spin lattice relaxation time (T_1) in ^{19}F NMR

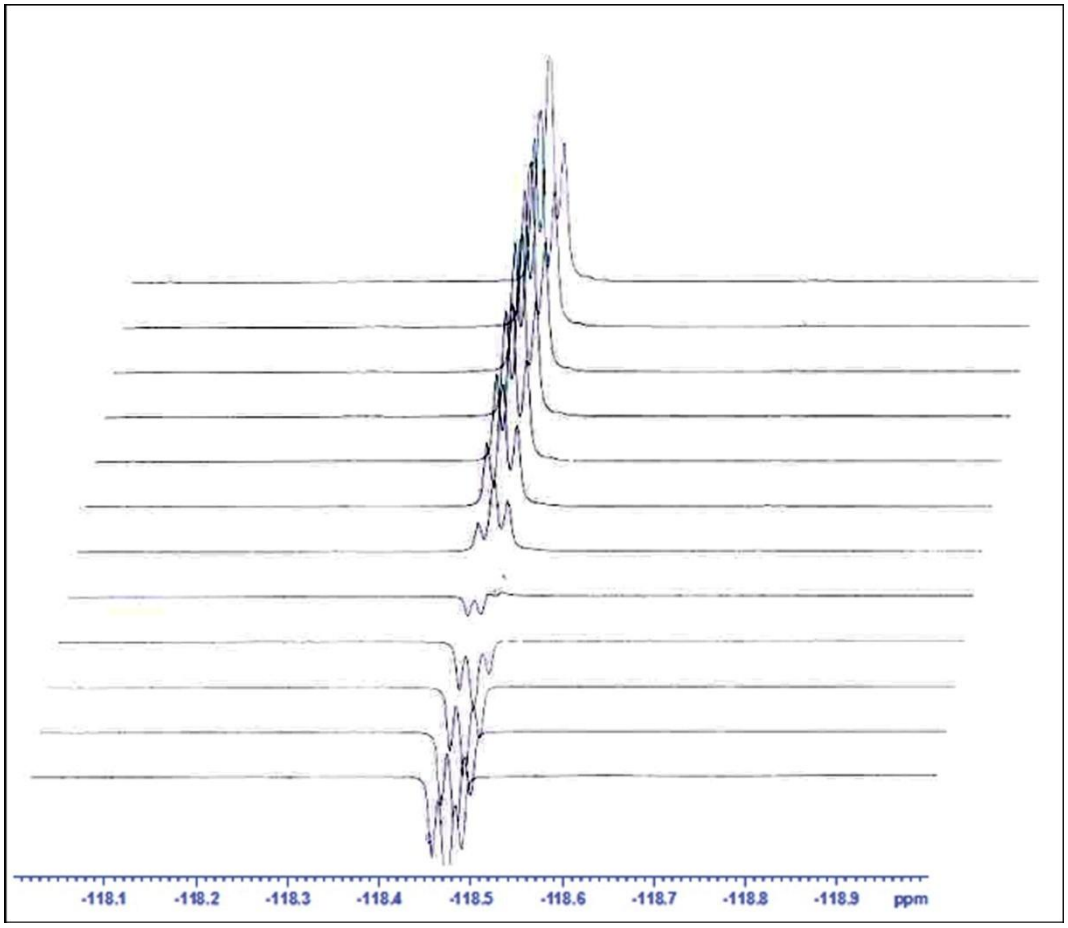

Figure 2.III.5: Inversion recovery plot of ^{19}F-NMR in Flurbiprofen at various delay time

The above experiments were also performed by using same variable delay for aromatic multiplet proton signals due to the presence of adjacent ^{19}F nucleus. The results of these experiments reveal that ortho-effects as well as cross correlation factors have significant effect on spin lattice relaxation time. (Table 2.III.3 and Figure 2.III.6) This may be the reason why in compound A, B and C, T_1 drastically varies with temperature. The aromatic protons of Flurbiprofen also exhibit only a slight change in relaxation time in the temperature range of 20 °C and 40 °C.

Sr. No.	Temp.	Compound A	Compound B	Compound C	FLB
1	10	5.471	4.296	2.956	1.687
2	20	9.930	5.182	3.820	2.358
3	30	9.460	2.799	3.952	2.100
4	40	11.762	3.855	3.537	2.319

Table 2.III.3: Temperature effect of spin lattice relaxation time (T_1) in $CDCl_3$ of ^{1}H-NMR

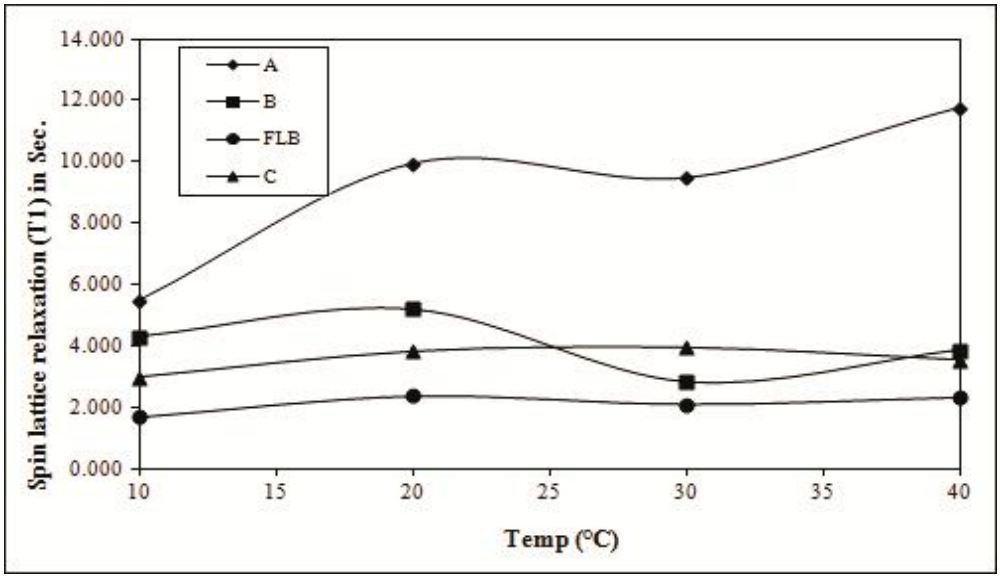

Figure 2.III.6: Variation of Temperature with spin lattice relaxation time (T_1) in ^{1}H-NMR

Sr. No.	Fluorinated compound	Spin lattice relaxation (T_1)
1	A	5.989
2	B	2.872
3	C	2.557
4	FLB	1.341

Table 2.III.4: Spin lattice relaxation time (T_1) of ^{19}F nucleus in $CDCl_3$ at 25 °C

Due to the presence of different functional group at *ortho*, *meta* and *para* positions of compounds A, B and C, they have different affinity to form intra-molecular hydrogen bonding within the molecule and non-bonding interactions with solvent molecules. When the spin lattice relaxation times (T_1) were measured by using inversion recovery experiments for ^{19}F nucleus in $CDCl_3$ at 25 °C from 10 s to 0.01 s variable delay, Flurbiprofen molecule showed lowest T_1 value among all the related compounds presented in Table 2.III.4 and Figure 2.III.7. Hence, it should be possible to accomplish Flurbiprofen assay and purity quantification by giving recycle delay time of about 7 s in $CDCl_3$ whereas in methanol-d_4 (CD_3OD) a recycle delay time of 12 s is considered optimum for the complete magnetization recovery of ^{19}F nucleus.

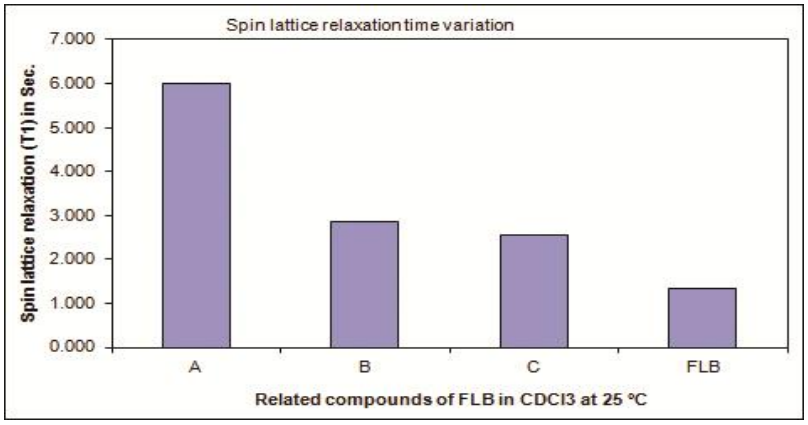

Figure 2.III.7: Related compounds of Flurbiprofen vs T_1 of in $CDCl_3$ at 25 °C

Compound A

Sr. No.	δ ppm	T_1
1	6.690	9.936
2	6.787	9.787
3	6.920	9.547
4	6.945	10.441

Table 2.III.5: Variation of T_1 with peak splitting of compound A in ^{1}H-NMR

Compound B

Sr. No.	δ ppm	T_1
1	7.247	5.977
2	7.277	6.446
3	7.405	3.124
4	8.224	5.394

Table 2.III.6: Variation of T_1 with peak splitting of compound B in ^{1}H-NMR

Compound C

Sr. No.	δ ppm	T_1
1	7.294	3.457
2	7.373	4.019
3	7.436	3.604
4	7.491	3.633

Table 2.III.7: Variation of T_1 with peak splitting of compound C in ^{1}H-NMR

Flurbiprofen (FLB)

Sr. No.	δ ppm	T_1
1	7.205	2.266
2	7.414	2.937
3	7.466	2.702
4	7.548	2.763

Table 2.III.8: Variation of T_1 with peak splitting of FLB in ^{1}H-NMR

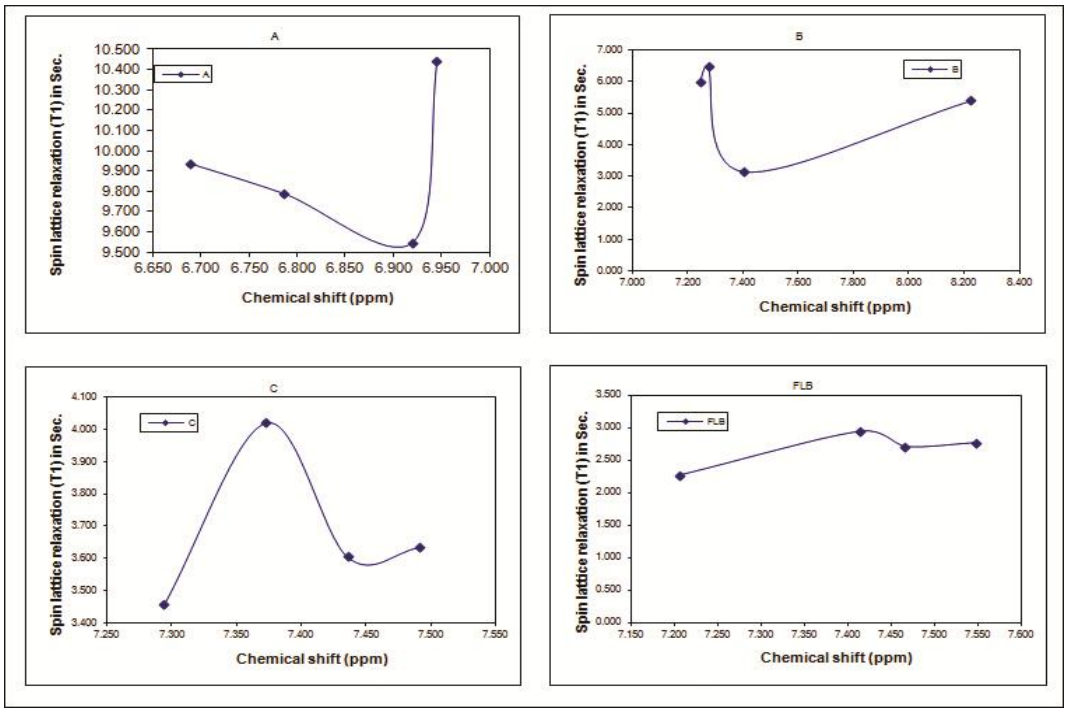

Figure 2.III.8: Graphical representation of T_1 against chemical shift of compound A, B, C and FLB in ^{1}H-NMR

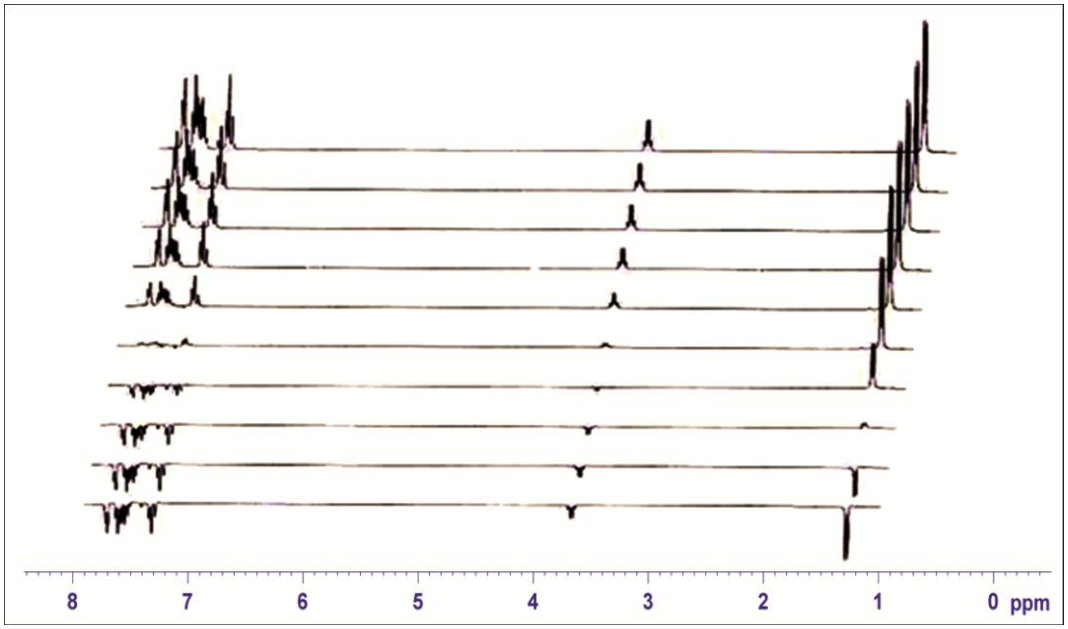

Figure 2.III.9: Inversion recovery plot of ^{1}H in Flurbiprofen at various delay time

From the above spectral data it evident that the presence of ^{19}F nucleus in the aromatic ring of all related compound A (Table 2.III.5), B (Table 2.III.6), C (Table 2.III.7) and also in Flurbiprofen (Table 2.III.8), gives rise to *ortho* effect as well as the cross correlation splitting of the proton signals. Hence, the proton signal observed is a complex multiplet due to ^{19}F coupling with neighboring protons, having different relaxation time (Fig.2.III.8) with respect to their chemical shift (δ) as shown in Fig.2.III.9. Further it indicates that cross correlation and ortho effect factors contribute to the irregular variation of spin lattice relaxation (T_1) time.

The equivalent NOE enhancement as well as the conversion of ^{19}F signal to sharp singlet with optimum signal to noise ratio in proton decoupled ^{19}F NMR spectra was developed using a pulse programme "zgfhigqn.2" with a decoupling power of 6.46 dB (0.22588 Watt) and optimum recycle delay time of 20 s. Due to the above conditions the ortho effect, cross correlation factors were adequately removed and also due to the sharpness of ^{19}F signal it is possible to quantify at lower level in dilute matrix solution with good linearity, high accuracy and recovery.

^{19}F NMR spectral analysis and spectral calibration

The ^{19}F NMR signal was calibrated with respect to external reference sample of trifluorotoluene (TFT) signal at chemical shift (δ) value of - 62.6 ppm recorded with same experimental conditions. The analyte ^{19}F signal was observed at -118.45

ppm as a triplet (Fig.2.III.10) and a complex multiplet of 4-fluoro benzoic acid IS at -105.96 ppm (Fig.2.III.11).

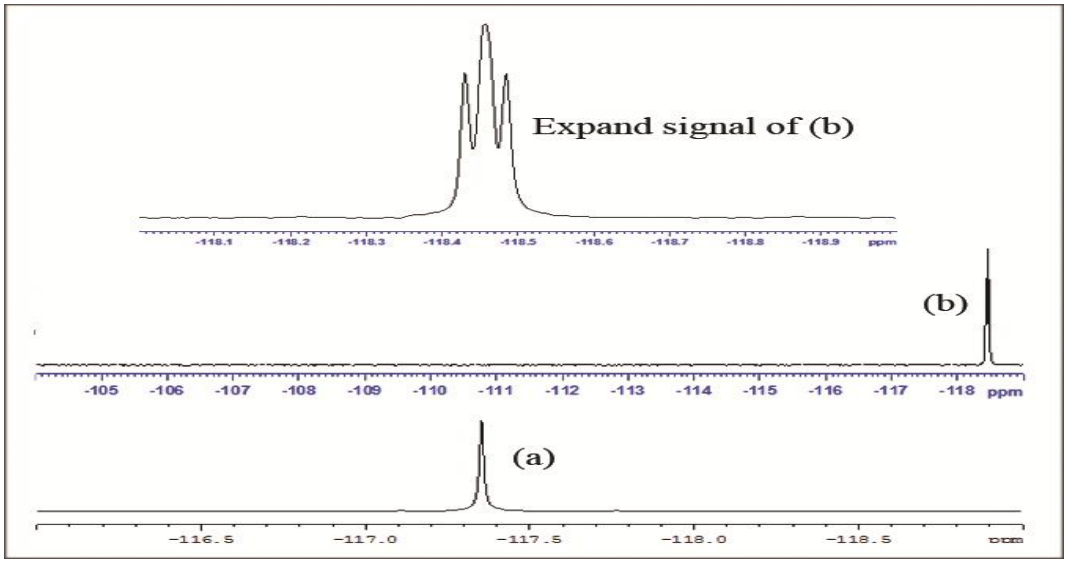

Figure 2.III.10: ^{19}F-NMR of Flurbiprofen with (a) proton decoupling and (b) without proton decoupling

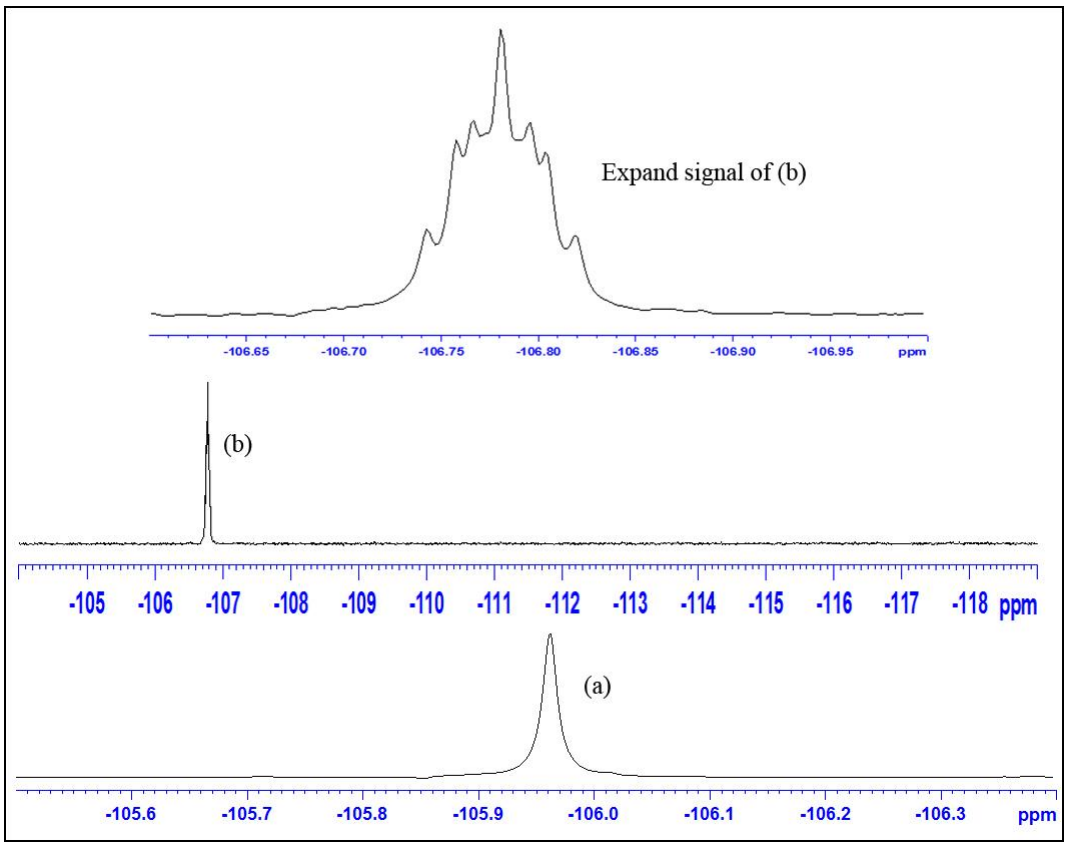

Figure 2.III.11: ^{19}F-NMR of 4-fluorobenzoic acid with (a) proton decoupling and (b) without proton decoupling

2.III.5: Quantitative ^{19}F qNMR method:

The area of the peak of a known amount of IS was compared with the area of the peaks originating from the analyte. In the current study, apart from its solubility, the choice of 4-fluoro benzoic acid as IS was made, because it supplies a well-separated signal without any interference from analyte drug signal in the integration region. The singlet area of 4-fluoro benzoic acid chosen for quantification was assigned a value of 100.00 in each NMR spectrum.

Validation of ^{19}F qNMR method

Similarly the ^{19}F qNMR method was validated with parameters like, system suitability, specificity and selectivity, linearity, precision and intermediate precision, LOD and LOQ, range, accuracy, recovery and robustness.

2.III.5.1: System suitability:

In the present study, system suitability was performed for every parameter by replicate acquisition of standard mixture sample of analyte with IS. The signal to noise ratio (S/N) of the analyte and IS signal was found to be 2090 : 1 and 614 : 1 respectively while the difference of the chemical shift (δ ppm) value of analyte signal with respect to IS was 11.39 ppm (Fig.2.III.12).

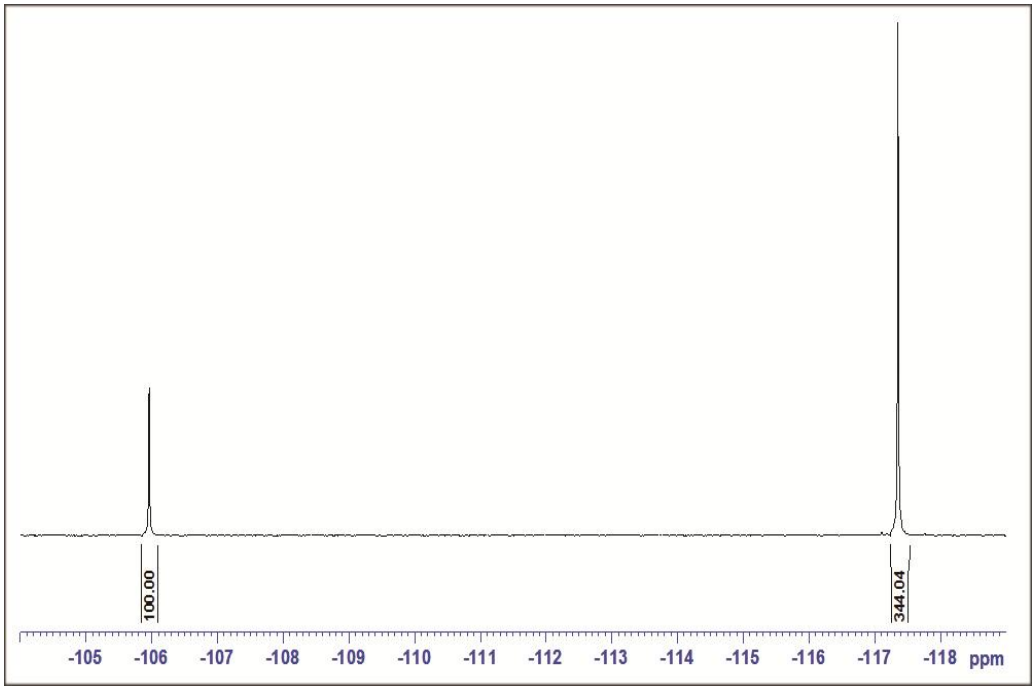

Figure 2.III.12: ^{19}F-NMR of FLB and 4-Fluorobenzoic acid with proton decoupling

2.III.5.2: Specificity and selectivity:

The selectivity and specificity of the proposed method was evaluated by considering the possible interference due to the presence of fluorinated excipients in the pharmaceutical formulations. Specificity study was performed by analyzing the diluent (CD_3OD), placebo solution preparation, Flurbiprofen standard preparation, 4-fluoro benzoicacid IS preparation and sample preparation. The results show (Fig.2.III.12) that there is no interference at the signals obtained at -117.35 ppm and -105.96 ppm for analyte and IS respectively due to diluent and placebo because it does not have any ^{19}F nucleus. Hence the method is very specific and also selective.

2.III.5.3: Precision and intermediate precision:

In the present study, the precision was assessed by six separate sample preparations. The content of drug (% assay) for each preparation was calculated by using the Equation (2-8) and the statistical results of the determinations are presented in Table 2.III.9.

The method precision was evaluated as the repeatability, by calculating the relative standard deviation (% RSD) of the ^{19}F qNMR signal areas of Flurbiprofen for six determinations under the same experimental conditions presented in Table 2.III.10. The % RSD of Flurbiprofen so calculated is 1.62 which is well within the acceptable limit of not more than 2.

Sr. No.	m	I_x	W_x	P_x	Mean	%RSD
1	15.10	44.18	14.98	98.21	96.35	1.62
2	14.59	328.15	14.28	96.91		
3	14.42	314.21	13.68	93.89		
4	16.05	359.80	15.66	96.59		
5	14.90	329.08	14.32	95.16		
6	15.03	339.44	14.77	97.31		

Table 2.III.9: Method precision of Flurbiprofen by ^{19} F qNMR

Sr. No.	m	I_x	W_x	P_x	Mean	%RSD
1	15.38	343.82	14.96	96.32	96.71	0.93
2	14.76	331.27	14.42	96.71		
3	15.89	351.77	15.31	95.39		
4	15.79	354.79	15.44	96.82		
5	15.05	338.28	14.72	96.85		
6	15.23	346.96	15.10	98.16		

Table 2.III.10: Intermediate precision (Different Analyst) of Flurbiprofen by ^{19}F qNMR

2.III.5.4: Linearity:

The linearity was established by preparing standard solutions at seven different concentration levels ranging from approximately 2 % to 166 %, according to the content of analyte in test sample given in Table 2.III.11. Linearity curve was generated by plotting the amount of the drug (mg) on x- axis against the amount of drug found (mg) on y-axis shown in Figure 2.III.13. Good linearity was evident with the equation $y = 0.9402\ x \pm 0.0259$ with a correlation coefficient of 0.9997 over the examined concentration range.

Sr. No.	m	I_x	W_x	P_x
1	0.32	6.49	0.28	87.34
2	0.38	7.74	0.34	87.80
3	0.83	16.76	0.73	87.01
4	1.59	34.58	1.51	93.72
5	4.47	98.03	4.27	94.49
6	9.12	197.12	8.58	93.13
7	11.23	251.38	10.94	96.45
8	16.51	354.58	15.43	92.54
9	19.89	430.97	18.76	93.36
10	24.51	527.70	22.97	92.77

Table 2.III.11: Linearity data of Flurbiprofen by ^{19}F qNMR

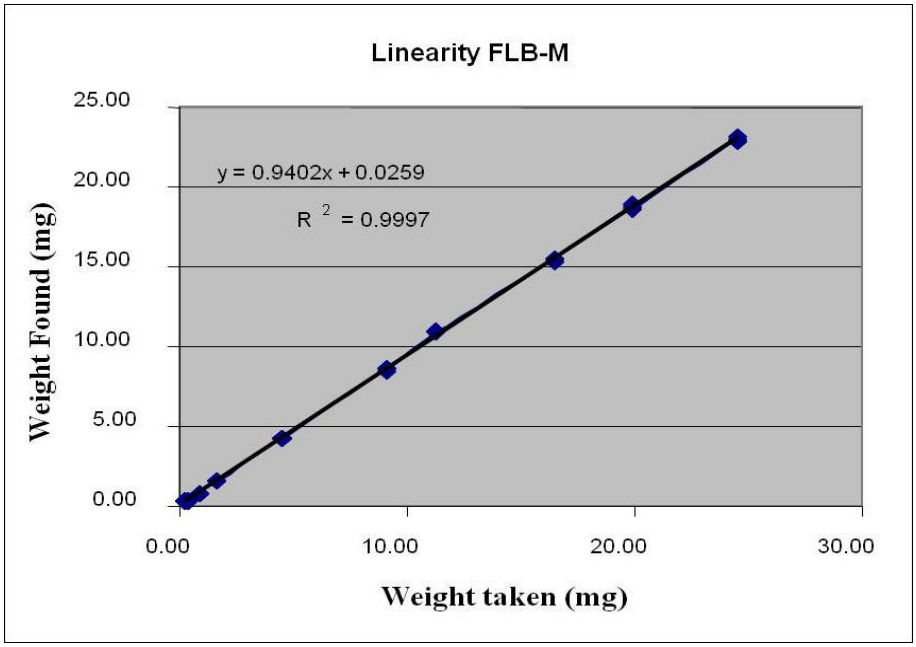

Figure 2.III.13: Linearity plot of Flurbiprofen by ^{19}F qNMR

2.III.5.5: LOD and LOQ:

In the case of NMR with Lorentzian lines as response signals, the LOD and LOQ have to be calculated by the standard deviation of the response 'σ' and the slope 's' of a calibration curve obtained in linearity study. The LOD and LOQ were calculated using Equation (2-9) and (2-10) respectively**.**

$$\text{LOD} = \frac{3.3\,\sigma}{s} \qquad (2\text{-}9)$$

$$\text{LOQ} = \frac{10\,\sigma}{s} \qquad (2\text{-}10)$$

LOD and LOQ are found to be 0.22 mg and 0.68 mg per mL of diluent respectively.

2.III.5.6: Solubility range:

The solubility range study was performed by preparing solutions of drug up to saturated concentration in solution using diluent methanol-d_4. Saturated solution was prepared by adding excess amount of drug and analyzing supernatant solution for determining the dissolved concentration of drug. Saturation concentration was found to be about ~100 mg per 1.0 mL diluent.

2.III.5.7: Accuracy:

The accuracy was studied at 80%, 100% and 120% levels, specified range covered under ICH guidelines, with respect to the sample by preparing the solutions in triplicate at each level. From the results as per Table 2.III.12, 2.III.13 and 2.III.14 respectively, it can be seen that method for assay content is accurate within the specified range. The % RSD at each level is less than 2.00 which is well within the acceptable limit.

Level	m	I_x	W_x	P_x	Mean	% RSD
80 %	12.11	272.92	11.88	97.10	95.72	1.44
	12.89	286.26	12.46	95.69		
	12.03	263.44	11.47	94.36		

Table 2.III.12: Accuracy at 80% level of Flurbiprofen by ^{19}F qNMR

Level	m	I_x	W_x	P_x	Mean	% RSD
100 %	15.01	335.51	14.60	96.31	96.81	0.47
	15.24	342.77	14.92	96.91		
	15.32	345.58	15.04	97.20		

Table 2.III.13: Accuracy at 100% level of Flurbiprofen by ^{19}F qNMR

Level	m	I_x	W_x	P_x	Mean	% RSD
120 %	18.12	402.69	17.53	95.76	94.36	1.28
	18.05	392.74	17.09	93.75		
	18.21	395.47	17.21	93.57		

Table 2.III.14: Accuracy at 120 % level of Flurbiprofen by ^{19}F qNMR

2.III.5.8: Recovery:

The recovery was performed at 50 %, 100 % and 150 % levels, again specified range covered under ICH guidelines, with respect to the sample by preparing the solutions in triplicate at each level. The results of recovery data obtained from matrix of Flurbiprofen by using ^{19}F qNMR at different levels are given in Table 2.III.15, 2.III.16 and 2.III.17. It can be seen that the % RSD at each level is 1.2, 1.08 and 0.17 which is well within the acceptable limit of not more than 10 %.

Level	m	I_x	W_x	P_x	Mean	% RSD
50 %	7.90	176.08	7.66	96.03	96.88	1.2
	7.82	178.24	7.76	98.21		
	7.69	172.04	7.49	96.39		

Table 2.III.15: Recovery at 50 % level of Flurbiprofen by ^{19}F qNMR

Level	m	I_x	W_x	P_x	Mean	% RSD
100 %	14.53	325.00	14.14	96.38	96.83	1.08
	15.06	342.64	14.91	98.03		
	15.11	336.97	14.67	96.09		

Table 2.III.16: Recovery at 100 % level of Flurbiprofen by ^{19}F qNMR

Level	m	I_x	W_x	P_x	Mean	% RSD
150 %	21.59	486.67	21.18	97.12	97.23	0.17
	21.86	492.91	21.45	97.16		
	21.32	482.06	20.98	97.42		

Table 2.III.17: Recovery at 150 % level of Flurbiprofen by ^{19}F qNMR

2.III.5.9: Solution stability of analyte:

Solution stability of standard preparation and sample preparation were studied at ambient temperature (~25 °C) at 0 h (initial), 3 h, 12 h, 24 h and 36 h intervals and % assay was calculated for each interval. The observed results of % assay at different time intervals shows no major change upto 12 h at an ambient temperature given in Table 2.III.18. Hence the solution can be considered stable upto at least 12 h.

Time interval (h)	m	I_x	W_x	P_x
0	8.05	259.49	7.99	98.55
3	8.05	259.43	7.99	98.52
12	8.05	259.25	7.98	98.26
24	8.05	250.53	7.71	94.95
36	8.05	250.44	7.71	94.92

Table 2.III.18: Solution stability of Flurbiprofen by ^{19}F qNMR

2.III.5.10: Robustness study:

The method robustness was determined by analyzing the same sample at normal operating conditions and also by changing following analytical parameters of instrument such as the variation in sample depth (Table 2.III.19), mode of shimming (Table 2.III.20), spinning rate (Table 2.III.21), sweep width (Table 2.III.22), offset position (Table 2.III.23), pulse length (Table 2.III.24) and temperature (Table 2.III.25). By changing only one operating parameter at a time while keeping all other parameters fixed and using the same sample showed either no change and in some cases very close to the results obtained with normal instrumental conditions. The results indicate that the influence of sample depth below 3.0 cm, offset position below -105 ppm and temperature above 32 °C due to degradation of IS does not complies as per the specification and other parameters is not significant therefore the proposed method is robust.

Parameter	Change	I_x	m	W_x	P_x	Difference
Sample depth	1.5 cm	333.91	12.93	12.22	93.57	5.88
	3.0 cm	325.51	12.93	12.43	96.13	3.32
	4.5 cm	320.14	12.93	13.02	99.66	-0.21
	6.0 cm	318.30	12.93	12.94	99.08	0.37
	7.5 cm	319.48	12.93	12.99	99.45	N/A

Table 2.III.19: Sample depth variation of Flurbiprofen by ^{19}F qNMR

Parameter	Change	I_x	m	W_x	P_x	Difference
Mode of shimming	Non	316.80	12.93	12.88	98.62	0.83
	Manual	317.09	12.93	12.89	98.71	0.74
	Top	316.25	12.93	12.99	99.45	N/A
	Auto	320.38	12.93	13.03	99.73	-0.28
	Simplex	321.09	12.93	13.05	99.95	-0.50

Table 2.III.20: Mode of shimming variation of Flurbiprofen by ^{19}F qNMR

Parameter	Change	I_x	m	W_x	P_x	Difference
Spinning rate in rps	0	266.84	10.91	10.85	98.44	-0.64
	8	267.01	10.91	10.86	98.51	-0.71
	12	267.27	10.91	10.87	98.60	-0.8
	16	267.26	10.91	10.87	98.60	-0.8
	20	265.10	10.91	10.78	97.80	N/A
	24	264.86	10.91	10.77	97.72	0.08
	28	266.66	10.91	10.84	98.38	-0.58
	32	267.04	10.91	10.86	98.52	-0.72

Table 2.III.21: Spinning rate variation of Flurbiprofen by ^{19}F qNMR

Parameter	Change	I_x	m	W_x	P_x	Difference
Sweep width in ppm	70	274.69	11.09	11.17	99.70	-0.45
	80	271.88	11.09	11.05	98.68	0.57
	90	272.47	11.09	11.08	98.89	0.36
	100	273.41	11.09	11.12	99.23	0.02
	110	273.46	11.09	11.12	99.25	N/A
	120	274.10	11.09	11.14	99.48	-0.23
	130	275.05	11.09	11.18	99.83	-0.58

Table 2.III.22: Sweep width variation of Flurbiprofen by ^{19}F qNMR

Parameter	Change	I_x	m	W_x	P_x	Difference
Offset at ppm	-80	267.71	11.09	10.88	97.16	1.31
	-90	273.62	11.09	11.12	99.31	0.84
	-100	271.32	11.09	11.03	98.47	N/A
	-105	268.81	11.09	10.93	97.56	0.91
	-110	261.46	11.09	10.63	94.89	3.58
	-115	255.15	11.09	10.37	92.60	5.87

Table 2.III.23: Offset variation of Flurbiprofen by ^{19}F qNMR

Parameter	Change	I_x	m	W_x	P_x	Difference
Pulse length in µs	2.11	252.70	10.33	10.27	98.46	1.43
	4.22	254.11	10.33	10.33	99.01	0.88
	6.33	254.74	10.33	10.36	99.26	0.63
	9.5	251.96	10.33	10.24	98.18	1.71
	12.60	252.55	10.33	10.27	98.40	1.49
	15.84	256.12	10.33	10.41	99.79	0.10
	19.00	256.36	10.33	10.42	99.89	N/A

Table 2.III.24: Pulse width variation of Flurbiprofen by ^{19}F qNMR

Parameter	Change	I_x	m	W_x	P_x	Difference
Temperature in K	295	255.88	10.35	10.40	99.48	N/A
	305	259.13	10.35	10.54	100.77	-1.29
	310	290.03	10.35	11.79	112.79	-13.31
	315	293.85	10.35	11.95	114.27	-14.79
	320	294.75	10.35	11.98	114.63	-15.51

Table 2.III.25: Temperature variation of Flurbiprofen by ^{19}F qNMR

2.III.6: Recovery and stability study of Flurbiprofen in human plasma by ^{19}F qNMR spectroscopy:

The fresh human plasma was collected and taken for the linearity and stability study of Flurbiprofen in human plasma matrix.

2.III.6.1: Linearity study of plasma:

5 mg, 10 mg and 15 mg of each Flurbiprofen API sample in triplicate was accurately weighed and dissolved in 1.0 mL of 0.1 N NaOH solutions and transferred into 2 mL micro centrifugation tubes. From this, nine stock solutions, each of 100 µL, were transferred to the centrifuge tube and 900 µL of human plasma was added into the centrifuge tube. After vigorously vortex-mixing for 1 min, the solution was diluted with 1.0 mL of IS solution and centrifuged for 5 min. The linearity study was performed on the supernatant solution by the proposed ^{19}F qNMR method at room temperature.

Sr. No.	Drug level	Area with respect to same concentration of IS	Average
1	0.5	16.95	16.69
2		16.10	
3		17.03	
4	1.0	35.39	34.21
5		35.84	
6		31.39	
7	1.5	47.84	47.43
8		46.13	
9		48.32	

Table2.III.26: Linearity data of Flurbiprofen in human plasma

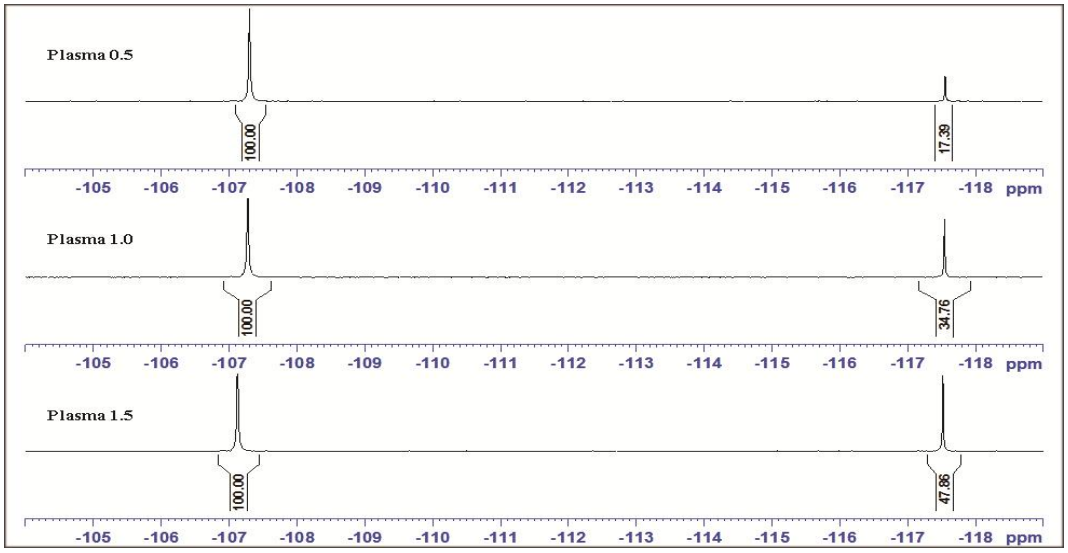

Figure 2.III.15: Comparison of ^{19}F qNMR spectra of Flurbiprofen in human plasma for linearity study

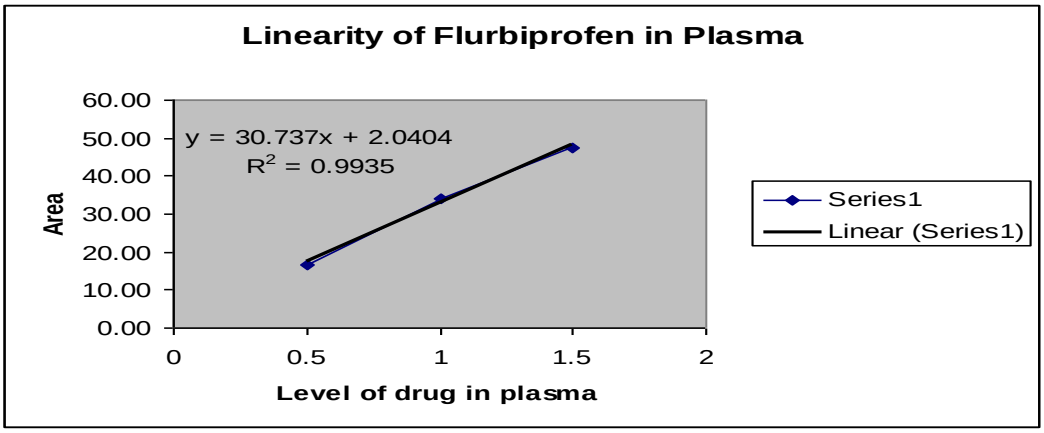

Figure 2.III.14: Linearity curve of Flurbiprofen in human plasma

From the data presented in Table 2.III.26 and linearity curve was plotted taking area of the signal on y-axis against the amount of the drug (mg) on x-axis added in plasma (Fig. 2.III.14). The equation for the linearity curve (Fig. 2.III.14) so obtained is $y = 30.737 x \pm 2.0404$ with a correlation coefficient of 0.9935, indicating good linearity with human plasma matrix.

Stock human plasma sample preparation for stability

10 mg of each Flurbiprofen API sample was accurately weighed and transferred into three 1.0 mL micro centrifugation tubes and dissolved in 1.0mL of 0.1 N NaOH solution. From the above three stock solutions, 100 µL sample solution in triplicate was transferred to the centrifuge tube and 900 µL of human plasma was added into it. The above plasma samples were vigorously vortex-mixed for 1 min and were kept for the stability study in human plasma matrix upto 48 h at room temperature.

2.III.6.2: Stability plasma sample preparation for ^{19}F qNMR spectral analysis :

10 µL of each stability sample was taken in triplicate at the time point selected and diluted with IS solution upto 1 mL and centrifuged for 5 min and the supernatant solution was taken for the ^{19}F qNMR study. Stability time point at ambient temperature (~25 °C) chosen are initial 2 h, 4 h, 8 h, 24 h and 48 h. The ^{19}F qNMR signal area obtained for each interval with triplicate preparations at different time interval showed no major change with % RSD 1.75 as presented in Table 2.III.27. From the observed data it is concluded that the ^{19}F signal of Flurbiprofen are linear and stable as shown in Fig.2.III.16 with human plasma matrix.

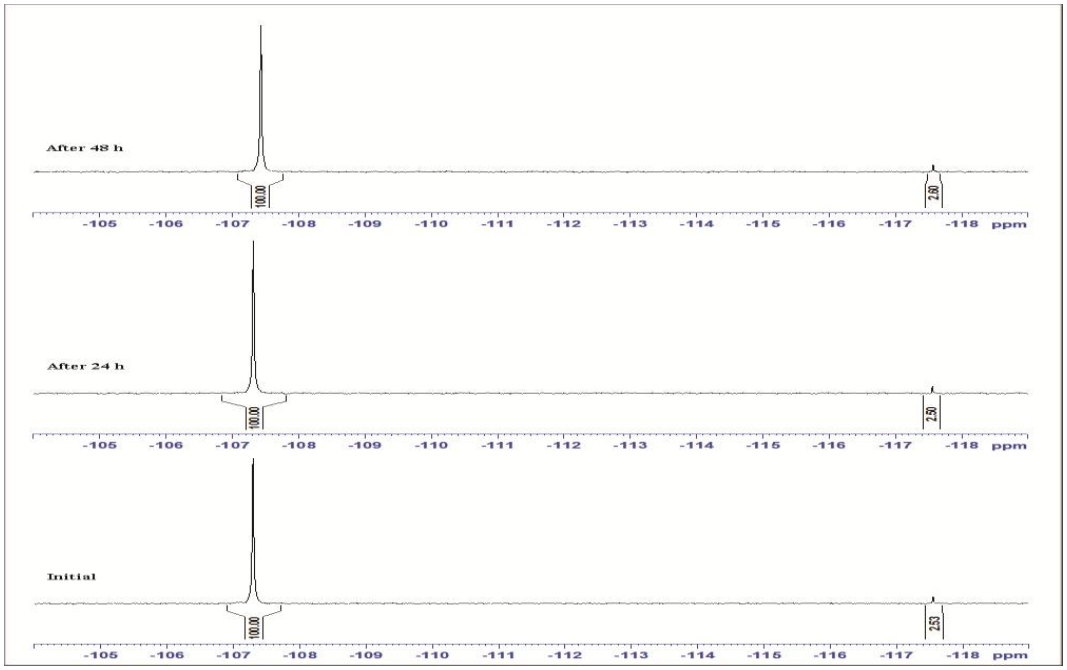

Figure 2.III.16: Comparison of ^{19}F qNMR spectra of Flurbiprofen in human plasma for stability study

Sr. No.	Time interval	Area with respect IS	Average	% RSD
1	0 hr	2.60	2.73	1.75
2		2.89		
3		2.71		
4	2 hr	2.57	2.75	
5		2.90		
6		2.77		
7	4 hr	2.83	2.70	
8		2.90		
9		2.36		
10	8 hr	2.72	2.71	
11		2.76		
12		2.65		
13	24 hr	2.62	2.63	
14		2.83		
15		2.45		
16	48 hr	2.82	2.64	
17		2.52		
18		2.58		

Table 2.III.27: Stability data of Flurbiprofen in human plasma

2.III.7: Commercial sample analysis by ^{19}F qNMR :

Commercially available eye drops of Flurbiprofen, one from Allergan (FLUR™, B.No.PT0109) label claim, 0.3 mg/mL and the other from Entod Pharmaceuticals Ltd. (FLUBI™, B.No.BB2022) label claim 0.03% w/v were purchased from the local market. 0.7 mL of each eye drop solutions were directly taken into the NMR tube, 0.3 mL of IS solution was added in each tube and mixed thoroughly and quantification were performed by using above ^{19}F qNMR method in triplicate. The sampling was done in duplicate and the observed results shown in Table 2.III.28 are in good agreement with the label claim, ^{19}F qNMR spectra of both samples used for the calculation are presented in Fig. 2.III.17 and 2.III.18.

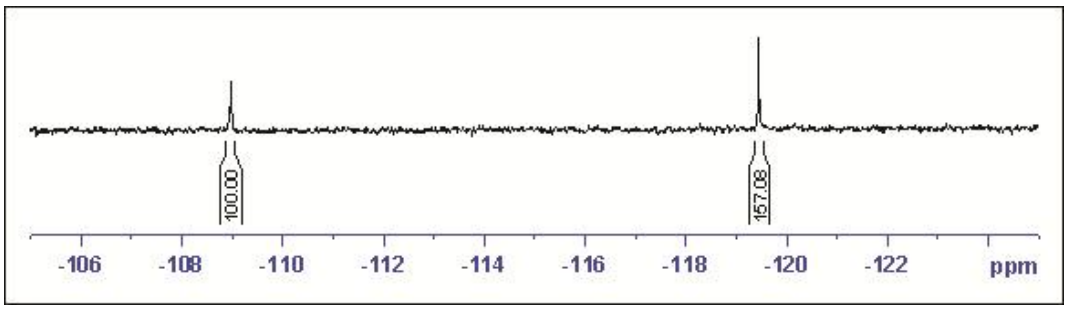

Figure 2.III.17: ^{19}F qNMR spectrum of FLUR (0.3 mg/mL) from Allergan.

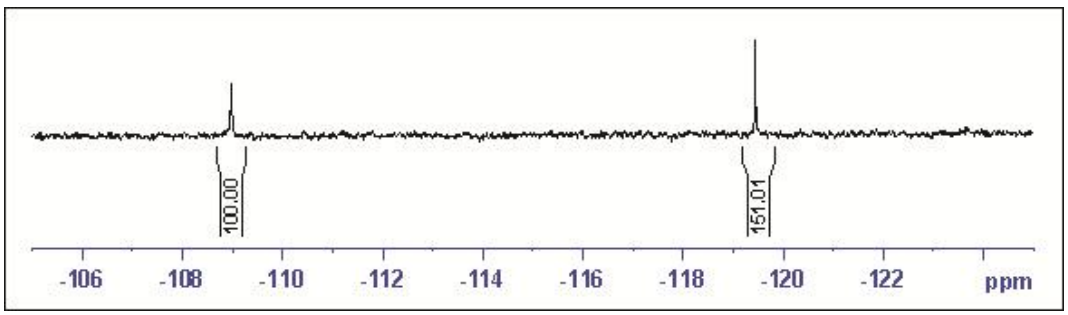

Figure 2.III.18: ^{19}F qNMR spectrum of FLUBI (0.03 %w/v) from Entod Pharmaceuticals Ltd.

Sr. No.		Label claim in mg	W_x in mg	P_x
1	Sample - 1	0.21	0.209	98.52
2		0.21	0.209	98.76
3	Sample - 2	0.21	0.208	98.11
4		0.21	0.214	101.06

Table 2.III.28: Assay of Flurbiprofen by ^{19}F qNMR in commercial samples

Conclusion

^{19}F qNMR spectroscopy provides a highly specific tool for detection, identification and quantification. In a single run all the fluorine nucleus including unexpected substances in the bulk solutions of biofluids or any type of fluorinated pharmaceutical formulations observed with minimal signal overlap and not hampered by dynamic range problems due to presence of water.

The ^{19}F qNMR method developed for the quantification of Flurbiprofen in this study has been shown to be rapid as well as easy to perform. The different aspects of performance of the method such as linearity, precision, accuracy, recovery, robustness, ruggedness and solution stability were studied and in each case showed satisfactory results against the limit. Hence, it can be concluded that, the ^{19}F qNMR method can serve very well as an alternative method for the determination of assay of Flurbiprofen in tablets and eye drops. It offers an excellent alternative choice over previously reported procedures for Flurbiprofen and can be used for in-process, routine quality control for assay and its different pharmaceutical formulation products where there is no interference from excipients and diluents.

Furthermore, linearity and stability of Flurbiprofen in human plasma has shown that the method is very sensitive, linear and stable and hence it can be routinely quantitative used for the direct study at the molecular level of biological samples and their metabolic studies. The equipment operating at a field of 400 MHz or more equipped with suitable data processing software is sufficient for the purpose.

References

1. Dolbier, W.R. *Guide to Fluorine NMR for Organic Chemists*, **2009**, Jhon-Wiley and Sons, New Jersey.
2. (a) Wenyi, H.; Fengpei, D.; Yan, W.; Yinghong, W.; Xin, L.; Hongyue, L.; Xiaodong, Z. *Fluorine Chem*. **2006**, *127*, 809. (b) O'Hagan, D. *J. Fluorine Chem*. **2010**, *131*, 1071.
3. Navratilova, H. *Magn. Reson. Chem.* **2001**, *39*, 727.
4. Fardella, G. P.; Barbetti, I.; Chiappini, G.; Grandolini. *Int. J. Pharm.* **1995,** *121*, 123.
5. Waibel, B.; Holzgrabe, U. *J. Pharm. Biomed. Anal.* **2007**, *43*, 1595.
6. Shamsipur, M.; Leila Shafiee, D.; Zahra, T.; Soheila, H. *J. Pharm. Biomed. Anal.* **2007**, *43*, 1116.
7. Mortino, R.; Veronique, G.; Franck, D.; Myriam, M. *J. Pharm. Biomed. Anal.* **2005**, *38*, 871.
8. Everett, J. R.; Jennings, K.; Woodnutt, G. *J. Pharm. Pharmacol.* **1985**, *37*, 869.
9. Martino, R.; Malet-Martino, M.; Gilard, V. *Curr. Drug Metab.* **2000**, *1*, 271.
10. Malet-Martino, M. C.; Martino, R.; Lopez, A.; Beteille, J. P.; Bon, M.; Bernadou, J.; Armand, J. P. *Biochem. Pharmacol.* **1985**, *34*, 429.
11. Corcoran, O.; Lindon, J. C.; Hall, R.; Ismail, I. M.; Nicholson, J. K. *Analyst*, **2001,** *126*, 2103.
12. Pouremad, R.; Bahk, K. D.; Shen, Y. J.; Knop, R. H.; Wyrwicz, A. M. *NMR Biomed.* **1999**, *12*, 373.
13. Hoeltzli, S. D.; Freiden, C. *Biochem. J*. **1994**, *33*, 5502.
14. Hoeltzli, S. D.; Freiden, C. *Biochem. J.* **1996**, *35*, 16843.
15. Gerig, J. T. *Methods Enzymol.* **1989**, *177*, 3.
16. Gerig J. T.; *NMR Spectroscopy*, **1994**, *26*, 293.
17. Wade, K. E.; Troke, J.; Macdonald, C. M.; Wilson, I. D.; Nicholson, J. K. *Methodoi Surv. Biochem. Anal.* (*Bioanal. Drugs Metab.*) **1988**, *18*, 383.
18. Hull, W. E.; Kunz, W.; Port, R. E.; Seller, N. *NMR Biomed.* **1988**, *1*, 9.
19. Meeh, L. A.; Ackerman, J. J. H.; Thorpe, S. R.; Daugherty, A. *Biochem. J.* **1992**, *286*, 785.

20. Taylor, R.; Abdul-Sada, A. K.; Boltalina, O. V.; Street, J. M. *Perkin* 2, **2000**, *5*, 1013.
21. Stebbins, J. F.; Zeng, Q. *J. Non-Cryst. Solids*, **2000**, *262*, 1.
22. Loewen, M. C.; Klein-Seetharaman, J.; Getmanova, E. V.; Reeves, P. J.; Schwa, I. H.; Khorana, H. G. *Proc. Natl. Acad. Sci. U.S.A.* **2001**, *98*, 4888.
23. Mabury, S. A.; Wilson, R. I.; Ellis, D. A. *Proceedings of 220th AGRO-093, Am. Chem. Soc.* **2000**, USA.
24. Krebs, H. C.; Kemmerling, W.; Habermehl, G. *Toxicon*, **1994**, *32*, 909.
25. Charton. M. *Prog. Phys. Org. Chem.* **1971**, *8*, 235.
26. Dorai, K.; Kumar, A. *Chem. Phys. Lett.* **2001**, *176*, 335.
27. Peng. J. W. *J. Magn. Reson.* **2001**, *32*, 153.
28. Kehrmann. F. *Ber. J. Prakt. Chem.* **1888**, *21*, 3315; **1889**, *22*, 3263; **1890**, *23*, 130.
29. Arunima.; Kurur, N. D. *Magn. Reson. Chem*. **2005**, *43*, 132.
30. *The Merck Index,* **1996,** 12th ed. Merck and Co. Inc. Whitehouse Station, NJ, USA.
31. Shamsipur, M.; Sarkouhi, M.; Hassan, J.; Haghgoo, S. *Afr. J. Pharm.* Pharmacol. **2011**, *5*, 1573.
32. Malz, F.; Jancke, H. *J. Pharm. Biomed. Anal.* **2005**, *38*, 813.

Section-IV

Quantification of Amifostine trihydrate by ^{31}P qNMR and new HPLC method

Introduction:

Phosphorus chemistry has received different classification and systemization since 1970's and has now become into an important branch of chemistry and biochemistry. High-resolution ^{31}P NMR has been widely used to solve different problems in phosphorus chemistry. Published literature provides insight the potential of ^{31}P NMR for the identification, structural determinations and quantification.[1-3]

The first method for quantitative phosphorous nucleus was developed by Gard by optimization of parameters with respect to accuracy, precision and analysis time.[4] The authors quantitatively determined short chain phosphates, in controlled inter laboratory analyses using commercial sodium Tripolyphosphate as internal standard. These results were comparable to that of chromatography and also superior to IR and XRD. The other internal standards which have been used include Dimethyl-methylphosphonate, Methylphosphonic acid (MPA), Phenylphosphinic acid (PPA), Triphenylmethyl-phosphonium bromide and 3-Aminopropylphosphonic acid.

Hanssum determined the spin-lattice relaxation time values for many phosphorous compounds using fast recovery FT experiments.[5] Similarly, Becker[6] and Rabenstein[7] developed the computational simulation methods to ensure sufficient relaxation of spin systems for accurate integration in quantification.

Ruppel *et al,* Stothers *et al* and Paul *et al* reported the different features of high-resolution ^{31}P NMR as a technique in elucidating complex chemical structures, different pulse techniques for sensitivity enhancement by FT- NMR (pulsed FID) and the ^{31}P chemical shifts variations of phosphonates.[8-10] West *et al,* Lumsden *et al* and Dransfeld *et al* studied the prediction of phosphorus NMR shift values.[11-13] Chesnut *et al,* Patchkovskii *et al* reported the theoretical determination of phosphorus chemical shielding tensor by using ^{31}P NMR spectroscopy.[14,15]

Qualitative application of ^{31}P qNMR has now become popular, due to advancement and rapid development in pulsed field gradient (PFG) NMR technology

with probe head design. Several specific publications have appeared in the literature for diverse applications. Miyata *et al* developed ^{31}P qNMR techniques for quantifying an internal standard to confirm its purity before being used for further quantification.[16]

Maniara and coworkers demonstrated[17] the significance of NMR as an independent and intrinsically reliable technique in establishing the purity of organic compounds especially, agrochemicals with both high accuracy and precision of the method. ^{31}P qNMR spectroscopy method offered non-chromatographic alternatives for quantifying organic materials as well as the quality assessment of reference compounds, qNMR was introduced and developed with the focus on its potential for the certification and quality control of reference compounds.

Product identification of commercial technical grade phosphates,[2] used for detergent products and their structure elucidation.[3] Chelating agents,[4] food,[9] medicine,[18-20] and in pharmaceuticals[21] are also routinely analyzed in many analytical laboratories.

2.IV.1: Applications of ^{31}P qNMR:

Pharmaceutical sciences

Appleton *et al* and Trevor *et al* studied qualitative application of ^{31}P qNMR in several areas such as organo phosphate complexes.[22-23] In 1993, Rana and coworkers identified the composition of binary mixtures of phospholipids by IR spectroscopy combined with ^{31}P qNMR, and showed that NMR method is well suited for quantitating the relative molar amounts of analytes through their optimization of spin lattice relaxation time.[24]

Recently, Nouri-Sorkhabi developed a method for the quantification of phospholipids and was able to resolve the narrow resonance lines of phospholipids in the erythrocyte membranes of human. The reported method was rapid, and significantly more accurate than conventional methods of time-consuming extractions.[25]

Teleman and coworkers applied quantitative measurement of ^{31}P qNMR for all low-molecular weight phosphorylated compounds in yeast by the use of high field and the neutral pH extracts, which are suitable for NMR analysis. The low concentration

of trimetaphosphate (0.2 mM intracellular concentration) was also detected in cold methanol-chloroform as well as perchloric acid extracts.[26]

Martino *et al* developed a suitable analytical technique for quantitative in-vitro metabolic studies of fluorinated or phosphorylated drugs using ^{19}F or ^{31}P qNMR spectroscopy.[27]

Medical science

^{31}P NMR spectroscopic technique is the only physical absolute method used routinely for the direct study at the molecular level of biological samples from biofluids, cell or tissue extracts. As phosphorus metabolites are found in human bodies, in medical science it has now become possible to utilize ^{31}P qNMR for the quantification of these metabolites as studied by Doyle.[28] The ^{31}P MRI spectra is also another application area in medicine.

The metabolic changes in the rat brain after acute and chronic ethanol intoxication was studied by the Denays by ^{31}P qNMR spectroscopy in which the variations in phosphodiester signal intensities suggested that concentration increases in the rat brain of membrane phospholipids and change in the cerebral atrophy in chronic alcoholism.[29]

Matson and coworkers developed a methodology for the quantification of *in vivo* ^{31}P MRS results through computer simulations.[30] Various studies and quantification methods have been developed by Chow *et al*, Wehrli *et al*, Odahara *et al*, Cady *et al* and Elliott *et al* utilizing changes in T_1 values, 2D, MRI, artificial neural network, and ^{31}P NMR spectroscopy in medical applications.[31-35] Hetherington and coworkers developed the methodology for the determination of phosphocreatine in human brain by quantitative ^{31}P NMR imaging[36] and subsequently Tosner *et al* used the similar methodology for the content of phosphocreatine in human liver.[37]

The use of ^{31}P NMR in quantifying membrane vesicle subtractions has been reported by Larijani and coworkers.[38] Subsequently, Belloque and coworkers quantified phosphorylated compounds in milk by this technique.[39] Bretthost, Kotyk reported ^{31}P qNMR method having high potential for quantification of biological fluids, by using principal component analysis (PCA).[40,41] Authors also introduced the

Bayesian Probability Theory (BPT), a new formalism for NMR parameter estimation. It is a rigorous statistical methodology to estimate NMR parameters.

Other applications of ^{31}P qNMR

Spyros and coworkers determined the mono and diglyceride composition of olive oil by phosphorylation of the free hydroxyl groups of glycerides and quantifying them by using ^{31}P qNMR techniques with the mole ratio method.[42] The water content of glassy silver metaphosphate was determined by Mustarelli and coworkers and the results complied well with those of thermal analysis.[43]

In 1999, Argypoulos group developed a quantitative method based on the measurement of relaxation time of quinonoid in isolated lignins which form adducts with trimethyl phosphite in which triphenyl phosphate was used as internal standard.[44]

Solid state ^{31}P NMR

Kirszensztejn and coworkers studied the acidic sites on Al_2O_3 by solid-state ^{3l}P NMR.[45] Peters *et al* and Roberie *et al* developed a method for quantification of Lewis-acid sites of solid acid catalysts by using ^{31}P solid-state NMR and thereby confirming its diversity.[46,47]

2.IV.2: Drug:

Amifostine is an organic thiophosphate cytoprotective agent known chemically as 2-[3-(Aminopropyl) amino] ethanethiol dihydrogen phosphate ester. It is a white crystalline powder which is freely soluble in water having empirical formula $C_5H_{15}N_2O_3PS$ with molecular weight of 214.22. The structural formula of Amifostine trihydrate (Fig.2.IV.1) is given below: [48,49]

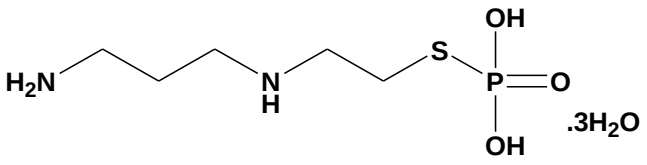

Figure 2.IV.1: Amifostine trihydrate

Amifostine is used therapeutically to reduce the incidence of neutropenia-related fever and also to reduce infection induced by DNA-binding chemotherapeutic (radio protective) agent.[50] It is also used to decrease the cumulative nephrotoxicity

associated with platinum-containing agents.[51] It is generally supplied as a sterile lyophilized powder requiring reconstitution for IV (intra venous) infusion under the brand name Ethyol® which is the trihydrate form of amifostine.[48-51] Amifostine also reduces the cumulative renal toxicity associated with repeated administration of cisplatin in patients with advanced ovarian cancer as well as the incidence of moderate to severe xerostomia in patients undergoing post operative radiation treatment for head and neck cancer.

Accurate, quantitative measurements by NMR are of considerable interest for quality control, in stability studies, and in answering process-related questions.

There are many analytical methods in various Pharmacopeias for the quantification of different drugs but almost all the methods are based on HPLC using absorption detectors which require presence of chromophore in the drug for detection.[20] For the analysis of pharmaceutical products containing phosphorous like Amifostine trihydrate, ^{31}P qNMR has a high potential due to its simplicity, reliability and simultaneous identification. The quantification method can be easily validated as per the ICH guidelines.[52]

Since chromophore limitation is unavoidable in HPLC with UV-Vis detector, the efforts in the present study are directed towards developing a competitive and selective ^{31}P NMR method,[53-56] for the assay determination of API and its injection of amifostine drug by using di-potassium hydrogen ortho-phosphate (K_2HPO_4) as an internal standard.[57,58] In addition, a new reversed phase HPLC method has also been developed by using newly available zwitterions solid phase column chemistry. The results and analytical parameters obtained from both ^{31}P qNMR and new HPLC methods have been well validated which have many advantages over the official US pharmacopeia HPLC method.

2.IV.3: Experimental:

2.IV.3.1: Materials and reagents:

High purity analytical and ICH grade materials were used throughout the study, Amifostine USP was provided by Sun Pharmaceuticals Industries Ltd. (Vadodara, India). K_2HPO_4 analytical reagent grade was purchased from Qualigens, India (99.0 %), Deuterium Oxide (D_2O) diluent was purchased from Merck Germany (99.96 % D). The following materials were also used in HPLC method: Acetonitrile HPLC grade (Merck, India), Analytical Grade Ammonium acetate (Rankem, India) as a buffer. All solutions were prepared in MilliQ water.

2.IV.3.2: Instrumentation:

All the ^{31}P qNMR spectra were recorded on a Bruker AV-III 500MHz (11.7 T) spectrometer operating at proton frequency 500.13 MHz and ^{31}P frequency 202.45 using 5 mm Broad Band Observe probe head. All data were processed using Topspin 2.1 software from Bruker. For all the ^{31}P-NMR measurements carried out for method development, 16 scans were collected into 32k data points over a spectral width of 15151.51Hz with a transmitter offset in the centre of the spectrum. The acquisition time was 9.49 min followed by a relaxation delay of 35 s. All spectra were recorded at 295 K using a flip angle 90°. An exponential line broadening window function at 5.0 Hz was used in the data processing and baseline corrections were done automatically while phasing was always performed manually.

For accurate quantitative NMR analysis, the proper value of relaxation delay (d_1) was generally set to more than or equal to five times the value of the longest spin-lattice relaxation time (T_1) of the integrated resonance signals in order to ensure full relaxation of the corresponding phosphorous nuclei. The T_1 relaxation times were measured by using the inversion-recovery pulse sequence. The maximum T_1 values for ^{31}P so obtained was 6.96 s for K_2HPO_4 peak at 2.3 ppm, while in the case of Amifostine it was 4.21s at 15.78 ppm.

***Diluent*:** Deuterium Oxide (D_2O)

Internal Standard (IS) stock solution

K_2HPO_4 (IS), 834.24 mg was dissolved in a small amount of D_2O taken in a 100 mL volumetric flask and the volume was made up to the mark with diluent. Then 25 mL of this solution was further diluted to 50 mL in a volumetric flask using D_2O as diluent. The resulting solution was used as diluent throughout study.

Sample preparation

10 mg of Amifostine trihydrate was accurately weighed and dissolved in 1 mL of IS solution in a 2 mL vial.

HPLC Column

The silica based zwtterionic hydrophilic interaction liquid chromatography (HILIC) column, **ZIC®-HILIC** manufactured by SeQuant™ Merck, Germany was used. The stationary phase of this column is made up of a covalently bonded, permanently zwtterionic, functional group of the sulfobetaine type polymer particles. This stationary phases were designed for efficient HILIC separation of acidic, basic and neutral hydrophilic compounds.

Gradient programme

The quantitative gradient HPLC method for analysis of Amifostine trihydrate was performed on Waters Model-2695, HPLC system with 2487 dual wavelength detector using Empower software using ZIC-HILIC column with dimensions 100×4.6 mm, pore size 100A°, particle size 5µm. Mobile phases used were A: consisting of 10 mM solution of ammonium acetate in water and B: 100% Acetonitrile. The HPLC system was operated at flow rate of 1.0 mL/min, the detection wavelength was set at 220 nm, injection volume 50µL, run time 17 min and the column temperature at 40°C.

A mixture of ammonium acetate buffer and acetonitrile in the ratio of 85 : 15 and was used as diluent. Optimized gradient condition used was : from 70 % B to 40 % B in 0 to 10 min, stayed at 40 % B from 10 to 12 min, then changed gradient from 40 % B to 70 % B from 12 min to in 12.1minutes and stayed at 70 % B till 17 min as given in Table 2.IV.1.

Time in min	% Mobile phase A	% Mobile phase B
0	30	70
10	60	40
12	60	40
12.1	30	70
17	30	70

Table.2.IV.1: Gradient program for HPLC method

Stock preparation (sample)

The stock solution was prepared by accurately weighing 20.092 mg of Amifostine trihydrate and transferring it into 10 mL volumetric flask. Then about 5 mL of the diluent was added into the flask and sonicated for 1 min to dissolve the sample completely and the content was diluted up to mark with the diluent.

Standard preparation

20.040 mg of Amifostine trihydrate standard was weighed accurately and transfer into a 100 mL volumetric flask, then about 25 mL of diluent was added into the flask and sonicated for 1 min to dissolve it completely and diluted up to the mark with diluent.

Sample preparation

Similarly six (A-1 to A-6) sets of Amifostine trihydrate sample given in Table 2.IV.2 was accurately weighed and transferred into a 100 mL volumetric flask then about 25 mL of diluent was added into the flask and sonicated for 1 min to dissolve completely and diluted up to mark with diluent.

Sample name	**A-1**	**A-2**	**A-3**	**A-4**	**A-5**	**A-6**
Weight in mg	20.044	20.059	20.065	20.071	20.075	20.080
Final dilution in mL	100	100	100	100	100	100
Final concentration in (μg/mL)	200.44	200.59	200.65	200.71	200.75	200.80

Table: 2.IV.2: Sample preparation for method precision study

2.IV.4: Results and discussion:

2.IV.4.1: ^{31}P qNMR spectroscopy method:

The ^{31}P NMR spectrum of the amifostine sample containing the internal standard is shown in Figure 2.IV.2 The signals at (δ) 2.3 ppm and 15.78 ppm (chemical shift calibrated with external standard signal of H_3PO_4 δ = 0 ppm in D_2O) are due to IS (K_2HPO_4) and amifostine trihydrate. ^{31}P signal of amifostine at (δ) 15.78 ppm appears as a triplet with approximate coupling constant *J* = 14 Hz due to the presence of neighboring -CH_2-protons. The integral values of the ^{31}P signals are found to be directly proportional to the number of nuclei and weight of the sample.

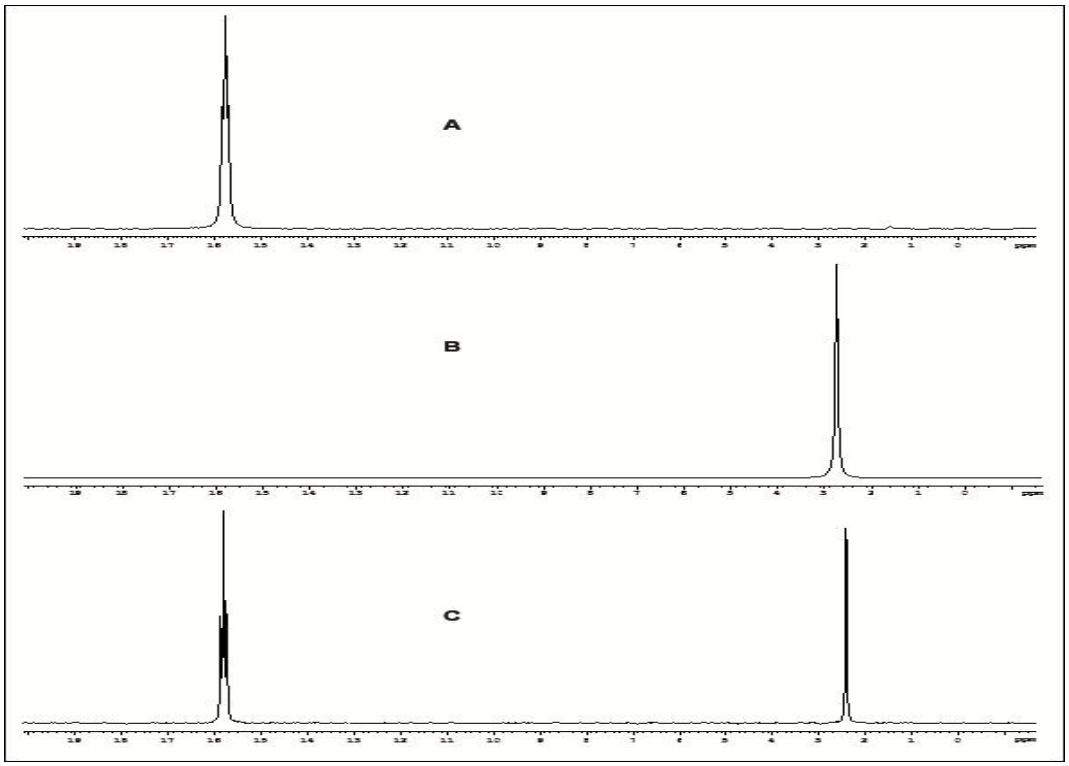

Figure 2.IV.2: ^{31}P qNMR spectrum of (A) Amifostine trihydrate (B) K_2HPO_4 and (C) mixture of Amifostine trihydrate and K_2HPO_4 in D_2O

The triplet pattern (J_{P-H} = 14.1 Hz) observed in the ^{31}P NMR spectrum of Amifostine trihydrate is due to methylene (-CH_2-) protons β– to phosphorous nucleus and which was confirmed by proton decoupling NMR spectra shown in Figure 2.IV.3. Similarly, the irradiation of γ–methylene group protons from the phosphorous atom by homonuclear proton decoupled spectra given in Figure 2.IV.4 shows a doublet (J_{P-H} = 14.1 Hz) which reveals that triplet pattern is only due to methylene group proton coupling phosphorous nuclei.

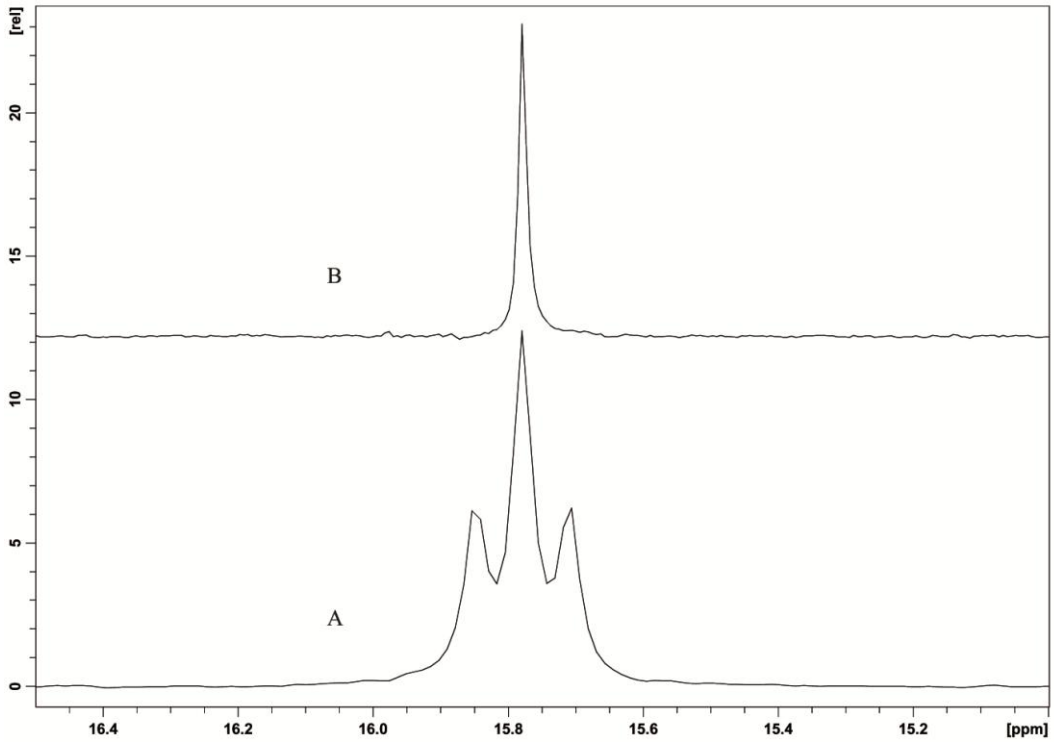

Figure 2.IV.3: (A) Proton coupled ^{31}P NMR of Amifostine trihydrate in D_2O and (B) Proton decoupled ^{31}P NMR of Amifostine trihydrate in D_2O

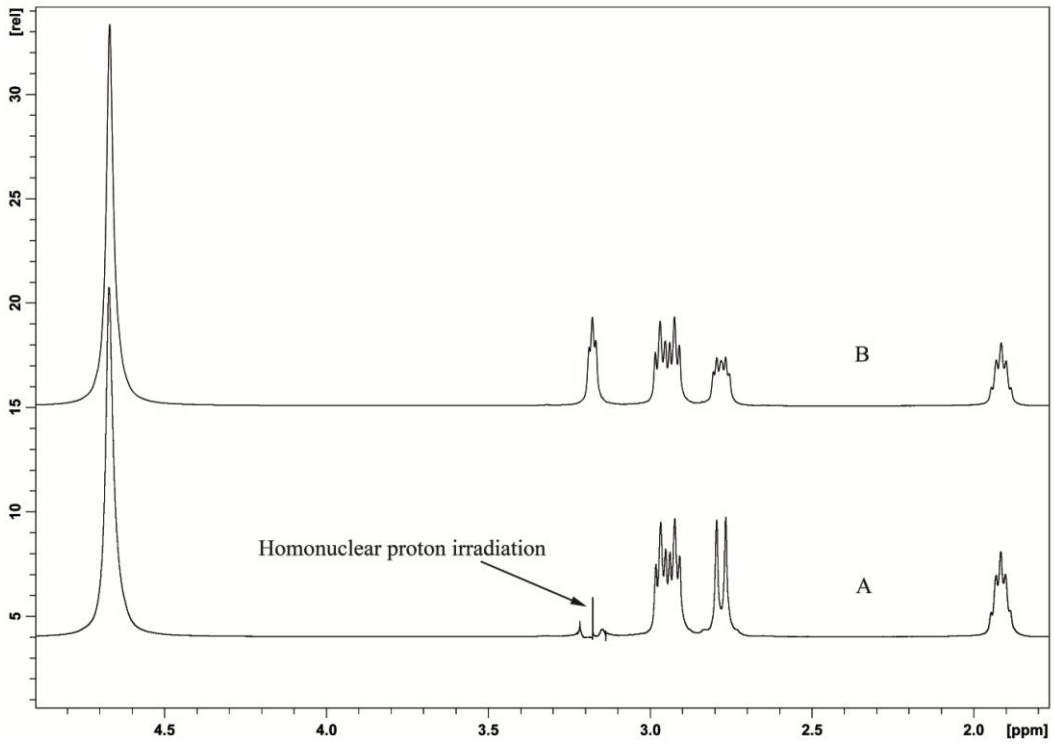

Figure 2.IV.4: ^{1}H-NMR spectrum of (A) Amifostine trihydrate irradiated at 3.2 ppm and (B) ^{1}H-NMR spectrum of Amifostine trihydrate in D_2O

2.IV.4.2: ^{31}P qNMR assay calculation:

For assay determination a known potency substance, K_2HPO_4, was used as an internal standard, and found to be most suitable for the ^{31}P qNMR assay determination.

Assay was determined by using the Equation (2-11) given below:

$$P_x = \frac{I_x}{I_{std}} \times \frac{N_{std}}{N_x} \times \frac{M_x}{M_{std}} \times \frac{W_{std}}{W} \times P_{std} \qquad (2\text{-}11)$$

where, P_x = Assay of the Amifostine (in % w/w) on as is basis

I_x , I_{std} = Integral value of amifostine at 15.78 ppm and of K_2HPO_4 IS obtained at 2.31 ppm respectively, (Chemical shift (δ) values are reported with the external calibration standard phosphoric acid in D_2O at δ= 0.0ppm)

N_{std} , N_x = Number of phosphorous nuclei for K_2HPO_4 IS and Amifostine respectively

M_x , M_{std} = Molar mass of the amifostine drug (214.26 g/mol), and K_2HPO_4 IS (174.18 g/mole) respectively

W_{std}, W = Weight of the K_2HPO_4 IS (in mg), the amifostine (mg) respectively

P_{std} = Potency of the K_2HPO_4 IS (99.0%)

The LOD and LOQ were calculated (Equation 2-12 and 2-13) by using the standard deviation of the response ‘σ’ and the slope ‘s’ of a calibration curve obtained in linearity study.

$$LOD = \frac{3.3\,\sigma}{S} \qquad (2\text{-}12)$$

$$LOQ = \frac{10\,\sigma}{S} \qquad (2\text{-}13)$$

The validity of the proposed ^{31}P qNMR method was established through linearity, method precision, LOD, LOQ, ruggedness, robustness, solution stability and recovery studies.

2.IV.4.3: Linearity:

The linearity was evaluated and established by triplicate analysis of standard solutions at eleven different concentration levels according to the content of analyte in test sample as given in Table 2.IV.3. Linearity curve was plotted for amount of drug

taken in (mg) on x-axis against amount of drug found in (mg) on y-axis (Fig.2.IV.5). Good linearity is evident (r^2 = 0.9975) from the figure over the examined concentration range from 5 % to 200 % with respect to label claim. Equation for the curve is y = 0.7687x ± 0.1598.

Sr. No.	m	I_x	W_x	P_x
1	0.41	10.30	0.32	77.43
2	0.62	15.55	0.48	77.53
3	1.53	37.14	1.14	74.65
4	2.59	67.72	2.08	80.42
5	5.00	129.78	4.00	79.83
6	7.61	209.25	6.44	84.57
7	10.09	266.21	8.20	81.15
8	12.46	325.29	10.01	80.29
9	15.14	390.50	12.02	79.33
10	17.49	436.79	13.45	76.81
11	20.01	489.36	15.07	75.22

Table 2.IV.3: Linearity data of Amifostine trihydrate by ^{31}P qNMR

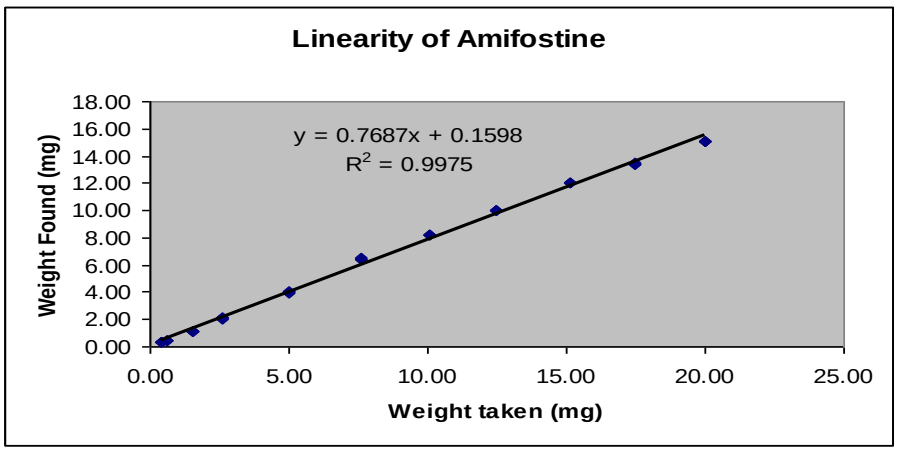

Figure 2.IV.5: Linearity plot of Amifostine trihydrate by ^{31}P qNMR

2.IV.4..4: LOD and LOQ:

From the ^{31}P qNMR spectral pattern with Lorentzian lines as response signals, the LOD and LOQ were calculated using Equation (2-12) and (2-13) respectively**.** LOD and LOQ were found to be 0.08 mg and 0.25 mg per 1.0 mL of diluents respectively.

2.IV.4.5: Solubility range:

The range study was carried out by preparing saturated solution by adding excess drug amount and analyzing supernatant solution to determine the dissolved concentration of the drug. In the case of Amifostine saturation concentration was found to be approximately ~250 mg per 1 mL diluent.

2.IV.4.6: Precision and intermediate precision (Ruggedness):

The method precision was evaluated as the repeatability, by calculating the relative standard deviation (% RSD) of the ^{31}P NMR signal areas of Amifostine trihydrate for six determinations under the same experimental conditions presented in Table 2.IV.4. The % RSD of amifostine trihydrate so calculated is 1.64 which is well within the acceptable limit of not more than 5.

Ruggedness of the method was ascertained by allowing a different analyst to carry out the experiment, magnetic field (400 MHz instrument instead of 500 MHz instrument) and by using different probe head (QNP-F) under the same acquisition parameters and data processing. The results of this investigation are presented in Table 2.IV.5 and Table 2.IV.6 respectively. The % RSD of Amifostine trihydrate determined are 1.59 and 2.49 which are well within acceptable limit of not more than 5.

Sr. No.	m	I_x	W_x	P_x	Mean	% RSD
1	10.03	256.54	7.88	78.48	79.63	1.64
2	9.99	264.29	8.13	81.32		
3	10.18	267.83	8.23	80.76		
4	10.02	257.95	7.93	79.09		
5	10.12	263.49	8.12	80.13		
6	10.01	254.35	7.82	78.03		

Table 2.IV.4: Method precision of Amifostine trihydrate by ^{31}P qNMR

Sr. No.	m	I_x	W_x	P_x	Mean	% RSD
1	10.03	255.69	7.87	78.41	80.96	1.59
2	9.99	265.76	8.18	81.82		
3	10.18	269.95	8.31	81.56		
4	10.02	263.57	8.11	80.90		
5	10.12	267.99	8.25	81.44		
6	10.01	265.66	8.18	81.62		

Table 2.IV.5: Method precision (Different Analyst) of Amifostine trihydrate by ^{31}P qNMR

Sr. No.	m	I_x	W_x	P_x	Mean	% RSD
1	10.61	269.39	8.29	78.09	80.11	2.49
2	10.55	269.64	8.30	78.61		
3	9.94	268.78	8.27	83.17		
4	10.10	268.32	8.26	81.71		
5	10.27	268.05	8.25	80.27		
6	10.48	268.60	8.27	78.83		

Table 2.IV.6: Method precision (Instrument change) of Amifostine trihydrate by ^{31}P qNMR

2.IV.4.7: Accuracy and recovery study:

The accuracy was studied at 80 %, 100 % and 120 % levels, specified range covered under ICH guidelines, with respect to the sample by preparing the solutions in triplicate at each level. The values given in the Table 2.IV.7, Table 2.IV.8 and Table 2.IV.9 for the concentrations when compared to the nominal values produced an accuracy of 83.00 %, 81.80 % and 80.02 % with an average % RSD value 0.73, 0.87 and 1.66 respectively. The results are within limit of accuracy 80 % to 120 % and % RSD not more than 10.

Similarly, the recovery data corresponding to 50 %, 100 % and 150 % of the analytical concentrations as given in Table 2.IV.10, Table 2.IV.11 and Table 2.IV.12 respectively are 81.86 %, 81.86 %, and 81.09 % with an average % RSD value 0.30, 1.23 and 0.29 respectively, the acceptable limit for % RSD is not more than 10. Thus the developed method proofs to be acceptable from both accuracy and recovery point of view.

Level	m	I_x	W_x	P_x	Mean	%RSD
80 %	9.21	249.01	7.67	83.16	83.00	0.73
	10.98	293.91	9.05	82.33		
	10.23	277.76	8.55	83.51		

Table 2.IV.7: Accuracy at 80 % level of Amifostine trihydrate by ^{31}P qNMR

Level	m	I_x	W_x	P_x	Mean	%RSD
100%	12.12	319.36	9.83	81.04	81.80	0.87
	13.56	364.08	11.21	82.46		
	13.68	364.25	11.21	81.89		

Table 2.IV.8: Accuracy at 100 % level of Amifostine trihydrate by ^{31}P qNMR

Level	m	I_x	W_x	P_x	Mean	%RSD
120%	14.73	379.46	11.68	79.07	80.02	1.66
	15.59	402.77	12.40	79.46		
	15.83	419.70	12.92	81.54		

Table 2.IV.9: Accuracy at 120 % level of Amifostine trihydrate by ^{31}P qNMR

Level	m	I_x	W_x	P_x	Mean	%RSD
50%	5.10	135.46	4.17	81.69	81.86	0.30
	5.25	140.20	4.32	82.14		
	5.30	140.86	4.34	81.74		

Table 2.IV.10: Recovery at 50 % level of Amifostine trihydrate by ^{31}P qNMR

Level	m	I_x	W_x	P_x	Mean	%RSD
100%	10.90	292.94	9.02	82.66	81.86	1.23
	10.23	273.40	8.42	82.20		
	10.15	266.43	8.20	80.73		

Table 2.IV.11: Recovery at 100 % level of Amifostine trihydrate by ^{31}P qNMR

Level	m	I_x	W_x	P_x	Mean	%RSD
150%	14.99	395.91	12.19	81.23	81.09	0.29
	14.99	395.83	12.19	81.22		
	15.21	399.63	12.30	80.81		

Table 2.IV.12: Recovery at 150 % level of Amifostine trihydrate by ^{31}P qNMR

2.IV.4.8: Solution stability of analyte:

In this investigation, standard preparation and sample preparation were analyzed at ambient temperature (~25 °C) at 0 h (Initial), 24 h, 36 h, 60 h, 90 h and 180 h intervals and % assay for each interval was calculated. The observed results at different time intervals are very close to that of the freshly prepared sample and no major change upto 36 h at ambient temperature presented in Table 2.IV.13. Hence the solution can be considered stable upto 36 h.

Time interval (h)	m	W_x	P_x	Difference
0	10.05	7.99	79.41	N.A.
24	10.05	7.99	79.39	0.02
36	10.05	7.98	79.34	0.07
60	10.05	7.71	76.64	2.77
90	10.05	7.71	76.67	2.74
180	10.05	7.71	76.68	2.73

Table 2.IV.13: Solution stability of Amifostine trihydrate by ^{31}P qNMR

2.IV.4.9: Robustness:

The robustness of the method was evaluated by varying two parameters independently such as number of scans and amount of internal standard up to 40 % variation (2.5 ± 1.2 mg). The experimental results of this study are given in Table 2.IV.14. The results observed at different number of scans from 8 to 40 rather than 16 do not show much difference. Similarly variation of internal standard (Table 2.IV.15) amount also did not appreciably change the measured amount of drug. Therefore, this method is quite robust in terms of the parameters that are varied in these experiments.

Parameter	Change	I_x	m	W_x	P_x	Difference
No. of scan	8	317.95	12.3	9.79	79.50	0.04
	16	318.11	12.3	9.79	79.54	N/A
	24	318.15	12.3	9.79	79.55	-0.01
	32	318.24	12.3	9.80	79.57	-0.03
	40	318.34	12.3	9.80	79.60	-0.06

Table 2.IV.14: Number of scan variations of Amifostine trihydrate by ^{31}P qNMR

Parameter	Change	I_x	m	W_x	P_x	Difference
Std. conc. with matrix	2.5	318.11	12.3	9.79	79.54	N/A
IS variation with matrix	1.58	274.9	6.83	5.34	78.15	1.39
IS variation with std.	3.61	154.51	8.67	6.86	79.06	0.48

Table 2.IV.15: IS variation of Amifostine trihydrate by ^{31}P qNMR

Additional parameters of robustness study

The robustness of the method was further evaluated by varying several instrumental parameters independently such as variation in sample depth (Table 2.IV.16), mode of shimming (Table 2.IV.17), spinning rate (Table 2.IV.18), sweep width (Table 2.IV.19), offset (Table 2.IV.20), pulse length (Table 2.IV.21) and temperature (Table 2.IV.22). The following results indicate that if the sample depth is more than 3.0 cm, offset value within 5 to 12 ppm and temperature within 5 °C to 37 °C then the method can be successfully used. The influence of other parameters was not significant and therefore the proposed method is robust.

Parameter	Change	I_x	m	W_x	P_x	Difference
Sample depth	1.5 cm	129.21	8.33	2.66	79.87	-45.94
	3.0 cm	124.72	8.33	6.13	77.09	-4.28
	4.5 cm	127.30	8.33	6.56	78.69	-0.82
	6.0 cm	125.71	8.33	6.48	77.71	0.16
	7.5 cm	125.97	8.33	6.49	77.87	N/A

Table 2.IV.16: Sample depth variation of Amifostine trihydrate by ^{31}P qNMR

Parameter	Change	I_x	m	W_x	P_x	Difference
Mode of shimming	Non-spin	147.49	9.71	7.60	78.21	-0.53
	Manual	148.07	9.71	7.63	78.52	-0.84
	Topshim	146.48	9.71	7.55	77.68	N/A
	Autoshim	146.40	9.71	7.64	78.58	-0.90
	Simplex	146.82	9.71	7.62	78.40	-0.72

Table 2.IV.17: Mode of shimming of Amifostine trihydrate by ^{31}P qNMR

Parameter	Change	I_x	m	W_x	P_x	Difference
Spinning rate in rps	0	140.20	9.33	7.23	77.37	0.09
	8	141.15	9.33	7.27	77.90	-0.44
	12	142.82	9.33	7.26	77.81	-0.35
	16	141.49	9.33	7.29	78.08	-0.62
	20	140.36	9.33	7.23	77.46	N/A
	24	141.14	9.33	7.27	77.89	-0.43
	28	141.66	9.33	7.30	78.18	-0.72
	32	140.24	9.33	7.23	77.39	0.07

Table 2.IV.18: Spinning rate variation of Amifostine trihydrate by ^{31}P qNMR

Parameter	Change	I_x	m	W_x	P_x	Difference
Sweep width in ppm	60	149.45	9.81	7.70	78.44	-0.19
	70	149.44	9.81	7.70	78.44	-0.19
	75	149.08	9.81	7.68	78.25	N/A
	80	149.33	9.81	7.70	78.38	-0.13
	90	149.82	9.81	7.72	78.64	-0.39
	100	148.55	9.81	7.66	77.97	0.28

Table 2.IV.19: Sweep width variation of Amifostine trihydrate by ^{31}P qNMR

Parameter	Change	I_x	m	W_x	P_x	Difference
Offset at ppm	-5	150.17	9.71	7.74	79.63	-1.95
	0	148.63	9.71	7.66	78.81	-1.13
	5	148.35	9.71	7.65	78.67	-0.99
	10	146.48	9.71	7.55	77.68	N/A
	12	148.54	9.71	7.66	78.77	-1.09
	20	149.98	9.71	7.73	79.53	-1.85
	25	148.77	9.71	7.67	78.89	-1.21

Table 2.IV.20: Offset variation of Amifostine trihydrate by ^{31}P qNMR

Parameter	Change	I_x	m	W_x	P_x	Difference
Pulse length in µs	1.250	149.32	9.85	7.70	78.06	0.24
	2.500	149.64	9.85	7.71	78.22	0.08
	3.750	150.68	9.85	7.77	78.76	-0.46
	5.625	149.67	9.85	7.71	78.24	0.06
	7.500	149.87	9.85	7.72	78.34	-0.04
	9.375	151.22	9.85	7.79	79.05	-0.75
	11.250	149.78	9.85	7.72	78.30	N/A

Table 2.IV.21: Pulse width variation of Amifostine trihydrate by ^{31}P qNMR

Parameter	Change	I_x	m	W_x	P_x	Difference
Temperature in K	275	152.88	9.95	7.88	79.11	-0.02
	285	153.53	9.95	7.91	79.45	-0.36
	295	152.84	9.95	7.88	79.09	N/A
	305	154.04	9.95	7.94	79.71	-0.62
	310	153.44	9.95	7.91	79.40	-0.31
	320	150.51	9.95	7.76	77.89	1.20

Table 2.IV.22: Sample temperature variation of Amifostine trihydrate by ^{31}P qNMR

2.IV.5: HPLC assay method of Amifostine trihydrate:

Assay of Amifostine trihydrate was calculated by using following the Equation (2-14)

$$Assay\ of\ Amifostine\ trihydrate\ (on\ as\ is\ basis) = \frac{A_t}{A_s} \times \frac{W_s}{100} \times \frac{100}{W_t} \times P \qquad (2\text{-}14)$$

where, A_t = Average area count of Amifostine peak in sample preparation

A_s = Average area count of Amifostine peak in standard preparation

W_t = Weight of Amifostine sample in mg

W_s = Weight of Amifostine standard in mg

P = % Potency of Amifostine standard (as is basis)

Method precision

The proposed reversed phase HPLC method was performed by injecting blank and Amifostine trihydrate standard separately with a run time of 17 min during which Amifostine peak was found to appear at about 9.4 min. The system precision was checked by injecting five replicates of standard solution, the detector response was

calculated from average area of the peak and corresponding % RSD are given in Table 2.IV.23. The theoretical plates and tailing factor were calculated from the standard chromatograms by using Waters Empower software version 2.0. Typical chromatograms are shown in Fig. 2.IV.6. From the above data it can be concluded that the instrument is precise and suitable for the assay determination of Amifostine trihydrate.

Injection No.	Area of standard	Limit
1	862239	Acceptable limit not more than 2.0%
2	866080	
3	868292	
4	868067	
5	861867	
Mean	865309	
Std. deviation	3097	
%RSD	0.36	
Retention time	9.4 min	
Theoretical plates	22045	
Tailing factor	1.13	

Table 2.IV.23: Method precision data of Amifostine trihydrate by HPLC

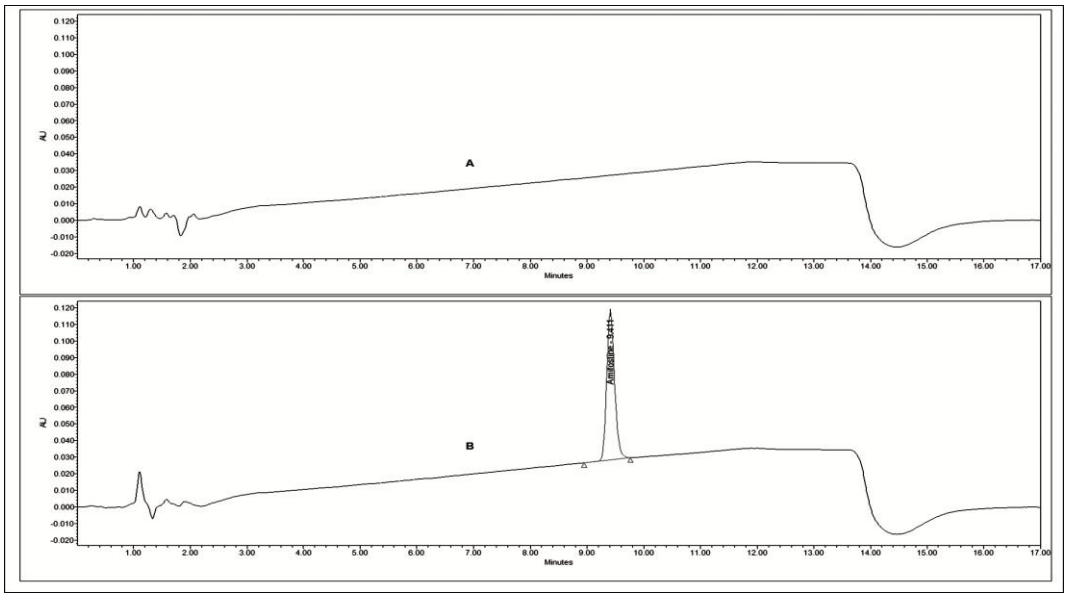

Figure 2.IV.6: HPLC chromatogram of (A) Blank and (B) Amifostine trihydrate

2.IV.5.1: HPLC method validation:

The method validation of the proposed reversed phase HPLC method was performed with following parameters as per the ICH guide lines such as linearity, method precision, LOD, LOQ, ruggedness, robustness, solution stability and forced degradation study.

2.IV.5.2: Linearity:

The linearity was evaluated and established by triplicate analysis of standard solution of Amifostine trihydrate. The sample stock solution, 50 % to 150 % level solutions (with respect to assay concentration chosen) were prepared by dilution as presented in Table 2.IV.24. Each of the following solutions was injected into chromatographic system and from the resulting chromatograms mean area counts of the peaks were calculated.

% Level of standard	Volume of stock solution (mL)	Final dilution (mL)	Final conc. (µg/mL)
50	0.5	10	100.46
75	0.75	10	150.69
100	1	10	200.92
125	1.25	10	251.15
150	1.5	10	301.38

Table: 2.IV.24: Dilution of Amifostine trihydrate for HPLC linearity study

The eluted peak areas given (Table 2.IV.25) were plotted against the corresponding concentration to generate calibration curve given in Figure 2.IV.7 which shows good linearity with linearity Equation $y = 4291.39x \pm 20024.53$ and regression coefficient of $r^2 = 0.999$ within the concentration range studied. The observed data clearly indicates that the proposed Amifostine trihydrate HPLC assay method shows very good linearity from 100 ppm to 300 ppm.

% Level of standard	Area of Amifostine peak			Mean Area	%RSD	Limit
50	407635	408328	409417	408460	0.2	NMT 2.0%
75	637747	634948	632640	635112	0.4	
100	839349	838538	840200	839362	0.10	
125	104950	1048005	104813	1048548	0.1	
150	127771	1279775	128108	1279524	0.1	
Slope					4291.39	
Intercept					-20024.53	
Correlation coefficient					1.000	NLT 0.999

Table: 2.IV.25: Linearity data of Amifostine trihydrate by HPLC method

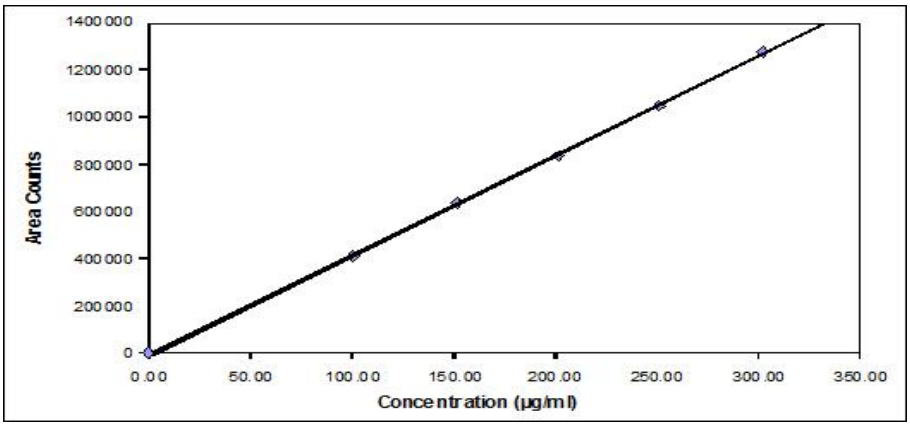

Figure 2.IV.7: Linearity plot of Amifostine trihydrate by HPLC method

2.IV.5.3: Specificity:

The method specificity was determined by carrying out following forced degradation studies. The sample solution was treated separately with acid, alkali, peroxide and heated upto 70°C for degradation study. The sample was also exposed to UV light at 289 nm and sun light for 4 h.

The solutions of the treated samples were prepared as per the procedure given below. These samples were injected into HPLC system under the same chromatographic conditions as fixed for assay. From the recorded chromatograms, the peak purity of Amifostine trihydrate was determined and percentage of residual drug was calculated with respect to the standard drug solution.

Peak purity of Amifostine trihydrate was determined by using PDA detector and results are presented in Table 2.IV.26 which confirms the spectral purity of Amifostine trihydrate peak.

Acid degradation

Accurately weighed 20.0960 mg of Amifostine trihydrate sample was transferred into 100 mL volumetric flask. About 25 mL of diluent was added into the flask and sonicated for 1 min to dissolve it completely. To this, 1 mL of 1M HCl was added and mixed well. Then the resulting solution was diluted up to mark with the diluent and injected into the HPLC study acid degradation.

Alkali degradation

Accurately weighed 20.105 mg of Amifostine trihydrate sample was transferred into 100 mL volumetric flask. About 25 mL of diluent was added into the flask and sonicated for 1 min to dissolve it completely. To this 1 mL of 1M NaOH was added and mixed well. Then the resulting solution was diluted up to mark with diluent and injected into the HPLC study alkali degradation.

Peroxide degradation

Accurately weighed 20.1120 mg of Amifostine trihydrate sample was transferred into 100 mL volumetric flask. About 25 mL of diluent was added into the flask and sonicated for 1 min to dissolve it completely. To this 0.1 mL of 30% H_2O_2 was added and mixed well. Then the resulting solution was diluted up to mark with diluent and injected into the HPLC study oxidation degradation.

Degradation under UV light

Accurately weighed 20.0720 mg of Amifostine sample was exposed to UV light at wavelength 254 nm for 4 h and transferred into 100 mL volumetric flask. About 25 mL of diluent was added into the flask and sonicated for 1 min to dissolve the sample completely and the solution was diluted up to the mark. This solution was injected into the HPLC for UV degradation study.

Degradation under Sun light

Accurately weighed 20.08 mg of Amifostine sample was exposed to direct sunlight for 4 h and transferred in to 100 mL volumetric flask then about 25 mL of diluent was added into the flask and sonicated for 1 min to completely dissolve the sample and the contents were diluted up to mark. The resulting solution was injected into the HPLC to study degradation by sun light.

Thermal degradation

Accurately weighed 20.1180 mg of Amifostine trihydrate sample was transferred in to 100 mL volumetric flask, then about 10 mL of diluent was added into the flask and sonicated for 1 min to dissolve completely. The resulting solution was heated at 70 ºC for 5 min and allowed to cool to room temperature and then diluted up to the mark. The above solution was injected into the HPLC for thermal degradation study.

The results of all the above experiments are presented in Table 2.IV.26. and the results reveal that Amifostine trihydrate is susceptible to acid, heat and oxidative condition. However, degradation impurities formed during acidification, heating, and oxidation are not interfere with Amifostine trihydrate peak.

Degradation study	% Assay of degraded sample	Purity angle	Purity threshold	Peak purity
Acid degradation	78.3	0.980	1.625	Complies
Alkali degradation	81.6	1.294	1.843	Complies
Peroxide degradation	75.5	0.702	1.111	Complies
UV light exposure	80.8	0.549	0.910	Complies
Sun light exposure	80.6	0.642	1.005	Complies
Thermal degradation	63.6	0.564	0.843	Complies

Table 2.IV.26: Method specificity data of Amifostine trihydrate by HPLC

2.IV.5.4: Method precision:

To check the repeatability and precision of the method, six sample solutions were used and 50 µL of each sample was injected in duplicate under the same experimental conditions and on the same day. From the mean area count of the concerned peaks, the assay was calculated against the standard and the results so

obtained are given in Table 2.IV.27. The repeatability of the method was ascertained by calculating the % RSD from the assay results of six replicate studies. The calculated % RSD was 0.3 % which is well within acceptable limit not more than 2 % which confirms that the proposed method is precise.

Sr. No.	Final con. (µg/mL)	Individual area counts		Mean area counts	% Assay (On as is basis)
		Inj.1	Inj.2		
1	200.44	855639	854949	855294	80.5
2	200.59	862787	857984	860386	80.9
3	200.65	852291	857761	855026	80.4
4	200.71	860493	863167	861830	81.0
5	200.75	859326	861200	860263	80.8
6	200.80	857237	862131	859684	80.8
Mean					80.7

Table: 2.IV.27: Method precision data of Amifostine trihydrate by HPLC

2.IV.5.5: Robustness:

Amifostine trihydrate test solution was prepared as described earlier and analyzed by changing chromatographic conditions like change in mobile phase flow rate (± 0.2 mL/min), column oven temperature (± 2°C), detector wavelength (± 2 nm). The assay results of these experiments are presented in Table 2.IV.28. The results are comparable with the results obtained under the set of conditions need for original experiment which shows that the proposed method is robust.

Changed parameter from the proposed chromatographic condition	% Assay of Amifostine
Mean assay result from the proposed chromatographic condition	80.7
1) Change in flow (1.0 ± 0.2 mL /min)	
a) Increase by 0.1 mL /min, i.e. 1.1 mL / min)	80.6
b) Decrease by 0.1 mL /min, i.e. 0.9 mL / min)	80.2
2) Change in column oven temp. (± 2.0°C)	
a) Increase column oven temp + 2°C i.e. 38°C	81.0
b) Decrease column oven temp - 2°C i.e. 42°C	80.9
3) Change in wavelength. (± 2 nm) (Data was extracted from method precision)	
a) Increase wavelength + 2 nm i.e. 218 nm	80.7
b) Decrease wavelength – 2 nm i.e. 222 nm	80.6

Table 2.IV.28: Robustness data of Amifostine trihydrate by HPLC

2.IV.5.6: Sensitivity (LOD and LOQ):

The detector sensitivity was determined by calculating the limit of detection (LOD) and limit of quantification (LOQ) for Amifostine trihydrate was calculated from the calibration curve and the results are given in Table 2.IV.25. Within the range of detection level, the residual standard deviation of y intercepts of the regression line is used as the standard deviation. From the value of σ and slope it is found that LOD = 21.83 µg/mL and LOQ = 61.16 µg/mL for the proposed method.

2.IV.5.7: Solution stability:

To study the solution stability, Amifostine trihydrate solution of known concentration was prepared and stored in vials in a sample cooler at 5°C. These samples (50 µL) were injected into HPLC system at different intervals from the time of preparation. The area count of the peak obtained after different time intervals against initial peak area count was compared. The calculated deviation from the initial value is given in Table 2.IV.29. The results show that maximum deviation of 1.49 % was observed upto 26 h which is well within acceptable limit of not more than 2.0 % in such cases.

Interval (h)	Parameters	Amifostine	Limit
Initial	Mean area	863479	NMT ± 2.0 %
	% Deviation from initial	0.00	
7	Mean area	861591	
	% Deviation from initial	-0.22	
12	Mean area	860861	
	% Deviation from initial	-0.30	
17	Mean area	867647	
	% Deviation from initial	0.48	
22	Mean area	870337	
	% Deviation from initial	0.79	
26	Mean area	876333	
	% Deviation from initial	1.49	

Table: 2.IV.29: Solution stability data of Amifostine trihydrate by HPLC

The validation and performance characteristics of quantification of Amifostine trihydrate obtained, given in Table 2.IV.30 by ^{31}P qNMR, were also confirmed by comparing with proposed HPLC technique. The results of HPLC method did not show any marked differences from those of qNMR method. Hence, both the proposed methods are comparable.

Sr. No.	Parameters	qNMR method	HPLC method
1	Correlation coefficient (r^2)	0.9975	1.000
2	Slope	0.7687	4291.39
3	Intercept	0.1598	-20024.53
4	Solution stability	36 h	26 h
5	Method Precision (%RSD)	1.64%	0.3%
6	Limit of Detection (LOD)	0.08 mg/mL	0.022 mg/mL
7	Limit of Quantification (LOQ)	0.25 mg/mL	0.066 mg/mL

Table 2.IV.30: Comparison of performance characteristics of qNMR and HPLC method

2.IV.6: Commercial injection sample analysis:

Three samples from production batches of amifostine injection including innovator sample were analyzed for the assay by the developed methods based on ^{31}P qNMR and HPLC. Results of this analysis shown in Table 2.IV.31 reveal that the two methods provide comparable results of Amifostine trihydrate assay on as is basis.

Sr. No.	Batch No.	^{31}P qNMR (%)	HPLC method (%)
1	Amifostine API	80.60	81.45
2	Cytofos injection	81.64	81.50
3	Ethyol injection	80.37	79.70

Table 2.IV.31: Comparative % assay of Amifostine by ^{31}P qNMR and HPLC method

Conclusion

The ^{31}P qNMR method developed for quantification of Amifostine trihydrate and HPLC method is rapid as well as easy to perform. Based on different aspects of performance of the method such as linearity, precision and accuracy, the ^{31}P qNMR method stands validated. It offers an excellent choice over previously described procedures and can be used for in-process, routine quality control assay of Amifostine trihydrate API and its pharmaceutical injection. Any modern NMR equipment operating at a field of 400 MHz or more may be used, provided that suitable processing of data is performed.

Assay results obtained by ^{31}P qNMR have been confirmed by comparing with those of an interesting reversed phase HPLC method developed. The proposed HPLC method has high capacity factor on the zwitterion based stationary phase. Consequently this newly introduced column gives better peak shape having more than 22000 theoretical plate count as well as very good peak symmetry and shorter run time in comparison with US pharmacopeia method.

Hence, it can be concluded that the two methods stand validated and can be used for the assay of Amifostine trihydrate API as well as its injection.

References

1. Crutchfield, M. M.; Dungan, C. H.; Letcher, J. H.; Mark, V.; Van-Wazer, J. R. *^{31}P Nuclear Magnetic Resonance* (*Topics in Phosphorus Chemistry*, **1967**, *Vol. 5),* Interscience Publishers, St. Louis, Missouri.
2. Gorenstein, D. G. *Phosphorus-31 NMR, Principles and Applications*, **1984**, Issue 8, Academic press, New York.
3. Verkade, J. G.; Quin, L. D. (Eds.) *Phosphorous-31 NMR Spectroscopy in Stereo Chemical Analysis*. **1987**, VCH, New York.
4. Gard, D. R.; Burquin, J. C.; Gard, J. K. *Anal. Chem.* **1992**, *64*, 557.
5. Hanssum, H. *J. Magn. Reson.* **1981**, *45*, 461.
6. Beckar, E. D.; Ferretti, J. A.; Gambhir, P. N. *Anal. Chem.* **1979**, *51*, 1413.
7. Rabenstein, D. L. *J. Chem. Educ.* **1984**, *61*, 909.
8. Ruppel, M. L.; Marvel, J. T. *Org. Magn. Reson.* **1976**, *8*, 19.
9. Stothers, J. B.; Robinson, J. R. *Can. J. Chem.* **1964**, *42*, 967.
10. (a) Paul, E. G.; Grant, D. M. *J. Amer. Chem. Soc.* **1963**, *85*, 1701. (b) Paul, E. G.; Grant, D. M. *J. Amer. Chem. Soc.* **1964**, *86*, 2977.
11. West, G. M. J. *J. Chem. Inf. Comput. Sci.* **1993**, *33*, 577.
12. Lumsden, M. D.; Eichele, K.; Wasylishen, R. E.; Cameron, T. S.; Britten, J. F. *J. Amer. Chem. Soc*. **1994**, *116*, 11129.
13. Dransfeld, A.; Schleyer, P. V. *Magn. Reson. Chem.* **1998**, *36*, 29.
14. (a) Chesnut, D. B.; Quin, L. D. *Adv. Mol., Str. Res.* **1999**, *5*, 189.(b) Chesnut, D. B.; Byrd, E. F. C. *Heteroat. Chem.* **1996**, *7*, 307.
15. Patchkovskii, S.; Ziegler, T. *J. Phys. Chem.* **2002**, *106*, 1088.
16. Miyata, Y.; Ando, H. *J. Health Sci*. **2001**, *47*, 75.
17. Maniara, G.; Rajamoorthi, S. R.; Stockton, G. W. *Anal. Chem*. **1998**, *70*, 4921.
18. Rabenstein, D. L. *J. Chem. Educ.* **1984**, *61*, 909.
19. Malet-Martino, M.; Holzgrabe, U. *J. Pharm. Biomed. Anal.* **2011**, *55*, 1.
20. *United States Pharmacopoeia 32*, **2009**, NF27, Rockville, Maryland, USA.
21. Holzgrabe, U.; Diehl, B.; Wawer, I. *NMR Spectroscopy in Pharmaceutical Analysis*, **2008,** Elsevier, Oxford, UK.
22. (a) Appleton, T. G.; Berry, R. D.; Davis C. A.; Hall, J. R.; Kimlin, H. A. *Inorg. Chem.* **1984**, *23*, 3514. (b) Appleton, T. G.; Hall, J. R.; Harris, A. D.; Kimlin, H. A. McMahon, I. J. *Aust. J. Chem.* **1984**, *37*, 1833.

23. Trevor, G. A.; Hall, J. R.; McMahon, I. J. *Inorg. Chem.* **1986**, *25*, 726.
24. Rana, F. R.; Mautone, A. J.; Dluhy, R. A. *Appl. Spectrosc.* **1993**, *47*, 1015.
25. Nouri-Sorkhabi, M. H.; Wright, L. C.; Sullivan, D. R.; Kuchel, P. W. *Lipids*, **1996**, *31*, 765.
26. Teleman, A.; Richard, P.; Toivari, M.; Penttila, M. *Anal. Biochem.* **1999**, *272*, 71.
27. Mortino, R.; Veronique, G.; Franck, D.; Myriam, M. *J. Pharm. Biomed. Anal.* **2005**, *38*, 871.
28. Doyle, V. L.; Payne, G. S.; Collins, D. J.; Verill, M. W.; Leach, M. *Phys. Med. Biol.* **1997**, *42*, 691.
29. Denays, R.; Chao, S. L.; Mathur-Devre, R.; Jeghers, O.; Fruhling, J.; Noel, P.; Ham, H. R. *Magn. Reson. Med.* **1993**, *29*, 719.
30. Matson, G. B.; Meyerhoff, D. J.; Lawry, T. J.; Lara, R. S.; Duijn, J.; Deicken, R. F.; Weiner, M. W. *NMR Biomed*. **1993**, *6*, 215.
31. Chow J. L.; Levitt, K. N.; Kost, G. J. *Ann. Biomed. Eng.* **1993**, *21*, 247.
32. (a) Wehrli, S. L.; Palmieri, M. J.; Reynolds, R. A.; Segal, S. *Magn. Reson. Med.* **1993**, *30*, 494. (b) Wehrli, S. L.; Reynolds, R.; Chen, J.; Yager, C.; Segal, S. *NMR Biomed*. **2001**, *14*,192.
33. Odahara, T.; Nishimoto, S.; Katsutani, N.; Kyogoku, Y.; Morimoto, Y.; Matsushiro, A.; Akutsu, H. *J. Biochem.* **1994**, *115*, 270.
34. Cady, E. B.; Wylezinska, M.; Penrice, J.; Lorek, A.; Amess, P. *Magn. Reson. Imag.* **1996**, *14*, 293.
35. Elliott, M. A.; Walter G. A.; Swift, A.; Vandenborne, K.; Schtland, J. C.; Leigh, J. S.; *Magn. Reson. Med.* **1999**, *41*, 450.
36. Hetherington, H. P.; Spencer, D. D.; Yaughan, J. T.; Pan, J. W. *Magn. Reson.* **2001**, *45*, 46.
37. Tosner, Z.; Dezortova, M.; Tinera, J.; Hajek, M. *Magn. Reson. Mater. Phys. Biol. Med.* **2001**, *13*, 40.
38. Larijani, B.; Poccia, D. L.; Dickinson, L.C. *Lipids*, **2000**, *35*, 1289.
39. Belloque, J.; De-La, F.; Miguel, A.; Ramos, M. *J. Dairty Res.***2000**, *67*, 529.
40. Brettorst, G. L.; Kotyk, J. J.; Ackerman, J. J. H. *Magn. Reson. Med*. **1989**, 9, 282.
41. Koytk, J. J.; Hoffman, N. G.; Hutton, W. C.; Bretthorst, G. L.; Ackerman, J. J. H. *J. Magn. Reson*. **1992**, *98*, 483.

42. Spyros, A.; Dais, P. *J. Agric. Food Chem.* **2000**, *48*, 802.
43. Mustarelli, P.; Tomasi, C.; Magistris, A.; Scotti, S. *J. Non-Cryst. Solids,* **1993**, *163*, 97.
44. Argypoulos, D. S.; Zhang, L. *J. Agric. Food Chem.* **1998**, *46*, 4628.
45. Kirszensztejn, P.; Czajka, B.; Sheng, T. C.; Bell, T. N.; Gay, I. D. *Catal. Lett.* **1995**, *32*, 305.
46. Peters, A. W.; Mueller, K. T.; Sutovitch, K. J.; Rakiewicz, E. F.; Wormsbecher, R. F. *Proc. Int. Zeolite Conf.* 12th, **1999**, *4*, 2331.
47. Roberie, T. G.; Sutovich K. J.; Koranne, M. M.; Yaluris, G. *Abstracts of papers*, **2001**, *26*, 222nd ACS National Meeting, Chicago, IL, USA.
48. Brown, D. Q.; Graham, W. J.; MackKenzie III, L. J.; Pittock III, J. W.; Shaw, L. M. *Pharmacol. Ther.* **1988**, *39*, 157.
49. Devita, V. T.; Hellman, S.; Rosenberg, S. A.; Eds.; Lippincott, J. B. *Biological Therapy of Cancer Updates*, **1995**, New York.
50. Kouvaris, J. R.; Kouloulias, V. E.; Vlahos, L. J. *The Oncologist,* **2007**, *12*, 738.
51. Andreassen, C. N.; Grau, G.; Lindegaard, J. C. *Chemical Radioprotection: A Critical Review of Amifostine as a Cytoprotector in Radiotherapy*, **2003**, *13*, 62-72, *Seminar in Radiation Oncology*, Denmark.
52. ICH Harmonized Tripartite Guidelines. *Validation of Analytical Procedures: Text and Methodology, Q2 (R1)*, **2005**.
53. Malz, F.; Jancke, H. *J. Pharm. Biomed. Anal.* **2005**, *38*, 813.
54. Holzgrabe, U.; Diehl, B. W.; Wawer, I. *J. Pharm. Biomed. Anal.* **1998,** *17*, 557.
55. Jungnickel, J. L.; Forbes, J. W. *Anal. Chem.* **1963**, *35*, 938.
56. Hollis, D. P. *Anal Chem.* **1963**, *35*, 1682.
57. Liu, S. Y.; Hu, C. Q. *Anal. Chim. Acta,* **2007**, *602*, 114.
58. Shao, G.; Kautz, R.; Peng, S.; Cui, G.; Giese, R. W. *J. Chromatogr. A.* **2007**, *1138*, 305.

Chapter 3

Drug Excipients Interaction Study

Introduction:

Amino acid

Amino acids are molecules containing an amine group, a carboxylic acid group and a side-chain that varies between different amino acids NH_2-CH(R)-COOH (where R is side chain). Davies *et al* reported twenty naturally occurring amino acids and their polymerization to give peptides, polypeptides and proteins.[1a]

Peptide and peptide bond

Peptides (from the Greek word "to digest") are short polymers of amino acid monomers linked by peptide bonds. Peptides are distinguished from proteins on the basis of the size of their molecule, typically containing less than fifty amino acid units. The shortest peptides are dipeptides, consisting of two amino acids joined by a single peptide bond shown in Figure 3.1. Similarly there are also tripeptides, tetrapeptides and polypeptides.

A peptide bond is a covalent bond that is formed between two amino acids when the carboxyl group of one amino acid reacts with the amino group of the same or another amino acid.

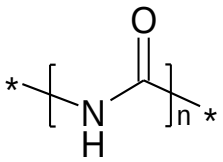

Figure 3.1: Amino acid peptide linkage

Protein

Amino acids which have been incorporated into a peptide are termed "residues"; every peptide has an N-terminus and C-terminus residue on the ends of the peptide (except for cyclic peptides). A polypeptide is a long, continuous, and unbranched peptide. Proteins consist of one or more polypeptides arranged in a biologically functional way and are often bound to cofactors, or other proteins.[1b]

Primary structure

As mentioned earlier, the condensation reaction between carboxyl group of one amino acid and amino group of other amino acid forms a peptide bond. This bond is responsible for the **primary structure** of all peptides and proteins. Peptide bond is a single bond between the carbonyl carbon and the amide nitrogen, hence free rotation around the bond is possible but it does not happen due to mesomeric effect.[2a]

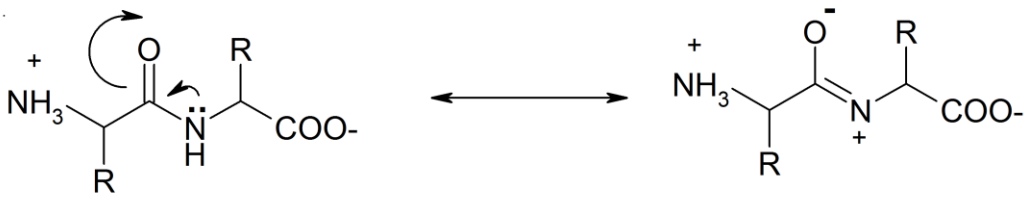

Figure 3.2: Resonating structures of amino acid

Presence of lone pair of electron on nitrogen atom is responsible for above resonating structures (Fig.3.2) due to delocalization; hence the peptide bond takes on a partial (approx. 40%) double bond character and is more resistant to rotation. The atoms involved in the group, O=C-NH, are coplanar, known as the **peptide plane**. Two possible conformations (Fig.3.3) of the planar peptide bond are "***trans* peptide group**" (the C_α atoms are on opposite side of the peptide bond) and "***cis* peptide group"**, (the C_α atoms are on the same side of the peptide bond).

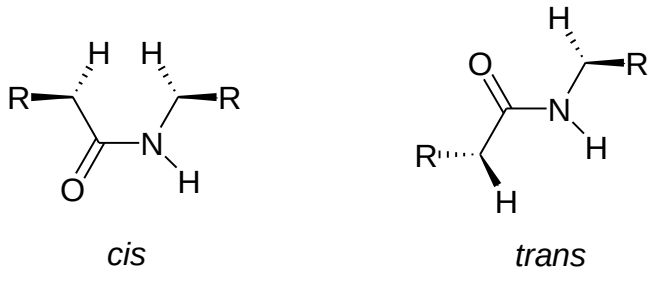

cis *trans*

Figure 3.3: -*cis* and -*trans* configuration of amino acid corresponding to the peptide C-N bond linkage

Mostly peptide bonds exist in the *trans* conformation, but *cis* forms can occur in peptide bonds that contain a proline residue. Hence *cis* form is more stable due to the proline side-chain which offers lower steric hindrance with minimum energy.[1b]

Dihedral angles ω, Φ and ψ

The repeating torsion angles or dihedral angles along the peptide backbone chain are known as ω, Φ and ψ due to the partial double bond character of -C-N- peptide bond (1.32 A°) with favored planarity arrangement. Omega (ω) angle tends to be planar (0° or 180°) due to delocalization of the carbonyl π electrons and the lone pair electrons at nitrogen. The atoms of N—C_α bond (1.47 A°) and C_α—C bonds are free to rotate, constrained only by steric interferences. The angle of rotation for the N—C_α bond is designated Φ and for C_α—C bond is Ψ. Due to steric constraints, the values of Φ and ψ favor the different conformations of the peptide. A conformational plot of Φ against ψ for a particular residue is known as a Ramachandran plot.[2b]

Secondary structure

Hydrogen bond is formed between >C=O and >N-H groups due to their proximity. The cumulative effect of many weak hydrogen bonds along with peptide backbone creates well defined geometries of the forms called **secondary structure.** Some geometric patterns observed in peptides are α-Helix, β-Sheet, β-Turn etc.[2c]

Tertiary structure

Tertiary structure is the folding of the total chain, the combination of the elements of secondary structure linked by turns and loops. The stability of tertiary structure is determined by non-bonding interactions and the disulfide bond. The forces that give rise to the tertiary structure of a peptide and protein are, ionic bonding, hydrogen bonding, hydrophobic interaction (van der Waals interaction) and disulphide linkage.[2d]

Quaternary structure

Quaternary structure is usually applicable only to proteins in which large number of molecules gets covalently bound through amino acid residue and result into still larger structure due to peptide bond. Two or several subunits are linked through hydrogen bond, polar or non-polar interactions are called quaternary structure. Some therapeutic peptides are prone to self association such as Glucagon and Insulin.[3,4]

3.1: Peptide structure, conformation, and dynamics:

Peptides and proteins are biological molecules whose 'building blocks' are amino acids attached by peptide bonds shown in Figure 3.4. The primary, secondary and tertiary structural analysis and its interaction of peptides are to provide insight into the physical and chemical properties of peptides. The folding of a disordered peptide chain to a highly ordered compact structure occurs as the system reaches its kinetically accessible free energy minimum.

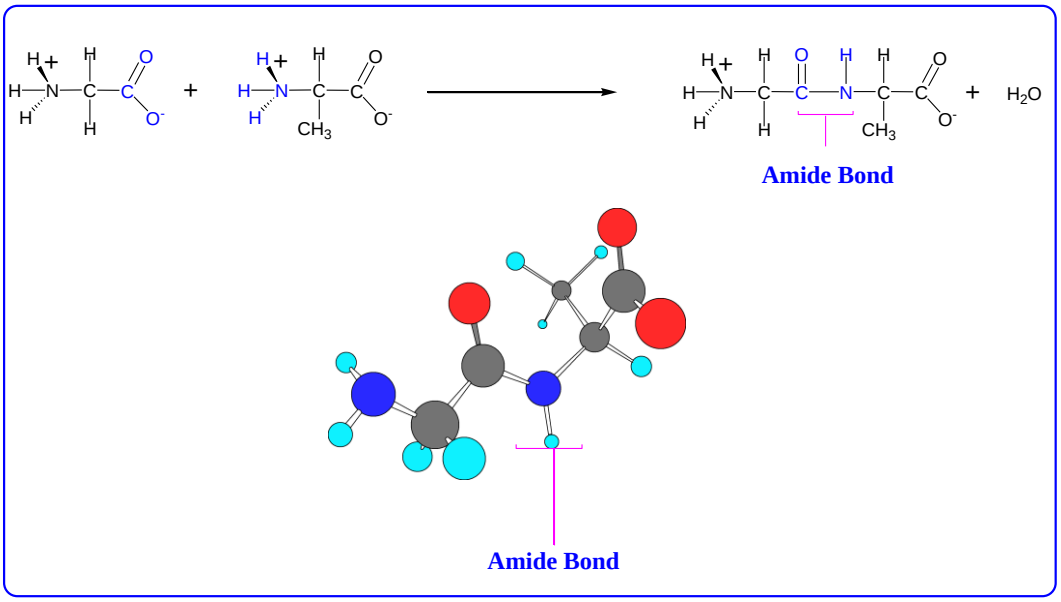

Figure 3.4: Schematic diagram of peptide bond formation

Dill and coworkers observed that in order to achieve a stable peptide structure, intra molecular forces such as steric hindrance, van der Waals interactions, hydrogen bonding, ionic interactions and entropic forces must be balanced against each other.[5] Similarly, interactions of preservatives with peptides are the dominant forces in peptide folding.

In peptides and proteins the non-covalent bio-molecular interactions are not simple to predict since they are made up of many components, both attractive and repulsive. Where possibilities for strong bonding (ionic or hydrogen bonding) exist a good match can often be recognized by consideration of molecular models. Usually, reasonable predictions of bio-molecular interactions require the use of sophisticated computer programs and specific pulsed programming with optimum experimental designs.

3.2: Therapeutic peptides:

Badelin *et al* studied the recent advances in the structural elucidation of numerous natural peptides and proteins, and the understanding of their role in several physiological processes[6] as given in Table 3.1. Use of pharmaceutical development techniques in their production have stimulated considerable interest in establishing peptides as drugs in therapy. Hokfelt *et al* recently reported that peptides have been found in neurons with classical neurotransmitters,[7] but it has revealed that they can have a variety of biological actions. Peptides can be used as good drugs in challenging situations. They may be more expensive and time consuming to produce than traditional small molecules, may also have low oral bioavailability, fast clearance in the body and even, in some cases may be immunogenic.

Gellman and coworkers studied peptidomimetic (peptidemimic) compound which is nothing but the ligand of a receptor that can block the biological effect of a peptide at the receptor level.[8] Costantino *et al* concluded that peptides can be extensively utilized in therapeutic formulations due to their participation in various metabolic pathways.[9] Their capability to act as a drug is confined to a particular conformation and is lost on conformational transition due to interactions, binding or aggregations as reported by Saudek *et al* and Mayer *et al*.[10,11]

In recent years peptides have emerged as potential candidates for drug delivery though drugs in various dosage forms has been used since long.[7-8] Costantino *et al,* Meyer *et al* and Mayer *et al* studied the isolation of specific genes and their production in bulk as a polypeptide product like insulin.[9-11] Conventional formulations for insulin show hepatic first pass metabolism which affects directly its therapeutic efficacy. Noordwijk and coworkers introduced an alternative approach for systemic administration by passing hepatic metabolism that was achieved in therapeutic proteins by site-directed mutagenesis instead of chemical modification. This was also investigated by Weatherall *et al*, Nispen *et al* through the substitution of one amino acid with other amino acid.[12-14] Hess *et al* reported synthesis of the smallest possible sequence, and the systematic shortening of natural peptides and have shown that only parts of the molecule are required for particular effects[15].

Despite having immense problems in using peptides and proteins as drugs, a significant numbers are already available like insulin and growth hormone, supplied

in their natural forms, as well as several luteinizing hormone-releasing hormone (LHRH) analogues studied by Bachmayer *et al.*[16]

Freter *et al* observed that particular parts of the molecule are recognized by the enzymes which can be chemically modified to lengthen the half-life of activity[17] in order to make pathway for peptide drug delivery through oral route.

Morley *et al* and Holienberg *et al* examined different ways of determining the three-dimensional shapes of peptides in solution.[18,19] Hruby *et al,* Dutta *et al,*and Sasaki *et al* studied these at the receptor level.[20-22] Lauz and coworkers investigated the production of peptides, in modified[23] and unaltered forms for use as possible drugs. The ways of testing their biological activity were investigated by Hagler *et al.*[24] Crippen *et al* and Godford *et al* reviewed drug delivery,[25,26] further supported by Humblet *et al* and Fauchere *et al* with respect to drug targeting,[27,28] and finally Lewis *et al* with regard to clinical trials.[29] These are the key parameters to be investigated prior to commercialization of a drug.

Lee *et al* proposed that while stabilizing the chemical structure, delivery and targeting to oral route are to be taken into account.[30,31] Hunt *et al,* Read *et al* and Hodgson *et al* revealed that without altering the conformation of the active form,[32-34] nonspecific interactions which leads to acute toxicity can be prevented. The progress in bio-pharmaceuticals has led to the development of large number of peptides being discovered with important physiological roles as reported by Veber *et al.* [35]

Degradation pathway of naturally occurring peptides has well-defined mechanism. Peptide hormones that control the amount of molecule in circulation through homeostasis are the regulators of physiological conditions within a certain range. Since injecting a sample of natural hormone will cause the body to down-regulate its own production and therefore, there will be no change in end effect.

Biological active peptide and their therapeutics use:			
Sr. No	**Name**	**Sequence**	**Therapeutics Use**
1	**Bivalirudin**[41] Warkentin *et al 2005*	H-D-Phe-Pro-Arg-Pro-Gly-Gly-Gly-Gly-Asn-Gly-Asp-Phe-Glu-Glu-Ile-Pro-Glu-Glu-Tyr-Leu-OH **(20 -residue)**	Anticoagulant (Direct thrombin inhibitor)
2	**Thymosin alpha**[42] Chien *et al 2004*	Ac-Ser-Asp-Ala-Ala-Val-Asp-Thr-Ser-Ser -Glu-Ile-Thr-Thr-Lys-Asp-Leu- Lys -Glu-Lys-Lys-Glu-Val-Val- Glu-Glu-Ala-Glu-Asn-OH**(28-residue)**	Immunomodulator, Anti-viral, Hepatitis-B Hepatitis-C,
3	**Salmon Calcitonin**[43] Brugee *et al 2008*	H-Cys-Ser-Asn-Leu-Ser-Thr-Cys-Val-Leu-Gly-Lys-Leu-Ser-Gln-Glu-Leu-His-Lys-LeuGln-Thr-Tyr-Pro-Arg- Thr-Asn-Thr-Gly-Ser-Gly-Thr-Pro-NH_2 cyclic(1→7)-disulfide	Hypocalcaemic hormone.
4	**Exenatide**[44] Heine *et al 2005*	H-His-Gly-Glu-Gly-Thr-Phe-Thr-Ser-Asp-Leu-Ser-Lys-Gln-Met-Glu-Glu-Glu-Ala-Val-Arg-Leu-Phe-Ile-Glu-Trp-Leu-Lys-Asn-Gly-Gly-Pro-Ser-Ser-Gly-Ala-Pro-Pro-Pro-Ser-NH_2 **(39-residue)**	To improve glycemic control in patients with Type 2 diabetes mellitus
5	**Liraglutide**[45] Bode *et al 1999*	H-His-Ala-Glu-Gly-Thr-Phe-Thr-Ser-Asp-Val-Ser-Ser-Tyr-Leu-Glu-Gly-Gln-Ala-Ala-Lys(γ-Glu-palmitoyl)-Glu-Phe-Ile-Ala-Trp-Leu-Val-Arg-Gly-Arg-Gly-OH **(31-residue)**	For use/treatment in diabetes mellitus type 2 and obesity.
6	**Pramlintide**[46] Nyholm *et al 2001*	H-Lys-Cys-Asn-Thr-Ala–Thr-Cys-Ala-Thr-Gln-Arg-Leu-Ala-Asn-Phe-Leu-Val-His-Ser- Ser-Asn-Asn-Phe-Gly-Pro-Ile-Leu-Pro-Pro-Thr-Asn-Val-Gly-Ser-Asn-Thr-Tyr-NH2 (2-7 Disulfide bond) **(37-residue)**	For the treatment of type 1 and type 2 diabetes mellitus
7	**Glucagon**[47] White *et al 1999*	H-His-Ser-Gln-Gly-Thr-Phe-Thr-Ser-Asp-Tyr-Ser-Lys-Tyr-Leu-Asp-Ser-Arg-Arg-Ala-Gln-Asp-Phe-Val-Gln-Trp-Leu-Met-Asn-Thr-OH **(29-residue)**	For treatment of severe hypoglycemia
8	**Teriparatide**[48] Meltzer *et al 1998*	H-Ser-Val-Ser-Glu-Ile-Gln-Leu-Met-His-Asn-Leu-Gly-Lys-His-Leu-Asn-Ser-Met-Glu-Arg-Val-Glu-Trp-Leu-Arg-Lys-Lys-Leu-Gln-Asp-Val-His-Asn-Phe-OH **(34-residue)**	For the treatment of osteoporosis
9	**Enfuvirtide**[49] Greene *et al 2007*	Ac-Tyr-Thr-Ser-Leu-Ile-His-Ser-Leu-Ile-Glu-Glu-Ser-Gln-Asn-Gln-Gln-Glu-Lys-Asn-Glu-Gln-Glu-Leu-Leu-Glu-Leu-Asp-Lys-Trp-Ala-Ser-Leu-Trp-Asn-Trp-Phe-NH_2	Human immunodeficiency virus type 1 (HIV-1) infection
10	**Octreotide**[50] Uhl *et al 1999*	H-D-Phe-Cys-Phe-D-Trp-Lys-Thr-Cys-L-threoninol **(8-residue)**	For treatment of acromegaly and cancer chemotherapy
11	**Leuprolide**[51] Saleh *et al 2004*	Pyr-His-Trp-Ser-Tyr-D-Leu-Leu-Arg-Pro-NHEt **(9-residue)**	Anti-Cancer

12	**Atosiban**[52] Roel de *et al 2010*	3-Mercaptopropionyl-D-Tyr(Et)-Ile-Thr-Asn-Cys-Pro-Orn-Gly-NH2 (1-6 Disulfide bond) **(9-residue)**	To Halt Premature labor
13	**Cetrorelix**[53] Volker *et al 2002*	Ac-D-2-Nal-4-chloro-D-Phe-β-(3-pyridyl)-D-Ala-Ser-Tyr-D-Cit-Leu-Arg-Pro-D-Ala-NH_2 **(10-residue)**	(GnRH) antagonistic
14	**Desmopressin**[54] Del *et al 2008*	3-Mercaptopropionyl-Tyr-Phe-Gln-Asn-Cys-Pro-D-Arg-Gly-NH_2 acetate salt (1-6 Disulfide bond) **(9-residue)**	Nocturnal enuresis Central diabetes insipidus, polyuria, polydipsia
15	**Terlipressin**[55] Boson *et al 2006*	H-Gly-Gly-Gly-Cys-Tyr-Phe-Gln-Asn-Cys-Pro-Lys-Gly-NH_2 acetate salt (4-9 Disulfide bond) **(12-residue)**	Acute variceal hemorrhage (esophageal varices) Hepatorenal syndrome
16	**Eptifibatide**[56] Amoroso *et al 2001*	3-Mercaptopropionyl-Homoarg-Gly-Asp-Trp-Pro-Cys-NH_2 acetate salt (1-7 Disulfide bond) **(7-residue)**	For treatment of myocardial infarction and acute coronary syndrome.
17	**Nesiritide**[57] Chen X *et al 2002*	H-Ser-Pro-Lys-Met-Val-Gln-Gly-Ser-Gly-Cys-Phe-Gly-Arg-Lys-Met-Asp-Arg-Ile-Ser-Ser-Ser-Ser-Gly-Leu-Gly-Cys-Lys-Val-Leu-Arg-Arg-His-OH (10-26 Disulfide bond) **(32-residue)**	For tretment of acutely decompensated congestive heart failure
18	**Vapreotide**[58] Fortune *et al 2009*	H-D-Phe-Cys-Tyr-D-Trp-Lys-Val-Cys-Trp-NH**2** (2-7 Disulfide bond) **(8-residue)**	For the treatment of esophageal variceal bleeding in patients with cirrhotic liver disease
19	**Lanreotide**[59] Carmichael *et al 2012*	H-D-2-Nal-Cys-Tyr-D-Trp-Lys-Val-Cys-Thr-NH_2 (2-7 Disulfide bond) **(8- residue)**	Acromegaly Carcinoid syndrome Thyrotrophic adenomas
20	**Oxytocin**[60] Spyranti *et al 2010*	H-Cys-Tyr-Ile-Gln-Asn-Cys-Pro-Leu-Gly-NH2 (1-6 Disulfide bond) **(9-residue)**	Used to induce labor or to enhance uterine contractions during labor
21	**Icatibant acetate**[61] Privitera *et al 2003*	H-D-Arg-Arg-Pro-Hyp-Gly-Thi-Ser-D-Tic-Oic-Arg-OH **(10-residue)**	Acute coronary syndrome, unstable angina undergoing PCI
22	**Sermorelin**[62] Esposito *et al 2003*	H-Tyr-Ala-Asp-Ala-Ile-Phe-Thr-Asn-Ser-Tyr-Arg-Lys-Val-Leu-Gly-Gln-Leu-Ser-Ala-Arg-Lys-Leu-Leu-Gln-Asp-Ile-Met-Ser-Arg-NH_2 **(29-residue)**	Growth hormone deficiency

23	**Secretin Human**[63] Overington *et al 2006*	H-His-Ser-Asp-Gly-Thr-Phe-Thr-Ser-Glu-Leu-Ser-Arg-Leu-Arg-Glu-Gly-Ala-Arg-Leu-Gln-Arg-Leu-Leu-Gln-Gly-Leu-Val-NH_2 **(27-residue)**	Diagnosis of pancreatic exocrine dysfunction, and gastrinoma,
24	**Teduglutide**[64] Palle *et al 2012*	H-His-Gly-Asp-Gly-Ser-Phe-Ser-Asp-Glu-Met-Asn-Thr-Ile-Leu-Asp-Asn-Leu-Ala-Ala-Arg-Asp-Phe-Ile-Asn-Trp-Leu-Ile-Gln-Thr-LysIle-Thr-Asp-OH **(33-residue)**	Treatment of Short Bowel Syndrome
25	**Goserelin**[65] Kirby *et al 2009*	Pyr-His-Trp-Ser-Tyr-D-Ser(tBu)-Leu-Arg-Pro-Azagly-NH_2 **(10-residue)**	Anti-Cancer
26	**Gonadorelin**[66] Lu ZL *et al 2005*	Pyr-His-Trp-Ser-Tyr-Gly-Leu-Arg-Pro-Gly-NH_2 **(10-residue)**	Ovarian follicular cysts (veterinary medicine)
27	**Nafarelin**[67] Barbieri *et al 1990*	Pyr-His-Trp-Ser-Tyr-D-2-Nal-Leu-Arg-Pro-Gly-NH_2 **(10-residue)**	Endometriosis Use in reproductive medicine

Table 3.1: Different therapeutic peptides and its applications in biomedicines

3.2.2: Theoretical aspects of peptide drug design:

Marshall *et al* developed computer-aided drug design[68,69] for different peptide and polypeptide drugs. Levitt *et al*, Cammon *et al*, Osguthrope *et al* and Hardy *et al* carried out different studies for energy minimization[70], molecular dynamics[71]and molecular graphics for ligand-receptor interaction.[72,73] Berg *et al* applied quantitative structure-activity relationships (QSAR) to peptides[74], while Blankley *et al* considered modeling as QSAR technique[75]. The receptor is usually a peptide or protein with the absence of crystal structure [73], but having specific sequence homology which was investigated by Bacon *et al*.[76]

The quantum mechanical techniques[77] were applied to small drug molecules by Richards *et al* and binding and catalytic region[78] of a molecular mechanical interpretation was studied by Zheng *et al*. Recently, Gunsteren *et al* and Bash *et al* reported the development of free-energy perturbation methods,[79, 80] with the potential for predicting changes in binding affinity of residue modification. Ullman *et al*, Holley *et al* and Gregor *et al* studied the drug development using parallel processing[81, 82] and artificial intelligence.[83]

3.2.3: Experimental aspects of peptide drug design:

The conformational structures of constrained peptides[23] and proteins[73], were developed by Nuclear Magnetic Resonance (NMR) spectroscopy[84] and X-ray crystallography techniques were adopted by Lautz *et al*, Hardy *et al* and Morris *et al*. Kaiser *et al* reported that structural environments induce well-defined conformations of flexible peptides i.e. amphipathic helices were favored in lipids.[85] The experimental and theoretical approach for molecular recognition in drug-receptor interaction[86] and drug delivery systems [87] were studied by Jellife *et al* and Eppstein *et al.*

3.2.4: NMR applications for interaction study:

NMR is a sophisticated and powerful analytical technology which has many applications in the field of scientific research, medicine, and various industries. Modern NMR spectroscopy emphasizes the application in bio-molecular systems and plays an important role in structural biology. NMR is one of the most powerful and versatile spectroscopic techniques for the analysis of bio-macromolecules with developments in both methodology and instrumentation in the past two decades, allowing characterization of bio-macromolecules and their complexes up to 100 kDa.[88] X-ray crystallography and NMR spectroscopy are two sophisticated technologies for the structural determination of bio-macromolecules at atomic resolution. Also NMR provides unique and important molecular motional and interaction profiles containing pivotal information on protein function which is critical in drug development.

3.2.5: NMR studies of peptide:

Leopold *et al*, Clore *et al*, Kay *et al*, and Wagner *et al* studied conformation of proteins by NMR methods. Interaction of proteins with small ligands and biopolymers has provided a potent driving force for the development of new NMR techniques for structural and dynamic characteristics of peptide complexes. The methodologies and strategies that are developed to study complexes between proteins and peptide ligands act as models of larger protein-protein complexes.[89-92]

3.2.6: NMR methodology:

The nature of the non-covalent complex of a protein with a ligand molecule and its dissociation can be determined by NMR. Using transferred NOE[93] significant

structural information is gained in the fast exchange limit which was studied by Jarori *et al*, Prog *et al* and Lian *et al.*[94,95] Fisher *et al* and Zhang *et al* studied the ligand in the protein bound state including the characterization of interactions between Calmodulin and small peptides.[96] The power of multinuclear, multidimensional, heteronuclear NMR and isotopic enrichment of the ligand and/or the protein methods can be applied to the structural and dynamic characterization of the complex.[97]

Bax *et al* developed experiments that provide a reliable path to the assignment of methionine methyls,[98] which are often at the center of hydrophobic interfaces, to the stereospecific assignment of the primary amide -NH_2 group. Mc Intosh *et al* and Yamazaki *et al* studied the asparagine and glutamine,[99] and similarly arginine guandino group[100] which often participate in ionic interactions. Pascal *et al* designed NMR experiments which rely on isotopic enrichment.[101] Otting *et al* and Wuthrich *et al* developed homonuclear and heteronuclear NMR approaches to study bound water molecules that is critical to the structural integrity of a variety of protein complexes.[102a,102b]

3.2.7: Solution structure of peptides:

The different principles used for atomic-resolution and structure determination of bio-macromolecules in aqueous solution, under near physiological conditions or membrane mimetic environment are given below:

- **Molecular dynamics**: for quantifying motional properties of bio-macromolecules.
- **Protein folding**: for determining the residual structures of unfolded proteins and the structures of folding intermediates.
- **Ionization state**: for determining the chemical properties of functional groups in bio-macromolecules, such as the ionization states of ionisable groups at the active sites of enzymes.
- **Weak intermolecular interactions and hydrogen bonding**: Allowing weak functional interactions between macro-bio molecules (e.g., those with dissociation constants in the micro molar to milli molar range) to be studied, which is not possible with other techniques. Hydrogen bonding also a unique technique for the direct detection of hydrogen bonding interactions.

- **Protein hydration**: for the detection of interior water and its interaction with bio-macromolecules.
- **Drug screening and design**: Particularly useful for identifying drug leads and determining the conformations of the compounds bound to enzymes, receptors, and other proteins.
- **Native membrane protein**: Solid state NMR has the potential for determining atomic-resolution structures of domains of membrane proteins in their native membrane environments, including those with bound ligands.
- **Metabolite analysis**: A very powerful technology for metabolite analysis.

3.2.8: Peptide drug delivery:

Major challenge for peptide drug delivery technology in its drug active form is closely related to the magnitude of enzymatic degradation of peptides which are administered parenterally, orally, bucally, rectally, nasally, transdermally, ocularly or vaginally.[103a] An understanding of the nature of this barrier is essential to the development of metabolically stable analogs, to the selection of protease inhibitors to control proteolytic activity, and to the selection of a route for peptide drug delivery.[103b]

The popularity of the oral route of drug administration will make it the dominant approach for drug delivery in the foreseeable future, but the nasal route of delivering peptides and proteins is a promising alternative, especially for the young, the very old, the blind, and the debilitated patients. The use of intranasal delivery[104] for peptides dated back to the early 1920s. Oxytocin, Vasopressin, Lypressin, Desmopressin, Glucagon are few examples of peptide drug given by the intranasal route of administration.[105-107] Some of the lipophilic preservatives[108] used for the peptide nasal spray are chlorobutanol, chlorocresol, methyl paraben and propyl paraben. Similarly polar preservatives used are Benzalkonium chloride, Benzethonium chloride and EDTA.

Molecular weight and particle size of the drug

It has been reported that for small drug molecules with molecular weight up to 300 Dalton a linear inverse correlation exists between the absorption of drugs and

molecular weight. But drug absorption decreases significantly if the molecular weight is greater than 1000 Dalton and this drug profile can be modified by the use of absorption enhancers. In the case of therapeutic peptide molecules, the drug absorption characteristics through nasal cavity is affected by molecular weight, secondary structure, formulation pH, pK_a of molecule, presence of salt and preservative, and delivery volume. Fischer *et al* showed that molecular weight represents the best correlation to the absorption and apparent cut-off point for molecular weight is upto 1000 Dalton. Shape also plays an important role. Linear molecules always have lower absorption than branched or cyclic molecules but in peptide chemistry shape and structure play a dominating role for drug absorption.[109]

Jones *et al* determined the effect of particle size of the drug with respect to absorption in lungs.[110] Corbo *et al* studied the correlation between drug bioavailability and hydrophilicity of therapeutic peptides.[111] It has been reported that particle size greater than 10 µm are deposited in the nasal cavity. Fry *et al* and Chein *et al* concluded that particle size between 2 to 10 µm can be retained in the lungs and particles of less than 1 µm are exhaled.[112,113]

Solubility and dissolution rate

The absorption power of a drug through nasal spray depends on the drug solubility and dissolution rates of powders and suspensions. The particles deposited in the nasal cavity need to be dissolved prior to absorption. If a drug remains as particles or is cleared away, no absorption occurs.[114]

3.2.9: Factors affecting in Formulation development:

pH of the solution medium

The solution pH of a formulation is another important factor for absorption. The systemic absorption optimization depends on both the pH of the nasal cavity and pK_a of a particular drug. Conley *et al* observed that the nasal irritation of products is minimum in the pH range of 4.5 to 6.5 when delivered with a specific volume and concentration.[115] Mostly the delivery volume is limited by the size of the nasal cavity with an upper limit of 25 mg/dose and a volume of 25 to 150 µL/ nostril.

The solution pH of a nasal formulation is important in order to avoid irritation of nasal mucosa, to ensure drug availability in unionized form for absorption and to

prevent growth of pathogenic bacteria in the nasal passage. It is also important for proper functioning of excipients such as preservatives, and to sustain normal physiological ciliary movement.

Lysozyme is found in nasal secretions, which is responsible for destroying certain bacteria at acidic pH. Thompson *et al* observed that in alkaline conditions, lysozyme is inactivated and the nasal tissue becomes susceptible to microbial infection.[116]

Buffer capacity and Osmolarity

Peptide drug nasal formulations are commonly administered in small volumes ranging from 25 to 150 µL with adequate buffer capacity because the nasal secretions may alter the pH and can affect the physicochemical structure and concentration of drug available for absorption. Drug absorption also depends upon the tonicity of the formulation. In many cases due to the presence of hypertonic saline solution shrinkage of epithelial cells may occur thereby hindering ciliary activity.[117]

Viscosity improver agents or gel-forming reagents

Pennington *et al* observed that solution viscosity plays an important role in prolonging the therapeutic effect of nasal preparations.[118] Suzuki and Makino found that a drug carrier such as hydroxyl propyl cellulose was effective for improving the absorption of low molecular weight drugs but did not produce the same effect for peptide products.[119]

Achari *et al* designed a liquid composition with excipients that gels in the presence of ions. Monovalent and/or divalent cations are added to the composition so that it is close to the point of electrolyte induced gelation.[120] The ionic strength of the composition is kept sufficiently low to obtain a low viscosity formulation for easy to administer form and also with sufficiently high gelation capacity while in the nasal cavity due to the presence of cation.

Solubilizers

As per Gattefosse bulletin in 1997 the solubility of a drug for nasal delivery always has a limitation in aqueous condition. To overcome this problem, surfactants or complexing agents that serve as a biocompatible solubilizer and stabilizer in combination with lipophilic absorption enhancers have been used.[121]

Preservatives

Hallen along with Graf and Bernstein showed that most nasal formulations are aqueous based and need preservatives like benzalkonium chloride to prevent microbial growth.[122,123] Hillardal *et al* reported that parabens, phenyl ethyl alcohol, EDTA, chlorobutanol and benzoyl alcohol as some of most commonly used preservatives in nasal formulations.[124] van de Donk *et al* have cautioned that mercury-containing preservatives have a fast and irreversible effect on ciliary movement and should not be used in nasal systems.[125,126]

Antioxidants

A small quantity of antioxidant sometimes is required to prevent drug oxidation without affecting drug absorption or causing nasal irritation. However, during the formulation process, chemical and physical interaction of antioxidants and preservatives with drugs, excipients, manufacturing equipment and packaging components are undesirable. Some commonly used antioxidants are sodium *meta* bisulfite, sodium bisulfite, butylated hydroxyl toluene and tocopherol.[127]

Humectants

Dryness of crusts and drying of mucous membrane may cause many allergic and chronic diseases. Hence, adequate moisture is essential for preventing the dehydration. Many preservatives, and antioxidants with other excipients may also cause nasal irritation especially when used in higher quantities.[128] Therefore, it is essential to incorporate humectants especially in gel based nasal products for avoiding nasal irritation and not to affect drug absorption. Some of the commonly used humectants are glycerin, sorbitol and mannitol.

Drug Concentration, Dose and Dose Volume

Drug concentration, dose and volume of administration are three interrelated parameters that impact the performance of the nasal delivery. Nasal absorption of L-Tyrosine was shown to increase with drug concentration in nasal perfusion experiments. Hirai *et al* reported that aminopyrine was absorbed at a constant rate as a function of concentration.[129] Hence, the above three parameters should be optimized or else the nasal mucosal cells may be permanently damaged.

Role of absorption enhancers

When the expected absorption profile is not attained by the nasal product, the use of absorption enhancers is recommended and their selection is based upon their acceptability by FDA and their impact on the physiological functioning of the nose. Morimato *et al* showed that the absorption enhancers are required when a drug exhibits poor membrane permeability, large molecular size, lack of lipophilicity and enzymatic degradation by amino peptidases.[130]

The absorption enhancers work by inhibiting enzymatic activity, reducing mucus viscosity or elasticity and decreasing mucociliary clearance. They may also help solubilize or stabilize the drug. Absorption enhancers are classified into two types as physical and chemical enhancers. Chemical enhancers act by destructing the nasal mucosa very often in an irreversible way, whereas physical enhancers affect nasal clearance reversibly by forming a gel.[131] The enhancing effect continues until the gel is swallowed. Chemical enhancers are chelating agents, fatty acids, bile acid salts, surfactants, and preservatives.

Effect of enzymatic activity

Protein and peptide based drug nasal products are subject to degradation in presence of proteases and amino-peptidases at the mucosal membrane. As the concentration of amino-peptidases present is much lower than that in the gastrointestinal tract, it does not degrade the product. Mathison *et al* observed that peptides sometimes form complexes with immunoglobulin (Igs) in the nasal cavity leading to an increase in the molecular weight and a reduction of permeability.[132]

The present chapter deals with development of ideas and approaches listed earlier for the design of peptide-based drug Salmon Calcitonin.

3.3: Salmon Calcitonin :

Peptides have been extensively utilized in therapeutic formulations due to their participation in various metabolic pathways.[133] Their capability to act as a drug is confined to a particular conformation and is lost on conformational transition due to interactions, binding or aggregations.[134,135] Salmon Calcitonin (sCT) a thirty two residue amino acid peptide is a man-made version of hormone, which is found in

Salmon. Salmon Calcitonin (sCT) is used worldwide as a therapeutic agent for the treatment of various bone disorders resulting due to altered calcium-phosphorus metabolism.[136,137] Calcitonin is used for treating postmenopause, osteoporosis, paget's disease of bone, and hypocalcaemia.

In humans, Calcitonin is produced by thyroid gland which acts primarily on bone.[138] The similarity of an intranasal Salmon Calcitonin (sCT) employing Benzethonium chloride as a preservative (Calcitonin Salmon Nasal spray) was compared with the reference listed drug (RLD) employing Benzalkonium chloride as a preservative (Miacalcin ® nasal spray). The concentration of Salmon Calcitonin (sCT) being 0.36 mg/mL along with 0.20 mg/mL of Benzethonium chloride (BTC) and 8.5 mg/mL of sodium chloride in our nasal spray provide various orthogonal methods to assess peptide structuring, dynamics and aggregation state. Mass spectroscopy, amino acid analysis and N-terminal sequencing, all of them demonstrated similarity in primary structure of sCT. Near and far circular dichroism also supported the secondary structure of sCT.[133,139]

a) H-Cys^{1}-Ser^{2}-Asn^{3}-Leu^{4}-Ser^{5}-Thr^{6}-Cys^{7}-Val^{8}-Leu^{9}-Gly^{10}-Lys^{11}-Leu^{12}-Ser^{13}-Gln^{14}-Glu^{15}-Leu^{16}-His^{17}-Lys^{18}-Leu^{19}-Gln^{20}-Thr^{21}-Tyr^{22}-Pro^{23}-Arg^{24}-Thr^{25}-Asn^{26}-Thr^{27}-Gly^{28}-Ser^{29}-Gly^{30}-Thr^{31}-Pro^{32}-NH_2

Structure of Salmon Calcitonin (sCT)

b)

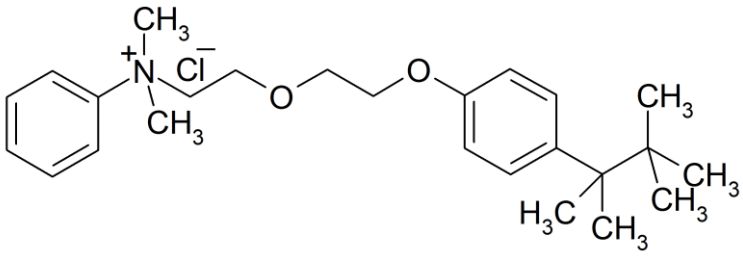

Structure of Benzethonium chloride (BTC)

The knowledge of weak molecular interaction between (sCT) employing BTC as a preservative is crucial to the stability of pharmaceutical products (Calcitonin Salmon Nasal Spray) as it affects the bioavailability, efficacy and toxicity of sCT. In the present work, NMR studies of sCT and BTC systems have been carried out to prove their molecular interactions/binding.[140,141]

3.3.1: Objectives:

Salmon Calcitonin is used as a therapeutic peptide to treat various disorders and is available in marketed formulations as a nasal spray in which various preservatives are used to prevent the microbial growth without compromising the efficacy of Calcitonin. The similarity between developed intranasal Salmon Calcitonin (sCT) employing Benzethonium chloride as a preservative (Calcitonin Salmon Nasal spray) has been compared with the reference listed drug (RLD) employing Benzalkonium chloride as a preservative (Miacalcin® nasal spray).

The work includes:

- Preparation of different mole equivalent peptide salmon Calcitonin and preservative Benzethonium chloride mixtures with diluent 90% H_2O with 10% D_2O.
- Selection of NMR experiments and optimisation of pulse programme with appropriate mixing time.
- Characterization of different mole equivalent mixtures through ^{1}H NMR, ^{13}C NMR, DOSY-NMR, CD-Spectroscopy, Fluorescence spectrometry, Zeta potential, DLS, TEM and ITC.
- Identification of molecular interaction of BTC with a bioactive peptide molecule like Salmon Calcitonin form in order to form a 1:1 stoichiometry complex with BTC which may lead to change in the secondary structure of Salmon Calcitonin.

In this chapter, we have tried to study the molecular interaction of Salmon Calcitonin, a therapeutic peptide and Benzethonium chloride, a preservative, used for the nasal spray preparation in presence sodium chloride by using NMR and other spectroscopic techniques. Focus is directed towards identification of interaction which changes the secondary structure which in turn affects the bioavailability, efficacy and toxicity of sCT.

3.3.2: Experimental:

3.3.2.1: Materials and reagents:

Drug

Salmon Calcitonin was obtained as a gift sample from Sun Pharmaceuticals Industries Ltd (Vadodara, India). Salmon Calcitonin (sCT) a thirty two residue amino acid peptide having molecular formula $C_{145}H_{240}N_{44}O_{48}S_2$ with molecular weight 3431.85 is a man-made version of hormone, which is found in salmon. Salmon Calcitonin (sCT) is a worldwide used therapeutic agent for the treatment of various bone disorders resulting due to altered Calcium-phosphorus metabolism. Calcitonin is approved for sale in various countries including U.S. under the brand name (Miacalcin ® Nasal Spray) to the reference listed drug (RLD) employing Benzalkonium chloride as a preservative. Salmon Calcitonin peptide is a white colored powder and has a logP -11.758 ± 1.207 at 25 ºC and is highly soluble in water.

Benzethonium chloride

Benzethonium chloride (BTC) having molecular formula $C_{27}H_{42}ClNO_2$, molecular weight 448.08, pharmaceutical grade with assay value 99.90%, manufactured by Spectrum Chemical Mfg. Corp.USA was used as received.

Benzalkonium chloride solution 50% (BKC) pharmaceutical grade manufactured by Spectrum Chemical Mfg. Corp.USA was used as received. Chlorobutanol hemihydrate (CBT) having molecular formula $C_4H_7Cl_3O{\cdot}0.5H_2O$, molecular weight 186.47, pharmaceutical grade manufactured by Athenstadt Pharmaceuticals Chemicals. Germany was used as received.

Solvents and reagents

AR grade trifluoroethanol (TFE), hydrochloric acid and sodium chloride from Merck, India were used as received.

Deuterium oxide (D_2O)

(99.99%) for NMR solvent were purchased from Merck, Germany and Milli-Q water (0.22 micron nylon filtered) was used throughout the experiments with 90 % H_2O and 10 % D_2O.

Diluent

Accurately weighed 75 mg of analytical grade sodium chloride was dissolved in 50 ml volumetric flask with 90 % H_2O and 10 % D_2O at room temperature.

3.3.3: Methods:

Nuclear Magnetic Resonance (NMR) studies

NMR Spectroscopy is a versatile method not only used as a tool for structure determination of molecules but has also been applied in a broader manner, to study the three dimensional structure, its flexibility, identification and characterization of molecular interactions as well as conformational changes in large molecules.[142] The ability to identify weak molecular interactions and structurally characterize them is a unique feature of NMR spectroscopy. Besides changes in chemical shift of the target peptide induced by ligand binding there are also other NMR parameters commonly exploited in the investigation of protein ligand binding. When a ligand is bound to a peptide, the ligand behaves like the peptide in its dynamic properties and it tumbles more slowly.[140,143]

NMR spectroscopic measurements were carried out for isolated sCT with BTC at three NMR titration points. All spectra were acquired at 25 °C on a Bruker BioSpin AV-III 500 MHz Spectrometer equipped with 5 mm Broad Band Observe probehead with Topspin 2.1 software.

The one dimensional NMR spectra were recorded by utilizing pre-saturation at the water resonance prior to 90° pulse using ‘zgpr’ pulse sequence. Similarly proton decoupled ^{13}C NMR spectra were acquired by using ‘zg30’ pulse programme.[144]

$T_{1\rho}$ is the spin-lattice relaxation time in the rotating frame (Fig.3.5). The NMR signal intensity (M) is measured as a function of the spin-lock duration τ. $T_{1\rho}$ is obtained by fitting the Equation (3-1),

$$M = M_\infty + (M_o - M_\infty)\, e^{-\tau/T_1} \qquad (3\text{-}1)$$

where, M_o is the initial magnetization, and M_∞ is the magnetization when the spin system and the lattice reach a quasi-equilibrium during the spin-lock ($M_\infty = 0$ at resonance).

Pulse sequence

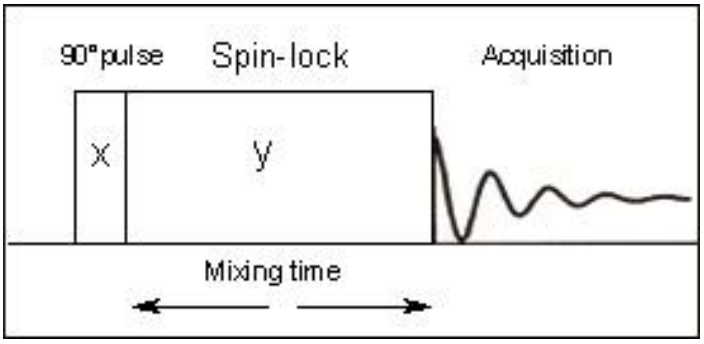

Figure 3.5: Measurement of $T_1\rho$ in two situations where nuclei are excited by a 90°pulse (X) and then Spin-lock (Y) for a time τ

Diffusion Ordered Spectroscopy (DOSY) NMR is a method particularly well suited for uncovering mixture of different drugs with preservatives (stabilizer), or adulterated herbal medicines as it provides both comprehensive information on the formulation and a virtual separation of the components of the mixture based on difference in their translational self diffusion coefficients in solution.[145,146]

A brief description of typical DOSY-NMR experiment is given below. A more detailed description of the method, is found elsewhere.[12] The use of NMR for measuring self diffusion coefficients of molecules in solutions is based on a pulsed field gradient (PFG) stimulated spin-echo (STE) experiment,[147] which is particularly well suited for the analysis of high resolution DOSY of complex mixtures where many signals are observed with a wide dynamic range. Typically a series of one dimensional PFG-STE experimental data is acquired with systematic variations of the gradient pulse amplitude. The Brownian motion in the liquid results in translational diffusion of various solutes and a mean molecular displacement is observed at the end of the delay Δ, which is the delay between coding and decoding gradients.[148,149] This displacement has the effect of reducing the signal intensity with an exponential equation which is based upon Stokes-Einstein Equation (3-2).

$$I(q) = I_0 \exp[-Dq^2(\Delta - L/3)] \qquad (3\text{-}2)$$

where, D = Diffusion Coefficient, $q = \gamma G\delta$ (γ = Gyromagnetic ratio, G = Amplitude of the applied gradient), Δ = Diffusion Time, L = Correlation for finite gradient length.

Hence DOSY signal intensity I(q) depends on molecular weight and other hydrodynamic properties (size, shape and charge) of the solute as well as on its surrounding environment (temperature, viscosity, interaction and state of aggregation).

DOSY spectra were recorded for isolated sCT, BTC and mixtures of the two in different molar ratio. The separation of signals from different components, which is based on differences in their relative diffusion rates are determined.

3.3.4: Circular Dichroism spectroscopy:

The spectra were recorded with quartz cuvettes between 195 and 260 nm with a CD Spectrometer (Model: JASCO J-815) on nitrogen flush with of 5 mm path length at room temperature. To investigate the conformational changes of sCT, different solvents viz mixture of 90 % H_2O and 10 % D_2O, Trifluoroethanol (TFE) and TFE : D_2O (1 : 1) were used. Moreover, for detailed information of conformational changes, different equivalents of BTC were added as shown in the spectra given in the results.[134,150]

3.3.5: Dynamic Light Scattering (Particle size):

A Zetasizer (Nano ZS, Model-Zen 3600, Make-Malvern Instruments, UK) dynamic light scattering equipment with a 15 mW solid state laser source operating at 688 nm was used to measure the hydrodynamic peptide[151] diameter and size distribution of freshly prepared sCT and BTC and its different molar equivalent solutions in a dynamic mode. The scattering intensities from the samples were measured at 90^o using photomultiplier tube. Average hydrodynamic radius of latex particles (R_h) was calculated by using Equation (3-3) from the intrinsic diffusion coefficient (D_0) as,

$$R_h = \frac{KT}{(6\ \pi\eta D_0)} \qquad (3\text{-}3)$$

where, *K* is a Boltzmann constant, T is the absolute temperature and η is the viscosity of the dispersing medium. The polydispersity index (π), which is the variance of the size distribution, was obtained with polystyrene latex standard (60 nm and 200 nm) from Thermo Scientific Inc. provided with the instrument.

Sizes were analyzed using a noninvasive back scatter system with a scattering angle of 173°.The sample and its different mole equivalents were analyzed at 25 °C using disposable low volume cuvettes in 90 % H_2O and 10% D_2O.

3.3.6: Zeta Potential:

Zeta potential was measured using dynamic laser light scattering with a Zetasizer (Nano ZS, Model- Zen 3600, Make-Malvern Instruments). Zeta potential values were determined by laser doppler anemometry at 25 °C, zeta potentials were calculated from three independent measurements.[152] The peptides were analyzed at 25 °C using disposable low volume cuvettes. Solutions of sCT, BTC and their mixtures with different mole ratio were prepared at various concentrations in a mixture of 90 % H_2O and 10 % D_2O (medium). For zeta potential measurements, samples were diluted 10-100 times with medium and placed in the electrophoretic cell where a potential of ± 150 mV was applied. All measurements were performed in triplicate. The performance of the Zetasizer was checked for its consistency by determining the zeta potential value of a standard colloidal zeta transfer standard (Zeta potential -68.4 mV) supplied by the Malvern Instruments, UK.

3.3.7: Fluorescence spectroscopy:

Fluorescence emission spectra were collected using a Spectrofluorophotometer (Model- RF-5301PC, Make-Shimadzu) equipped with a temperature-controlled cuvette compartment. Solution samples prepared at various concentrations in the medium were placed in a 3 x 3 mm quartz cuvette maintained at 25 °C. The excitation monochromator was set at 308 nm and the emission intensity from 200-400 nm was scanned in 1 nm steps with a 1s integration time per step. Both the emission and excitation slits were set to 1 nm. Spectral raw data intensities were normalized with respect to peptide concentration. Spectral intensity is represented in arbitrary units whereby the most intense spectrum was normalized to a value of 1.0 at λ_{max}.

3.3.8: Transmission Electron Microscopy (TEM):

The morphology of different compositions of sCT and BTC was examined by Transmission Electron Microscopy[153] (Model-TECNAI G2 SPIRIT bio TWIN, Make-FEI Company). A high accelerating voltage of 120 kV with spot size 3 of 6 µL

sample solutions (i.e sCT and BTC and their mixtures having different mole ratio) were placed on a copper grid during the course of imaging.[154]

3.3.9: Isothermal Titration Calorimetry (ITC):

Isothermal Titration Calorimetry[155] was performed by using Microcal iTC 200 (Make-MicroCal). The complete binding parameters[156, 157] of sCT and BTC were determined using a cell volume of 200 µL of 200 µM sCT solution and titrated with 40 µL of 2000 µM BTC in water at 25ºC.

3.4: Results and discussion:

3.4.1: Proton, Proton decoupled ^{13}C NMR:

Binding of small molecules to any large peptide causes the ligand T_2 (spin-spin relaxation) values to decrease and the signals to broaden.[140] The degree of broadening observed is dependent on the affinity of the ligand towards the peptide. The increase in relaxation rates simultaneously affects the signal broadening and decrease in signal intensity.

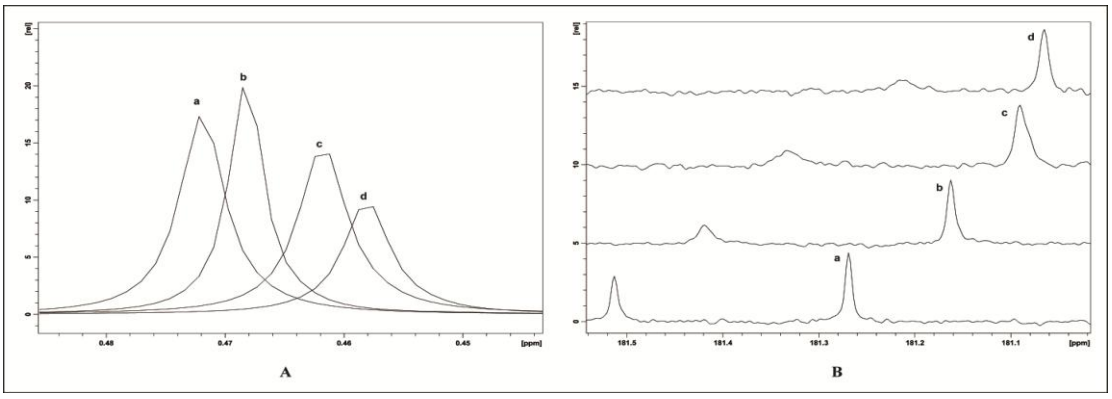

Figure 3.6: (A) ^{1}H-NMR chemical shift (δ) of (a) pure BTC, (b) 0.5 eqvt., (c) 1.0 eqvt. and (d) 2.0 eqvt. of BTC with respect sCT, (B) Variation in ^{13}C chemical shift of (a) pure sCT, (b) 0.5 eqvt., (c) 1.0 eqvt. and (d) 2.0 eqvt. of BTC with respect sCT

The signal shift of ^{13}C-NMR, ^{1}H-NMR titration consistently supports that BTC, CBT and BKC is interacting to sCT at different mole equivalent. The proton decoupled ^{13}C spectra of sCT at δ =181.5 ppm with BTC, CBT and BKC shows chemical shift variation along with line broadening shown in Fig.3.6(B), Fig.3.7(B) and Fig.3.8(B). In case of CBT relatively less downfield shift was observed with respect to BKC, whereas in case of BTC there is a upfield shift. The line broadening and chemical shift of respective ^{1}H signal of BTC, CBT and BKC at 0.48-0.45 ppm

(Fig. 3.6 (A)), 0.80-0.86 ppm (Fig. 3.7(A)), 0.75 - 0.80 ppm (Fig. 3.8(A)) respectively shows a upfield shift for BTC and CBT whereas BKC shows a downfield shift.

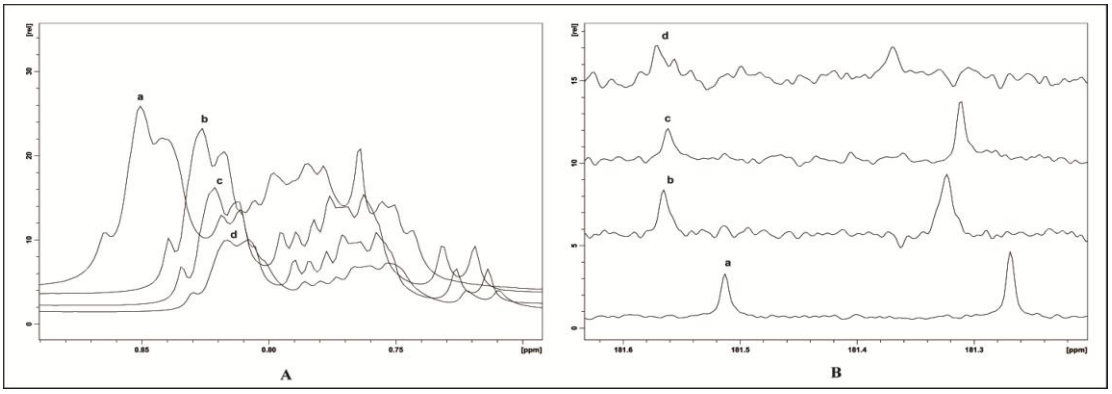

Figure 3.7: (A) ^{1}H-NMR chemical shift (δ) of (a) pure CBT, (b) 0.5 eqvt., (c) 1.0 eqvt. and (d) 2.0 eqvt. of CBT with respect sCT, (B) Variation in ^{13}C chemical shift of (a) pure sCT, (b) 0.5 eqvt., (c) 1.0 eqvt. and (d) 2.0 eqvt. of CBT with respect sCT

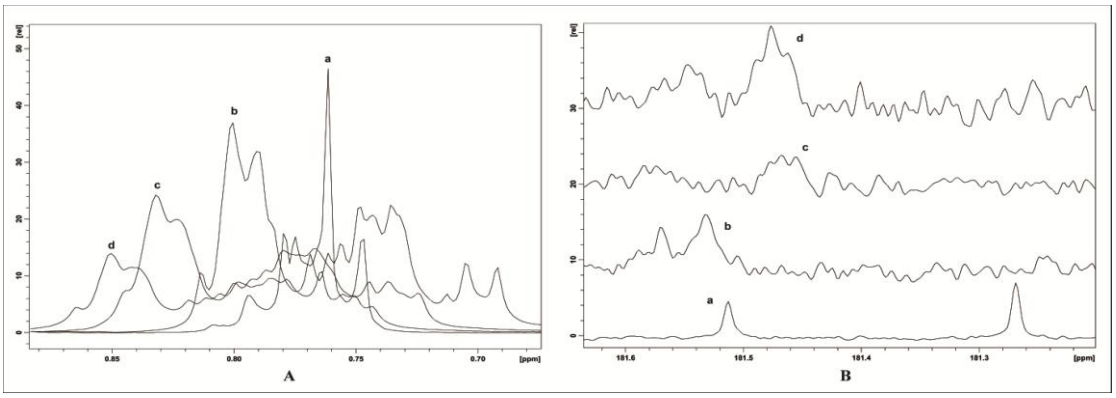

Figure 3.8: (A) ^{1}H-NMR chemical shift (δ) of (a) pure BKC, (b) 0.5 eqvt., (c) 1.0 eqvt. and (d) 2.0 eqvt. of BKC with respect sCT, (B) Variation in ^{13}C chemical shift of (a) pure sCT, (b) 0.5 eqvt., (c) 1.0 eqvt. and (d) 2.0 eqvt. of BKC with respect sCT

3.4.2: $T_1\rho$ experiments:

Alternatively, transferred $T_1\rho$ relaxation study has been applied for determining the changes in relaxation rates upon binding to a peptide. As we know the increase in relaxation rates simultaneously affects the signal broadening and decrease in signal intensity.

3.4.2.1: Effect of mixing time against intensities in sCT and BTC:

18.3 mg of sCT was accurately weighed and dissolved it completely in 1 mL of diluent and the pH of the resulting solution was 3.77 at 25ºC. Similarly 50 mg of BTC was weighed accurately and completely dissolved in 5 mL volumetric flask and diluted upto the mark with diluent, the pH of the solution was 3.5 at 25 °C.

$T_1\rho$ experiments of the above solution were performed with varying mixing time from 10 ms to 190 ms at 25°C and the results of variation of intensities are presented in Table 3.2. and Table 3.3 respectively. From the data it was observed that by increase in mixing time the intensities of a specific signal decreases exponentially as shown in Figure 3.9.

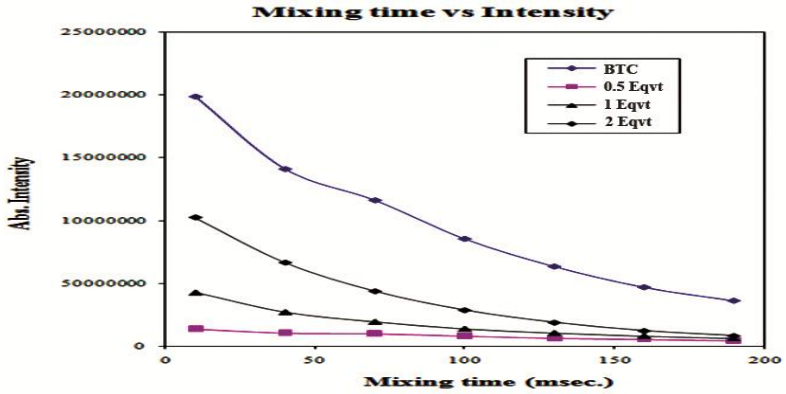

Figure 3.9: ^{1}H-NMR absolute intensity vs mixing time (τ) variations at different mole equivalent

Sr. No.	Mixing Time(ms)	Abs. Intensity of signal x 10^5 at ~0.80 ppm
1	10	2.82
2	40	2.50
3	70	2.22
4	100	1.97
5	130	1.73
6	160	1.51
7	190	1.34

Table 3.2: sCT signal intensity with variation of mixing time

Sr. No.	Mixing time τ in ms	Abs. Intensity of signal x 10^8 at ~ 0.45ppm
1	10	3.74
2	40	2.97
3	70	2.48
4	100	2.24
5	130	2.06
6	160	1.70
7	190	1.32

Table 3.3: BTC signal intensity with variation of mixing time

3.4.2.2: pH effect on chemical shift in sCT and BTC:

One equivalent mole ratio of sCT with BTC was prepared by mixing accurately weighed 18.3 mg of sCT and 3.41 mg BTC were dissolved completely in 1 mL of diluent. Similar $T_1\rho$ experiments were performed with a mixing time of 10 ms by varying pH. The observed results are given in the Table 3.4 and concluded that the pH having no substantial effect on chemical shift.

Sr. No.	pH	δ sCT peak at 0.79 ppm	δ BTC peak at 0.45 ppm
1	3.12	0.7804	0.4514
2	3.77	0.7883	0.4522
3	5.30	0.7859	0.4526
4	5.97	0.7890	0.4529

Table 3.4: pH effect of sCT with 1 equivalent of BTC

Alternatively transferred $T_1\rho$ relaxation study has been applied to BTC, CBT and BKC to determine the change in signal intensities upon binding to sCT at different mole ratio solution in 10% D2O and 90% H2O against variation of mixing time from 10 ms to 190 ms at 25°C.

The $T_1\rho$ experiments data reveal that BTC clearly displays faster relaxation in presence of sCT compared to isolated BTC which is evident from the decrease in absolute intensity with respect to mixing time in milliseconds (Fig.3.10A) whereas CBT displays very small variations in relaxation time upon addition to sCT in comparison to isolated CBT (Fig.3.10B) and BKC displays moderate relaxation (Fig. 3.10C) upon addition to sCT when compared to isolated BKC.

Finally it can be concluded that BTC strongly interacts with sCT in comparison to BKC and CBT as shown in Figure 3.11.The dual ionic property of BTC and its optimum size makes it a less stable nasal spray formulation in comparison to BKC

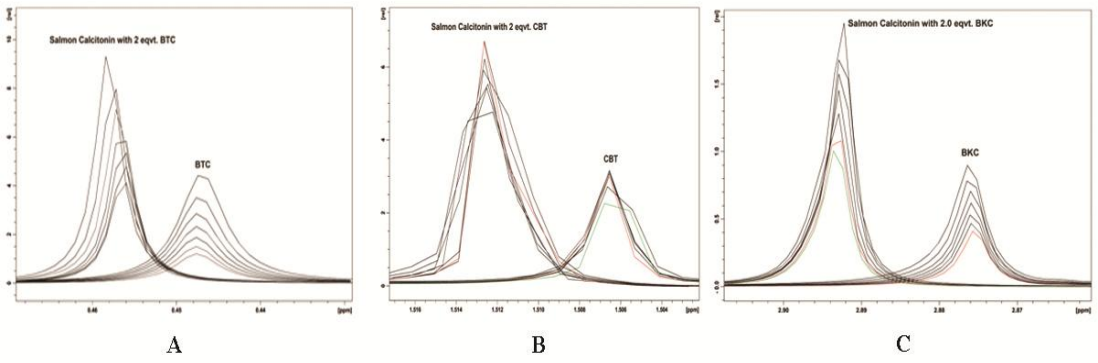

Figure 3.10: ^{1}H-NMR absolute intensity of pure (A) BTC, (B) CBT and (C) BKC as compared to their mixture of sCT with mixing time (τ) variation

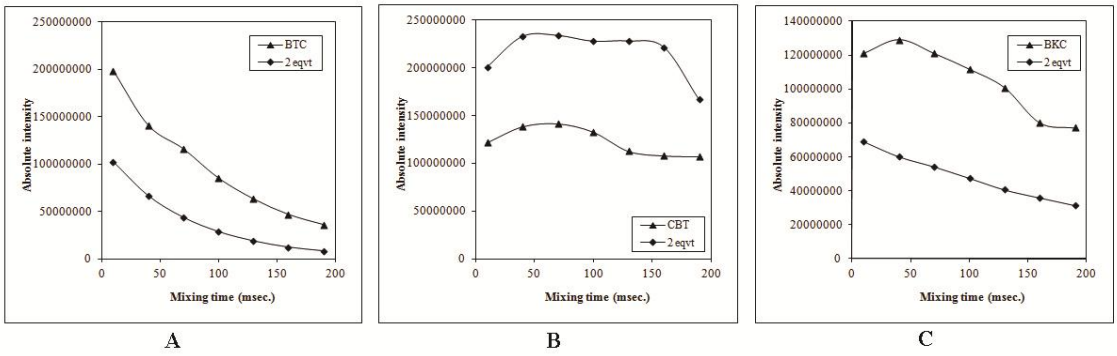

Figure 3.11: Graphical representation of ^{1}H-NMR absolute intensity of pure (A) BTC, (B) CBT and (C) BKC as compared to their mixture of sCT with mixing time (τ) variation

3.4.3: DOSY-NMR experiments:

The size of sCT and BTC, CBT, BKC and their mixtures of different mole ratios were evaluated by comparing their self diffusion coefficients with those of monomeric units using the DOSY experiments spectra as shown in Figure 3.12. The identical experimental conditions were applied for all the samples. The hydrodynamic radius calculated from Stokes-Einstein equation using the value of diffusion constant obtained from DOSY experiments is correlated to the shape and size of the molecules.

The signals used for the determination of self diffusion coefficients are at 0.45 ppm for BTC and 1.78 ppm for sCT and results indicates that increase in amount of BTC in the mixture leads to its slower exchange with sCT presented at Table 3.5. Hence, there appears to be shrinkage in the size of sCT to partial symmetrical shape with respect to free sCT. At 1 : 1 mole ratio sCT shows an optimum diffusion constant as shown in Figure 3.13.

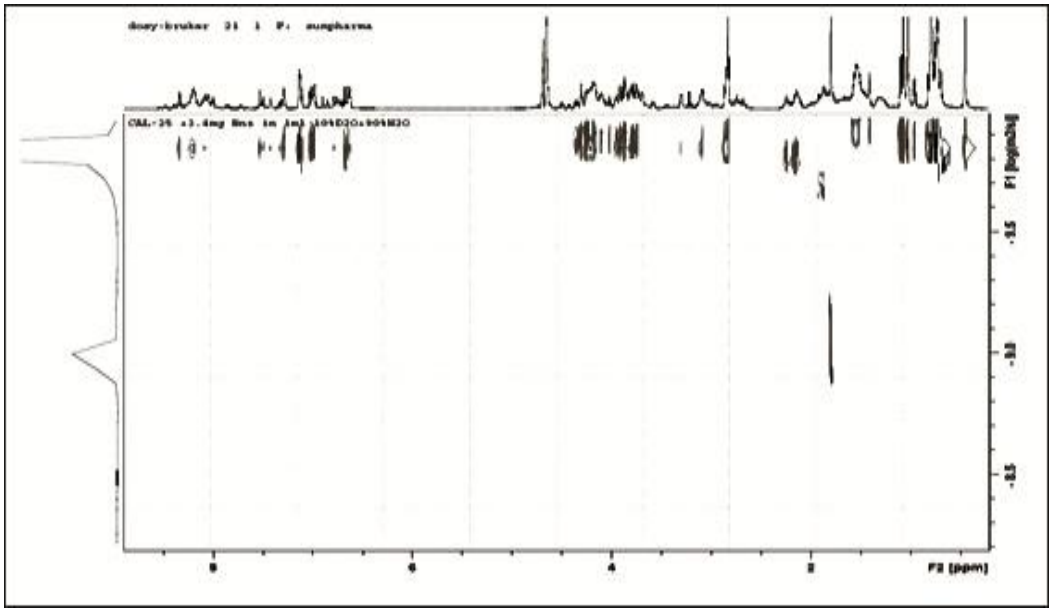

Figure 3.12: DOSY NMR spectrum of sCT and BTC (1 : 1) in 10% D_2O in H_2O

Sr. No.	(sCT+BTC) mole ratio	Diffusion constant of BTC	Diffusion constant of sCT
1	1 + 0	---	7.413
2	0 + 1	2.66	---
3	1 + 0.5	2.312	8.146
4	1 + 0.75	1.456	8.477
5	1 + 1	1.282	8.905
6	1 + 1.5	1.084	8.625
7	1 + 2.0	0.997	8.401

Table 3.5: Diffusion constants of sCT, BTC and their mixtures with different mole equivalents

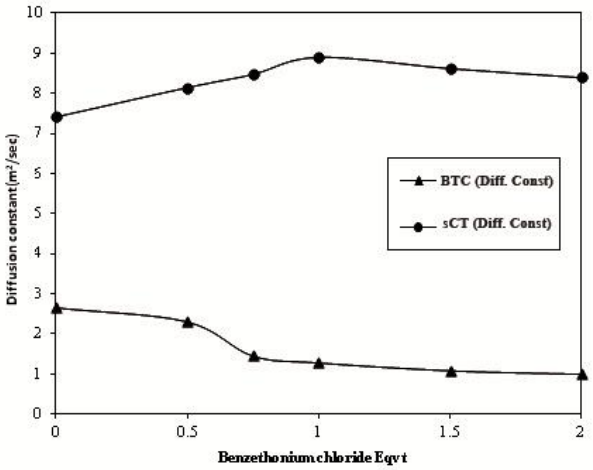

Figure 3.13: Variation of diffusion constant of sCT and BTC with different mole equivalent of BTC

Sr. No.	(sCT+CBT) mole ratio	Diffusion constant of CBT	Diffusion constant of sCT
1	1 + 0	---	7.413
2	0 + 1	6.890	---
3	1 + 0.5	5.404	8.351
4	1 + 0.75	5.943	7.325
5	1 + 1	5.870	7.395
6	1 + 1.5	6.143	7.421
7	1 + 2.0	6.368	7.545

Table 3.6: Diffusion constants of sCT, CBT and their mixtures with different mole equivalent

The self diffusion coefficients are at 1.5 ppm for CBT indicates that increase in amount of CBT in the mixture leads to its very slower exchange with sCT (Table 3.6). Hence, there appears to be negligible shrinkage at all mole ratio in the size of sCT to partial symmetrical shape with respect to free sCT. Similarly for BKC at 3.2 ppm it shows minimal exchange upto 1 : 1.5 , while at 1 : 2 mole ratio it shows very fast exchange with sCT (Table 3.7) . Hence, it seems to be a drastic shrinkage in the size of sCT to partial symmetrical shape with respect to free sCT at 1 : 2 mole ratio.

Sr. No.	(sCT+BKC) mole ratio	Diffusion constant of BKC	Diffusion constant of sCT
1	1 + 0	---	7.413
2	0 + 1	1.246	---
3	1 + 0.5	1.340	8.372
4	1 + 0.75	1.302	7.981
5	1 + 1	1.360	8.509
6	1 + 1.5	1.377	8.533
7	1 + 2.0	1.844	15.03

Table 3.7: Diffusion constants of sCT, BKC and their mixtures with different mole equivalent

Hence, comparison of DOSY experiments reveals that CBT shows very less interaction at all molar ratios while BKC exhibits sudden increase in interaction at 2 equivalent mole ratio. Under same experimental conditions BTC shows maximum interaction with sCT at 1 : 1 mole equivalent.

3.4.4: Dynamic Light Scattering and Zeta Potential:

Light Scattering represents an exquisitely sensitive method for the detection of a small fraction of a large species. The present study was performed to investigate the capability of dynamic light scattering to distinguish various mole ratio solutions of sCT and BTC differing their complex form in soluble aggregate content shown in Table 3.8, which is also inversely proved by diluting the 1 : 1 mole equivalent aggregated mixture solution. Similar results were also observed from Zeta Potential experiments. The dynamic light scattering intensity profiles of various mole ratio solutions and Zeta potential were graphically represented below (Fig.3.14). The dilution effect was studied by light scattering technique for sCT with one equivalent BTC (Table 3.10 and Fig.3.15).

Sr. No.	(sCT+BTC) mole ratio	Z-Average (nm)
1	1 + 0	908.5
2	0 + 1	288.0
3	1 + 0.5	724.9
4	1 + 0.75	498.1
5	1 + 1	105.3
6	1 + 1.5	170.3
7	1 + 2.0	222.8

Table 3.8: Variation in Z-Average molecular weight with mole ratio of sCT and BTC

3.4.5: Zeta Potential:

It can also be used to determine zeta potential of such species. Variation in zeta potential with mole ratio of sCT and BTC is shown in Table 3.9. It is evident that zeta potential curve shows a maximum at 1 : 1 mole ratio thereby lending support to the conclusion drawn from NMR studies.

Serial No.	(sCT+BTC) mole ratio	Zeta Potential (mV)
1	1 + 0	19.4
2	0 + 1	38.7
3	1 + 0.5	27.9
4	1 + 0.75	29.6
5	1 + 1	32.2
6	1 + 1.5	30.1
7	1 + 2.0	25.1

Table 3.9: Variation in Zeta potential with mole equivalents of sCT and BTC

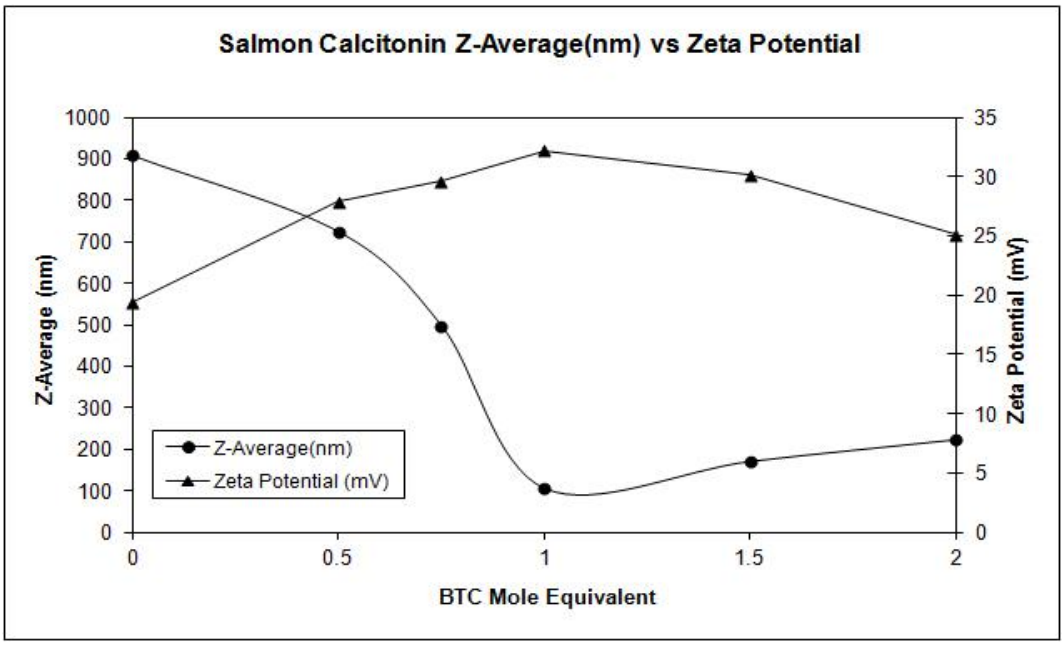

Figure 3.14: Comparison of Z-Average molecular weight and Zeta Potential of sCT at different mole equivalent of BTC

The dilution study of 1 : 1 sCT and BTC reveals that after three fold dilution, the size observed from DLS is equivalent with the size of free sCT shown in Table 3.10, hence it can be concluded that the minimal size is due to the soluble aggregates of 1 : 1 mole ratio complex which separates out on further dilution and achieves and optimal size.

Sr. No.	Salmon Calcitonin with 1.0 Equivalent Benzethonium chloride	
	Dilution in mL	Z-Average (nm)
1	10	105.3
2	20	455.5
3	40	963.1
4	80	1022
5	160	1070
6	320	919
7	640	790.5

Table 3.10: Results of dilution effect on sCT with 1 equivalent of BTC

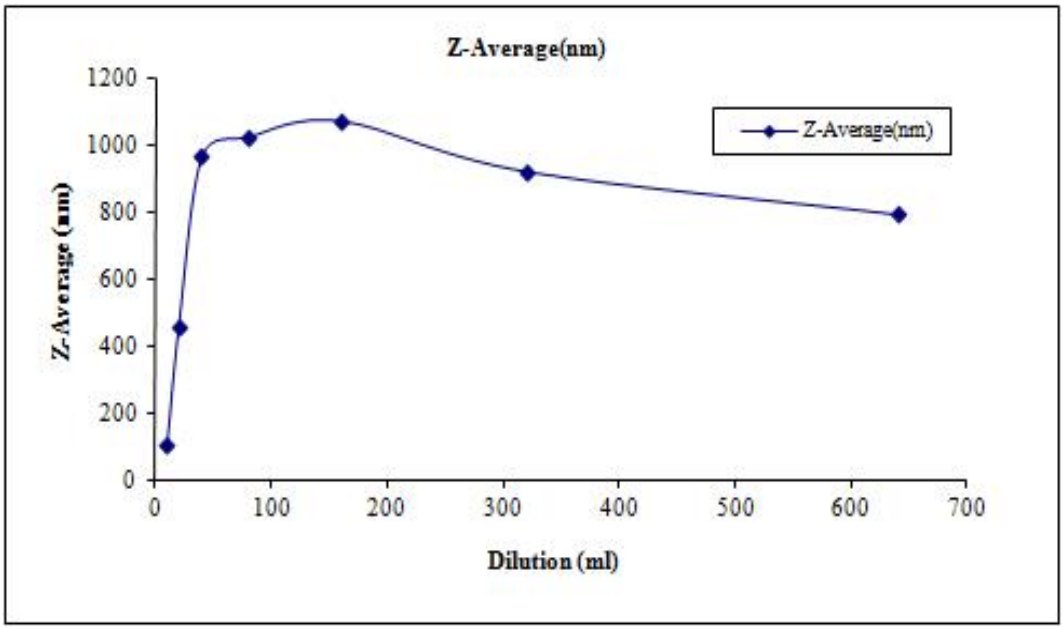

Figure 3.15: Dilution effect curve of sCT with 1.0 equivalent of BTC

3.4.6: Fluoroscence spectroscopy:

Free sCT has a fluorescence wavelength at 308 nm with high intensity. Upon addition of BTC the intensity decreases with a hypsochromic shift and in a 1 : 1 mixture the decrease in intensity is found to be maximum with highest hypsochromic shift due to a perturbation in the energy levels of sCT due to interaction with BTC (Fig.3.16). These observations confirm the formation of 1 : 1 complex (Table 3.11).

Serial No.	Concentration of BTC	Wavelength	Intensity
1	0	305	11.307
2	0.5	307	3.814
3	0.75	306	3.095
4	1.0	304	2.202
5	1.5	302	2.477
6	2.0	305	1.613

Table 3.11: Effect of concentration variation of BTC on fluorescence intensity of sCT

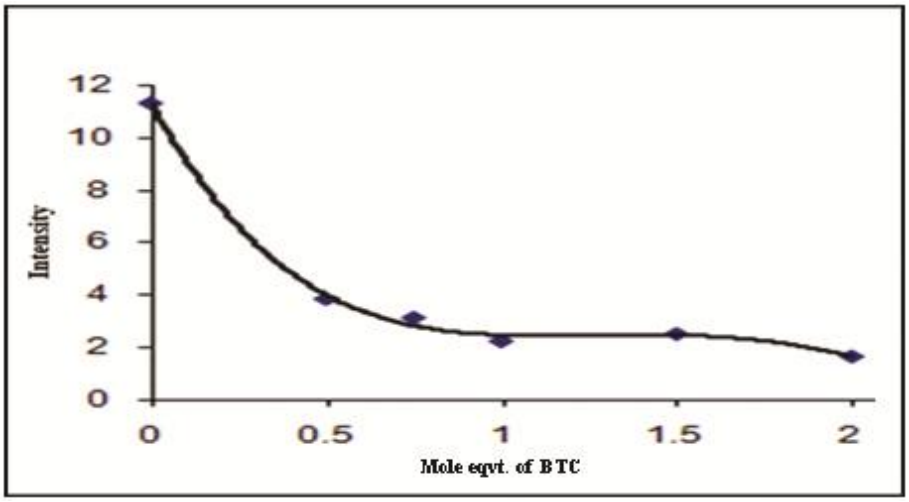

Figure 3.16: Plot of Fluoroscence intensity of sCT with different mole equivalent of BTC

3.4.7: CD spectroscopy:

3.4.7.1: Solvent effect:

The CD spectra of 100 ppm sCT were typically recorded as an average of 16 scans, obtained in millidegree, and converted to molar ellipticy [θ] (deg.cm^{-2}.dmol^{-1}). When dissolved in a mixture of 90 % H_2O and 10 % D_2O it shows a negative peak at ~ 201 nm (Fig.3.17a) which indicates a random coil conformation. Further in pure trifluoroethanol (TFE) (Fig.3.17b) and TFE: D_2O (1 : 1) (Fig.3.17c), sCT displays a strong alpha-helical structure as it exhibits two negative bands 222 and 207 nm and a positive band at about 194 nm.[2] Nevertheless, the intensity of the minimum at 222 nm is less than expected for a pure alpha-helix and the peaks are somewhat broader indicating the presence of other secondary structural features, possibly 40 % alpha-helical, 40 % beta- pleated sheet and 20 % random coil.[2] In a mixture of 90 % H_2O and 10 % D_2O there is drastic loss of structure in the CD spectra (Fig.3.17a). Probably

sCT assumes nearly random coil conformation, although a small positive maximum in the far UV indicates that some preferred conformation is still left due to the presence of Cys^{1}-Cys^{7} ring system.[2] Comparison CD spectra of sCT with same mole equivalent of BTC,CBT and BKC as shown in Figure 3.18. The final formulation product of sCT nasal spray was manufactured with preservatives and sodium chloride salt, hence the salt effect also studied by CD spectroscopy and the result are presented in Table 3.13.

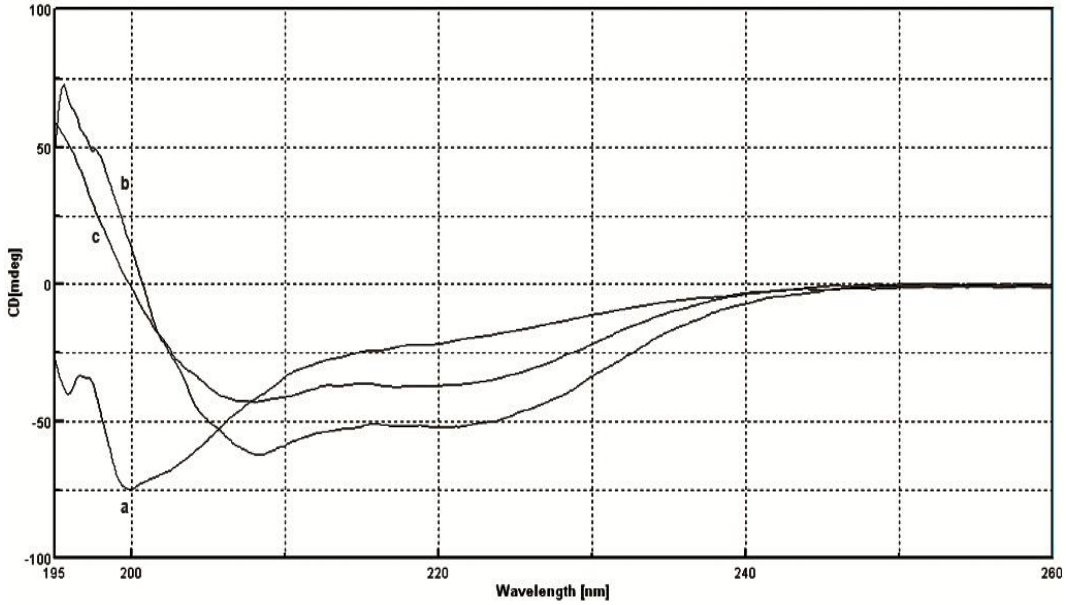

Figure 3.17: Solvent dependant CD spectra of sCT

The CD spectra of 100 ppm sCT recorded with different equivalents of BTC, CBT and BKC (i.e. 0.50, 0.75, 1.0, 1.5 and 2.0 eqvt.) are given in Figure 3.19, Figure 3.20 and Figure 3.21 which show broadening of peaks indicating the presence of other secondary structure (Table 3.12). At different equivalents of CBT there is no significant change in secondary structure as seen from the CD spectra comparison with respect to free sCT but after 48 hours there is change in secondary structure of % β-Sheet from 17 to 3 %, whereas for different equivalents of BKC it shows a similar pattern compared to free sCT upto 1 : 1 equivalent, but there is a drastic loss in the secondary structure above 1.5 equivalent.

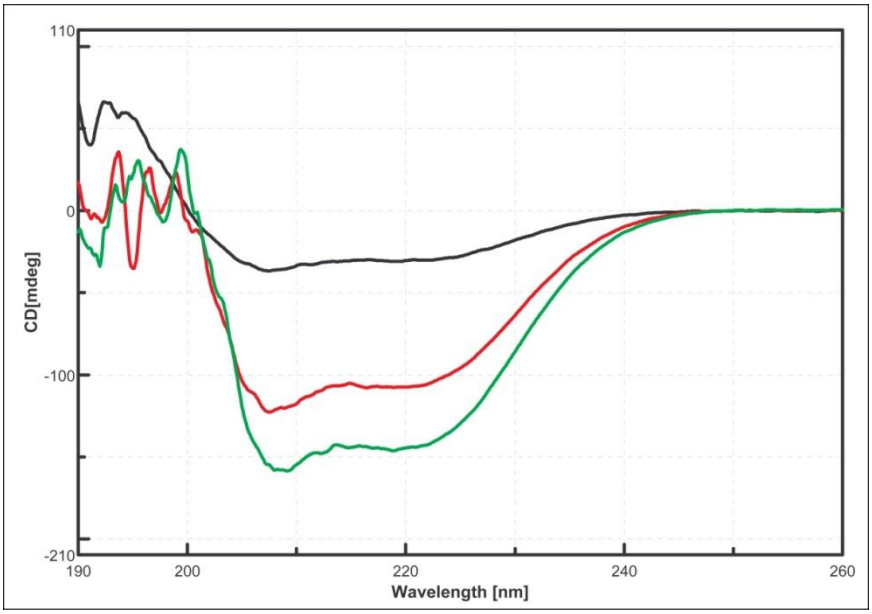

Figure 3.18: Comparison of CD spectra of sCT with same equivalent of CBT (Green line), BKC (Red line) and BTC (Black line)

3.4.7.2: Comparison study of sCT with different preservatives:

Similar CD experiments was performed for BTC, CBT and BKC with 1 mole equivalent of sCT and the results are represented Table 3.12.

Sample at 25 °C	Solvent	% Random coil	% α-Helix	% β-Sheet
sCT	90 % H_2O + 10 % D_2O	59.1	2.3	38.6
sCT	TFE	26.7	21.4	38.2
sCT	TFE + D_2O	33.5	33.0	33.4
sCT + 1 eqvt. BTC	TFE + D_2O	28.7	30.6	40.7
sCT + 1 eqvt. CBT	TFE + D_2O	33.9	22.6	17.3
sCT + 1 eqvt. BKC	TFE + D_2O	34.8	21.4	20.3
sCT + 1 eqvt. BTC (after 48 hours)	TFE + D_2O	26.9	34.6	38.5
sCT + 1 eqvt. CBT (after 48 hours)	TFE + D_2O	37.3	27.7	2.9
sCT + 1 eqvt. BKC (after 48 hours)	TFE + D_2O	35.2	21.4	19.6

Table 3.12: Variation of secondary structure of sCT with BTC, CBT and BKC along with time

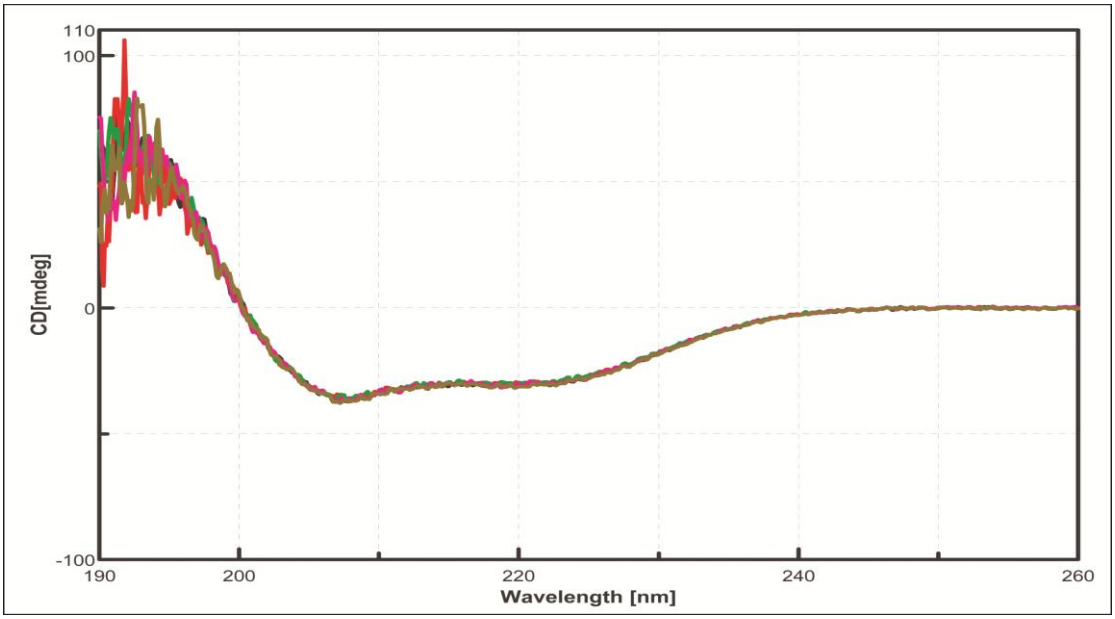

Figure 3.19: Comparison of CD spectra of sCT with different equivalent of BTC [(a)- Green line (0.5 eqvt.), (b)-Pink line (0.75 eqvt.), (c)-Black line (1.0 eqvt.), (d)-Tan line (1.5 eqvt.), (e)-Orange line (2.0 eqvt.)]

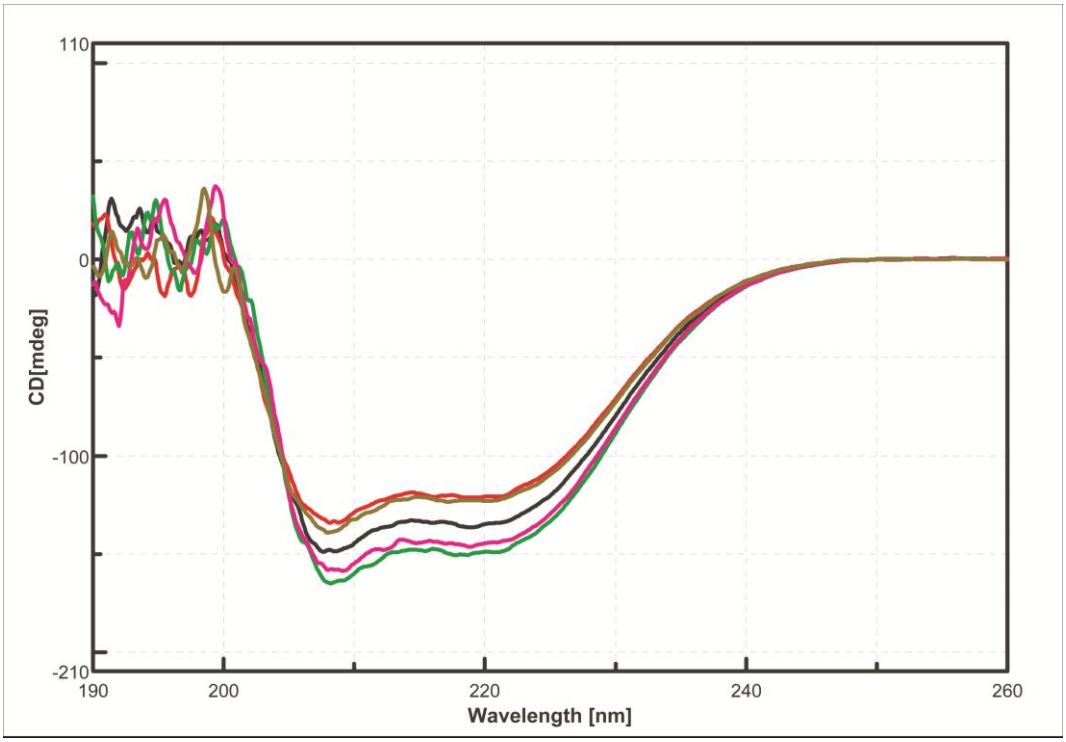

Figure 3.20: Comparison of CD spectra of sCT with different equivalent of CBT [(a)- Green line (0.5 eqvt.), (b)-Pink line (0.75 eqvt.), (c)-Black line (1.0 eqvt.), (d)-Tan line (1.5 eqvt.), (e)-Orange line (2.0 eqvt.).]

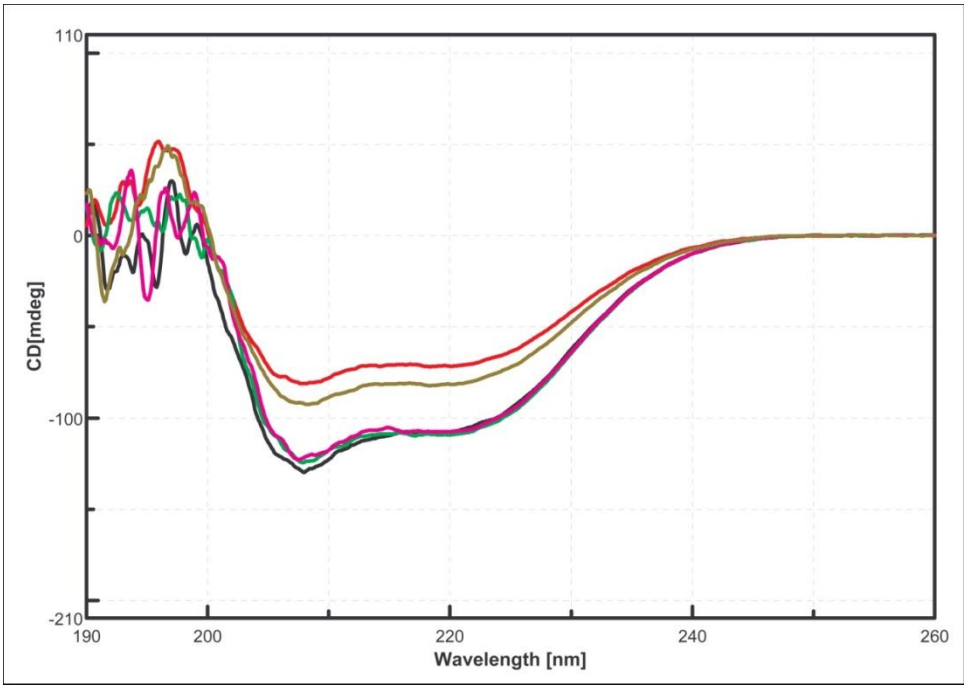

Figure 3.21: Comparison of CD spectra of sCT with different equivalent of BKC [(a)- Green line (0.5 eqvt.), (b)-Pink line (0.75 eqvt.), (c)-Black line (1.0 eqvt.), (d)-Tan line (1.5 eqvt.), (e)-Orange line (2.0 eqvt.)]

From the initial data it is observed that there is a significant change in the secondary structure of BTC when compared to CBT and BKC. But after 48 h it is seen that there is no significant change in secondary structure of BKC and BTC while for CBT there is a drastic change in the percentage of β-Sheet.

3.4.7.3: Salt effect:

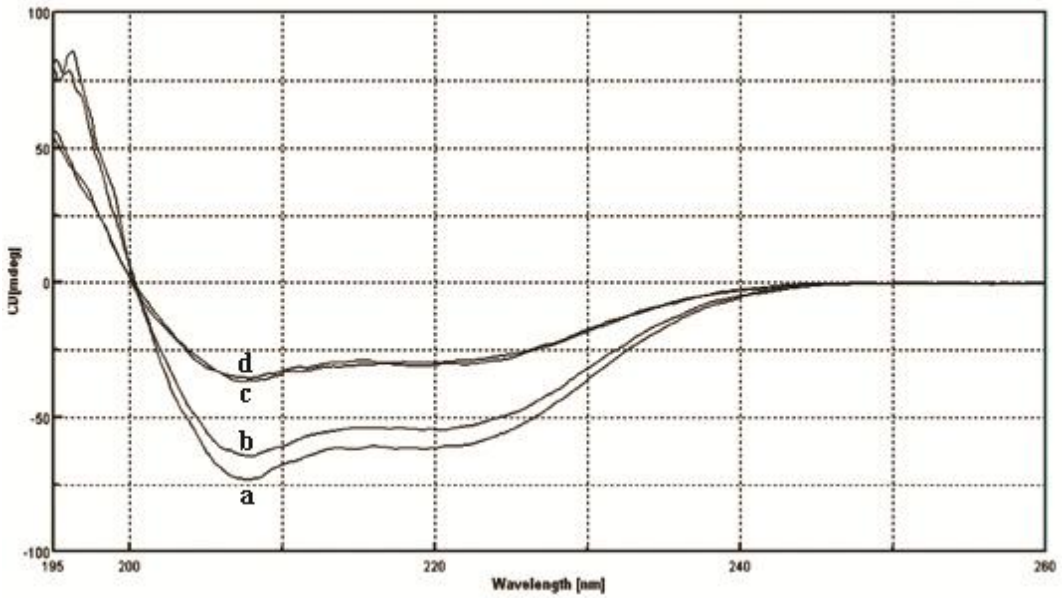

Figure 3.22: CD spectra of pure sCT with BTC and its effect with NaCl

Further, due to addition of NaCl i.e pure sCT with salt (Fig.3.22c) and 1 : 1 sCT : BTC with salt (Fig.3.22d)] to pure sCT (Fig.3.22a) and 1:1 sCT: BTC (Fig.3.22b), there is a loss of secondary structure from the CD spectra which is not observed in the case of CBT and BKC.

Sample + preservative	Solvent	% Random coil	% α-Helix	% β-Sheet
sCT + 1 eqvt. BTC+ NaCl	TFE + D_2O	21.8	16.1	50.6
sCT + 1 eqvt. CBT+ NaCl	TFE + D_2O	35.6	27.0	6.7
sCT + 1 eqvt. BKC+ NaCl	TFE + D_2O	37.2	26.7	5.9

Table 3.13: Variation of secondary structure of sCT with BTC, CBT and BKC with NaCl

3.4.8: Transmission Electron Microscopy (TEM) study:

The morphology of sCT and BTC and their mixtures was studied by Transmission Electron Microscopy (TEM). The TEM micrographs shown in Figure 3.23 of pure solution of sCT (A), BTC (B) and their mixtures are shown in images (C and D). TEM studies show that with increasing mole equivalents of BTC, agglomerised sCT expands as compared to the pure agglomerised rod type sCT. Moreover, the image of BTC merges with that of sCT.

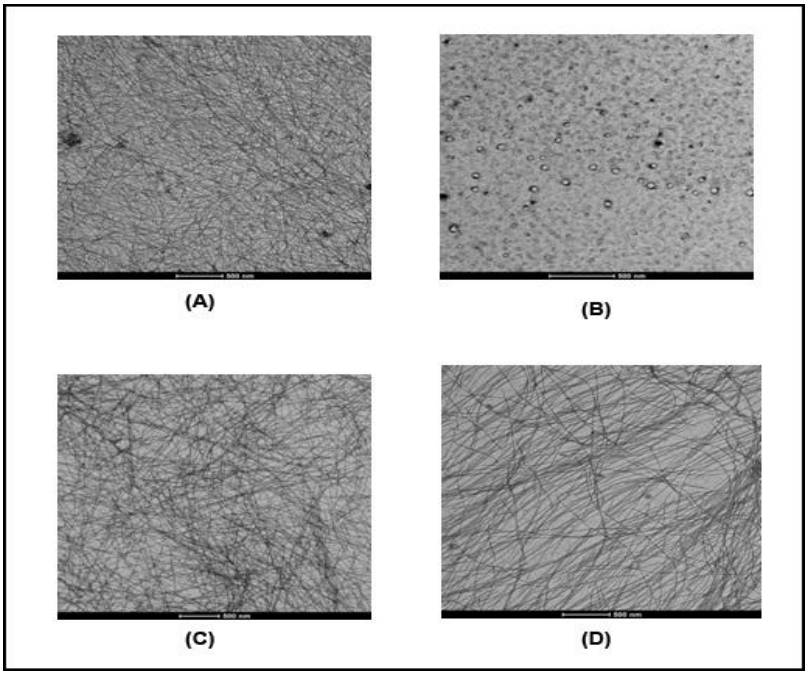

Figure 3.23: TEM images of (A) sCT (B) BTC (C) 1:1 mole eqvt. of sCT and BTC (D) 1:2 mole eqvt. of sCT and BTC

3.4.9: Isothermal Titration Calorimetry (ITC):

Isothermal Titration Calorimetry is a technique that directly measures the heat released or absorbed during a molecular binding event. Measurement of this heat enables accurate determination of binding constant (K_B), reaction stoichiometry (n), enthalpy (ΔH) and entropy (ΔS), thereby providing complete information of the molecular interactions.[25] The experiment was performed in duplicate at 25°C with high reproducibility results. The following features of the isothermal titration curve against time as shown in Figure 3.24 and the average binding parameter datas are given in Table 3.14 which reveals that the binding of sCT with BTC is very weak but interestingly shows 1 : 1 stoichiometry as shown in Figure 3.25.

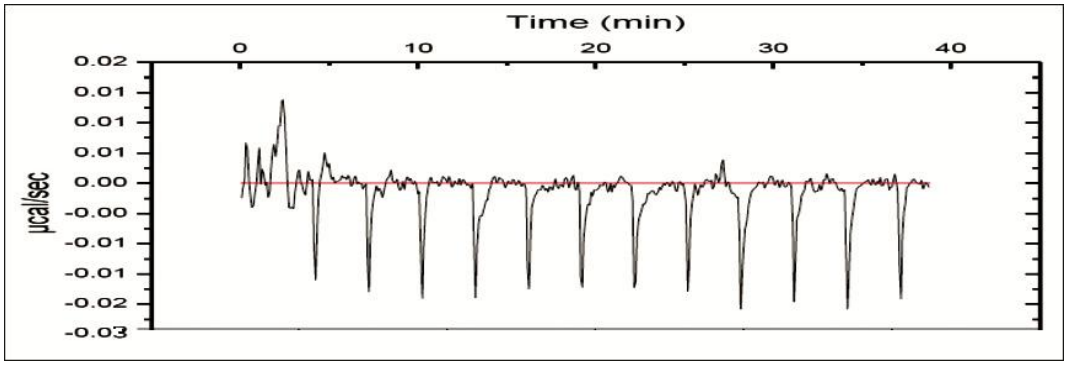

Figure 3.24: Isothermal titration calorimetry curve

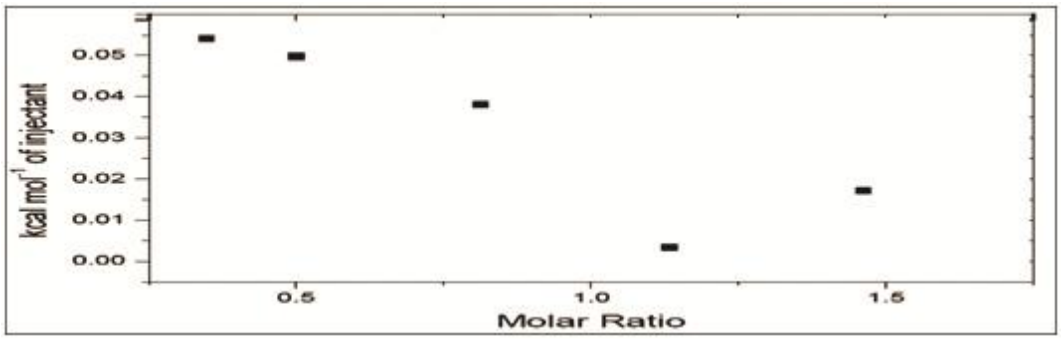

Figure 3.25: Isothermal titration stoichiometric points between sCT and BTC

Sr. No.	Binding parameter	Average result
1	Binding constant (K_B)	2.235 E5 M^{-1}
2	Reaction stoichiometry (n)	0.84 ± 0.1164
3	Enthalpy (ΔH)	86.67 cal/mol
4	Entropy (ΔS)	22.45 cal/mol/deg

Table 3.14: Binding parameters of sCT with BTC

3.4.10: Effect on preservative efficacy:

10 mL each of the different mole equivalent sample solution with sCT were taken in a preservative efficacy tube (PET) and comparative preservative capacity of BTC, CBT and BKC was studied by using two different standard test organism (*viz*: S. aureus and E. coli) of 100 CFU/mL (CFU= Colony Forming Units). Exactly 1 mL each of the 100 CFU/mL was taken in sterilized petri-dish, then 10 to 15 mL SCDA (Soyabean Casein Digest Agar) was added to it as a control and incubated at 30 to 35 °C for 24 to 48 h. The results were collected at different intervals up to 96 h. No growth was observed in any mole equivalent concentration of BKC with sCT, where as uncountable growth was observed in all three mole equivalent BTC with sCT solution while CBT solution showed intermediate growth. Hence it is evident that BTC preservative efficacy got modified or reduced in comparison with BKC and CBT due to interaction with sCT.

Conclusion

The knowledge of weak molecular interaction between sCT employing BTC as a preservative is crucial to the stability of pharmaceutical products of Salmon Calcitonin as it affects the bioavailability, efficacy and toxicity of sCT. The different sets of experiments carried out in the present study point to the fact that Benzethonium chloride (BTC) interacts / binds with Salmon Calcitonin (sCT). The chemical shift variations, broadening in the proton spectra, $T_1\rho$ experiments and DOSY NMR spectral analysis support that, in the concentration range of sCT employed, the BTC is in intermediary exchange between a bound and free form at the current NMR timescale with 1 : 1 stoichiometry with BTC due to the presence of carboxylic group of glutamic acid (-Glu^{15}-) in peptide chain. Hence, the secondary structure of sCT is distorted due to the presence of BTC as a preservative in the nasal spray. This is actually responsible for the toxicity and lower efficacy of the preservative. The reference compounds used in this study namely BKC and CBT, show lower interaction with sCT and therefore are preferred over sCT.

The above observations are also supported by Fluorescence emission spectrophotometry, Circular Dichrosim spectroscopy, Dynamic Light Scattering (DLS), Zeta potential and Isothermal Titration Calorimetry.

Reference

1. (a) Davies, J. S. *Amino Acids, Peptides and Proteins,* **2006**, 1-73, *RSC* Publishing. (b) Sanger, F. *Adv. Protein. Chem.* **1952**, *7*, 1.
2. (a) Pauling, L.; Corey, R. B.; Branson, H. R. *Proc. Natl. Acad. Sci. U.S.A.* **1951**, *37*, 205. (b) Ramachandran, G.N.; Ramakrishnan, C.; Sasisekharan, V. *J. Mol. Biol.* **1963**, *7*, 95. (c) Richards, F. M.; Kundrot, C. E. *Proteins,* **1988**, *2*, 71. (d) Kauzmann, W. *Adv. Protein Chem.* **1959**, *14*, 1.
3. Koltz, I. M.; Darnall, D. W.; Langerman, N. R. *The Proteins*, **1975**, *Vol.1*. Academic Press, New York, p.293-411.
4. Sund, H. Weber, K. *Angew. Chem. Int. Ed.* **1966**, p.231-245.
5. Dill, K. A. *Biochemistry***, 1990**, *29*, 7133.
6. Badelin, V. G.; Kulikov, O. V.; Vatagin, *V. S. Thermochim. Acta*, **1990**, *169*, 81.
7. Hokfelt, T.; Millhorn, D.; Seroogy, K.; Tsuruo, Y.; Ceccatelli, S.; Lindh, B.; Meister, B.; Melander, T.; Schalling, M.; Bartfai T.; Terenius, L. *Experientia,* **1987**, *43*, 768.
8. Gellman. S.; Wu. Y. D. *Acc. Chem. Res*. **2008**, *41*, 1231.
9. Costantino, H.; Philo, J. S.; Eidenschink, L. *J. Pharm. Sci.* **2009**, *98*, 3691.
10. Meyer, J-P.; Pelton, J. T.; Hoflack, J.; Saudek, V. *Biopolymers*, **1991**, *31*, 233.
11. Mayer, M.; Mayer, B. Angew. *Chem. Int. Ed.* **1999**, *38*, 1784.
12. Weatherall, M. *Pharm. J*. **1987**, *238*, 210.
13. Nispen, J. W.; Pinder, R. M. *Annu.Rep.Med.Chem*. **1987**, *22*, 51.
14. van Noordwijk, J. *Arzneim.-Forsch./Drug Res.* **1988**, *38*, 943.
15. Hess, P. N. *Arzneim.-Forsch./Drug Res.* **1987**, *37*, 1210.
16. Bachmayer, H. *Arzneim.-Forsch./Drug Res.* **1988**, *38*, 590.
17. Freter, K. R. *Pharm. Res*. **1988**, *5*, 397.
18. Morley, J. S. *Annu. Rev. Pharmacool. Toxicol*. **1980,** *20*, 81.
19. Holienberg, H. D. *Trends Pharmacol. Sci*. **1987**, *8*, 197.
20. Hruby, V. J.; Wilkes, B. C.; Hadley, M. E.; Al-Obeidi, F.; Sawyer, T. K.; Staples, D. J.; deVaux, A. E.; Dym, O.; de L. Castrucci, A. L.; Hintz, M. F.; Riehm, J. P.; Rao, K. R. *J. Med. Chem*. **1987**, *30*, 2126.
21. Dutta, A. S. *Chem. Br.* **1989**, *2*, 159.
22. Sasaki, Y.; Murphy, W. A.; Heiman, M. L.; Lance, V. A.; Coy, D. H. *J. Med. Chem.* **1987**, *30*, 1162.

23. Lautz, A. J.; Kessler, H.; Blaney, J. M.; Scheek, R. M.; van Gunsteren, W. F. *Int. J. Pept. Protein Res*. **1989**, *33*, 281.
24. Hagler, A. T. *The Peptides*, **1985**, *vol.7*, pp. 213. (Udenfriend S.; Meienhofer, J. ed.), Academic Press, New York.
25. Crippen, G. M. *Med. Chem*. **1979**, *22*, 988.
26. Goodford, P. J. *J. Med. Chem*. **1984,** *27*, 557.
27. Humblet, C.; Marshall, G. R. *Annu. Rep. Med. Chem*. **1980**, *15*, 267.
28. Fauchere, J. L. *Int. Adv. Drug Res.* **1986**, *15*, 29.
29. Lewis, D. A.; Bloom, F. E. *Annu. Rev. Med.* **1987**, *38*, 143.
30. Lee, T. Y.; Notari, R. E. *Pharm. Res.* **1987**, *4*, 311.
31. Lee, T. Y.; Notari, R. E. *Pharm. Res*.**1987**, *4*, 385.
32. Hunt, C. A.; MacGregor, R. D.; Siegal, R. A. *Pharm. Res.* **1986**, *3*, 333.
33. Read, N. W.; Sugden, K. CRC *Crit. Rev. in. Ther. Drug Carrier Systems*, **1987**, *4*, 221.
34. HodgSon, J. *Bioechnology*, **1990**, *8*, 720.
35. Veber, D. F.; Freidinger, R. M. *Trends Neurosci.* **1985**, *8*, 392.
36. Evans, B. E.; Bock, M. G.; Rittle, K. E.; DiPardo, R. M.; Whitter, W. L.; Veber, D. F.; Anderson, P. S.; Freidinger, R. M. *Proc. Natl. Acad. Sci. U.S.A.* **1986**, *83*, 4918.
37. Hruby, V. J.; Kao, L. F.; Pettitt, B. M.; Karplus, M. *J. Amer. Chem. Soc*. **1988**, *110*, 3351.
38. Gage, L. P. *Am. J. Pharma. Edu.* **1986**, *50*, 368.
39. Werner, R. G. *Arzneim.-Forsch./Drug Res.* **1987**, *37*, 1086.
40. Dibner, M. D.; Timmermans, P. B. M. *Hypertension*, **1986**, *8*, 965.
41. Warkentin, T. E.; Koster, A. *Expert Opin. Pharmacother.* **2005**, *6*, 1349.
42. Chien, R. N.; Liaw, Y. F. *Anti. Infect. Ther.* **2004**, *2*, 9.
43. Brugge, V. A.; Schooley, D. A.; Orchard, I. *J. Exp. Biol*. **2008**, *211*, 382.
44. Heine, R. J.; Van Gaal, L. F.; Johns, D.; Mihm, M. J.; Widel, M. H.; Brodows, R. G. *Ann. Intern. Med.* **2005**, *143*, 559.
45. Bode, H. P.; Moorman, B.; Dabew, R.; Goke, B. *Endocrinology*, **1999**, *140*, 3919.
46. Nyholm, B.; Brock, B.; Orskov, L.; Schmitz, O. *Expert Opin. Invest. Drugs*, **2001**, *10*, 1641.
47. White, C. M. *J. Clin. Pharmacol.* **1999**, *39*, 442.

48. Meltzer, S.; Leiter, L.; Daneman, D.; Gerstein, H. C.; Lau, D.; Ludwig, S.; Yale, J. F.; Zinman, B.; Lillie, D. *J. Can. Med. Assoc.* **1998**, *15*, 1.
49. Greene, W. C. *Eur. J. Immunol.* **2007**, *37*, 94.
50. Uhl, W.; Anghelacopoulos, S. E.; Friess, H.; Buchler, M. W. *Int. J. Gastroenterology*, **1999**, *60*, 23.
51. Saleh, F. M.; Niel, T.; Fishman, M. J. *J. Forensic Sci.* **2004**, *49*, 1343.
52. Eduard, R. de H.; Mulder, J. H.; Gerard, H. A. *Intern. J. Womens Health*, **2010**, *2*, 137.
53. Volker, P.; Grundker, C.; Schmidt, O.; Schulz, K. D.; Emons, G. *Am. J. Obstet. Gynecol.* **2002**, *186*, 171.
54. Del Tredici, A. L.; Vanover, K. E.; Knapp, A. E.; Bertozzi, S. M.; Nash, N. R.; Burstein, E. S.; Lameh, J.; Currier, E. A.; Davis, R. E.; Brann, M. R.; Mohell, N.; Olsson, R.; Piu, F. *Biochem. Pharmacol.* **2008**, *76*, 1134.
55. Boson, W. L.; Della, M. T.; Damiani, D.; Miranda, D. M.; Gadelha, M. R.; Liberman, B.; Correa, H.; Romano-Silva, M. A.; Friedman, E.; Silva, F. F.; Ribeiro, P. A.; De Marco, L. *Genet. Test. Fall.* **2006**, *10*, 157.
56. Amoroso, G.; van Boven, A. J. van Veldhuisen, D. J.; Tio, R. A.; Balje-Volkers, C. P.; Petronio, A. S.; van Oeveren, W. *J. Cardiovasc. Pharmacol.* **2001**, *38*, 633.
57. Chen, X.; Ji, Z. L.; Chen, Y. Z. *Nucleic Acids Res.* **2002**, *30*, 412.
58. Fortune, B. E.; Jackson, J.; Leonard, J.; Trotter, J. F. *Expert Opin. Pharmacother.* **2009**, 10, 2337.
59. Carmichael, J. D. *Patient Preference and Adherence J.* **2012**, *6*, 73.
60. Spyranti, Z.; Fragiadaki, M.; Magafa, V.; Borovickova, L.; Spyroulias, G. A.; Cordopatis, P.; Slaninova, J. *Amino Acids*, **2010**, *39*, 539.
61. Privitera, P. J.; Beckstead, R. M.; Yates, P.; Walgren, R. *Cell Mol. Neurobiol.* **2003**, *23*, 805.
62. Esposito, P.; Barbero, L.; Caccia, P.; Caliceti, P.; D-Antonio, M.; Piquet, G. *Adv. Drug Delivery Rev.* **2003**, *55*, 1279.
63. Overington, J. P.; Al-Lazikani, B.; Hopkins, A. L. *Nat. Rev. Drug Discovery*, **2006**, *5*, 993.
64. Bekker, P.; Jeppesen, P. B. *Therap. Adv. Gastroenterol.* **2012**, *5*, 159.
65. Kirby, R. S.; Fitzpatrick, J. M.; Clarke, N. *BJU. Int.* **2009,** *104*, 1580.

66. Lu, Z. L.; Gallagher, R.; Sellar, R.; Coetsee, M.; Millar, R. P. *J. Biol. Chem.* **2005**, *280*, 29796.
67. Barbieri, R. L. *Am. J. Obstet. Gynecol.* **1990**, *162*, 581.
68. Marshall, G. R. *Annu. Rev. Pharmacool. Toxicol*. **1987**, *27*, 193.
69. Hopfinger, A. J. *J. Med. Chem*. **1985**, *28*, 1133.
70. Levitt, M. *J. Mol. Biol*. **1983**, *170*, 723.
71. Mc Cammon, J. A.; Harvey, S. *Prediction of Protein Structure and the Principle of Protein Conformation*, **1987,** Cambridge University Press, New York.
72. Dauber-Osguthorpe, P.; Roberts, V. A.; Osguthorpe, D. J.; Wolff, J.; Genest, M.; Hagler, A. T. *Proteins: Struct., Funct. Genet.* **1988**, *4*, 3147.
73. Hardy, L. W.; Finer-Moore, J. S.; Montfort, W. R.; Jones, M. O.; Santi, D. V.; Stroud, R. M. *Science*, **1987**, *235*, 448.
74. Hell berg, S.; Sjostrom, M.; Skagerberg, B.; Wold, S. *J. Med. Chem*. **1987**, 30, 1126.
75. Blankley, C. J.; Topliss, J. G. *Quantitative Structure-Activity Relationships of Drugs*, **1983**, p.1-21. Academic Press, New York.
76. Bacon, D. J.; Anderson, W. F. *J. Mol. Biol*. **1986**, *191*, 153.
77. Richards, W. G. *Quantum Pharmacology*, **1977,** Butterworth, London.
78. Zheng, C.; Wong, C. F.; McCammon, J. A.; Wolynes, P. G. *Nature*, **1988**, *334*, 726.
79. Van-Gunsteren, W. F. *Protein Eng.* **1988**, *2*, 5.
80. Bash, P. A.; Singh, U. C.; Langridge, R.; Kollman, P. A. *Science*, **1987**, *236*, 564.
81. Ullman, S. *Trends Neurosci*. **1986**, *9*, 530.
82. Holley, L. H.; Karplus, M. *Proc. Natl. Acad. Sci. U.S.A.* **1989**, *86*, 152.
83. McGregor, M. J.; Flores, T. P.; Sternberg, M. J. E. *Protein Eng.* **1989**, *2*, 521.
84. Morris, G. A. *Magn. Reson. Chem*. **1986**, *24*, 371.
85. Kaiser, E. T. *Biochem. Pharmacol*. **1987**, *36*, 783.
86. Jelliffe, R. W. *Fed. Proc.* **1987**, *46*, 2494.
87. Eppstein, D. A.; Longenecker, J. P.; *CRC Crit. Rev. in Ther. Drug Carrier Systems*, **1988**, *5*, 99.
88. Clore, G. M.; Gronenborn, A. M. *Prog. Biophys. Mol. Biol*.**1994**, *62*, 153.
89. Leopold, M. F.; Urbauer, J. L.; Wand. A. J. *Mol. Biotechnol*.**1994**, *2*, 61.

90. Kay. L. E. *Prog. Biophys. Mol. Biol.* **1995**, *63*, 277.
91. Wagner, G.; Walters, K.J.; Matsuo, H.J. *J. Amer. Chem. Soc.* **1997**, *119*, 5958.
92. Clore, G. M.; Gronenborn. A. *Nat. Struct. Biol.* **1997**, 849.
93. Jarori, G. K.; Murali, N.; Switzer, R. L.; Rao. B. D. *Eur. J. Biochem.* **1995**, *230*, 517.
94. Lian, L. Y.; Barsukov, I. L.; Sutcliffe, M. J.; Sze, K. H.; Roberts, G. C. K. *Methods Enzymology*, **1994**, *239*, 657.
95. Ni, F. *Prog. Nucl. Magn. Reson. Spectrosc.* **1994**, *26*, 517.
96. Fisher, P. J.; Prendergast, F. G.; Ehrhardt, M. R.; Urbauer, J. L.; Wand, A. J.; Sedarous, S. S.; McCromic, D. J.; Buckley. P. J. *Nature*, **1994**, *368*, 651.
97. Zhang, M.; Vogel, H. J.; Zwiers, H. *Biochem. Cell Biol.* **1994**, *72*, 109.
98. Bax, A.; Delaglio, F.; Grzesiek, S.; Vuister, G. W. *J. Biomol. NMR.* **1994**, *4*, 787.
99. Mcintosh, L. P.; Brun, E.; Le Kay, J. D. *J. Biomol. NMR.* **1994**, *4*, 306.
100. Yamazaki, T.; Pascal, S. M.; Singer, A. U.; Forman-Kay, J. D.; Le Kay. *J. Am. Chem. Soc.***1995**, *117*, 3556.
101. Pascal, S. M.; Yamazaki, T.; Singer, A. U.; Le Kay; Forman-Kay. J. D. *Biochemistry*, **1995**, *34*, 11353.
102. (a) Otting, G. E. Liepinsh.; Wuthrich, K. *Science*, **1991**, *254*, 974.(b) Wuthrich, K.; Otting, G. E.; Liepinsh. *Faraday Discuss.* **1992**, *93*, 35.
103.(a) Vermehren, C.; Johansen, P. B.; Hansen, H.S. *Drug Metab. Dispos.* **1997**, *25*, 1083. (b) Jitendra.; Sharma, P.K.; Bansal, S.; Banik, A. *Ind. J. Pharm. Sci.* **2011**, *73*, 367.
104. Hofbauer, J.; Hoerner, J. K. *Am. J. Obstet. Gynecol*. **1927**, *14*, 137.
105. Guhl, V .U.; Schweiz. *Med. Wochenschr*. **1961**, *91*, 798.
106. Spiegelman, A. R. *J. Am. Med. Assoc*. **1963**, *184*, 657.
107. Anderson, K. E.; Arner, B. *Acta. Med. Scand*. **1972,** *192*, 21.
108. Vande Donk, J. H. M.; UllerPlantema, I. P.; Zuidema, J.; Merkus, F. W. H. M. *Rhinology*, **1980**, *18*, 119.
109. Fischer, A. N.; Brown, K.; Davis, S. S.; Parr, G. D.; Smith, D. A. *J. Pharm. Pharmacol.* **1987**, *39*, 357.
110. Jones, N. S.; Quraishi, S.; Mason, J. D. T. *Int. J. Clin. Pract.* **1997**, *51*, 308.
111. Corbo, D.; Liu, J.; Chein, Y. W. *Pharm. Res.* **1989**, *6*, 848.
112. Fry, F. A.; Black, A. *J. Aerosol Sci.* **1973**, *4*, 113.

113. Chien, Y. W.; Chang, S.; *Crit. Rev. Ther. Drug Carrier. Syst.* **1987**, *4*, 67.

114. Chien, Y. W.; Su, K. S. E.; Chang, S. *Nasal Systemic Drug delivery*, **1989**, p.1-38, Marcel Dekker Inc. New York.

115. Conley, S. F. *Ann. Allergy*, **1994**, *72*, 829.

116. Thompson, R. *Arch. Pathol.* **1940**, *30*, 1096.

117. Dominique, D.; Gilles. P. *Drug. Dev. Ind. Pharm.* **1993**, *19*, 101.

118. Pennington, A. K.; Ratcliffe, J. H.; Wilson, C. G.; Hardy, J. G. *Int. J. Pharm.* **1998**, *43*, 221.

119. Suzuki, Y.; Makino, Y. *J. Controlled Release*, **1999**, *62*, 101.

120. Achari, R. G.; Ahmed, S.; Behl, C. R.; de Meireles, J. C.; Liu, R.; Romeo, V. D.; Sileno, A. P. *Unites States Patent*, **2002**, USP 20020193397.

121. Gattefosse Bulletin. *New Lipidic systems enhancing the Bioavailability of problem Drugs*, **1997**, 1-81.

122. Hallen, H.; Graf, P. *Clin. Exper. Allergy*, **1995**, *25*, 401.

123. Bernstein, I. L. *J. Allergy. Clin. Immunol.* **2002**, *105*, 39.

124. Hillardal, G. *ORL. J. Otorhinolaryngol Relat. Spec*. **1985**, 47, 278.

125. Van de Donk, H. J. M.; Merkus, F. W. H. M. *J. Pharm. Sci.* **1982**, *71*, 595.

126. Van de Donk H. J. M.; Muller Plantema, I. P.; Zuidema, J.; Merkus, F. W. H. M. *Rhinology*, **1980**, *18*, 119.

127. Illum, L. *Bioadhesive Formulations for Nasal Peptide Delivery*, **1999**, p.507-541, Marcel Dekker, New York.

128. Hussain, A. A. *Adv. Drug Delivery Rev.* **1998**, *29*, 39.

129. Hirai, S.; Yashika, T.; Matsuzawa, T.; Mima, H. *Int. J. Pharm*. **1981**, *7*, 317.

130. Morimoto, K.; Katsumata, H.; Yabuta, T.; Iwanaga, K.; Kakemi, M.; Tabata, T.; Ikada, Y. *Eur. J. Pharm. Sci*. **2001**, *13*, 179.

131. Schipper, N. G. M.; Verhoef, J. C.; Romeijn, G.; Merkus, F. W. H. M. *Calcif. Tissue Int.* **1995**, *56*, 280.

132. Mathison, S.; Nagilla, R.; Kompella, U. B. *J. Drug Targeting*, **1998**, *5*, 415.

133. Costantino, H.; Philo, J. S.; Eidenschink, L. *J. Pharm. Sci.* **2009**, *98*, 3691.

134. Meyer, J.P.; Pelton, J. T.; Hoflack, J.; Vladimir S. *Biopolymers*, **1999**, *31*, 233.

135. Mayer, M.; Meyer, B. *Angew. Chem., Int. Ed.* **1999**, *38*, 1784.

136. Kenji, K.; Nosaka, A. Y. *Biochemistry*, **1995**, *34*, 12138.

137. Copp, D. H.; Chenny, B. *Nature*, **1962**, *193*, 381.

138. Gaudiano, M. C.; Colone, M.; Bombelli, C.; Chistolini, P.; Valvo, L.; Diociaiuti , M. *Biochim. Biophys. Acta*, **2005**, *1750*, 134.

139. Chang, X.; Keller, D.; O Donoghue, S. I.; Led, J. J. *FEBS Lett.* **2002**, *515*, 165.

140. Deese, A. J.; Dratz, E. A. Hymel, L.; Fleischer, S. *J. Biophys.* **1982**, *37*, 207.

141. Christy, R. R; Grace, R.; Mahajan, G.; Mahajan S.; Cowsik, S. *Peptide Science*, **2011**, *96*, 252.

142. Frazier, R. A.; Deaville, E. R.; Green, R. J. *J. Pharm. Biomed. Anal.* **2010**, *51*, 490.

143. Doyle, B. L.; Pollo, M. J.; Pekar, A. H.; Roy, M. L.; Thomas, B. A.; Brader, M. L. *J. Pharm. Sci.* **2005**, *94*, 2749.

144. Zheng, G.; Torres, A. M.; Ali, M.; Manolios, N.; Price, W. S. *Peptide Science*, **2011**, *96* , 177.

145. Dehner, A.; Kessler, H. *Chem. Bio. Chem*. **2005**, *6*, 1550.

146. Wang, S.; Jiayi, Y.; Wei, L.; Fei, L. *Peptide Science*, **2011**, *96*, 348

147. Coles, D. T.; Simerska, P.; Fujita, Y.; Toth, I. *Peptide Science*, **2011**, *96*, 172.

148. Smriti, K.; Mark, G.; Paul; Steve, S. H. *J. Pharm. Biomed. Anal.* **2010**, *51*, 164.

149. Bekiroglu, S.; Mylberg, O.; Ostman, K.; Ek, M.; Arvidsson, T.; Rundlof, T.; Hakkarainen, B. *J. Pharm. Biomed. Anal*. **2008**, *47*, 958.

150. Michael, H. F.; Niels, A. H. *Peptide Science*, **2004**, *76*, 298.

151. Cetin, M.; Aktas, S.; Mustafa, V. I.; Ozturk, M. *J. Microencapsulation*, **2012**, *29*, 156.

152. Vonhoff, S.; Condliffe, J.; Heiko, S. *J. Pharm. Biomed. Anal.* **2010**, *51*, 39.

153. Marigiolaki, I.; Wright, J. P. *Acta. Cryst.* **2008**, *A64*, 169.

154. Tuteja, N.; Tuteja, R. *Eur. J. Biochem*. **2004**, *271*, 1849.

155. Ababou, A.; Laudbury, J. E. *J. Mol. Recognit.* **2006**, *19*, 79.

156. Christensen, J. J.; Izatt, R. M.; Hansen, L. D.; Partridge, J. M. *J. Phys. Chem.* **1966**, *70*, 2003.

157. Doyle, M. L. *Curr. Opin. Biotechnol*. **1997**, *8*, 31.

Chapter 4

Drug Complex Formation and Application

Introduction:

The term "Ubermolekelan" (Supermolecule) was introduced by Wolf *et al* in the mid of 1930 to describe entities of higher organization resulting from the association of two or more coordinately saturated species.[1] The branch of science which deals with the study of structures and functions of supermolecules is called "Supramolecular chemistry" or "nanotechnology" as described by Lehn *et al.*[2]

Mascal *et al* defined supramolecular chemistry as a chemistry of noncovalent bonds, whose objects are 'supermolecules' of well defined structure and function.[3] Although supramolecular chemistry has an increasing impact on chemistry, especially organic chemistry, due to their chemical modifications and its unique features smoothly separate it from the conventional chemistry.

Organic supramolecular synthesis has gained much importance during the last few years and many strategies have been developed to create 'smart' functional, organized supramolecular materials like various types of 'hosts' which will bind to the specific receptors. Connors *et al* investigated these self-assembling nanostructures with the potential to be used as drug delivery systems.[4]

Supramolecular systems classified into two categories which are as follows

- **Host-Guest supramolecular systems**
- **Self-Assembling supramolecular systems**

In Host-Guest supramolecular systems one component known as "host" is perceived to spatially accommodate the guest and these systems are characterized by lack of chemical affinity between the combining species. These systems have been extensively studied by Whitesides *et al*.[5]

Self-assembly is the spontaneous organization of specifically engineered molecular components to form thermodynamically stable systems. Self-organization involves the design of systems capable of spontaneously generating supramolecular entities exhibiting well organized behavior by self-assembly from their components in

a given set of conditions. Bayley *et al* classified molecular crystals as self-organizing structures and co-crystals as self-assembling structures.[6]

These dynamic properties of bio-molecular materials can be realized in size range of nanometer or above and the use of various types of biomaterials for controlled release and encapsulation systems are important in Pharma applications. For encapsulation of sensors and implants various surface coatings exhibiting well defined physical properties like wettability, porosity and elasticity are needed. Rideout *et al* have developed various self-assembling biomolecular materials for medical applications.[7] A report by Dill *et al* highlights the potential of self-assembling drugs as an innovative approach to biochemical modulation in cancer chemotherapy.[8]

Non-covalent design principles

The weak intermolecular forces which operate over a range of few angstroms have the potential to be used in the design of self-assembling nanostructures. For the final assembly to be stable, these intermolecular forces must be favored energetically thereby lending stability. In other words, self-assembled structures represent thermodynamic minima. Weak intermolecular forces can be effectively used in the reversible assembly of the host around the guest, a phenomenon that is commonly encountered in biological chemistry as observed by Whitesides and group.[5]

Different types of intermolecular forces of interest in supramolecules are: van der Waals Forces (Keesom interactions, Debye interactions and London interactions), hydrogen bonding, hydrophobic interactions, charge-transfer interactions and ion-dipole and ion-ion interactions.

Hydrophobic interactions

Exclusion of the hydrophobic molecule or hydrophobic part of the molecule from water is an important phenomenon in the stability of biological structures. Dill *et al* have cautioned against the loose use of terminology 'hydrophobic effect', 'hydrophobicity' and 'hydrophobic hydration'.[8]

It is now well known that hydrophobic interactions play a significant role in maintaining protein folding for their secondary and tertiary structure, in micelle formation, lipid-bilayers and Langmuir-Blodgett monolayer on water. An important example to understand the role of hydrophobic interactions can be seen in the aggregation or self-assembling 40-42 residue peptide 'A beta'. The therapeutic

peptides which is associated with Alzheimer's disease has now been shown to display properties commonly associated with surfactants or detergents, which form micelles in solution in a report published by Soreghan.[10]

4.1: Co-crystals:

Co-crystals are long known but little studied class of compounds. Wohler and coworkers reported the first entry of 'co-crystal' in 1844 of Benzoquinone and Hydroquinone[11] as shown in Figure 4.1. Subsequently, Anderson *et al* studied systems consisting of organic molecular compounds.[12] However, until 1960 the structural information on co-crystals was not known and term complexes was generally used. Hoogsteen in 1963 developed first prototype co-crystal with the new base known as 'Hoogsteen base pair'.[13]

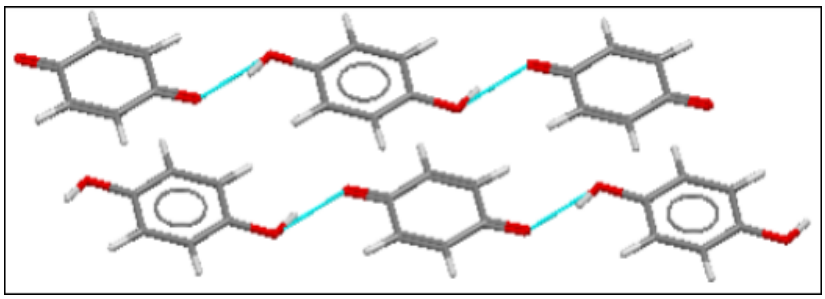

Figure 4.1: Crystal structure of the triclinic form of Quinhydrone

This emerging field of co crystal has now been used for modifying the composition of matter and physicochemical properties of a molecule without breaking or forming a covalent bond. This shows that there are many diverse applications of co-crystals.

4.1.1: Pharmaceutical co-crystals:

Pharmaceutical co-crystals are defined as "co-crystals in which the target molecule or ion is an Active Pharmaceutical Ingredient (API), which binds to the co-crystal forming agent(s) through ion pair, van der Waals interaction or hydrogen bonds".[14a]

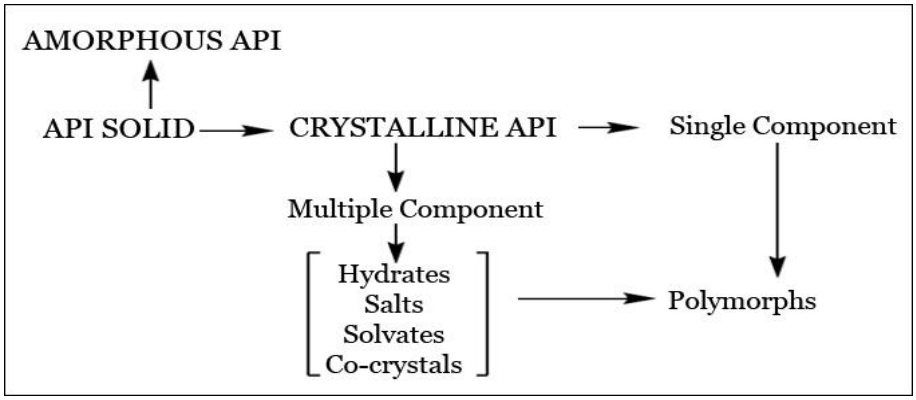

Figure 4.2: Representation of pharmaceutical solids

From the application point of view, delivery of an API is generally preferred in a solid dosage form. API's are developed in variety of solid forms and administered in different ways such as amorphous, salt, polymorphs and solvates[14b] as given in Figure 4.2. The properties such as stability, solubility and bioavailability of a drug are varied by its solid form. Thus it gives an opportunity to a researcher to develop the most suitable form of a drug with improved physicochemical properties. Factors such as dissolution rate, solubility, chemical stability and moisture uptake influencing therapeutic efficacy of many pharmaceuticals, and may significantly lower the market value of a drug. Multi-component crystals e.g. solvates, hydrates, co-crystals and salts play an important role in pharmaceutical technology.[14c]

First pharmaceutical co-crystal was reported in 1934 by Heyden *et al*.[15] The co-crystals of Barbiturates with 4-oxy-5-nitropyridine, 2-ethoxy-5-acetaminopyridine, N-methyl-alpha-pyridone and α-amino pyridine. The following example highlights the importance of co-crystals in pharma products. A major pet food crisis was observed in China in 2007 in which more than 24,000 clinical assessments were found with acute renal failure within 3 months. Investigations by Puschner *et al* [16a] showed that melamine present in protein content of the pet food, forms a co-crystal with cyanuric acid (QACSUI), another constituent of pet food. Even though melamine and cyanuric acid are nontoxic individually the resulting 1 : 1 co-crystal (Fig.4.3) is highly insoluble in water resulting in toxic kidney stones. This is the first example of co-crystals altering clinically relevant physical properties in a negative manner.

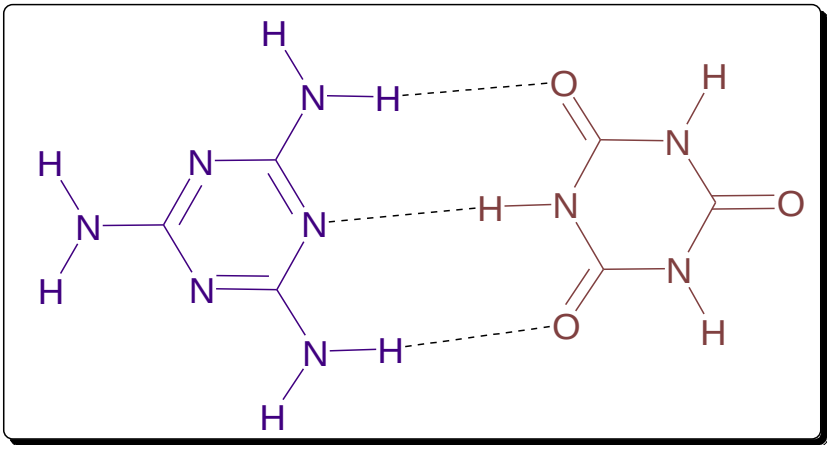

Figure 4.3: Co-crystal of Melamine and Cyanuric acid

Co-crystals or pharmaceutical co-crystals are novel as they can afford crystal form diversity. The utility in terms of improving physicochemical properties of a drug represents an opportunity to patent and market clinically improved crystal forms of available drugs in the form of new drugs. In conclusion, co-crystals and pharmaceutical co-crystals offer new avenues to the pharmaceutical industry.[16b]

4.1.2: Characterization of co-crystals:

Characterization of co-crystals involves both structure (infrared spectroscopy, single crystal x-ray crystallography and powder x-ray diffraction)[17-19] and physical property determination[19,20] (e.g. melting point, differential scanning calorimetry, thermogravimetric analysis). The analytical potential of NIR spectroscopy for co-crystal screening using Raman spectroscopy as a comparative method has been reported by Alleso *et al*.[21]

4.1.3: Application of co-crystals:

Compared to other solid-state modification techniques employed by pharmaceutical industry, co-crystal formation appears to be an advantageous alternative for drug discovery (e.g. new molecule synthesis, nutraceutical co-crystals), drug delivery (solubility, bioavailability) and chiral resolution.[14, 22-24]

Solubility and bioavailability

Solubility and bioavailability of a drug are important parameters in drug development process. Intrinsic solubility and dissolution of a drug are prerequisites for oral drug delivery. The fundamentals of the dissolution as studied by Noyes-

Whitney equation,[25a] and its correlation with bioavailability leads to a Bio-pharmaceutics Classification System (BCS).

BCS classification

According to BCS a substance is classified on the basis of its aqueous solubility and intestinal permeability. Based on this, four drug classes have been defined i.e. high solubility/high permeability (Class I), low solubility/high permeability (Class II), high solubility/low permeability (Class III) and low solubility/low permeability (Class IV) as shown in Figure 4.4. According to BCS a drug substance is considered to be highly soluble when the highest strength of permitted dose is soluble in 250 mL or less of aqueous media over the pH range of 1.0 - 7.5; otherwise, the drug substance is considered to be poorly soluble.[25b] BCS Class II drugs present a challenge to co-crystallization field where co-crystals can make a difference by altering the bulk solubility of a drug and hence altering the rate of dissolution and consequently the bioavailability of an API.

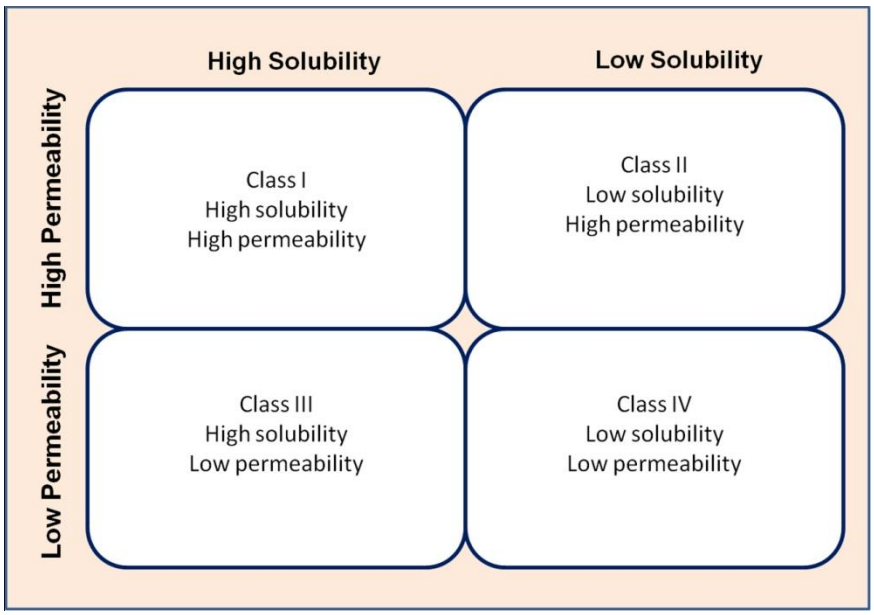

Figure 4.4: Biopharmaceutics Classification System as defined by FDA

Kastelic *et al* investigated the formation of co-crystals of Fluconazole, an antifungal drug with different dicarboxylic acid like maleic, fumaric and glutaric acids by solution evaporation method with an objective to modify the physicochemical properties.[26a]

Almarsson *et al* studied the formation of Carbamazepine : Saccharin (1 : 1) co-crystals and found that it exhibits similar physical and chemical stability to that of

Carbamazepine in marketed formulations (Tegretol) along with improved oral bioavailability.[22]

Itraconazole, an antifungal agent is poorly water soluble. Shevchenko *et al* demonstrated that Intraconazole forms co-crystal with malonic acid and succinic acid which exists as di and trihydrochloride salts. The dissolution rate of co-crystal of Itraconazole with succinic acid shows 5 fold increase compared to Itraconazole without compromising the hygroscopicity and stability.[26b]

Fluoxetine hydrochloride forms three co-crystals with benzoic acid (1 : 1), succinic acid (2 : 1) and fumaric acid (2 : 1). Prozac® is an antidepressant drug containing Fluoxetine hydrochloride as an API. Childs *et al* reported the intrinsic dissolution profile of above three co-crystals of Fluoxetine hydrochloride in water. Fluoxetine hydrochloride : Succinic acid co-crystal showed two fold increase in solubility as compared to Fluoxetine hydrochloride. It has also been observed that co-crystal decreases the solubility as in the case of Fluoxetine hydrochloride : Benzoic acid and Fluoxetine hydrochloride : Fumaric acid.[27a]

The co-crystal of Sildenafil citrate API (active pharmaceutical ingredient in Viagra®) with aspirin was patented in 2007 which showed improved solubility in acidic conditions and good thermodynamic stability up to 165 ºC.[27b]

4.2: Introduction of drug delivery technology:

Controlled drug delivery technology, one of the most rapidly developing areas of science in which several disciplines, such as chemistry, pharmaceutical technology and medicine, is contributing to human health care as reviewed by Orive *et al.*[28] For many years, the focus of both fundamental and applied research has been in the development of pharmaceutical formulates permitting maximization of the therapeutic efficacy and minimization of the adverse effects (Fig.4.5) of the drugs of interest.[29]

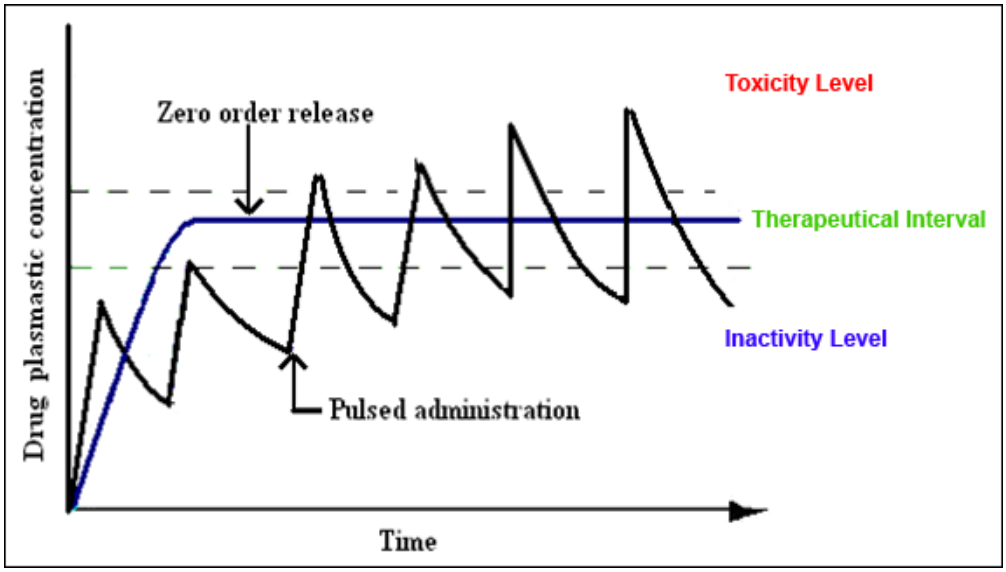

Figure 4.5: Variation of drug plasmatic concentration for conventional and controlled release drug products with time

In the development of drug delivery systems, the rationale should be modified according to the specific biological substance and/or the particular therapeutic situation.[30a,30b] Although clinical introduction of the first controlled release systems occurred 30 years ago, nowadays these systems have an incredible impact on nearly every branch of modern medicine, including cardiology, neurology, ophthalmology, endocrinology, oncology, pneumology, immunology and pain management.[30b]

For more than two decades, use of polymeric materials to deliver bioactive agents has attracted the attention of investigators throughout the scientific community. Polymer chemists and chemical engineers, pharmaceutical scientists and entomologists are engaged in bringing out design that is predictable, for controlled delivery of bioactive agents ranging from insulin to rodenticides.

Bio-degradable polymers are susceptible to degradation in biological fluids with progressive release of dissolved or dispersed drug. The most promising area of application involves drug-composites which are implanted, injected or inserted. The applications in which these bio-degradable systems may be used range from contraceptive implants or injections which are required to provide constant release of steroids for up to one year to some anti-cancer therapies which are required to maintain optimum concentration in specific sites in the body.

The term bio-degradation has been used in the broad sense to include non-enzymatic (chemical) and enzymatic processes. However, future approaches must be

oriented to give a more restrictive distinction between non-biological and biological degradations.[31]

4.2.1: Classes of biodegradable polymers:

- Slow dissolution and erosion by hydrolysis process
- Water insoluble polymers undergoing hydrolysis, ionization or protonation of pendent group without undergoing backbone cleavage
- Water insoluble polymer degradation to water soluble products by backbone cleavage.

Bio-degradable polymers investigated for controlled drug delivery are,

- Lactide/Glycolide polymers
- Poly anhydrides
- Poly-caprolactones
- Poly-orthoesters
- Poly-phosphagenes
- Pseudo poly amino acids
- Natural polymers

4.2.2: Lactide and Glycolide polymers:

The most widely investigated biodegradable polymer with regards to available toxicological and clinical data are the aliphatic polyesters based on lactic acid and glycolic acid. They are bio-compatible, exhibit predictable bio-degradation kinetics and ease of fabrication and have regulatory approval. William *et al* investigated the enzymatic catalysis of these biodegradable polymers *in vivo*.[32]

Maulding and coworkers observed an unusual acceleration in bio-degradation rate of polylactide / glycolide in presence of tertiary amino compound, Thioridazine.[33]

The 50 : 50 lactide / glycolide copolymers have the fastest degradation rate of the dl-lactide /glycolide materials with degradation time of about 50 to 60 days. The 65 : 35, 75 : 25 and 85 : 15 *dl*-lactide / glycolide have progressively longer *in-vivo* life time with the 85 : 15 lasting about 150 days where as poly dl-lactide requires about 12 to 16 months for biodegrading completely.[34]

Lactide and glycolides are the most widely investigated polymers in drug delivery research due to their ease of fabrication and bio-performance. Co-polymers of lactide and glycolide can be tailored particularly for getting optimum bio-degradation kinetics. In the recent past, lactide / glycolide branched with different polyols like poly vinyl alcohol have also been reported for contolled delivery of many drugs like steroids, hormones, antibiotics, narcotic antagonists, anti-cancer drugs etc.

4.2.3: Schizophrenia:

Schizophrenia is a mental disorder characterized by a breakdown of thought processes and by poor emotional responsiveness which commonly manifests itself as auditory hallucinations, paranoid or bizarre delusions or disorganized speech and thinking accompanied by significant social or occupational dysfunctions. Antipsychotic drugs are the most effective treatment for schizophrenia by changing the balance of chemicals in the brain and thus control symptoms.[35a,35b] The major limitations related to this antipsychotic drugs are adverse effects like tremor, sedation and long term use causes tardive dyskinesia, also in some cases extra pyramidal side effects. Psychotic disorders are difficult mental disorders to treat. The treatment of psychotic conditions requires the patient to take the medicament daily for prolonged periods of time. Unfortunately, the conventional immediate release oral delivery systems for antipsychotics yield effective plasma levels during a limited time interval, often deliver inaccurate doses and require frequent dosing which makes the treatment of the patient non-compliant. In-addition frequent dosing of immediate release formulations leads to peak and tough levels of antipsychotic agent causing undesirable side effects or inadequate efficacy.[36]

Long-acting injectable antipsychotic dosage forms would be valuable in maintenance therapy and would enhance patient compliance. Currently available long-acting neuroleptics include viscous oily solutions of oil-soluble ester derivatives of the neuroleptic compounds. Viscous oily depots are administered by deep intramuscular (IM) injection, repeated at intervals ranging from 14 to 35 days. Depending on the volume of injection / erythema, nodules / lumps, bleeding, pain, tenderness and/or seepage of formulation from site of injection.[37a]

4.2.4: Ion pair complex (co-crystal) and its Injectable sustained release products:

The two oppositely charged compounds of a co-crystal are the antipsychotic agents having basic group and the cholesteryl sulfate having acidic group. The cholesteryl sulphate or its alkali metal salt interacts with the oppositely charged antipsychotic agents having basic group can easily form an ion-pair complex which is able to exhibit a retardation effect on the release of the antipsychotic agent with or without incorporation into a biodegradable polymer.[36]

An injectable sustained release pharmaceutical composition contains a biodegradable polymer used for coating like poly (lactic-co-glycolic acid) or poly (lactic acid) and the molecular weight of poly (lactic-co-glycolic acid) ranges from about 10,000 Dalton to about 30,000 Dalton.

The term "biocompatible carrier" as used herein means a carrier, the degradation products of which are non-toxic, and which causes no significant deleterious or untoward effects, such as a significant immunological reaction at the injection site. The biocompatible carrier that may be used to incorporate the anti-psychotic agent cholesteryl sulphate complex (co-crystal) so as to provide sustained release of the antipsychotic agent. It can be biodegradable polymers or blends or copolymers there of or lipids selected from cholesterol and steroid derivatives. The term 'biodegradable' means the composition will degrade or erode in vivo to form smaller non-toxic chemical species. Helena *et al* studied the enzymatic degradation of biodegradable polymers and strategies to control their degradation route.[37b]

The term "Ion-pair complex" or "Ion-pair co-crystals" refers to an ionic interaction that occurs between two oppositely charged compounds. Kim *et al* studied (1 : 1) inclusion complex of Ziprasidone mesylate, an antipsychotic agent with beta-Cyclodextrin sulfobutyl ether which in turn enhances solubility of Ziprasidone.[38]

Iloperidone, an atypical antipsychotic agent which is generally well-tolerated, has a favorable safety profile with regard to extra pyramidal symptoms is used for the treatment of schizophrenia. It is approved by the USFDA as an atypical antipsychotic agent.[27,39a,39b] A low-dose Iloperidone therapy is required to control the psychotic symptoms and long-term treatment is needed to treat schizophrenia. Currently the conventional oral formulations of Iloperidone (12-24 mg / day) are the only available preparations for the short term management of manifestations of psychotic disorders. The drug is practically insoluble in water and undergoes significant "first-pass"

metabolism; slow initial dosage titration and need for twice daily dosing are potential disadvantages associated with Iloperidone.[40]

Common types of controlled drug release systems are,

- Oral systems
- Formulates for parenteral administration
- Therapeutic transdermal delivery systems
- Occular systems
- Intrauterine and intravaginal systems

4.3: Microsphere technology:

Microsphere based drug delivery systems have received considerable attention in recent years.[41,42] The most important characteristic of microspheres is the microphase separation morphology which endows it with a controllable variability in degradation rate and also drug release.

The range of techniques for the preparation of microspheres offers a variety of opportunities to control aspects of drug administration. The term 'control' includes phenomena such as protection and masking, reduced dissolution rate, ease of handling, and spatial targeting of the active ingredient. This approach facilitates accurate delivery of small quantities of potent drugs; considerable reduction in drug concentrations at sites other than the target organ or tissue; and protection of labile compounds before and after administration and prior to appearance at the site of action.[14c]

4.3.1: Matrix systems:

To address the issues of matrix systems, drug can be physically embedded in polymers at large enough concentration to create a series of interconnecting pores through which the drug can slowly diffuse. In this system, the matrix may consist of hydrophobic or viscous hydrophilic polymers in which the solid drug is dispersed as shown in Figure 4.6. Generally, the drug is sparingly soluble in the polymer matrix. These release systems are inexpensive and readily available, since they are prepared simply by mixing the polymer matrix and the drug. The desired device shape is obtained later by extrusion. The release mechanism is based on the diffusion of the drug molecules to the surface from where they are delivered. This process takes place

as long as the higher concentration of the drug in the system core affords a constant flow of drug molecules through the matrix.[30a]

In this dissolution–diffusion process, the interface between the drug reservoir and the release moiety progressively moves towards the core of the device.

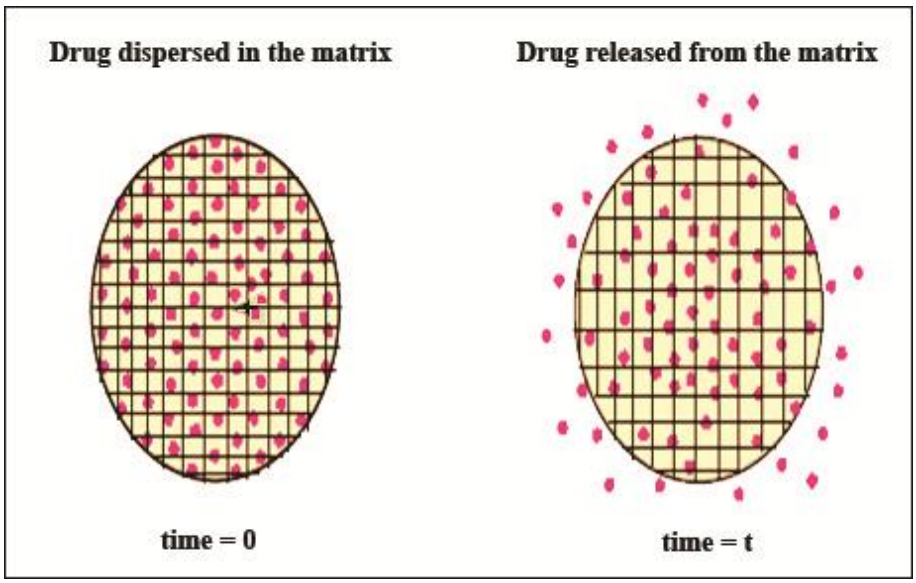

Figure 4.6: Diagramatic representation of matrix release systems

4.3.2: Biodegradable delivery systems:

In degradable delivery systems, the drug is loaded in a bio-erodible and/or biodegradable polymer matrix. The release takes place because of a combination of processes, such as matrix degradation and drug diffusion. The use of these materials was considered in order to avoid the problems related to the physiological secretion or mechanical removal of the non degradable drug delivery devices after their function is completed. Certainly, these devices are the preferred ones for internal application. It is important to note that the combination of diffusion through pores and polymer degradation process provides an additional control of the drug release rate. In ideal systems, the degradation occurs only at the surface of the device, affording a progressive delivery of the drug as shown in Figure 4.7.[30b]

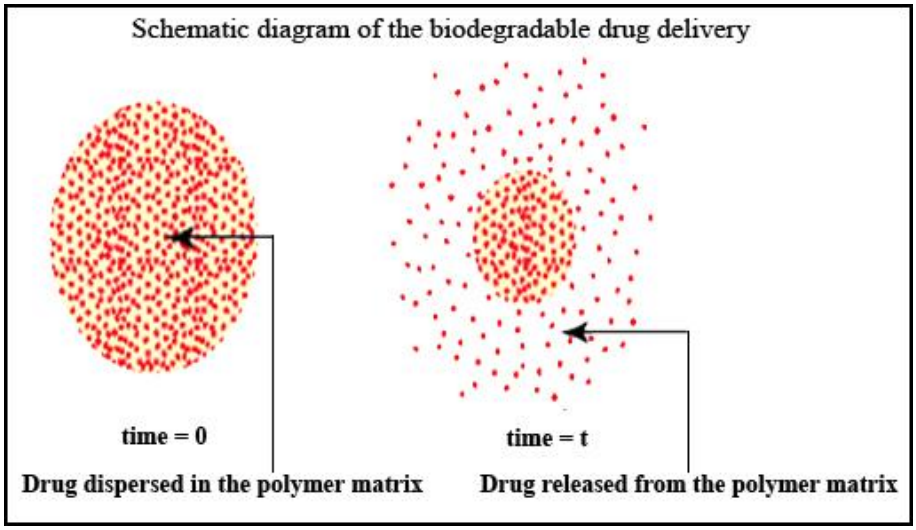

Figure 4.7: Diagramatic representations of degradable matrix systems

4.3.3: Definition of Microsphere:

Microspheres can be defined as solid, approximately spherical particles ranging in the size from 1 to 1000 μm. They are made of polymeric, waxy, or other protective materials, that is biodegradable synthetic polymers and modified natural products such as starches, gums, proteins, fats, and waxes. The natural polymers include albumin and gelatin,[43,44] the synthetic polymers include polylactic acid and polyglycolic acid.[45,46] The potential use of microspheres in the pharmaceutical industry has been considered since the 1960s,[47-49] for the following applications:

- Taste and odour masking
- Conversion of oils and other liquids to solids for ease of handling
- Protection of drugs against the environment[50] (moisture, light, heat, and/or oxidation) and vice versa (prevention of pain on injection)
- Delay of volatilization
- Separation of incompatible materials (other drugs or excipients such as buffers)
- Improvement of flow of powders
- Safe handling of toxic substances
- Aid in dispersion of water-insoluble substances in aqueous media.
- Production of sustained-release or controlled-release and targeted medications[51-54]
- Reduced dose dumping potential compared to large implantable devices

4.3.4: Pharmaceutical applications:

A number of pharmaceutical microencapsulated products are currently in the market, such as aspirin, theophylline and its derivatives, vitamins, pancrelipase, antihypertensives, potassium chloride, progesterone, and contraceptive hormone combinations.[55]

Microspheres have also found potential applications for injection as described by Kissel *et al* and Gurney *et al* [56, 57] or inhalation products by Gupta *et al.* [58-61] The number of commercially available products do not reflect the amount of research that has been carried out in this area, nor the benefits that can be achieved using this technology.

4.3.5: Other applications:

Applications of microencapsulation in other industries are numerous. The best known microencapsulated products are carbonless copying paper, photosensitive paper, microencapsulated fragrances, such as "scent-strips" (also known as "snap-n-burst") and microencapsulated aromas ("scratch-n-sniff'). All of these products are usually prepared by gelatin-acacia complex coacer-vation. Scratch-n-sniff has been used in children's books, food and cosmetic aroma advertising.[62] Microcapsules are also extensively used as diagnostics, such as temperature-sensitive microcapsules for thermographic detection of tumors and radioactive microspheres for radio immobilization of liver, spleen and bone marrow imaging.[63]

In the biotechnology industry microencapsulated microbial cells are being used for the production of recombinant proteins and peptides.[64] The retention of the product within the microcapsule can be beneficial in the collection and isolation of the product encapsulation of microbial cells which can increase the cell-loading capacity and the rate of production in bioreactors. Smaller microcapsules are better for these purposes; they have a larger surface area that is important for the exchange of gases across the microcapsule membrane. Microcapsules with semi permeable membranes are being used in cell culture.[65] A feline breast tumor line, which was difficult to grow in conventional culture has been successfully grown in microcapsules.[66] Microencapsulated activated charcoal has been used for hemoperfusion.[67] Paramedical uses of microcapsules include bandages with microencapsulated anti-infective substances.[38] A unique application of microencapsulation technology is for

feeding organisms. Sea bass larvae have been fed with all-protein microcapsules or with microcapsules containing lipids to supplement their diet.[68a]

In the light of the studies reported so far, biodegradable polymeric microspheres appear to have potential applications in controlled drug delivery. Development in polymer science has made it possible to synthesize polymers with a wide range of biodegradability. Biodegradability can be tailored to the desired degree by copolymerization of two or more monomers at varying ratios introducing cross-linking between the chains, blending one polymer with other etc. A number of methods have been devised to prepare microspheres of desired size, shape and surface properties. Dunne *et al* studied the influence of particle size on the degradation properties of PLGA biodegradable polymers and found the existence of linear relationship between particle size and degradation rate.[68b]

4.3.6: Preparation of microsphere:

The preparation of microspheres should satisfy certain criteria.[69] They are,

- The ability to incorporate reasonably high concentrations of the drug
- Microsphere stability after synthesis with a clinically acceptable shelf-life
- Controllable particle size and dispersability in aqueous vehicles for injection.
- Release of active agent with good control over a wide time scale
- Biocompatibility with a controllable biodegradability
- Susceptibility to chemical modification

The most important physicochemical characteristics that may be controlled in microsphere manufacture are particle size and distribution, polymer molecular weight, ratio of drug to polymer and total mass of drug and polymer. Each of these can be related to the manufacture and rate of drug release from the systems. The following discussion presents methods of manufacture of coated or encapsulated systems, referred to as microcapsules and matrix systems containing homogeneously distributed drug referred to as micro matrices.

Preparation of microspheres and encapsulation of proteins/growth factors into the microspheres are the steps that determine the efficiency of a microparticle-based delivery system

Single emulsion method

The single emulsion method normally involves an oil-in-water (o/w) emulsion and has been primarily used to encapsulate hydrophobic drugs.[70] The hydrophobic drug is dissolved or dispersed in an organic solvent into the polymer solution and the resulting mixture after emulsification by high-speed homogenization or sonication is added into an aqueous solution to make an oil-in-water emulsion with the aid of amphiphilic macromolecules, which are termed emulsifier/stabilizer/additive.[71] The solvent in the emulsion is removed by either evaporation at elevated temperatures or extraction in a large amount of water, resulting in formation of compact particles. The solvent evaporation method has been used extensively to prepare PLA and PLGA micro and nano-particles containing many different drugs.[72] Solvent extraction or evaporation from the emulsion then lead to hardening of the emulsified wet droplets into solid microspheres.[73]

Rapid solvent evaporation rates can lead to local explosion in the wet droplets, which in turn may cause the formation of porous microsphere surfaces.[74,75] Several variables have been identified which can influence the properties of the microspheres including drug solubility, internal morphology, solvent type, diffusion rate, temperature, polymer composition, viscosity, and drug loading.[76] This method, however is only available for the hydrophobic drugs because the hydrophilic drugs may diffuse out or partition from the dispersed oil phase into the aqueous phase, leading to poor encapsulation efficiencies.[77] Many types of drugs with different physical and chemical properties have been formulated into polymeric systems including anti-cancer drugs, narcotic agents, local anesthetics, steroids and fertility control agents.

Double emulsion method

Several water soluble drugs have been encapsulated by water-in-oil-in-water (w/o/w) methods. The aqueous solution of the water soluble drug is emulsified with polymer dissolved organic solution to form the water-in-oil (w/o) emulsion. The emulsification is carried out using either high speed homogenizers or sonicators. This primary emulsion is then transferred into an excess amount of water containing an emulsifier under vigorous stirring, thus forming a w/o/w emulsion. In the subsequent procedure, the solvent is removed by either evaporation or extraction process to allow

the formation of microsphere. One advantage of this method is encapsulation of hydrophilic drugs in an aqueous phase with high encapsulation efficiency. For this reason, the w/o/w emulsion system has been used widely for the development of protein delivery systems. The characteristics of the particles prepared by the double emulsion method are dependent upon the properties of the polymer (such as composition and molecular weight), the ratio of polymer to drug, the concentration and nature of the emulsifier, temperature, and the stirring/agitation speed during the emulsification process.[77] In w/o/w emulsion, the organic solvent diffuses out when it is transferred to large quantities of water. This diffusion coupled with solvent evaporation leads to the formation of solid microspheres. The solid microspheres can then be collected by filtration or centrifugation and stored after freeze dry.

Other methods are as follows:

- Phase separation method [78]
- Nanoprecipitation method [79-85]
- Dialysis method [86,87]
- Self assembling method [88-91]
- Rapid expansion of supercritical fluid solution method [92,93]
- Spray drying method [93-98]
- In-situ polymerization method [99-101]

Some of important biodegradable microspheres with PLGA and their method of encapsulation are presented in Table 4.1.

Sr. No.	Growth factor/protein	Polymer	Method of preparation	Reference
1.	Basic Fibroblast growth factor (bFGF)	PLGA	Double emulsion method	102
2.	Fibroblast growth factor-1 (FGF-1)	PLGA	Double emulsion method	103
3.	Human growth hormone	PLGA	Double emulsion method	104
4.	Insulin like growth factor-1 (IGF-1)	PLGA	Double emulsion solvent extraction method	105,106
5.	NGF	PLGA	Double emulsion method	107
6.	Recombinant human bone morphogenetic protein-2 (rhBMP-2)	PLGA	Double emulsion method	108,109
7.	Recombinant human glial cell line –derived neutrophilic factor (rhGDNF)	PLGA	Double emulsion method	110,111
8.	Transforming growth factor-ß (TGF- ß1)	PLGA	Double emulsion method	112,113
9.	Transforming growth factor-ß (TGF- ß3)	PLGA	Double emulsion method	114
10.	Vascular endothelial growth factor (VEGF)	PLGA	Solid encapsulation	115,116

Table 4.1: Biodegradable microspheres with PLGA and method of preparations

Factors determining the properties of microspheres

A range of production parameters influence the physicochemical parameters of the resulting microspheres.[117] Critical formulation parameters for the w/o/w preparation process are:

- Mechanical stirring
- Viscosity
- Osmotic gradient
- Volume of the phases
- Type of organic solvent-co solvent
- Temperature
- Stabilizers

4.3.7: Physico-chemical characterization of microspheres:

New applications of microspheres necessitate successful technology transfer, industrial scale-up, and reliable investigation methods both in pre formulation and in formulation steps.

- Design of experiment (DOE)
- Rheological measurements
- Morphological study
- Particle size analysis
- Drug entrapment and encapsulation efficiency (EE)
- Thermoanalytical measurements (TA)
- Analysis of residual organic solvents and co solvent
- Raman spectroscopy (RS)
- FTIR measurement
- PXRD
- Solid State NMR
- Electron microscopy

Cumulative drug release profile studies

The knowledge of the BCS characteristics of a drug can also be utilized by the formulator to develop a more optimized dosage form based on fundamental mechanistic rather than empirical information.[118]

The *in vitro* dissolution rates of the microparticles can be measured at defined rpm in 37 ± 1 ^{0}C buffer solution/deionized water mixture of defined pH according to the USP Drug Release Test 2 criteria. Since dissolution in the GI-tract takes place under heterogeneous conditions; different buffer solutions (citrate, acetate, phosphate or other) are used, although most of them do not correspond to the physiological

situation in the human GI-tract. The use of surfactants in the dissolution systems has physiological significance also as natural surfactants like bile salts (wetting, micellar solubilization, and / or deflocculation). Gastric juice has a relatively low surface tension, (42.7 $dyn.cm^{-1}$) compared with water (70 $dyn.cm^{-1}$) which aids in the wetting of both hydrophobic and hydrophilic particles. The controlled *in vitro* release data obtained from dissolution study should be fitted to various kinetic models in order to find out the drug release mechanism.[119,120] As *in vivo* animal studies, generally male New Zealand white rabbits, Rhesus monkeys, wild type and transgenic mice can be used,[121] therefore the correlation of the *in vitro / in vivo* evaluations should be clearly established.[122,123]

4.3.8: Objectives

Co-crystals or ion pair complex for pharmaceutical applications are in use since 1960's. Controlled drug delivery technology represents one of the most rapidly developing areas of science. The primary focus of the present work is the development and optimization of procedures for the preparation of co-crystals of Iloperidone and cholesteryl sulphate sodium. The work has been carried out with the practical end in mind of preparing more hydrophobic complex for the sustained drug delivery of optimum bio-available drug. In the undertaken research activity, biodegradable copolymer of lactic and glycolic acid (PLGA) with different composition of drug complex and other parameters (Organic solvent, emulsifier, homogenizer speed and stirring) are used for the optimum drug complex loading with uniform microsphere with high encapsulation efficiency of drugs in order to get a better understanding of the suitability and versatility of the methods applied for the preparation of sustain release drug delivery systems. Effects of microsphere morphology, size and surface charge on encapsulation efficiency as well as on *in vitro* controlled drug release profiles.

4.4: Experimental:

4.4.1: Materials and reagents:

Iloperidone

Iloperidone (Ilo) was obtained as a gift sample from Sun pharmaceutical Industries Limited, Vadodara, India. Iloperidone (FANAPT®) is an antipsychotic, psychotropic drug of the benzisoxazole class, is used for the treatment of

schizophrenia in adults. Its chemical name is 1-[4-[3-[4-(6-fluoro-1, 2-benzisoxazol-3-yl)-1-piperidinyl] propoxy]-3-methoxyphenyl]ethanone molecular formula : $C_{24}H_{27}FN_2O_4$, and molecular weight is 426.48. Iloperidone is a white crystalline powder and has a pK_a of 7.69. Iloperidone is practically insoluble in water and soluble in chloroform.

Cholesteryl sulphate sodium

Cholesteryl sulphate sodium (CSS), molecular formula : $C_{27}H_{45}NaO_4S$, and molecular weight : 488.71 (Analytical Grade 99.9 % pure obtained from Genzyme Pharmaceuticals LLC, Switzerland) was used as received.

Amberlite IR 120H cation exchange resin

Sigma-Aldrich, USA was used as received.

DL-Copoly lactic glycolic acid (PLGA)

(PLGA-7525) Wako Pure Chemical Industries Ltd, Japan was used as received.

Solvents and emulsifier

Analytical reagent grade glacial acetic acid, dichloromethane, methanol, acetone, n-hexane and polyvinyl alcohol (degree of hydrolysis: 88) were obtained from Merck, India and were used as received. Water for injection (WFI) and double distilled de-ionized water (0.22 micron nylon filtered) was used throughout the experiments.

4.4.2: Method of preparation Iloperidone-cholesteryl sulphate complex:

Iloperidone having one lone pair electron available on tertiary nitrogen atom of piperidine ring and molar equivalent of cholesteryl sulphate were considered for adduct formation. Hence 1 : 1 mole ratio of each sample was taken to form a non-bonding complex of electron rich species like Iloperidone to the electron deficient cholesteryl sulphate molecule in the same solvent with acidic pH. The ion-pair complex was least soluble in aqueous solvent as compared to organic solvent and also quantitatively extractable (Scheme 4.1).

Method I

To maintain 1 : 1 mole ratio, 474.3 mg of Iloperidone was dissolved in 4 ml of methanol containing 0.5ml of glacial acetic acid and 543.5 mg of cholesteryl sulphate sodium was separately dissolved in 10 mL methanol by gentle warming up-to 40°C for 5 min. The two solutions were mixed in 100 mL round bottom flask and stirred at 40 °C for 5 h. Methanol was removed by using rotatory evaporator assembly to get the solid complex. To this was added 30 mL of water for injection (WFI) and the supernatant was discarded. Similarly the precipitate was rewashed 3 times for the removal of acetic acid and methanol completely and dried at room temperature overnight. The dried complex was recrystalized by dissolving it in 30 mL of methanol to obtain a white crystalline solid having 95 % yields.

Method II

In this method, 543.5 mg cholesteryl sulphate solution methanol (50 mL) was passed through previously regenerated Amberlite IR 120H cation exchange resin, then it was mixed with Iloperidone (474.3 mg) in two drops of acetic acid and 5 mL methanol to obtain clear solution. The above solutions were mixed together and stirred at 40 ºC for 5 h, followed by evaporation using rotator evaporator. The solid so recovered was dried at room temperature overnight, washed with water, re-precipitated at -50 ^{o}C (methanolic dry ice, 5 min) and the supernatant was discarded. The precipitated solid was further reprecipitated from 30 mL methanol which gave an off-white amorphous solid having 92 % yield.

Complex synthesis

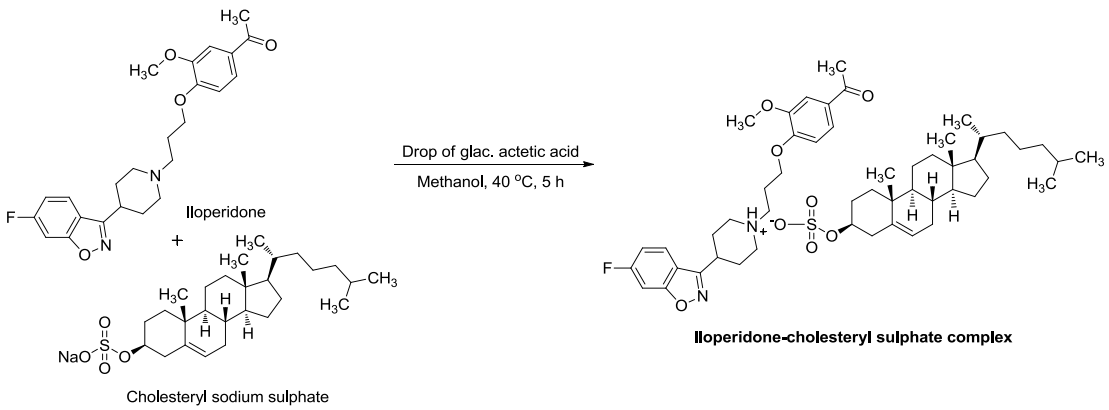

Scheme 4.1: Synthesis of Iloperidone-cholesteryl sulphate complex

The complexes so prepared were characterized by FT-IR, FT-NMR (^{1}H, ^{13}C), Mass spectroscopy, DSC, XRD and microanalysis. The drug-loading efficiency was determined by UV-Vis spectrometry and morphology by SEM.

4.4.3: PLGA (7525) Lactic acid and Glycolic acid mole ratio content by NMR:

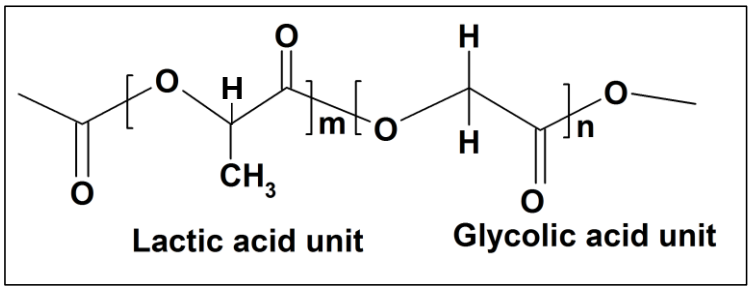

Figure 4.8: Molecular skeleton of PLGA co-polymer

About 100 mg of the PLGA sample (structure shown in Fig.4.8) was accurately weighed and dissolved in about 0.7 mL of deuterated chloroform as a test solution and transferred into a 5 mm NMR tube. NMR spectra (Fig.4.9) were scanned using TMS as reference at 0.0 ppm. Content of lactic acid, glycolic acid and the ratio of lactic acid and glycolic acid in the sample were calculated from the integral values of respective peaks.

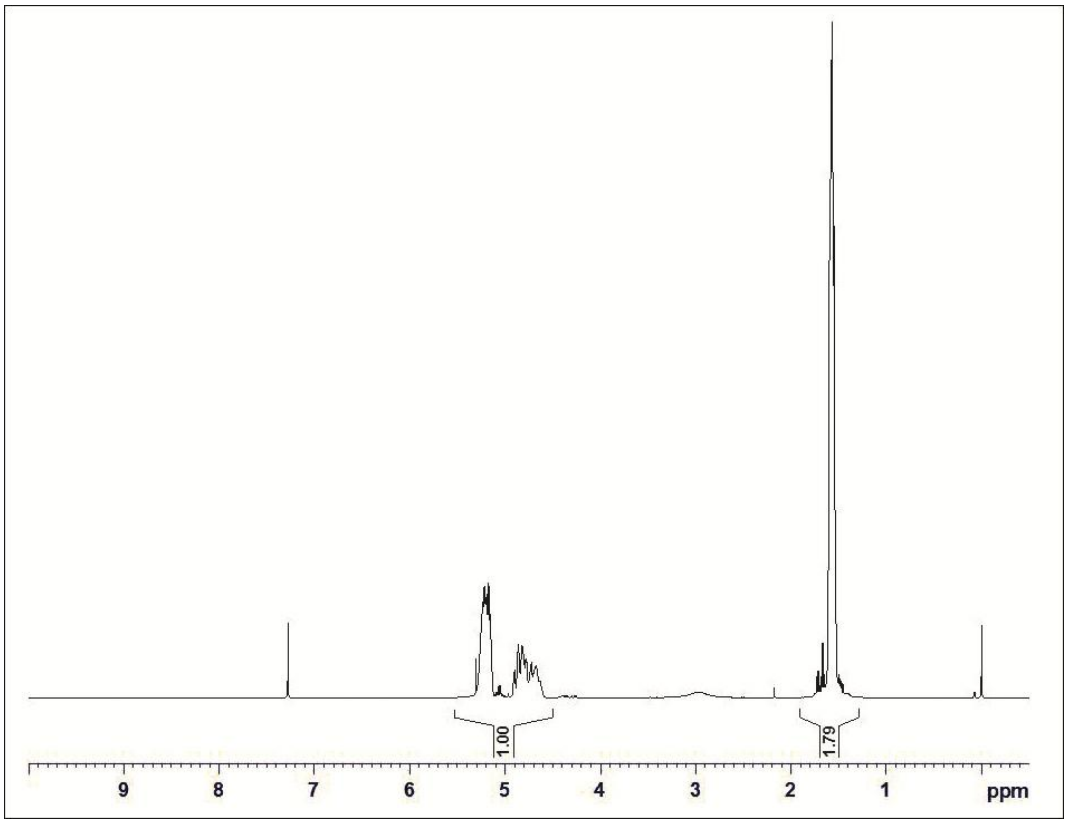

Figure 4.9: ^{1}H NMR spectra of PLGA (7525) in CDCl3

Mole ratio calculation

A = Integral value due to methyl ($-CH_3$) groups at 1.57 ppm

B = Integral value due to methine (-CH-) and methylene ($-CH_2-$) group between 4.2 ppm and 5.5 ppm

m = Mole fraction of lactic acid = A / 3

n = Mole fraction of Glycolic acid = (B - m) / 2

% Mole ratio of Lactic acid (LA) = [m / (m + n)] x 100 = 74.74

% Mole ratio of Glycolic acid (GA) = [n / (m + n)] x 100 = 25.26

Molecular ratio of lactic acid and glycolic acid = 2.96

4.5: Preparation of Iloperidone-CSS complex depot (Microsphere):

The both (crystalline and amorphous) ion-pair complexes of Iloperidone-CSS depot (microsphere) were prepared by solvent evaporation method with variable loading of drug complex and also with varying biodegradable polymer. In the present study, crystalline ion-pair complex of Iloperidone-CSS (Ilo-CSS_c) (30 mg), and PLGA (75 : 25) (900 mg) were dissolved completely in 25 mL methylene chloride which formed the polymer phase. This polymer phase was emulsified with an aqueous phase made up of 5% w/v polyvinyl alcohol (PVA) solution by using homogenizer (Make-Kinematica) at a speed of 8000 rpm. The solvent was evaporated by continuous stirring at 500 rpm under nitrogen atmosphere. Finally, the mother liquor was filtered off and solution was freezed at -50 °C with dry ice methanol bath .The freezed solution was attached to freezed dryer (Lyophylizer, Make-Martin Christ GMBH, Germany) with condenser temperature -52°C and vacuum 0.3 bar for 24 h. Same procedure was followed for amorphous ion-pair complex of the microsphere Iloperidone-CSS(Ilo-CSS_a). Polymer and drug complex ratios used in preparing the microsphere are given in Table 4.2 and Table 4.3.

The microspheres so prepared were characterized by XRD, FT-IR, DSC, PSD, drug-loading efficiency by UV-Vis, SEM and accelerated in-vitro studies were carried out by using rotating dissolution apparatus and the percentage of cumulative drug released was determined by UPLC with UV detector.

Formulation code	Polymer: Drug ratio	Polyvinyl Alcohol (g)	Dichloromethane (mL)	Water (mL)
A1	30:0.5	1.5	1.4	33
A2	30:1	1.5	1.4	33
A3	30:2	1.5	1.4	33
A4	30:0.5	1.5	1.4	33
A5	30:1	1.5	1.4	33
A6	30:2	1.5	1.4	33

Table 4.2: Different formulations of Ilo-CSS microsphere by varying drug ratio

Formulation code	Polymer: Drug ratio	Polyvinyl Alcohol (g)	Dichloromethane (mL)	Water (mL)
F1	20:1	1.5	1.4	33
F2	30:1	1.5	1.4	33
F3	40:1	1.5	1.4	33
F4	20:1	1.5	1.4	33
F5	30:1	1.5	1.4	33
F6	40:1	1.5	1.4	33

Table 4.3: Different formulations of Ilo-CSS microsphere by varying polymer ratio

4.5.1: Characterization of Ilo-CSS complex and its microsphere:

Fourier Transform Infrared Spectroscopy (FT-IR)

FT-IR spectrums of samples were scanned using an Infra red spectrometer (Model: Spectrum one, Perkin Elmer). Approximately 10 mg of each sample was mixed with 200 mg of dried potassium bromide of equal weight and compressed to form a KBr disc. The scanning range used was from 400 to 4,000 cm^{-1} and the resolution was 1 cm^{-1}.

Differential Scanning Calorimetry (DSC)

Differential Scanning Calorimetric (DSC) analysis was carried out by using a Model-DSC Q2000, TA Instruments, (Delaware, USA). The instrument was calibrated using indium as a standard and about 2mg samples of pure sample of Iloperidone, Cholesteryl sulphate sodium, PLGA and physical mixture of Iloperidone-cholesteryl sulphate, $ICSS_c$, $ICSS_a$ and these microspheres (about 5 mg) were placed

in standard aluminum pans sealed with a lid. The crimped aluminum pans were heated from 40-350 °C at a heating rate of 10 °C/min.

Mass spectroscopy (ESI-MS)

About 20 ppm of Iloperidone, cholesteryl sulphate sodium, Iloperidone-colesteryl Iloperidone-CSS complex ($ICSS_c$, $ICSS_a$) solution in dichloromethane was injected through a direct inlet of electrospray ionization with positive and negative mode by MicroMass Quattro micro API (Make-Waters) with mass range from 0.0 amu to1000.0 amu to get the mass spectrum.

Fourier Transform NMR Spectroscopy (FT-NMR)

About 10 mg of pure Iloperidone, Cholesteryl sulphate sodium and Iloperidone-cholesteryl sulphate complexes ($ICSS_c$, $ICSS_a$) in a 5mm NMR tube with deuterated NMR solvent and perfectly closed by the cap .^{1}H-NMR spectra were recorded in $CDCl_3$ (Merck 99.9% of D) on a Bruker Biospin AV-III 500 MHz spectrometer operating at proton frequency at 500.13 MHz using 5 mm Broad Band Observe probe head at room temperature (~30 ± 2 ºC). All data were processed using Bruker Biospin Topspin 2.1 version software.

Similarly proton decoupled ^{13}C-NMR spectra along with DEPT-90,135 were recorded by using 10% sample in $CDCl_3$ with spectrometer operating at carbon frequency at 125.76 MHz.

Elemental analysis:

All samples were accurately weighed (between 1.0 to 3.0 mg) in tin capsule by using micro balance and sealed properly then kept in auto sampler for the determination of elemental composition with following instrumental condition. The percentage of Carbon, Hydrogen and Nitrogen was determined by EA 2400 Series II analyzer, (Perkin Elmer, USA) attached with a GC packed column ALPHA 3 feet (2 meter x 1/8", Hayesep D 80/100 mesh) with instrumental condition, combustion temperature 925 °C, reduction temperature 640 °C and detector oven temperature 82.4° ± 0.2°C.

X-Ray Powder Diffractometry (XRPD)

Powder X-ray diffraction pattern (XRD) were recorded on a Philips X'Pert PRO, PAN Analytical, Netherlands, using a Ni-filtered equipped with Cu Kα1 radiation (1.5405 A^o) source (Cu anode), Solid-state Germanium detector with

spinning sample stage. The XRPD diffraction patterns of all samples i.e. Iloperidone, cholesteryl sulphate, PLGA and physical mixture of Iloperidone-cholesteryl sulphate, $ICSS_c$, $ICSS_a$ and microsphere formulations, were recorded using a diffractometer with a voltage of 45 kV and a current of 40 mA . The solids were exposed to Cu-K_α radiation (1.54 Å) and the scanning rate was 2 °/ min over a 2θ angular range of 4-40° with an interval of 0.008° in 2θ.

Scanning Electron Microscopy (SEM)

Surface morphology and shape of the Iloperidone-cholesteryl sulphate, $ICSS_c$, $ICSS_a$ and microsphere formulations were examined with Scanning Electron Microscope (Model-Quanta-200, Make-FEI Company, The Netherlands), with spot size 5, with carbon tape. The samples were mounted on a metal stub with double-sided adhesive tape with an accelerated voltage of 15 kV and a current of 20 mA prior to observation. The samples images of representative areas were captured at suitable magnifications.

Particle Size Distribution (PSD)

The various PLGA-drug complex formulation microspheres particle size distribution was measured by wet method using a particle size analyzer (Malvern Mastersizer-2000, UK). Samples were suspended in 1.0 % of tween-80 in distilled water as a dispersant and stirred continuously with 1500 rpm for particle size analysis.

Determination of loading efficiency and production yield

The UV-Vis spectrums of the purified Iloperidone, cholesteryl sulphate sodium, Iloperidone-cholesteryl sulphate, $ICSS_c$, $ICSS_a$ and PLGA were recorded on spectrophotometer (Model UV-1800 Series, Make-Shimadzu) in wave length range form 200-400nm after confirming the noninterference of cholesteryl sulphate sodium in the absorption region of Iloperidone with dichloromethane.

Accurately weighed 20-25 mg of Ilo-CSS complex loaded with PLGA microsphere were dissolved in 10 mL of dichloromethane entrapment efficiency (% EE) of Iloperidone-cholesteryl sulphate microsphere was calculated by using Equation (4-1) with the help of calibration plot constructed for pure Iloperidone at 275 nm.

$$Loading\ efficiency = \frac{Weight\ of\ actual\ drug\ content\ in\ microspheres}{Weight\ of\ theoretical\ drug\ content\ in\ microspheres}\ X\ 100 \quad (4\text{-}1)$$

The production yield (%) was expressed as percentage of the dried micro-particle with respect to the initial weight of the raw materials of drug and the polymer used. All the experiments were performed in duplicate.

4.5.2: In vitro release studies:

Correlation between real time in vitro release studies of Iloperidone-CSS complex PLGA microsphere up to one month and in vitro release using accelerated conditions at 55 °C was established which indicates 1 h accelerated study is equivalent with one day real time study.

The *in vitro* release studies of the drug loaded microspheres along with Iloperidone-CSS complex were carried out at 55°C with 2 % tween-80 in water medium using bottle rotating dissolution apparatus (Varian, Model-ERB 16W) up-to 36 h (eight stations). 1 mL of dissolution media sample was withdrawn at predetermined time intervals and the same volume of fresh dissolution media was added as replacement. After suitable dilution, the withdrawn samples were analyzed and the amount of Iloperidone released was determined by using UPLC (Waters). The whole study was carried out in triplicate.

The samples were analyzed by using a Waters make UPLC having UV detector with wavelength at 275 nm. All the experiments were repeated thrice and the average values were considered. Drug release kinetics study was also performed with the help of different mathematical models.

Drug release conditions

Apparatus	: Bottle rotating apparatus (Make : Varian)
Speed	: 6 rpm
Temperature of bath	: 55°C ± 0.5°C
Dissolution Medium	: 0.02% w/v tween-80 in water
Volume of Medium	: 90 mL
Time Points	: Initial, 0.5, 1, 4, 12, 18, 24 and 36 h

Preparation of 0.02 % w/v tween-80 *(Dissolution media)*

About 200 mg of tween-80 was weighed in a 100 mL glass beaker and dissolved it completely with the help of sonicator in 50 mL of water. Transfer the

resulting solution completely to 1000 mL volumetric flask and diluted with water up to the mark.

1 mL sample was withdrawn at specified time point in a micro centrifuge tube and replaced with fresh above dissolution media. The withdrawn sample was centrifuged for 5 min at 4000 rpm and clear supernatant solution was taken as analyte.

Standard solution preparation

20-25 mg of Iloperidone standard was dissolved in 40 mL of methanol in a 200 mL volumetric flask and the volume was made up to the mark with mobile phase.

Sample preparation

Each 100 mg of microsphere samples were accurately weighed and dissolved in 90 mL of dissolution media in a 90 mL capacity rotating bottle. (Each sample were prepared in triplicate for the *in vitro* study)

Column	: Acquity UPLC HSS C18 (100 mm x 2.1 mm, 1.8µm) make –Waters, USA.
Flow rate	: 0.3 mL/min
Temperature	: Ambient
Detection	: 275 nm
Injection volume	: 2 µL
Run time	: About 8 min
Mobile phase	: Buffer: Acetonitrile: Methanol (600:200:200), filter through 0. 22µ filter
Buffer	: 3.15 gm of Ammonium formate in 1000 mL of water, pH was adjusted to 3.5 with formic acid
Retention time	: About 5.5 min
Diluent	: Methanol and mobile phase

Percentage of Cumulative drug release calculation

First withdrawal

$$\%\, Iloperidone(R_1) = \frac{A_t}{A_s} \times \frac{W_s}{50} \times \frac{5}{25} \times \frac{100}{W_t} \times \frac{P}{L_c} \times A \times \frac{1}{90} \times \frac{100-W}{100} \qquad (4\text{-}2)$$

where, A_t : Area count of Ilo-CSS complex peak in test solution

A_s : Average area count of Ilo-CSS complex peak in standard solution

W_s : Weight of Ilo-CSS complex in mg in standard solution

W_t : Weight of depot mass taken in bottle (mg)

P : Percentage purity of Ilo-CSS complex (as on anhydrous basis)

A : Average weight in mg

L_c : Label claim in mg (1.5 mg in 100 mg of microsphere)

1 / 90 : Factor for overfill

W : Water content of Ilo-CSS complex (Freshly determined)

Second withdrawal

$$Content\ of\ \%\ Iloperidone(R_2) = \mathrm{R_1} + C_1 \quad (4\text{-}3)$$

$$C_1 = \mathrm{R_1} \times \frac{\mathrm{V_w}}{90} \quad (4\text{-}4)$$

where, C_1 = Correction factor for second withdrawal

$\mathrm{R_1}$ = % drug release at first withdrawal

$\mathrm{V_w}$= Volume withdrawn (1 mL) at the time of withdrawal

Third withdrawal

$$Content\ of\ \%\ Iloperidone(R_3) = \mathrm{R_2} + C_2 \quad (4\text{-}5)$$

$$C_2 = \left(\mathrm{R_2} \times \frac{\mathrm{V_w}}{90}\right) + \mathrm{C_1} \quad (4\text{-}6)$$

where, C_2 = Correction factor for third withdrawal

$\mathrm{R_2}$ = % drug release at second withdrawal

$\mathrm{V_w}$= Volume withdrawn (1 mL) at the time of withdrawal

Fourth withdrawal:

$$Content\ of\ \%\ Iloperidone(R_4) = \mathrm{R_3} + C_3 \quad (4\text{-}7)$$

$$C_3 = \left(\mathrm{R_3} \times \frac{\mathrm{V_w}}{90}\right) + \mathrm{C_1} + \mathrm{C_2} \quad (4\text{-}8)$$

where, C_3 = Correction factor for fourth withdrawal

$\mathrm{R_3}$ = % drug release at third withdrawal

$\mathrm{V_w}$= Volume withdrawn (1 mL) at the time of withdrawal

Fifth withdrawal

$$Content\ of\ \%\ Iloperidone(R_5) = \mathrm{R_4} + C_4 \quad (4\text{-}9)$$

$$C_4 = \left(R_4 \times \frac{V_w}{90}\right) + C_1 + C_2 + C_3 \quad (4\text{-}10)$$

where, C_4 = Correction factor for fifth withdrawal

R_4 = % drug release at fourth withdrawal

V_w= Volume withdrawn (1 mL) at the time of withdrawal

Sixth withdrawal

$$Content\ of\ \%\ Iloperidone(R_6) = R_5 + C_5 \quad (4\text{-}11)$$

$$C_5 = \left(R_5 \times \frac{V_w}{90}\right) + C_1 + C_2 + C_3 + C_4 \quad (4\text{-}12)$$

where, C_5 = Correction factor for sixth withdrawal

R_5 = % drug release at fifth withdrawal

V_w = Volume withdrawn (1 mL) at the time of withdrawal

Seventh withdrawal

$$Content\ of\ \%\ Iloperidone(R_7) = R_6 + C_6 \quad (4\text{-}13)$$

$$C_6 = \left(R_6 \times \frac{V_w}{90}\right) + C_1 + C_2 + C_3 + C_4 + C_5 \quad (4\text{-}14)$$

where, C_6 = Correction factor for seventh withdrawal

R_6 = % drug release at sixth withdrawal

V_w= Volume withdrawn (1 mL) at the time of withdrawal

4.6: Results and discussion:

4.6.1: Characterization of Ilo-CSS complex and its PLGA microsphere:

Characterization by FTIR

FT-IR spectra for (a) Iloperidone (b) cholesteryl sulphate (c) Physical mixture of Iloperidone and cholesteryl sulphate (d) Complex M1 (e) Complex M2 are presented in Figure 4.10. The FTIR spectrum of CSSNa ($ROSO_2O^-M^+$) shows asymmetric and symmetric stretching of > SO_2 group at 1383 -1246 cm^{-1} and 1137-1064 cm^{-1} respectively. However, with removal of Na^+, the asymmetric stretching disappears and symmetric stretching is shifted to higher wavelength. Iloperidone spectrum shows characteristic peaks for various functional groups of Iloperidone. The

spectra of complexes prepared by Method I and Method II are similar. In addition, the asymmetric stretching reappears for the complex ($ROSO_2O^-M^+$). There is disappearance, merging and decrease in intensity in C-H stretching peaks of Iloperidone in the range of 2746 to 3091 cm^{-1}. This suggests the formation of complex.

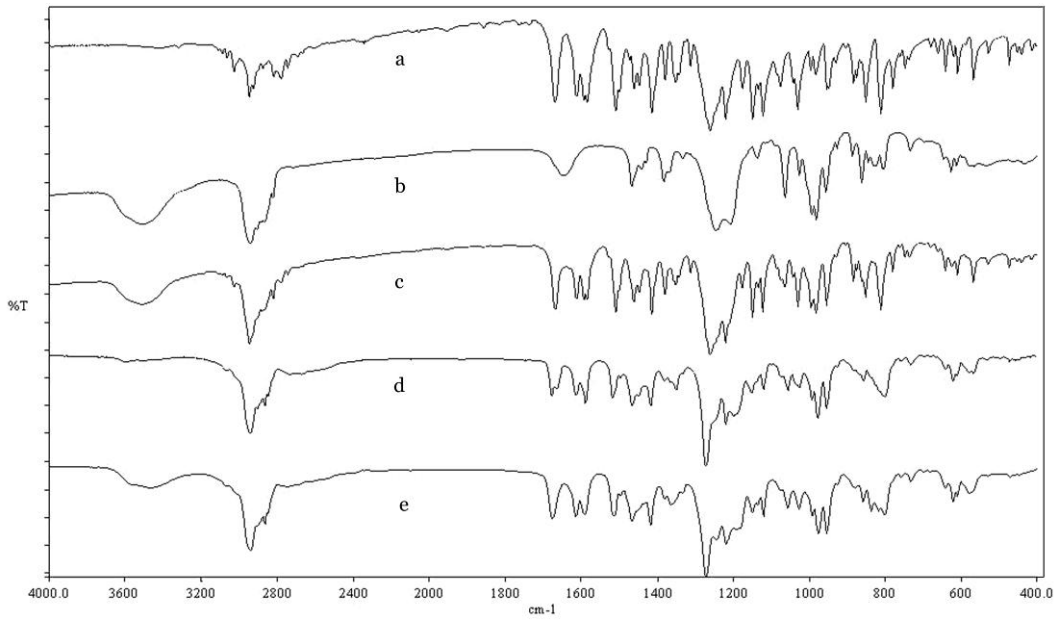

Figure 4.10: FTIR spectra of (a) Iloperidone (b) Cholesteryl sulphate sodium (c) 1:1 Physical mixture (d) M1 (Ilo-CSS_c) (e) M2 (Ilo-CSS_a)

IR (KBr): υ in cm^{-1} 2949-2779 (-C-H stretching), 1668 (-C=O stretching), 1607-1450 (Aryl -C=C- stretching), 1585 (-C=N- stretching), 1261 (-C-O stretching), 1149 (-C-F stretching), 1031 (-C-N- stretching), 812 (-N-O- stretching) $cm.^{-1}$

Differential Scanning Calorimetry (DSC)

The Differential Scanning Calorimetry (DSC) thermogram of pure Iloperidone and cholesteryl sulphate sodium exhibit sharp melting peaks around 122.5 ºC and 173.7 ºC respectively which are also seen in the physical mixture of the two, where as complexes give a sharp melting peak at 169 ºC. Similarly microspheres F1 to F6 do not show any melting peak of loaded Ilo-CSS complex with amorphous polymer. Comparison of thermograms can be seen from Figure 4.11, Figure 4.12 and Figure 4.13.

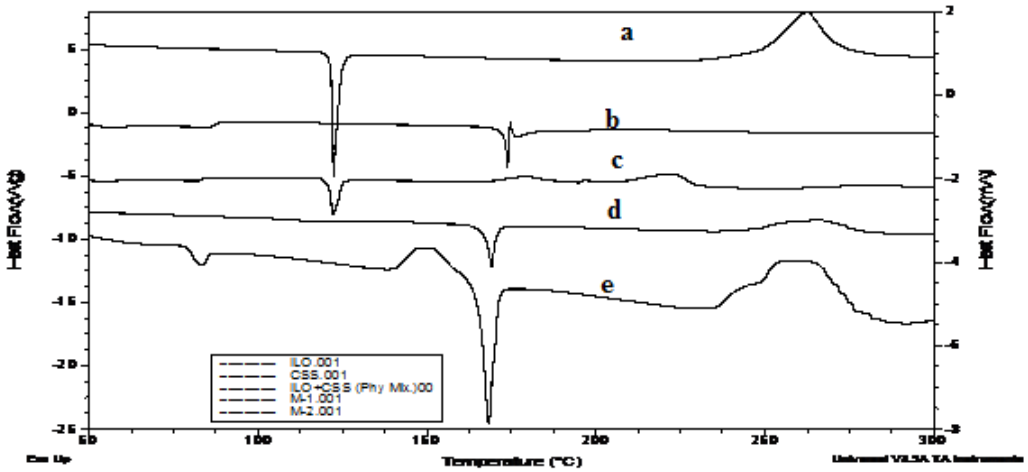

Figure 4.11: DSC thermogram (a) Iloperidone (b) Cholesteryl sulphate sodium (c) 1:1 Physical mixture (d) M1 (Ilo-CSS_c) (e) M2 (Ilo-CSS_a)

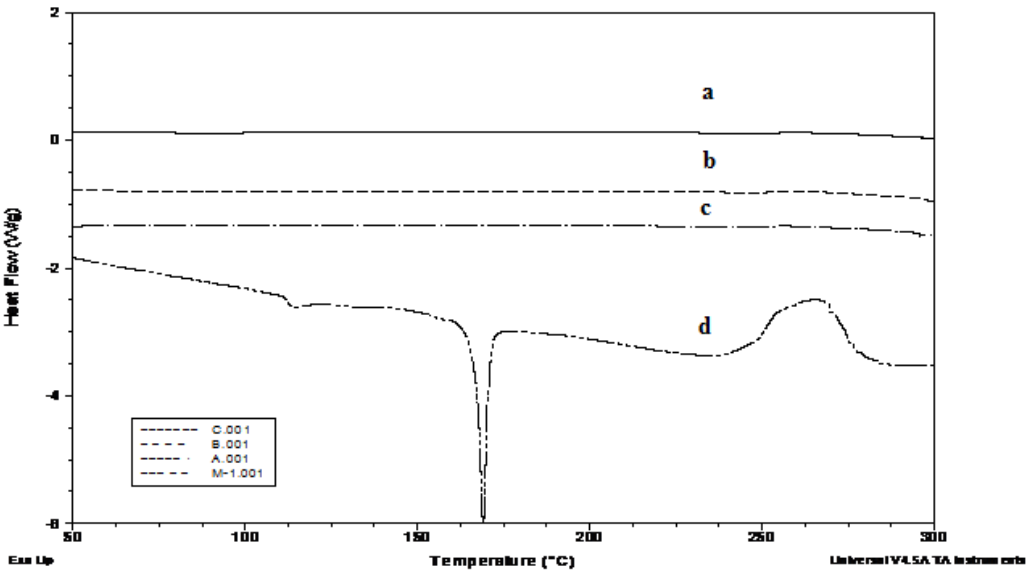

Figure 4.12: DSC thermogram of Ilo-CSS_c complex (M1) with its microsphere F1, F2 and F3

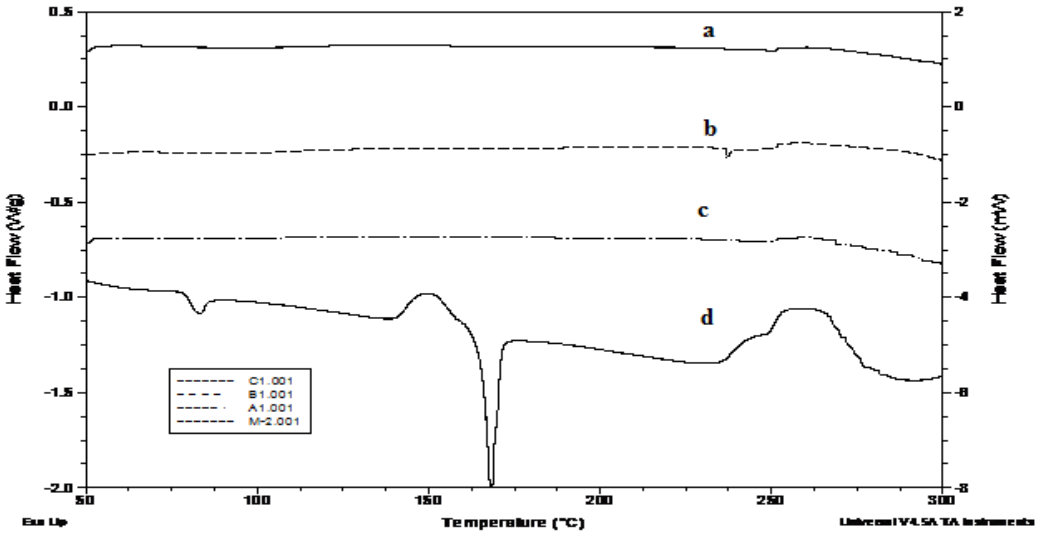

Figure 4.13: DSC thermogram of Ilo-CSS_a complex (M2) with its microsphere F4, F5 and F6

Electro Spray Ionization (ESI) mass spectroscopy

Mass Spectra of Iloperidone, cholesteryl sulphate and their complexes, both crystalline and amorphous (Fig. 4.14 and Fig.4.15) show molecular ion peak $[M+H]^+$ at 427.21 which indicates the presence of Iloperidone in cationic form, where as the ESI negative ion mode shows a molecular ion peak $[M]^-$ at 465.4 that indicates the presence of cholesteryl sulphate (free acid) in anionic form. Hence both the crystalline and amorphous complexes exhibit 1:1 mole ratio and ionic form which is further supported by molecular modeling and energy minimization data.

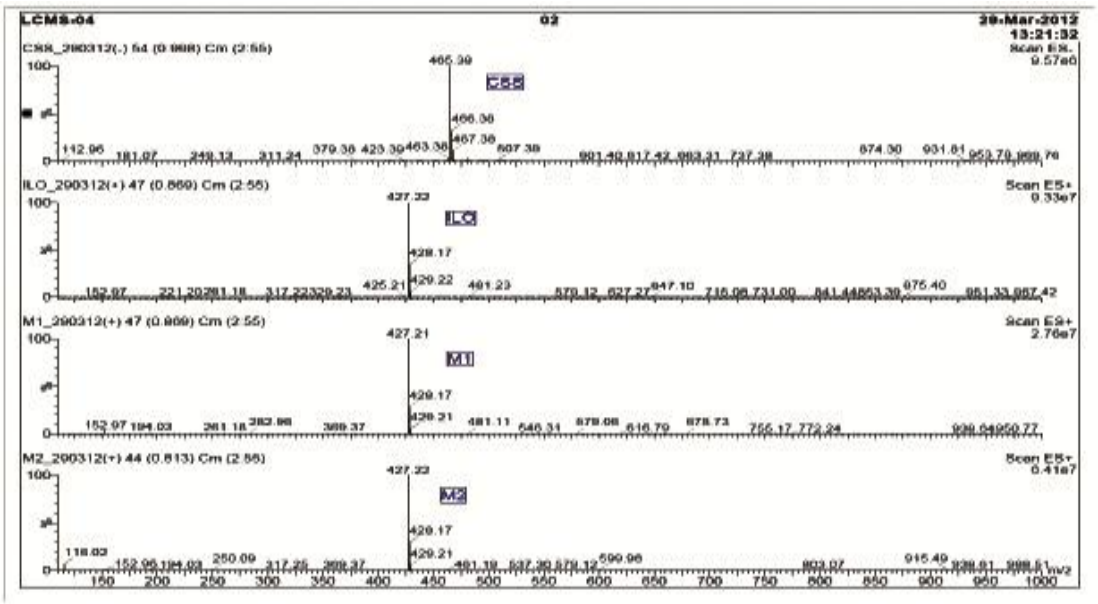

Figure 4.14: Mass spectra of in ESI positive ion mode (ILO) Iloperidone, (CSS) Cholesteryl sulphate sodium, (M1) Ilo-CSS_c, (M2) Ilo-CSS_a

ESI-MS: (+Ve ion mode) (For calcul. $C_{51}H_{73}N_2O_8SF$ = 893.19, Found = 427.21 due to Iloperidone moiety).

(-Ve ion mode) (For calcul. $C_{51}H_{73}N_2O_8SF$ = 893.19, Found = 466.27 due to cholesteryl sulphate moiety).

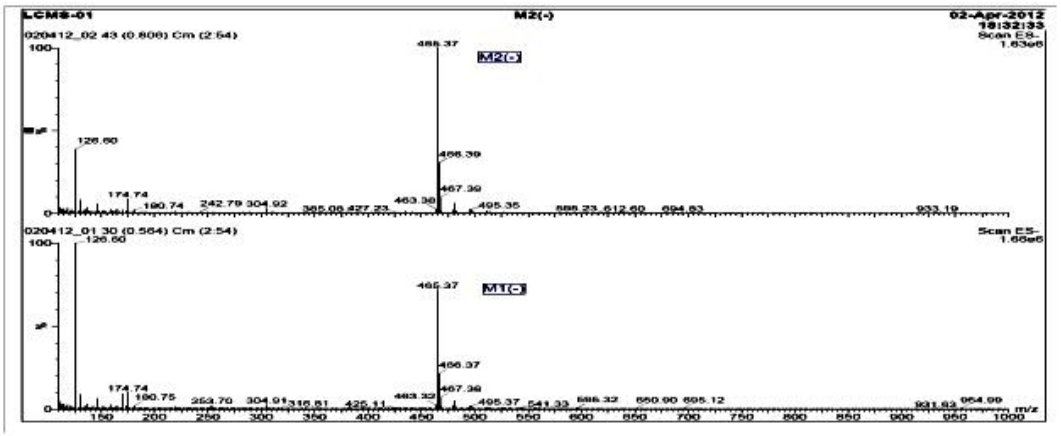

Figure 4.15: Mass spectra of (M1) Ilo-CSS_c and (M2) Ilo-CSS_a complex in ESI negative ion mode

^{1}H and ^{13}C NMR spectroscopy

^{1}H-NMR and proton decoupled ^{13}C-NMR spectra of all the samples are given in Fig.4.17 and Fig.4.19 respectively. ^{1}H-NMR signals of piperidine nucleus in Iloperidone-CSS complex is shifted to downfield with respect to Iloperidone such as, δ 2.07 - 2.26, 2.17 - 2.37, 3.07 - 3.33, 3.09 - 3.42 ppm in Fig.4.16. Similarly cholesteryl sulphate proton signals shifted to downfield δ 2.38 - 2.80, 2.47 - 2.99 ppm.

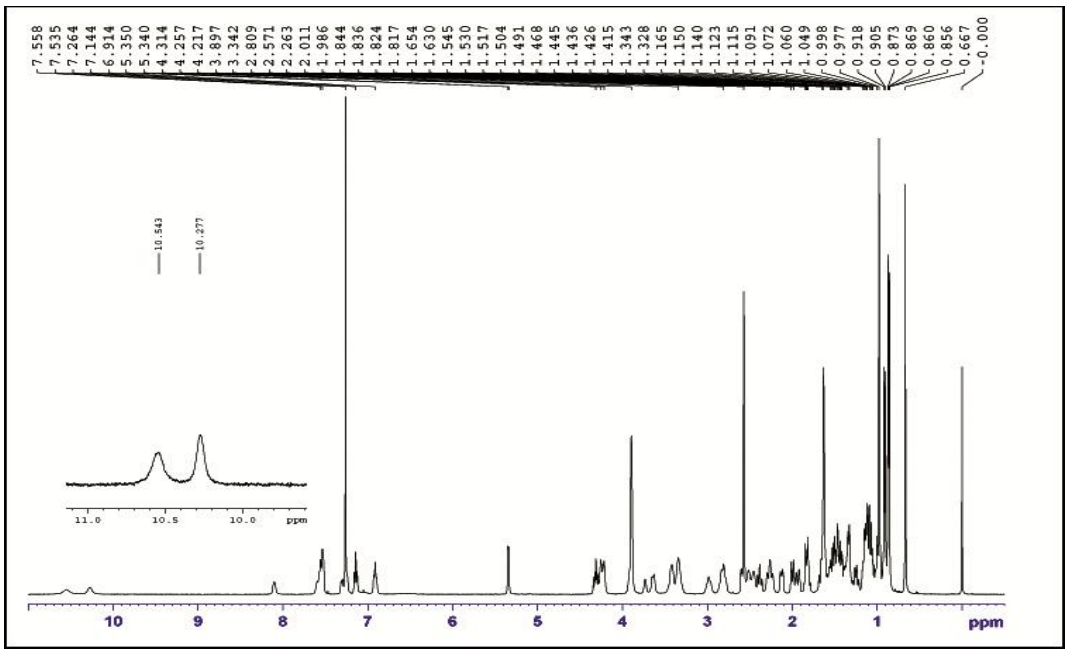

Figure 4.16: ^{1}H-NMR of M1 (Ilo-CSS_c) in $CDCl_3$

^{1}H-NMR (500 MHz, $CDCl_3$): δ 0.67 (s, 3H), 0.86 (dd, J=2.10, 6.55 Hz, 6H,), 0.91 (d, J=6.45 Hz, 3H), 0.98 (s, 3H), 0.93-1.56 (m, 20H), 1.83 (m, 2H), 1.94 (dd, J=2.50, 17.15 Hz, 1H), 2.00 (d, J=12.55 Hz, 1H), 2.13 (d, J=12.20 Hz, 1H), 2.26 (t, J=16.28 Hz, 2H,), 2.38 (t, J=11.33 Hz, 1H), 2.32-2.42 (t, 1H), 2.43-52 (m, 2H), 2.57 (s, 3H), 2.60 (d, J=3.00 Hz, 1H), 2.72-2.9 (m, 2H), 2.90-3.05 (t, 1H), 3.25-3.78 (m, 5H), 3.90 (s, merge with broad doublet 4H), 4.22-4.26 (d, J=19.91 Hz, 2H), 4.31-4.34 (m, 1H), 5.34 (d, J=4.95 Hz, 1H), 6.91-6.93 (t, 1H), 7.12-7.16 (t, J=8.75 Hz, 1H), 7.20-7.31 (dd, 1H), 7.47-7.55 (m, 1H), 8.10 (s, 1H), 10.27-10.54 (bs, due to NH, 1H).

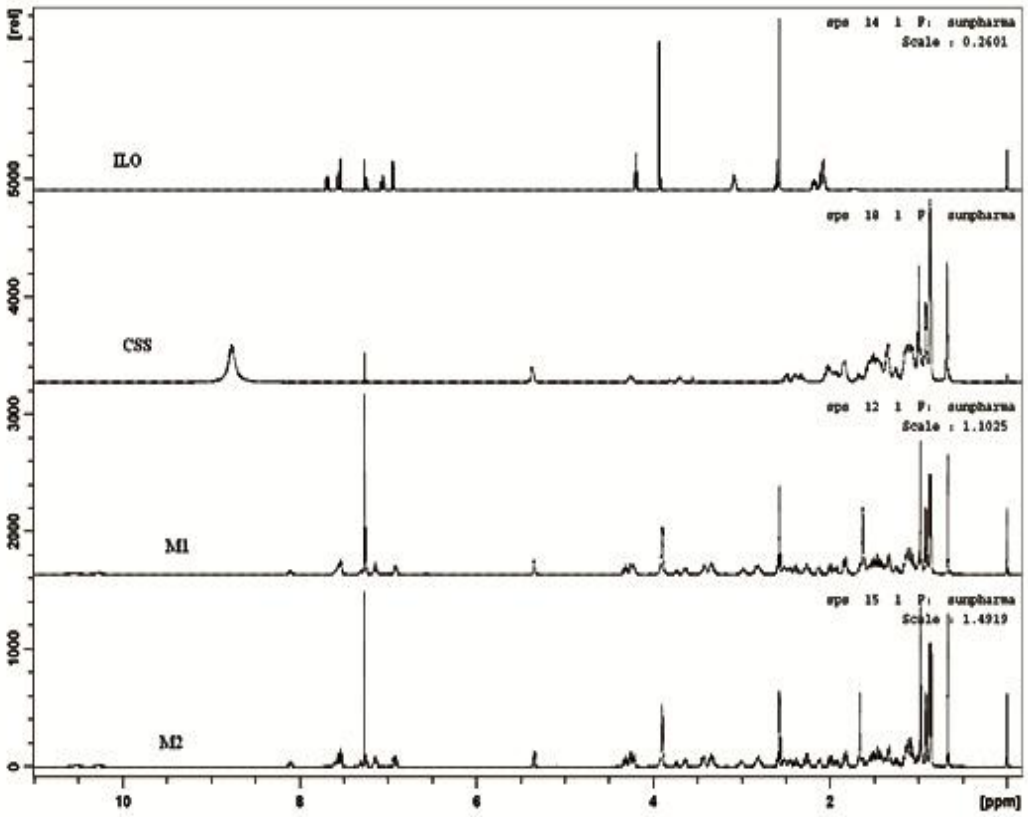

Figure 4.17: ^{1}H NMR spectra of (Ilo) Iloperidone, (CSS) Cholesteryl Sulphate Sodium, (M1) Ilo-CSS_c, (M2) Ilo-CSS_a

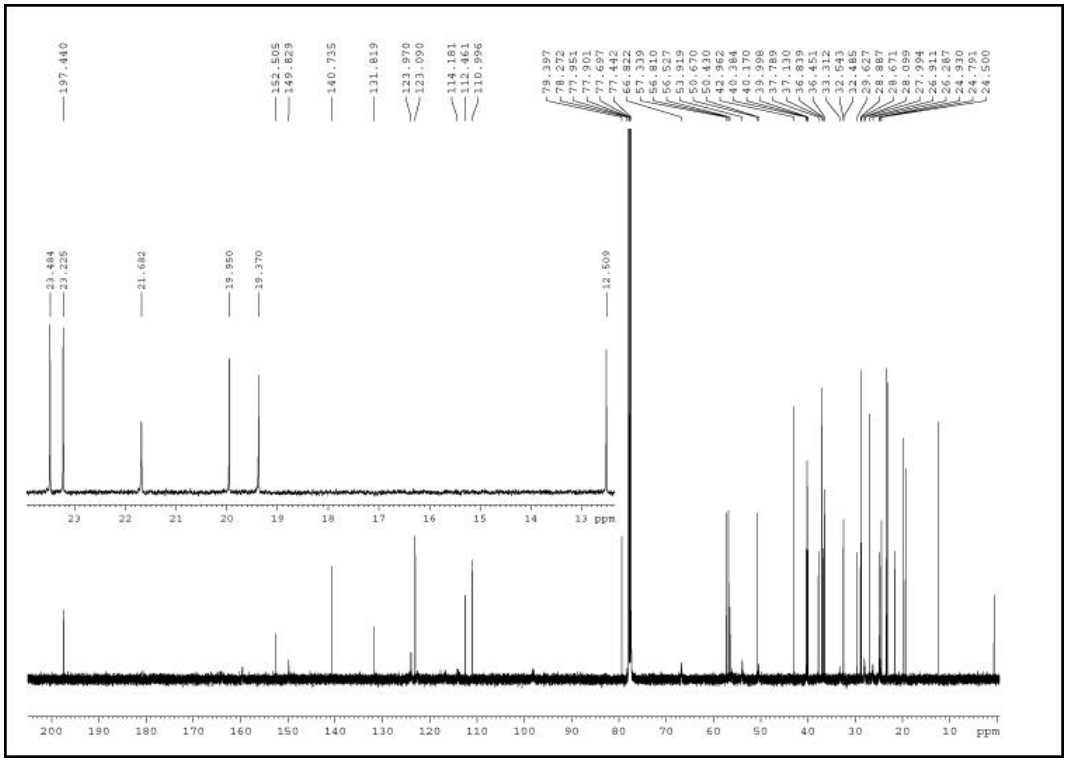

Figure 4.18: Proton decoupled ^{13}C-NMR of M1 (Ilo-CSS$_c$) in $CDCl_3$

^{13}C-NMR (125.76 MHz, $CDCl_3$): δ 197.41 (C=O), 159.70 (Cq), 152.51 (Cq), 149.75 (Cq), 140.68 (Cq), 131.72 (Cq), 124.16 (Cq), 124.11(CH), 123.93 (CH), 123.05 (CH), 116.85 (Cq), 113.98 (Cq), 113.79 (CH), 112.39 (CH), 110.95 (CH), 98.09 (CH), 79.33, 66.84 (CH_2), 57.29 (CH), 56.78 (CH), 56.48 (OCH_3), 56.35 (Cq), 53.73 (CH_2), 50.62 (CH), 50.41(CH_2), 42.92 (Cq), 40.34 (CH_2), 40.14 (CH_2), 39.98 (CH_2), 37.73 (CH_2), 37.07 (Cq), 36.81 (CH_2), 36.41, 32.99 (CH), 32.48 (CH_2), 32.43 (CH), 29.60 (CH_2), 28.85 (CH_2), 28.64 (CH), 28.19 (Cq), 28.03 (CH_2), 26.87 (CH_3), 26.25 (Cq), 24.89 (CH_2), 24.73 (CH_2), 24.47 (CH_2), 23.46 (CH_3), 23.20 (CH_3), 21.63 (CH_2), 19.89 (CH_3), 19.34 (CH_3), 12.47 (CH_3).

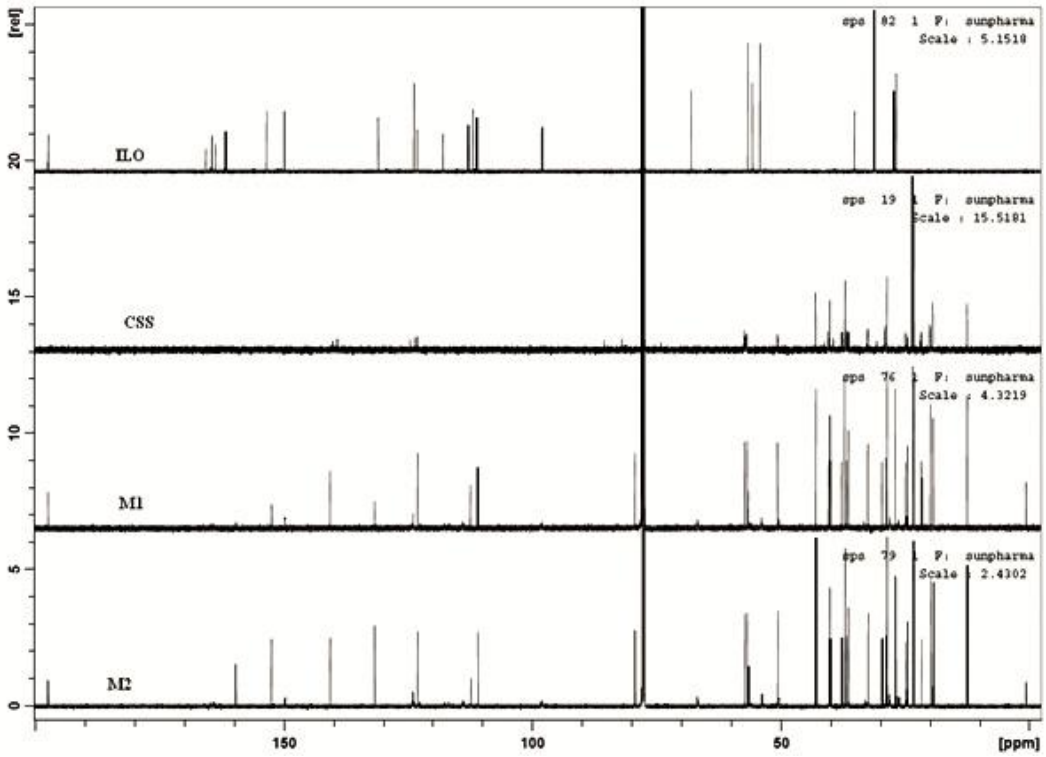

Figure 4.19: Proton decoupled ^{13}C-NMR spectra of (Ilo) Iloperidone, (CSS) Cholesteryl Sulphate Sodium, (M1) Ilo-CSS_c, (M2) Ilo-CSS_a

In ^{13}C-NMR spectrum the piperidine vicinal carbon signals to nitrogen are broadened and shifted to downfield (Fig.4.18). These observations support the fact that both the complexes exist in ionic form of piperidine moiety of Iloperidone and sulphate moiety of cholesteryl sulphate nucleus.

Elemental analysis (CHN)

The result obtained from elemental analysis presented in Table 4.4, show that the results of all the samples comply with the theoretical value with variations due to moisture content along with instrumental and analytical errors within the acceptable limits.

Sr. No.	Name of Compound	Observed value (%)			Theoretical value (%)		
		C	H	N	C	H	N
1.	Iloperidone	67.64	6.69	7.09	67.59	6.38	6.57
2.	CSS	64.14	9.12	-	66.36	9.28	-
3.	M1(Ilo-CSS_c)	68.17	8.03	2.96	67.26	8.58	3.27
4.	M2(Ilo-CSS_a)	67.58	8.26	2.83	67.26	8.58	3.27

Table 4.4: Elemental analysis data of Ilo, CSS and its complex

Powder XRD analysis

X-ray diffraction technique is a powerful tool to identify any changes in crystalinity of drug. The power XRD patterns for (a) Iloperidone, (b) cholesteryl sulphate sodium (CSS), (c) Physical mixture of Iloperidone and cholesteryl sulphate sodium (d) Ilo-CSS_c ,(e) Ilo-CSS_a are presented in Figure 4.20. Iloperidone shows characteristic intense peaks between 2θ angles between 15º and 26º (Fig. 4.20a). Similarly, CSS gives intense peaks between 2θ angles between 6º and 23º (Fig.4.20b), but the complex Ilo-CSS_c (Fig.4.20d) exhibits totally different diffraction pattern having intense peak from 7º to 28º in comparison with Iloperidone, CSS and its physical mixtures (Fig. 4.20c) whereas complex Ilo-CSS_a (Fig. 4.20e) shows no intense peak. On the contrary it shows a broad line from 10º to 30º which indicates that the complex is amorphous in nature.

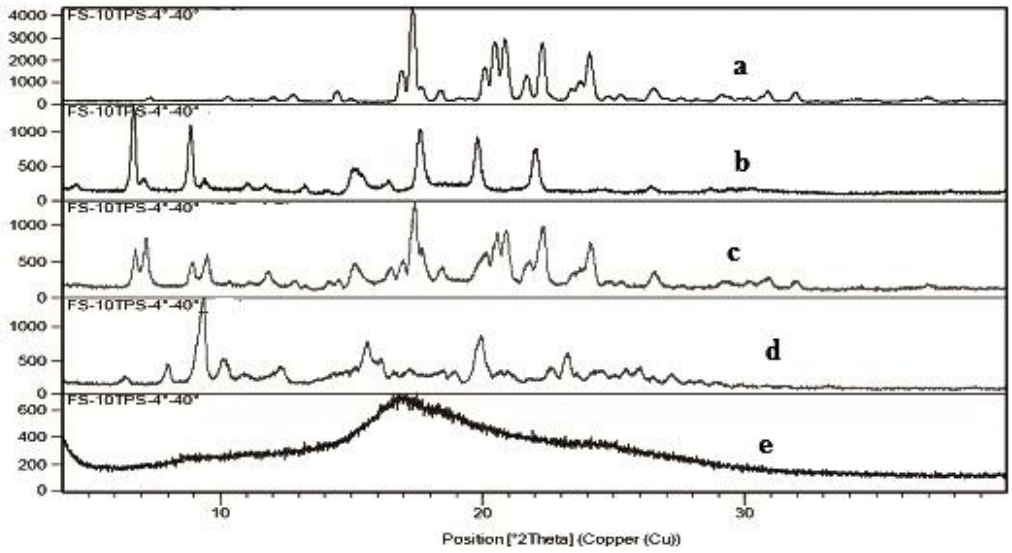

Figure 4.20: XRD powder pattern of (a) Iloperidone, (b) Cholesteryl sulphate sodium, (c) 1:1 Physical mixture, (d) M1(Ilo-CSSc), (e) M2 (Ilo-CSSa)

Further, no intense peaks are observed between 2θ angle from 4º to 30º for all the microspheres which indicates that the drug complex is completely entrapped within the biodegradable PLGA polymer. Hence the XRD patterns of different microsphere formulations F1 to F6 are similar to that of pure PLGA (Fig.4.21 and Fig.4.22).

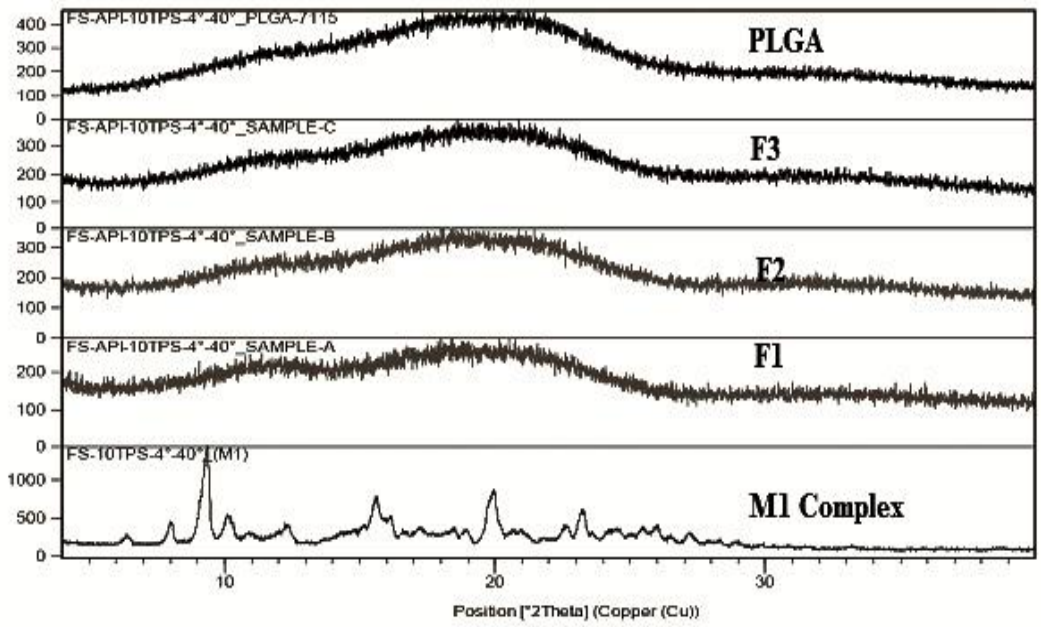

Figure 4.21: XRD powder pattern of (M1) Ilo-CSS_c complex with its microsphere F1, F2 and F3

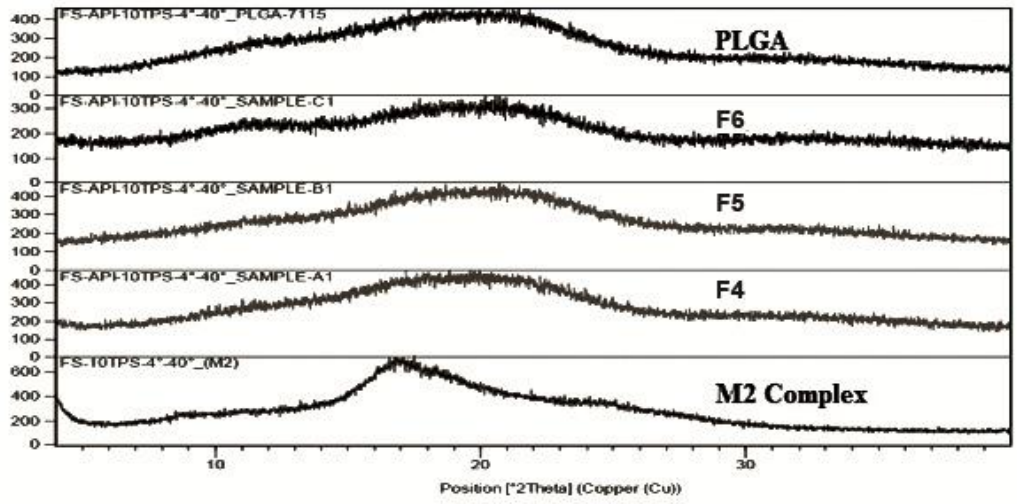

Figure 4.22: XRD powder pattern of (M2) Ilo-CSS_a complex with its microsphere F4, F5 and F6

Morphology of complex and its microspheres by SEM

The morphology of Ilo-CSS complexes both crystalline and amorphous, Ilo-CSS complex loaded PLGA microspheres were studied by SEM (Fig.4.23a and Fig. 4.23b, Fig. 4.23c and Fig. 4.23d).

The morphology of the prepared microspheres was studied by SEM and the micrographs taken at different magnifications are shown in (Fig.4.23c and Fig. 4.23d). SEM studies show that the microspheres are almost spherical with some pores at the surface.

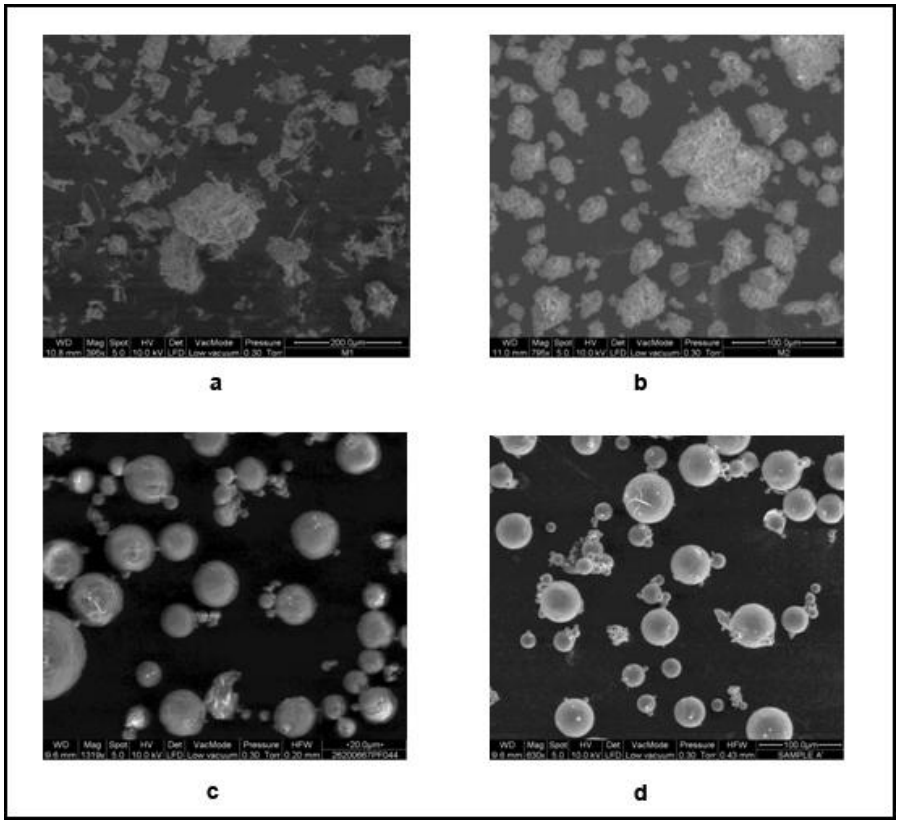

Figure 4.23: SEM images of Iloperidone-CSS complex (a) Ilo-CSS_c, (b) Ilo-CSS_a, (c) $ICSS_c$-PLGA microspheres, (d) $ICSS_a$-PLGA microspheres

Particle size distribution of complex and its microspheres

The particle size distribution of the ILO-CSS complex and its various PLGA loaded microspheres formulations was determined and the resulted histogram was shown in Figure 4.24 and averages of values obtained from two determinations were given in Table 4.7.

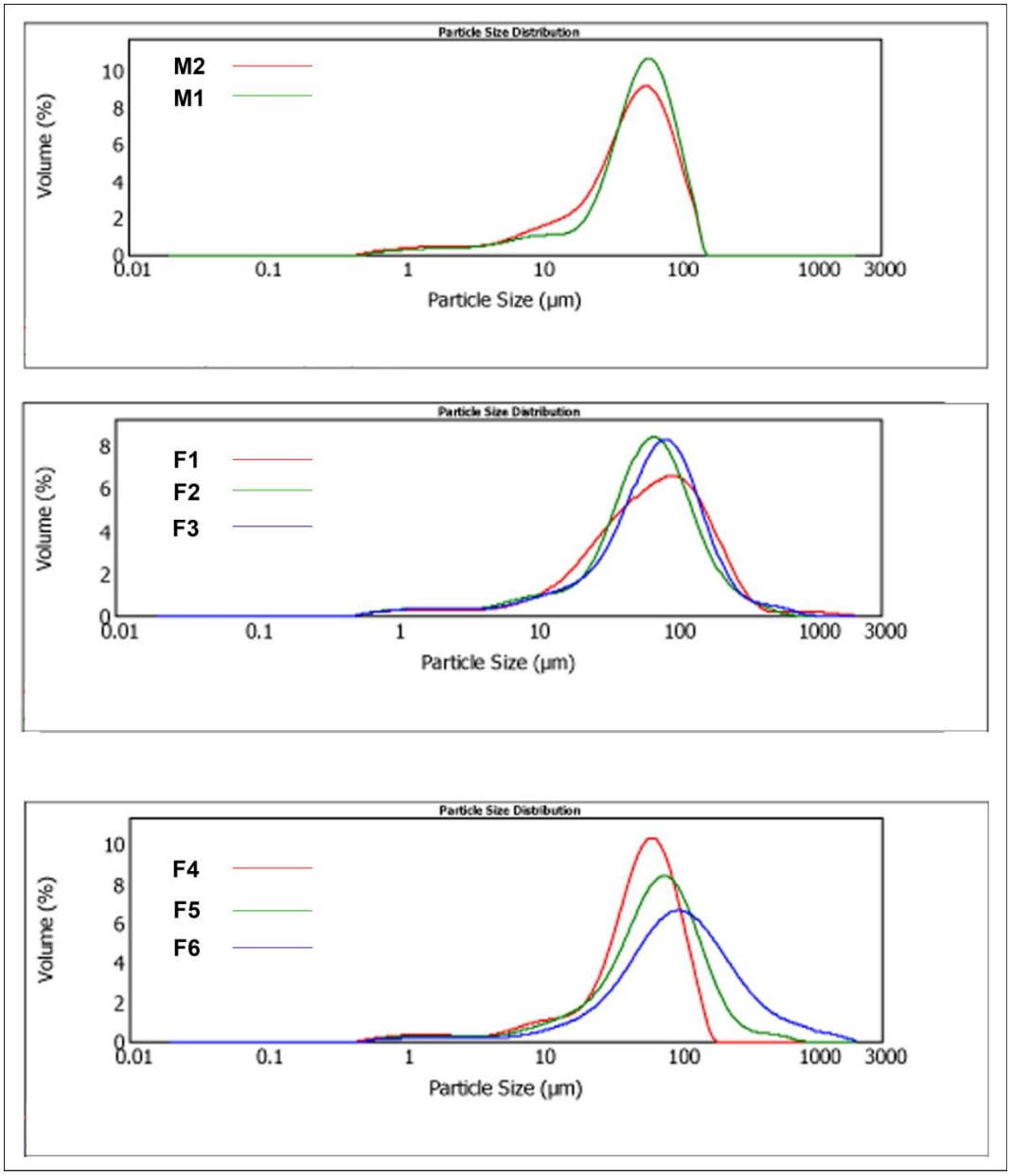

Figure 4.24: Comparative histograms of M1, M2 and its PLGA microspheres

4.6.2: Encapsulation efficiency by UV-Vis spectrometry:

The absorptivity of Iloperidone solution in dichloromethane at its two wavelength maxima at λ_{max} 275 nm and 229 nm, was calculated by using formula absorbance upon concentration in percentage. UV-Vis (Dichloromethane) : λ_{max} (ε) = 275 nm (375), 229 nm (526).

Accurately weighed (between 5 to 6 mg) of microsphere samples were finely ground and the powder so obtained was dissolved in dichloromethane and % assay was determined by using UV-Vis spectrophotometers for Iloperidone at 275 nm. Preliminary studies showed that the polymer and other additives did not interfere with

the drug absorption at 275 nm. The drug concentration was calculated and expressed in percentage of loading efficiency[13] as given below.

Similarly recorded UV-visible spectral pattern and its comparison with Iloperidone, cholesteryl sulphate sodium, Ilo-CSS complex (M1 and M2) are shown in Figure 4.25 and its microsphere F1 and F4 with PLGA (Fig.4.26) indicates that λ_{max} at 275nm, CSS and PLGA does not interfere. The linearity results were obtained from 3 µg / mL to 15 µg / mL and indicating good linearity with regression coefficient 0.9994. Therefore the average percentage of loading efficiency (percentage of drug entrapped) of various PLGA loaded microsphere was determined as presented in Table 4.5 by using the linearity equation y = 0.347 x ± 0.0021.

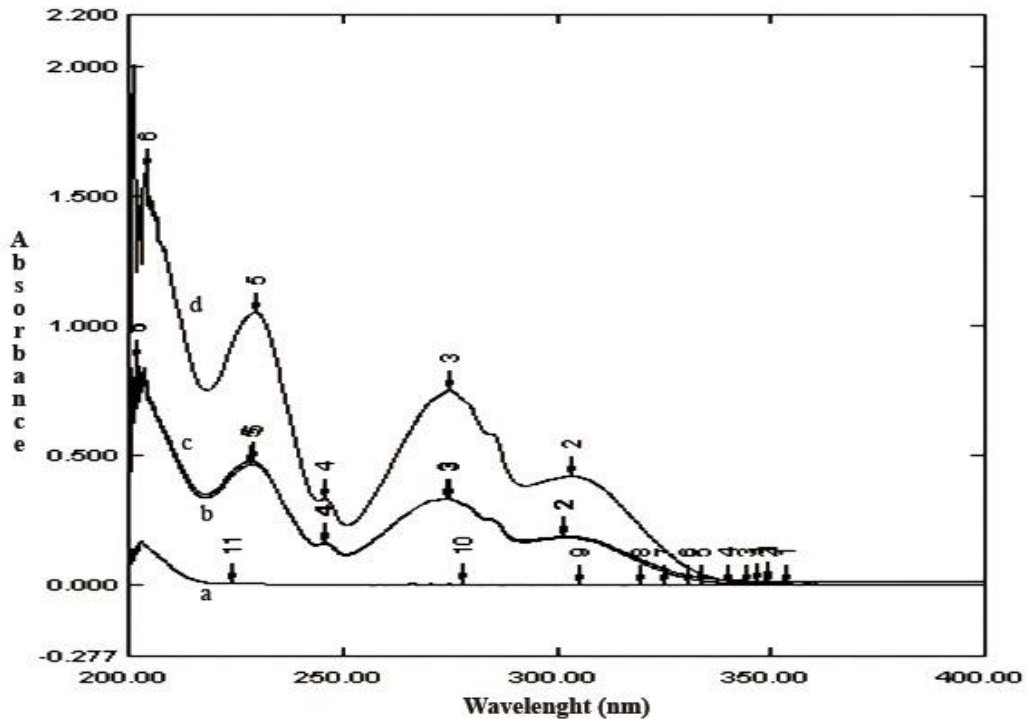

Figure 4.25: UV-Vis spectra of (a) Cholesteryl sulphate sodium (b) Complex Ilo-CSS_a (M2), (c) Complex Ilo-CSS_c (M1) and (d) Iloperidone

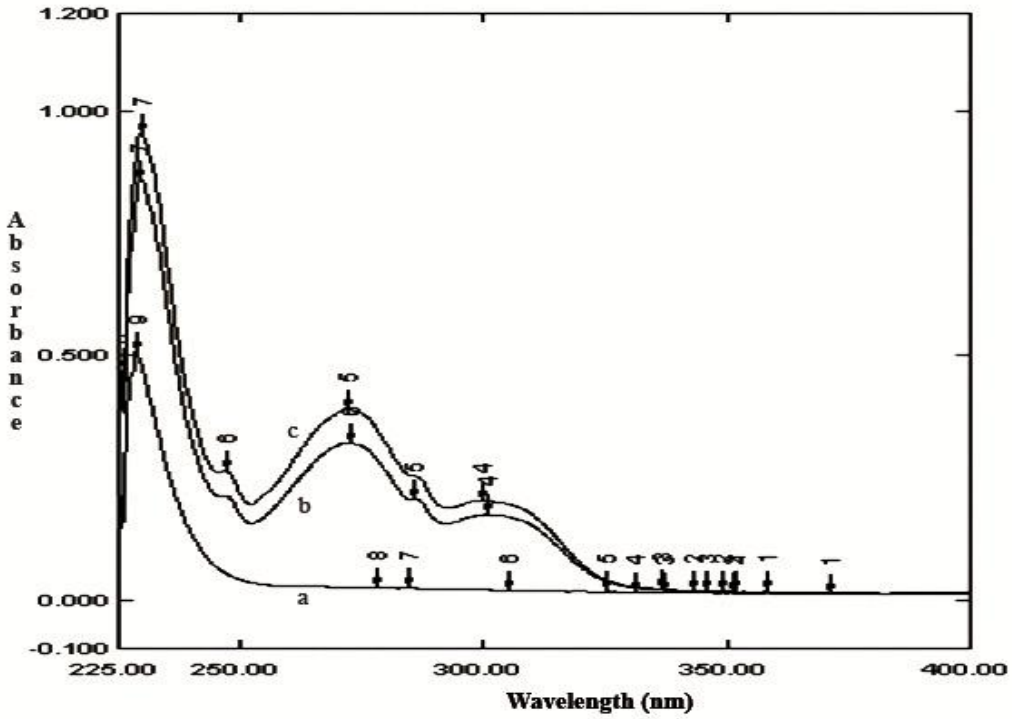

Figure 4.26: UV spectrum overlay of (a) Co-poly lactic glycolic acid (PLGA), (b) PLGA Microsphere with Ilo-CSS_a (F4), (c) PLGA Microsphere with Ilo-CSS_c (F1)

Sr. No.	Stock solution (mL)	Final dilution (mL)	Concentration ((µg/mL)	Absorbance
1	3	100	3	0.109
2	6	100	6	0.233
3	9	100	9	0.339
4	12	100	12	0.450
5	15	100	15	0.561
Slope	0.0374			
Intercept	0.0021			
Regression coefficient	0.9994			

Table 4.5: Linearity data of Iloperidone by UV-Vis spectrometry

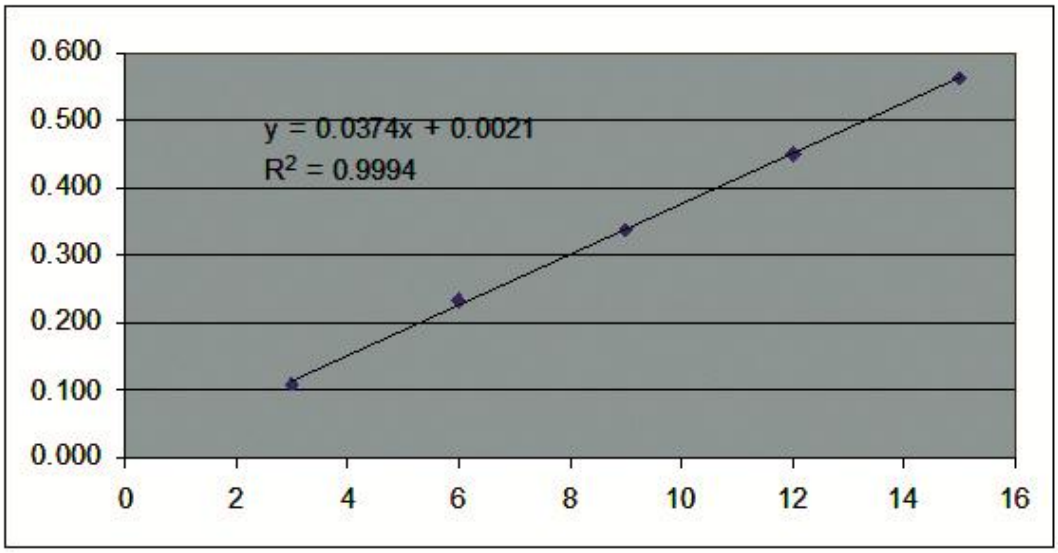

Figure 4.27: Linearity plot of Iloperidone by UV-Vis spectrometry

Sample name	Average absorbance	Average actual concentration (%)	Average observed concentration (%)	Average % of Iloperidone
F1	0.415	1.99	1.84	92.88
F2	0.245	1.35	1.20	88.64
F3	0.195	1.02	1.02	98.91
F4	0.391	1.98	1.91	96.70
F5	0.301	1.34	1.34	99.75
F6	0.224	1.01	1.00	98.51

Table 4.6: Percentage of drug entrapped in various microsphere

Microspheres were prepared as per the composition mentioned in Table 4.2. Formulation with polymer-drug ratio of 30 : 1 (A2) gives maximum yield of porous microspheres having optimum in-vitro release pattern where as formulation A5 with same ratio but amorphous complex gives maximum yield of microspheres with non-porous nature and consequently low release profile compared to A2. Similarly, in the case of formulations prepared by keeping fixed amount of drug and varying amounts of polymer present in Table 4.3, it is observed that both F1 and F4 give maximum yield of spherical porous microspheres and higher drug loading efficiency, with the

former slightly better in both respects. The production yield of microspheres varied from 56-83% and drug loading efficiencies varied from 98.9% to 88.6% as shown in Table 4.7. It is observed that increasing quantity of drug enhanced the encapsulation efficiency. Increasing the polymer PLGA amount also increased the percentage of drug encapsulation but the drug release pattern drastically diminished.

While selecting high polymer drug ratio (30 : 1) factors like particle size, porosity, particle shape, production yield as well as in vitro release are taken into account. Though F4 and F6 show good entrapment but mean particle size is more compared to other formulations and overall weight for these formulations to administer parenteral dose is high which is not feasible.

Formulation code	Production yield (%)	Theoretical drug content (%)	Mean amount of drug entrapped (%)	Mean Particle size (μm ± SD)
F1	83.17	2.04	92.88	199.26±0.41
F2	72.36	1.38	88.64	163.53±1.13
F3	56.66	1.04	98.91	184.07±0.45
F4	76.19	2.03	96.70	106.15±0.35
F5	57.58	1.38	99.75	158.55±4.18
F6	56.08	1.04	98.51	323.07±0.50

Table 4.7: Production yield, drug entrapment and particle size of different formulations of Ilo-CSS microsphere

4.6.3: Accelerated in vitro release profile:

Iloperidone release kinetics from PLGA biodegradable polymers are controlled by either diffusion and erosion or both. Also the cumulative release is dependent upon polymer characteristics such as molecular weight, co-polymer ratio and polymer crystallinity, drug properties as well as dosage form characteristics such as preparation of microsphere, its particle size and morphology, porosity and above all drug loading. Iloperidone release from PLGA microspheres shows a triphasic profile.[68b]

- An initial burst release of surface and pore associated drug
- A lag phase until sufficient polymer erosion takes place
- And a secondary release with approximately zero order kinetics

The initial burst release is controlled by diffusion where as the lag phase and secondary release phase are dependent on polymer erosion as well as diffusion. Accelerated *in vitro* % of cumulative drug release (% CDR) data of Iloperidone microspheres were presented in Table 4.8 and Table 4.9. The observed data shown that both Ilo-CSS_c and Ilo-CSS_a complex exhibits fast release as compared to its Ilo-CSS PLGA microspheres. Microspheres prepared by using crystalline complex of Ilo-CSS_c shows better and desired release pattern when compared to that of amorphous complex of Ilo-CSS_a. Also from Figure 4.28 and Figure 4.29, it is evident that increasing amount of polymer significantly retards the release of Iloperidone from Iloperidone-CSS microsphere. A2 formulation was prepared using Ilo-CSS_c crystalline complex (M1) where as A5 was prepared using Ilo-CSS_a amorphous complex (M2). In A5 initial burst is more compared to A2 since the texture of microsphere is smooth and spherical in case of A2 compared to A5 where the microsphere surfaces were uneven and more drugs was entrapped on surface.[124]

Release kinetics

The *in vitro* release data of optimized microsphere formulations prepared with Ilo-CSS complex and PLGA biodegradable polymer were treated with different kinetic models[120] such as Zero order, First order, Higuchi, Hixson-Crowell and Ritger-peppas to explain the release kinetics of Iloperidone from Ilo-CSS PLGA microspheres. Among all release kinetics, Zero order release kinetics was considered as the best fitting model with the highest value of co-relation coefficient. The value of correlation coefficient (r^2) for optimized formulation was found to be 0.959.

Sr. No.	Time interval (h)	% Cumulative Drug Release			
		M1 (Ilo-CSS_c)	F1	F2	F3
1	0	13.44	7.00	6.93	4.79
2	0.5	55.99	4.78	4.46	3.63
3	1	55.11	6.67	4.35	2.27
4	4	89.74	8.30	5.89	2.97
5	12	96.01	26.56	17.27	4.61
6	18	97.24	30.54	26.28	5.43
7	24	99.62	32.36	29.36	6.48
8	36	102.65	76.88	57.54	8.17

Table 4.8: % CDR of M1 (Ilo-CSS_c) with its different microspheres (F1, F2 and F3)

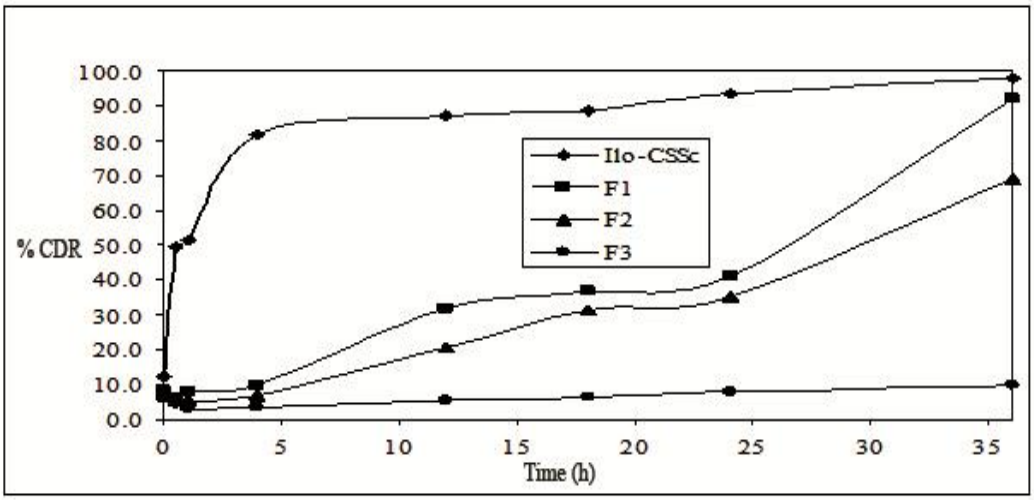

Figure 4.28: % CDR of Ilo-CSS_c along with PLGA microspheres (F1, F2 and F3)

Sr. No.	Time interval (h)	% Cumulative Drug Release			
		M2 (Ilo-CSS_a)	F4	F5	F6
1	0	9.33	10.02	7.79	4.05
2	0.5	14.71	3.89	2.48	2.89
3	1	15.05	4.50	3.69	2.62
4	4	30.56	8.02	7.14	5.54
5	12	69.21	25.49	32.73	13.39
6	18	81.36	29.41	45.85	16.66
7	24	83.17	31.17	45.98	47.81
8	36	99.63	74.79	74.23	42.37

Table 4.9: % CDR of M2 (Ilo-CSS_a) with its different microspheres (F4, F5 and F6)

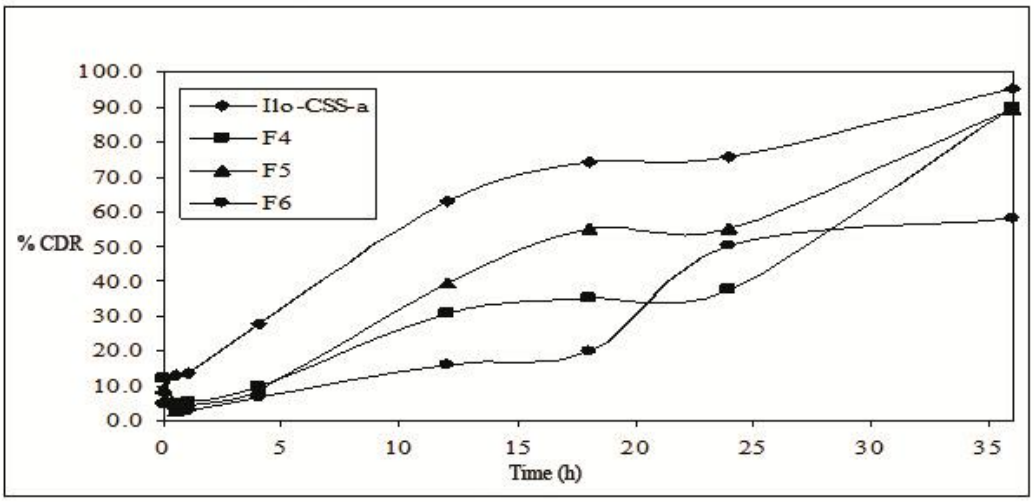

Figure 4.29: % CDR of Ilo-CSS_a along with PLGA microspheres (F4, F5 and F6)

Conclusion

The molecular modeling energy minimization data shows that Iloperidone-Cholesteryl sulphate co-crystal exists as an ion pair complex with slight distortion in piperidine ring of Iloperidone moiety. The spectroscopic characterization, thermo-analytical and quantification data indicates that Ilo-CSS complex has 1 : 1 stoichiometry and is highly hydrophobic in nature with respect to Iloperidone.

The optimization studies of preparation of microspheres using Ilo-CSS as a model hydrophobic drug complex reveals that the preparation conditions used in this method result in higher encapsulation efficiency which is likely to be due to the processing of microspheres in hydrophilic conditions that result in the rapid precipitation of polymer into microspheres. Iloperidone-CSS gets physically and molecularly dispersed in the PLGA forming almost a homogenous phase, resulting in spherical shape and some pores on the surface.

Characterization of the microsphere formulation by XRD pattern shows no evidence of Ilo-CSS complex, as it gets dispersed completely at molecular level in the polymer matrix. This is supported by DSC studies where a reduction in the glass transition temperature of the PLGA is observed. Most importantly the encapsulation of Ilo-CSS complex in PLGA using the optimized solvent evaporation method results in the sustained release of the drug upto more than 36 h. The *in vitro* percentage of cumulative drug release data suggests that the initial release of the drug complex is due to diffusion of the drug complex trapped near the surface followed by diffusion from the core through the pores in the matrix generated by swelling of polymer over the first 15 to 18 h. Further increase in the release of the drug is dependent on the degradation of PLGA matrix. Together these results indicate that the present optimized single emulsion solvent evaporation method is an effective way of encapsulating highly hydrophobic complex of an otherwise less hydrophobic small molecule drug, within PLGA microspheres for both therapeutic and tissue engineering applications in which continuous release over long periods of time is desirable.

References

1. Wolf, K. L.; Dunken, H.; Merkel, K. Z. *Phys. Chem. Abt.* **1940**, *46*, 287.
2. Lehn J. M. *Science*, **1993**, *260*, 1762.
3. Mascal, M. *Contemporary Organic Synthesis*, **1994**, *1*, 31.
4. Connors, K. Int. *Remington's Pharmaceutical Sciences*, **1990**, 18th ed. 189 Mack Publishing, USA.
5. Whitesides, G. M.; Mathias, J. P.; Seto, C. T. *Science*, **1991**, *254*, 1312.
6. Bayley, H. *J. Cell. Biochem.* **1994**, *56*, 177.
7. Rideout, D. *Cancer Invest*. **1994**, *12*, 189.
8. Dill, K. A. *Science*, **1990**, *250*, 297.
9. Baldwin, R. *Proc. Natl. Acad. Sci. U.S.A.* **1986**, *83*, 8069.
10. Soreghan, B.; Kosmoski, J.; Glabe, C. *J. Biochem.* **1994** ,*269*, 28551.
11. Wohler, F. *Justus Liebigs Ann. Chem.* **1844**, *51*, 153.
12. Anderson, J. S. *Nature*, **1937**, *140*, 583.
13. Hoogsteen, K. *Acta. Crystallogr*. **1963**, *16*, 907.
14. (a) Thayer, A. M. C & E. N. **2007**, *1*, 7. (b) French patent: von Heyden, F. *et al*, **1934**, *769*, 586. (c) Nair, R. H.; Sarah, J. N.; Adivaraha, J. *Encyclopedia of Pharmaceutical Technology*, vol.*1*, **2007**, 3rd ed. p. 615, Informa Healthcare, New York.
15. Eli lilly patent: Amos, J. G.; Indelicato, J. M.; Pasini C. E.; Reutzel, S. M. BicvcUc beta lactam/paraben complexes, **1995**, US 5412094 (Al), JP 7048383 (A), F1943081 (A), BR9402561 (A) and EP 0637587 (Bl)
16. (a) Puschner, B.; Poppenga, R. H.; Lowenstine, L. J.; Filigenzi M. S.; Pesavento, P. A. *J. Vet. Diagn. Invest.* **2007**, *19*, 616. (b) Andrew, V. *Mol. Pharm.* **2007**, *4*, 301.
17. Callcar S. K. University of Southampton, School of Chemistry, PhD Thesis, **2008**, 253pp. http://eprints.soton.ac. uk/51224.
18. Wengcr, M.; Bernstein, J. *Cryst. Growth Des.* **2008**, *8*, 1595.
19. Basavoju, S.; Bostrom, D.; Velaga, S. P. *Pharm*. *Res.* **2008**, *25*, 530.
20. Lu, J.; Rohani, S. *Org. Process Res. Dev.* **2009**, *13*, 1269.
21. Alleso, M.; Velaga, S.; Alhalaweh, A.; Cornett, C.; Rasmussen, M. A.; van den Berg, F.; de Diego, H. L.; Rantanen, J. *Anal*. *Chem*. **2008**, *80*, 7755.

22. Hickey, M. B.; Peterson, M. L.; Scoppettuolo, L. A.; Morrisette, S. L.; Vetter, A.; Guzman, H.; Remenar, J. F.; Zhang, Z.; Tawa, M. D.; Haley, S.; Zaworotko, M. J.; Almarsson, O. *Eur. J. Pharm. Biopharm.* **2007**, *67*, 112.
23. Remenar, J. F.; Morissette, S. L.; Peterson, M. L.; Moulton, B.; MacPhee, J. M.; Guzman, H. R.; Almarsson, O. *J. Amer. Chem. Soc.* **2003**, *125*, 8456.
24. Schultheiss, N.; Newman, A. *Cryst. Growth Des.* **2009**, *6*, 2950.
25. (a) Noyes, A. A.; Whitney, W. R. *J. Amer. Chem. Soc.* **1897**, *19*, 930. (b) Chi-Yuan, W.; Leslie, Z. *Benet Pharmaceutical Research*, **2005**, *22*, 1.
26. (a) Kastellic, J.; Hodnik, Z.; Sket, P.; Plavec, J.; Lah, N.; Leban, I.; Pajk, M.; Planinsek, O.; Kikelj. D. *Cryst. Growth Des.* **2010**, *10*, 4943. (b) Shevchenko, A.; Bimbo, L. M.; Miroshnyk, I.; Haarala. J.; Jelinkova, K.; van Veen, B.; Kiesvaars, J.; Santos, H. A.; Yliruusi. *Int. J. Pharm.* **2012**, *436*, 403.
27. (a) Childs, S. L.; Chyall, L. J.; Dunlap, J. T.; Smolenskaya, V. N.; Stahly, B. C.; Stahly, G. P. *J. Chem. Soc*, **2004**, *126*,13335. (b) Musenga, A.; Augusta, M.; Albers, J. L. *Expert Opin. Invest. Drugs*, **2008**, *17*, 61.
28. Orive, G.; Gascon, A. R.; Hernandez, R. M.; Dominguez Gil.; Pedraz, J. L. *Trends Pharmacol. Sci*. **2004**, *25*, 382.
29. Willis, R. C. *Mod. Drug Discovery*, **2004**, *31*, 30.
30. (a) Veronese, F. M.; Caliceti, P. *"Drug Delivery Systems"*, **2002**, p.600, Integrated Biomaterials Science, (Edn.) Barbucci R. Kluwer Academic, Plenum Publishers, New York. (b) Juergen, S.; Ronald, A.; Siegel; Michael, J.; Rathbone. *Fundamentals and Applications of Controlled Release Drug Delivery*, **2012**, 13th ed. p.156, CRS, NY.
31. Williams, D. F.; Mort, E. *Bioeng*. **1977**, *1*, 231.
32. Herman, J. B.; Kelly, R. J.; Higgnis, G. A. *Arch. Surg.* **1970**, 100.
33. Maulding, H. V.; Tice, T. R.; Cowsar, D. R.; Fong, J. W.; Pearson, J. E.; Nazareno, J. R. *J. Controlled Release*, **1986**, *3*, 103.
34. Brich, Z.; Nummerfall, F.; Kissel, T.; Bantle, S. *Proc. Int. Symp. Controlled Release Bioact. Mater.* **1988**, *15*, 95.
35. (a) Tandon, R.; Keshavan, S. M.; Nasrallah, A. H. *Scizophrenia Research*, **2008**, *102*, 1.(b) Tandon, R.; Keshavan, S. M.; Nasrallah, A. H. *Scizophrenia Research*, **2009**, *110*, 1.
36. *An Injectable Sustained Release Pharmaceutical Composition*: WO, 2010/119455 A2; October 21, **2010.**

37. (a) Zhornitsky, S.; Stip, E. *Scizophrenia Research and Treatment*, **2011**, *2012*, 1 (b) Helena, S.; Azevedo, Rui, L.; Reis. *Biodegradable Systems in Tissue Engineering and Regenerative Medicines*, **2004**, p. 177, *CRS Press*.
38. Kim, Y.; Oksanen, D. A.; Lassefski, W. Jr.; Blake, J. F.; Duffy, E. M.; Chrunyk, B. *J. Pharm. Sci.* **1998** , *87*, 1560.
39. (a) Citrome, L.; *Int. J. Clinical Pract*. **2010**, *64*, 61. (b) Citrome, L.; Meng, X.; Hochfeld, M. *Scizophrenia Research*, **2011**, *131*, 75.
40. Crabtree, B. L.; Montgomery, J. *Clin. Ther.* **2011**, *33*, 330.
41. Davis, S. S.; Illum, L.; McVie, J. G.; *Tomlinson, E. Microspheres and drug Therapy: Pharmaceutical, Immunological and Medical Aspects*, **1984,** Elsevier, Amsterdam.
42. Guiot, P.; Couvreur, P. *Polymeric Nanoparticles and Microspheres*, **1986**, 1st ed. CRC Press, Boca Raton.
43. Yapel, A. P. *US patent* 4,147,767, April 3, **1979**.
44. Burgess, D. J.; Carless, J. E. *Int. J. Pharm.* **1986**, *32*, 207.
45. Redmon, M. P.; Hickey, A. J.; DeLuca, P. P. *J. Controlled Release*, **1989**, *9*, 99.
46. Lzumikawa, S.; Yoshioka, S.; Aso, Y.; Takeda, J. *J. Controlled Release*, **1991**, *15*, 133.
47. Khalil, S. A. H.; Nixon, J. R.; Carless, J. E. *J. Pharm. Pharmacol.* **1968**, *20*, 215.
48. Luzzi, L. A.; Gerraughty, R. J. *J. Pharm. Sci.* **1964**, *53*, 429.
49. Phares, R. E.; Sperandio, G. J. *J. Pharm. Sci.* **1964**, *53*, 515.
50. Zhou, S.; Hickey, A. J.; Jay, M.; Warren, S. M.; Lord, M.; Deluca, P. P. *Pharm. Res.* **1988**, *5*, S76.
51. Nixon, J. R. *Microencapsulating*, Marcel Dekker, New York, **1976**.
52. Gutcho, M. H. *Microencapsulation's and Other Capsules, Advanced Science***,** **1979**, Noyes Data Corp, Park Ridge, NJ.
53. Lim, F. *Biomedical Applications of Microencapsulation*, **1984**, CRC Press Inc., Boca Raton, FL.
54. Kondo, T. *Microencapsulation; New techniques and Applications*, **1979**, Techno Books, Tokyo.
55. Donbrow, M. *Microcapsules and Nanoparticels in Medicine and Pharmacy*, **1991**, p.1-14, CRC Press, London.
56. Kissel, T.; Demirdere, A. *Controlled Drug Deliverey*, (Ed.) Muller, B.W. **1984**, 103, Wissen – Schaftliche Verlagsge-Sellschaft, Stutgart.

57. Gurney, R.; Peppas, N. A.; Harrington, D. D.; Banks, G. S. *Drug Dev. Ind. Pharm.* **1981**, *7*, 1.
58. Gupta, P. K.; Hickey, A. J. *J. Controlled Release,* **1991**, *17*, 129.
59. Masinde, L. E.; Hickey, A. *J. Pharm. Res.* **1991**, *8*, S120.
60. Masinde, L. E.; Hickey, A. J. *Int. J. Pharm.* **1993,***100*,123.
61. Gupta, P. K.; Hickey, A. J.; Mehta, R.; Deluca, P. P. *Pharm. Res.* **1990**, *7*, S82.
62. Versic, R. J. *Drug. Cosm. Ind.* **1989**, *144*, 30, 32, 34, 75.
63. Maggi, G. C.; Di Roberto, F. M. *Microencapsulation,* (Ed.) Nixon, J. R. **1976,** 103-111, Marcel Dekker, New York.
64. Jarvis, A. P.; Spriggs, T. A.; Chingura, W. R. *In Vitro,* **1982**, *18*, 276.
65. Lim, F.; Buchler, R. J. *Methods in Enzymology,* (Ed.) Langome, J. J.; Van-Vunakis, H. **1981,** 73, Academic Press, New York.
66. Lim, F. *Adv. Biotechnol. Progr.***1988**, *7*, 185.
67. Chang, T. M. S. *Biomedical Applications of Microencapsulations*, Lim, F.; (Ed.) **1984**, 85, CRC Press, Boca Raton, FL.
68. (a) Waalford, J.; Lim, T. J. *Aquaculture,* **1991**, *92*, 225. (b) Dunne, M.; Corrigan, O. L.; Ramtoola, Z. *Biomaterials*, **2000**, *21*, 1659.
69. Goldberg, E. P.; Longo, W. E.; Iwata, H. *U. S. Patent*, 4,671,954, **1987**.
70. O'Donnell, P. B.; Mcginity, J. W. *Adv. Drug Delivery Rev.* **1997**, *28*, 25.
71. Si-Feng. *Expt. Rev. Med. Dev.* **2004**, *1*, 115.
72. Kim, D. H.; Martin, D. C. *Biomaterials,* **2006**, *27*, 3031.
73. Jalil, R.; Nixon, J. R. *J. Microencapsulation*, **1990**, *7*, 25.
74. Wu, X. S. in *Encyclopedia handbook of Biomaterials and Bioengineering*, (Ed.) Wise, D.; Trantolo, D. J.; Altobelli, D. E.; Yaszemski, M. J.; Gressers, J. D.; Schwartz, E. R. **1995**, p.1151, Marcel Dekker, New York.
75. Arshady, R. *J. Controlled Release*, **1991**, *17*, 1.
76. Panyam, J.; Williams, D.; Dash, A.; Leslie-Pelecky, D.; Labhasetwar, V. *J. Pharm. Sci.* **2004**, *93*, 1804.
77. Park, J. H.; Ye, M.; Park, K. *Molecules,* **2005**, *10*, 146.
78. Yeo, Y.; Chen, A. U.; Basaran, O. A.; Park, K. *J. Pharm. Res.* **2004**, *21*, 1419.
79. Fessi, H.; Puisieux, F.; Devissaguet, J. P.; Ammoury, N.; Benita, S. *Int. J. Pharm.* **1989**, *55*, 1.
80. Bilati, U.; Allemann, E.; Doelker, E. *Eur. J. Pharma. Biopharm.* **2005**, *59*, 375.
81. Fonseca, C.; Simoes, S.; Gaspar, R. *J. Controlled Release,* **2002**, *83*, 273.

82. Cowdall, J.; Davies, J.; Roberts, M.; Carlsson, A.; Solaro, R.; Mazzanti, G.; Chiellini, E. E.; Chiellini, F.; Soderlind, E. *WO Patent*, **1999**, 002131.
83. Park, T. G.; Lu, W.; Crotts, G. *J. Controlled Release*, **1995**, *33*, 211.
84. Federica, C.; Bartoli, C.; Dinucci, D.; Piras, A. M.; Anderson, R.; Croucher, T. *Int. J. Pharm.* **2007**, *343*, 90.
85. Jeong, Y. I.; Cho, C. S.; Kim, S. H.; Ko, K. S.; Kim, S. I.; Shim, Y. H.; Nah, J. W. *J. Appl. Polym. Sci.* **2001**, *80*, 2228.
86. Zhang, Z ; Feng, S. S. *Biomacromolecules*, **2006**, *7*, 1139.
87. Gupta, K.; Ganguli, M.; Pasha, S.; Maiti, S. *Biophys. Chem.* **2006**, *119*, 303.
88. Liu, X. M.; Yang, Y. Y.; Leong, K.W. *J. Colloid Interface Sci.* **2003**, *266*, 295.
89. Hsiue, G. H.; Wang, C. H.; Lo, C. L.; Wang, C. H.; Li, J. P.; Yang, J. L. *Int. J. Pharm.* **2006**, *317*, 69.
90. De Wolf, H. K. ; Luten, J.; Snel, C. J.; Oussoren, C.; Hennink, W. E.; Storm, G. *J. Controlled Release,* **2005**, *109*, 275.
91. Shekunov, Y.; Chattopadhyay, P.; Seitzinger , J.; Huff, R. *Pharm. Res.* **2006**, *23*, 196.
92. Leuenberger, H. *J. Nanopart. Res.* **2002**, *4*, 111.
93. Jelvehgari, M.; Siahi-Shadbad, M. R.; Azarmi, S.; Gary, P.; Nokhodchi, M. A. *Int. J. Pharm.* **2006**, *308*, 124.
94. Mu, L.; Teo, M. M.; Ning, H. Z.; Tan, C. S.; Feng, S. S. *J. Controlled Release,* **2005**, *103*, 55.
95. Takada, S.; Uda, Y.; Toguchi, H.; Ogawa, Y. *J. Pharm. Sci. Technol.* **1995**, *49*, 180.
96. Elversson, J.; Fureby, M. *Int. J. Pharm.* **2005**, *294*, 73.
97. De Rosa, G.; Larobina, D.; La Rotonda, M.; Musto, P.; Quaglia, F.; Ungaro, F. *J Controlled Release,* **2005**, *102*, 71.
98. Johnson, O. L.; Cleland, J. L.; Lee, H. J.; Charnis, M.; Duenas, E.; Jaworowicz, W. *Nat. Med.* **1996**, *2*, 795.
99. Attwood, D. In Colloidal Drug Delivery Systems; Microemulsions, (Ed.) Kreuter, J. **1994**, 31, Marcel Dekker, New York.
100. Eccleston, J. *In Encyclopedia of Pharmaceutical Technology, Micro-emulsions*. (Ed.) Swarbrick, J.; Boylan, J. C. **1994**, *9*, 375, Marcel Dekker, New York.
101. Lawrence, M. J. *Eur. J. Drug Metab. Pharmacokinet.* **1994**, *3*, 257.

102. Perets, A.; baruch, Y.; Weisbuch, F.; Shoshany, G.; Neufeld, G.; Cohen, S. *J. Biomed. Mater. Res.* **2003**, *65A*, 489.

103. Royce, S. M.; Askari M.; Marra, K. G. *J. Biomater. Sci., Polym. Ed.* **2004**, *15*, 1327.

104. Clenland, L.; Mac, A.; Boyd, B.; Yang, J.; Duenas, E. T.; Yeung, D.; Brooks, D.; Hsu, C.; Mukku, V.; Jones, A. J. *Pharm. Res.***1997**, *14*, 420.

105. Carrascoa, C.; Torre-Aleman, I.; Lopez-Lopez, C.; Carro, E.; Espejo, S.; Torrado, J. J. *Biomaterials*, **2004**, *25*, 707.

106. Carrasco, C.; Espejo, L.; Torrado, S.; Torrado, J. J. *J. Biomater. Appl.* **2003**, *18*, 95.

107. Piotrowicz, A.; Shoichet, M. S. *Biomaterials*, **2006**, *27*, 2018.

108. Schrier, J. A.; Deluca, P. P. *Pharm. Dev. Technol.* **1999**, *4*, 611.

109. Ruhe, P. Q.; Boremon, O. C.; Russel, F. G. M.; Spauwen, P. H. M.; Mikos, A. G.; Jansen J. A. *J. Controlled Release*, **2005**, *106*, 162.

110. Andrieu-Soler, C.; Aubert-Pouselle, A.; Doat, M.; Picaud, S.; Halhal, M.; Simonutti, M.; Venier-Julliene, M. C.; Benoit, J. P.; Behar-Cohen, F. *Mol.Vis.* **2005,** *11*, 1002.

111. Aubert-Pouselle, A.; Venier-Julliene, M. C.; Clavreul, A.; Sergent, M.; Jollivet, C.; Montero-Menej, C.N.; Garcion, E.; Bibby, D.C.; Menei, P.; Benoit, J.P. *J. Controlled Release*, **2004**, *95*, 463.

112. Elisseeff, J.; McIntosh, W.; Fu., K.; Blunk, T.; Langer, R. *J. Ortho Res.* **2001**, *19*, 1098.

113. De-Fail, A. J.; Chu, C. R.; Izzo, N.; Marra, K. G. *Biomaterials*, **2006**, *27*, 1579.

114. Moioli, E. K.; Hong, L.; Guardado, J.; Clark, P. A.; Mao, J. J. *Tissue Eng.* **2006**, *12*, 537.

115. King, T. W.; Patrick, C. W. *J. Biomed. Mater. Res.* **2000**, *51*, 383.

116. Faranesh, A. Z.; Nastley, M. T.; Perez de la Cruz, C.; Haller, M. F.; Laquerriere, P.; Leong, K. W.; McVeigh, E. R. *Magn. Reson. Med.* **2004**, *51*, 1265.

117. Freiberg, S.; Zhu, X. X. *Int. J. Pharm.* **2004,** *282*, 1.

118. Lobenberg, R. G.; Amidon, L. *Eur. J. Pharm. Biopharm.* **2000**, *50*, 3.

119. Korsmeyer, R.W.; Gurny, R.; Doelker, E.; Buri, P.; Peppas, N.A. *Int. J. Pharm.* **1983,** *15*, 25.

120. Mohd, Y.; Bajpai, M.; Bhattacharyya, A. *J. Pharam. Res.* **2010**, *3*, 2265.

121. Cleland, J. L.; Duenas, E.; Daugherty, A.; Marian, M.; Yang, J.; Wilson, M.; Celniker, A. C.; Shahazamni, A.; Quarmby, V.; Chu, H.; Mukku, V.; Mac, A.; Ronssakis, M.; Gilette, N.; Boyd, B.; Yeung, D.; Brroks, D.; Maa, Y-F.; Hsu, C.; Jones, A. J. S. *J. Controlled Release*, **1997**, *49*, 193.
122. Besseghir, K.; Zerbe, O.; Andris, D.; Orsolini, P.; Heimgastner, F.; Merkle, H. P.; Gander, B. *J. Controlled Release*, **2000**, *67*, 19.
123. Chattaraj, S. C.; Rathinavelu, A.; Das, S. K. *J. Controlled Release*, **1999**, *58*, 223.
124. Allison, S. D. *Epert. Opin. Drug. Deliv*. **2008**, *5*, 615.

Chapter 5

Drug Polymorphism Quantification

Introduction:

In the middle of 18th century, Brittain had observed that many substances could exist in more than one crystalline forms which are known as polymorphs.[1] Bernstein *et al,* Grant *et al* and Vippagunta *et al* defined polymorphism in crystalline solids as materials having the same chemical composition but different lattice structures and/or different molecular composition.[2-4] Aguiar *et al* studied extensively polymorphism in drug molecules and its effect on dissolution and bioavailability of molecules like chloramphenicol palmitate.[5] Byrn *et al* and Nangia *et al* illustrated pseudo polymorphism in crystalline forms wherein solvent molecules form an integral part of the crystal structure.[6,7] In solvatomorphism, various pharmaceutical crystals are obtained due to the incorporation of solvent molecules in the crystal structure which are known as solvates, whereas if water is the solvent in the crystal lattice, they are called hydrates.[8] Polymorphs exhibit different solubility and dissolution rates and these differences also show existence of non-equivalence of bio-availabilities.[9]

Pharmaceutical solids are known to exhibit polymorphism. The different crystal forms are likely to show difference in solubility, intrinsic dissolution, melting point, biological and pharmaceutical properties which will have a direct bearing on their behavior when used. There are a wide variety of solid state analytical techniques available to characterize pharmaceutical solids and solid state transformations.

As per ICH guidelines,[10] polymorphs may exhibit a significant difference in dissolution, bioavailability and stability of the product and therefore, polymorphism is a crucial phenomenon in the manufacturing process. This makes Polymorphism a key factor for product patent and regulatory process like "New Drug Application" (NDA) and "Abbreviated New Drug Application" (ANDA) particularly in solid and related dosage forms, Byrn *et al* and Yu *et al* studied these aspects extensively.[11,12a]

Yu *et al,* Rodriguez-Spong *et al,* Pudipeddi *et al* and Hancock *et al* reported that amorphous solids show higher dissolution rate with higher bioavailability during

drug development process.[12b,13-15] Higher solubility of these solids is due to the higher energy and molecular mobility which renders amorphous solids physically unstable.

Formation of co-crystals may tend to overcome poor aqueous solubility of crystalline solids without affecting stability. Miroshynk and coworkers defined co-crystal as a multiple component crystal in which all components are solids under ambient conditions when in their pure form.[16]

Stahly and coworkers observed that 80 % to 90 % of organic compounds exist in polymorphic forms.[17] The toxic effect of some polymorphs in different dosage form of the drug product was studied and confirmed by Heinz *et al*, Knapman *et al*, Byrn *et al* and the same was further confirmed by various "Food and Drug and Administration" (FDA) agencies.[18-20] Buckton and coworkers reported that proper monitoring of solid-state forms both qualitatively and quantitatively ensure better, effective and high-quality products.[21]

Due to improvement of technologies and advancement of software, various analytical techniques become convenient for the qualitative and quantitative solid-state analysis of Active Pharmaceutical Ingredients (APIs) in its drug product.

5.1: Types of Polymorphisms:

Single component system

APIs that are amorphous solids exhibit better drug delivery compared to their crystalline forms leading to their improved bioavailability. Amorphous solids lack the three dimensional long range molecular order that characterizes crystalline solids but they exhibit short range order,[22,23,24] which in turn reflects their faster dissolution rates and kinetics or metastable solubility.[25]

Multi-component system

Multi-component systems are the systems of molecular assemblies composed of an API of amorphous or crystalline molecular dispersion with a complementary molecule. The complementary molecule that is chosen may be neutral or charged, which may be that of solvent, excipients and other substances. These systems are assembled from specific non-covalent interactions between molecules which may include hydrogen bonds, ionic, van der Waals and π - π interactions.[26-28]

Monotropy:

A polymorphic drug substance is said to be monotropic if only one form is stable at all temperatures below its melting point, while all other polymorphs, if any are unstable. Such a system of two or more solid phases is said to be monotropic.

Enantiotropy:

The two polymorphs of a drug are said to enantiotropes, if they exhibit lower free energy content and solubility over two different temperature range and pressure, the phenomenon of two such solid phases is said to exhibit enantiotropism.

5.1.1: Chemical stability of polymorphs and amorphous forms:

The thermodynamically more stable polymorph is expected to be more chemically stable than a metastable polymorph and contributes to higher crystal packing density as reported by Waterman *et al,* Hovorka *et al* and Yoshioka.[29-32] Selection of excipients and optimization of processes which minimize the chemical instability of drug is an important part for formulation development.

5.1.2: Solvates and hydrates:

Metastable solvates and hydrates of drug polymorphs affect the dissolution rate and solubility. Suleiman reported that pentanol and toluene solvates of Glibenclamide exhibit higher solubility and dissolution rate compared to its two non-solvated polymorphs.[32] Toxicity of the solvent, and its interactions with drug and excipients on storage should be investigated during formulation process of the solvates. Singhal *et al* studied physical stability of hydrates and anhydrate forms and their dependency on relative humidity and temperature of the environment which affect dissolution rate and bioavailability.[33]

5.1.3: Structural aspects of polymorphism:

An ideal crystal is formed by regular spatial repetition of identical structural lattice. Crystal modification of drug molecules occur by two different ways; one is packing polymorphism in which molecules exhibit a rigid grouping through different assembly modes of conformationally equivalent molecules to occupy the points of different lattices. The second one is termed as conformational polymorphism in which molecule is not rigidly constructed and can exist in distinct conformational states

reviewed by Bernstein *et al* in organic solid state chemistry.[34] The conformational polymorphism is defined as the existence of different conformers of the same molecule in different polymorphic modifications.

5.1.4: Thermodynamics of polymorphism:

Each polymorphic drug substance has its own characteristic interaction energies and Morse curve. These intermolecular Morse curves are similar in shape but have smaller energies and greater distance than the Morse potential energy curve for the interaction between two atoms linked by a covalent bond in a diatomic molecule or within a functional group in a polyatomic molecule.

The relative thermodynamic stability of polymorphs depends upon the condition and direction in which a transformation can occur, and the total time for transformation to reach equilibrium. Burger and Ramberger studied thermodynamic stability relationships of polymorphic crystals that are based on thermodynamic rules such as free energy change and temperature diagram which distinguishes monotropic and enantiotropic systems.[35]

5.1.5: Kinetics of polymorphism:

Kinetics of polymorphism process is the rate of change of the phase transformation which occurs at constant temperature to form the most stable low energy polymorphs. Thermodynamic study establishes the stability domain of the various solid states, structural elements of the molecular assembly which leads to crystallization and their control. Frankenbach and Etter studied the process of crystallization of molecular arrangement into energetically stable packing patterns by non-covalent and hydrogen bonds.[36] Zhang *et al* and Gu co-workers investigated the supramolecular process of crystallization and its utility, the role of solvents and additives in nucleation of polymorphs.[37,38] Crystallization process involves both nucleation and growth of a polymorphic phase. Approaches to identify the most stable polymorphs are important and must be used in order to guide the selection of the best form for drug development process.

5.1.6: Polymorphism and solubility:

Grant and Higuchi investigated and reported that crystals with different lattice energies and entropies have different physical properties like solubility and dissolution.[39] Crystal with higher lattice energy dissolves faster due to release of higher amount of stored lattice energy thus improving dissolution profile.

In 1997, Taylor and coworkers observed that dissolution profile was significant for drug product evaluation and its rate was typically influenced by particle size and wettability.[22] Similarly Lippold *et al* studied the influence of wettability on the dissolution rate of pharmaceutical powders.[40] As correlation exists between wettability and dissolution rate, hence particle size affects the rate of dissolution. As dissolution rate is proportional to the surface area therefore decrease in particle size increases the surface area.

Anon *et al* reported that Ritonavior, a protease inhibitor molecule (HIV drug) exists in a new undesirable crystalline polymorphic Form II along with Form I. Further they confirmed that Form II is thermodynamically more stable compared to Form I and also revealed that the two crystalline forms differ substantially in their physical properties such as solubility and dissolution rate.[41]

Grant *et al* studied the effect of intrinsic solubility of a substance on its particular solid phase (solvate or anhydrate),[42] lattice energies of physical forms (amorphous, polymorphs of solvates) of a compound and correlated it to their solubilities and dissolutions profile and found that the largest difference in solubility is observed between amorphous and crystalline materials.[43,44]

5.1.7: Different methods for generation of polymorphic drug:

As mentioned earlier, organic drug substances can exist in two or more solid phases and can provide some distinct advantages and/or disadvantages in particular applications. The metastable form of a solid may be preferred in those instances where better absorption of the drug or the dissolution rate is optimum upto their release profile. The stable phase is less susceptible to chemical decomposition and may be the only form that can be used in suspension formulations. A metastable polymorph can be used in solid state formulations, and the thermodynamically stable

form in suspensions. The following methods are used for the generation of different polymorphic drug substances.

- Sublimation
- Crystallization from a single solvent
- Evaporation from a binary mixture of solvents
- Vapor diffusion
- Thermal Treatment
- Crystallization from the melt
- Rapidly changing solution pH to precipitate acidic or basic substances
- Thermal desolvation of crystalline solvates
- Growth in the presence of crystalline solvates
- Growth in the presence of additives
- Grinding

5.1.8: Generation of polymorph:

An important method to prepare different polymorphs is by slow solvent evaporation of saturated solutions. Commonly used solvents are dipolar aprotic solvents *viz*. DMF, acetonitrile, DMSO and protic solvents such as water, methanol. Similarly Lewis acids i.e. dichloromethane, chloroform and Lewis bases like acetone, 2-butanone, aromatic solvents like toluene, xylene and non-polar solvents like cylohexane and n-hexane have also been used.

Another useful method is the crystallization method, which involves controlled changes in temperature and slow cooling of hot saturated solution. Hydrates are usually obtained by re-crystallization from water. Sasaki *et al* investigated the formation of Trazodone hydrochloride tetrahydrate by dissolving the anhydrate in hot distilled water.[45a] Some of the drug substances and their number of reported polymorphs are given in Table 5.3.

5.2: Physico-chemical characterization of polymorphs:

The analytical techniques available for the physical characterization of solid materials are crystallography, microscopy, thermal analysis, solubility studies, vibrational spectroscopy, and nuclear magnetic resonance. These are most useful for the characterization of polymorphs and solvates as shown in Table 5.2.

5.2.1: Single crystal X-ray diffraction and powder X-ray diffraction:

Most drug substances are obtained as microcrystalline powders. It is often difficult to obtain crystallographically adequate crystals for structural analysis. However, in many cases it is sufficient to establish only the polymorphic identity of the solid and to verify that the isolated compound is indeed of the desired structure. The techniques of powder X- ray diffraction (PXRD) and single crystal XRD are prominent tools for the study of crystalline materials, well suited for the routine characterization with respect to polymorphs, solvates and molecular structure.[45b]

5.2.2: Morphology by microscopy:

Both optical and electron microscopes have found wide spread use for the characterization of polymorphs and solvates. Although optical microscopy is more limited in the range of magnification suitable for routine work (working beyond 6000X is difficult when observing microcrystalline materials), the use of polarizing optics introduces enormous power into the technique that is not available with other methods.[45c] Electron microscopy can be performed at extraordinary high magnification levels (upto 90,000X), and the images that can be obtained contain a considerable degree of three dimensional information such as (a) Polarizing optical microscopy and (b) Thermal microscopy.

5.2.3: Phase transitions by thermal methods of analysis:

Measurements of thermal analysis are conducted for the purpose of evaluating the physical and chemical changes that may take place in heated samples and the events noted in a thermogram in terms of plausible reaction processes. Thermal reactions can be endothermic (melting, boiling, sublimation, vaporization, desolvation, solid-solid phase transitions, chemical degradations) or exothermic (crystallization, oxidative decomposition) in nature as shown in Table 5.1.

The following thermal methodology has extensive use in the pharmaceutical industry for the characterization of compound purity, polymorphism, solvation, degradation, and drug excipients compatibility study.

- Thermogarvimetry Analysis (TGA)
- Differential Thermal Analysis (DTA)
- Differential Scanning Calorimetry (DSC)

5.2.4: Molecular motion by vibrational spectroscopy:

The energies associated with the vibrational modes of a chemical compound lie within the range of 4000-400 cm^{-1}. The vibrational modes can be observed directly through their absorbance in the infrared region of the spectrum, or through the observation of the low-energy scattered bands that accompany the passage of an intense beam of light through the sample by Raman effect.

5.2.5: Raman Spectroscopy:

The vibrational modes of a compound can be studied by using Raman spectroscopy, by which it measures the inelastic scattering of radiation by a non absorbing medium.[46] When a beam of incident light passes through a material, approximately one in every million incident photons are scattered with a loss or gain of energy. The inelastically scattered radiation can occur at lower and higher frequencies relative to that of the incident light, and the energy displacements relative to the energy of the incident beam correspond to the vibrational transition frequencies.

Raman scattering lines are quite sharp, and also contain significantly less spectral overlap in comparison with infrared absorption spectra, which permits a more facile characterization of the structural differences between the two systems. Raman spectra are generally insensitive to water for which it is primarily used for the differentiation of polymorphs or solvates. The degree of spectral simplification associated with Raman data permits a more facile generation of band or lines for assignments.[46]

5.2.6: Phase transition of polymorphs:

A metastable polymorphic transition to the stable polymorph during processing can proceed via all four mechanisms enlisted in Table 5.1 below.[47-50]

Mechanism	Phase transition	Factors influencing
Solid-state	Polymorphic transition hydration/ dehydration amorphous crystallization/ vitrification	Temperature, Pressure, Relative humidity, Presence of crystalline defects, Particle size distribution and their impurities.
Melting	Polymorphic transitions, vitrification	Relative rates of Nucleation, Crystal growth, Cooling and impurities or excipients
Solution	Polymorphic transition hydration/ dehydration, amorphous crystallization/ vitrification	Rate of solvent evaporation, ease of nucleation, processing conditions, un-dissolved solids and excipients.
Solution mediated	Polymorphic transition hydration/ dehydration amorphous crystallization/ vitrification	Solubility and solubility difference between the phases, processing temperatures, contact surfaces, agitation and soluble excipients / impurities

Table 5.1: Phase transition of polymorphs

5.2.7: Pharmaceutical solid-state analytical techniques:

Hilfiker *et al* and Brittain *et al* studied variety of analytical techniques for the characterization of pharmaceutical solids.[9,51] A combination of techniques over single one are preferred for characterization of polymorphs that reflect the solid-state properties.

Analytical techniques	Information	Advantage	Reference
FT-IR Diffused Reflectance Infrared Transmission Spectroscopy **(DRIFTS)** Attenuated Total Reflectance **(ATR)**	Intramolecular vibrations, polymorphic form H-bonding, Amorphous with broadening of peaks	Small sample quantity, rapid, non destructive method for qualitative and quantitative measurement.	52-54
FT-Raman	Intramolecular vibrations for different polymorphic forms with unique bands, peak shifting, amorphous form with broadening of peaks	Simple non-destructive method, Ability to penetrate through glass containers, insensitive to water. At low frequencies Raman spectroscopy can be used to analyze lattice vibrations.	52, 54-59
NIR	Overtones and combinations of vibrations in the mid-IR region.	Rapid, non-destructive method with ability to penetrate glass containers through fiber optic probe.	54, 60-63
SS-NMR	Nuclei and chemical environment within a molecule Molecular dynamics interactions , drug-drug or drug-excipients	Non destructive method with qualitative and quantitative measurement.	54, 64-66
Particulate level Terahertz Pulsed Spectroscopy **(TPS)**	Intramolecular and lattice vibrations (phonon modes) Polymorphic forms with unique peaks, amorphous form no spectral features.	Small sample size with rapid data acquisition and processing	51,59, 67,68
PXRD	Structural information polymorphic forms with degree of crystallinity Amorphous form having broad halo peaks	Non-destructive method used for qualitative and quantitative measurement.	51, 69-71

SCXRD	To solve crystal structures	Non-destructive method	51, 69-71
SAXS	Structural information from 0.01 to 3.0 ° of 2θ.	Non-destructive method, probes relatively large-scale structures having nm to μm range.	72, 73
DSC	Thermal events, glass transition temperature (T_g), crystallization temperature (T_c) and melting temperature (T_m), heat capacity, heat of fusion, transition and crystallization. Interactions study of drug-drug or drug-excipients.	Qualitative and quantitative applications.	51, 74-76
MDSC	Separation into reversing and non-reversing heat flow	Improves clarity to small (T_g) and overlapping thermal events.	77-79
TGA/ DVS	Gain or a loss of mass Decomposition temperature		80, 81
Isothermal micro calorimetry **(IMC)**	Heat change in a reaction enthalpy relaxation of amorphous material, heat of crystallization	High sensitivity Non destructive method qualitative and quantitative measurement.	82-84
Solution calorimetry **(SC)**	Heat change in a reaction heat capacity of liquid, heat capacity of solids	Temperature variability	82-84
Microscopy Polarized Light Microscopy **(PLM)**	Crystallinity, morphology, color and crystal habit	Higher resolution than light microscopy	51, 85-88
SEM	Topographical properties	-	51, 88
Bulk level Karl Fischer Titration	Water content (adsorbed or hydrate) with use in conjunction with TGA/DVS	-	89, 90
Brunauer, Emmett and Teller method **(BET)**	Surface area of the samples of multilayer adsorption	Simple and straight forward non-destructive method	91

Table 5.2: Analytical techniques used for characterization of polymorphs

Sr. No.	Name of the drug	No of polymorph	Reference
1.	Maltol	2	92
2.	Ethyl Maltol	3	93
3.	Sulfamerazine	3	94, 95
4.	Carbmazepine	4	96
5.	Lapachol	2	97
6.	Nitrofurantoin	2	98
7.	Probucol	2	99
8.	Spiranolactone	2	100
9.	Lomeridine hydrochloride	2	101
10.	Indomethacin	2	102
11.	Paroxetine maleate	2	103
12.	Enalapril maleate	2	104
13.	Flurbiprofen	2	105
14.	Sertraline hydrochloride	5	106
15.	Methylprednisolone	2	107

Table 5.3: Drugs and their polymorphic Forms

5.3: Polymorphic quantification by FT-Raman spectroscopy:

Bell and coworkers in 2000, reported rapid and non destructive method for the identification and characterization of both the drug and excipients present, Raman spectroscopy can be used to distinguish chemically similar substances such as N-ethyl-3,4-methylenedioxyamphetamine (MDEA) and N-methyl-1-(1,3-benzodioxol-5-yl)-2-butanamine (MBDB) and differently hydrated forms of the same drug in the analysis of ecstasy and related phenethylamines in seized tablets.[108]

Novoselsky and Glasser studied the isotopic chemical shift values in solid-state CP/MAS ^{13}C NMR spectra of Form I and Form III conformational polymorphs of (1S,4S)-Sertraline hydrochloride. These were correlated with a γ- gauche effect resulting from the respective antiperiplanar and synclinal C(2)-C(1)-N-CH_3 torsion angles measured by X-ray crystallography. The similarity of the solution–state C(2) chemical shifts in CD_2Cl_2 and DMSO-d_6 with that for Form III [and other polymorphs having C(2)-C(1)-N-CH3 (+)-synclinal angles] strongly suggests that a

conformational bias about the C(1)-N bond exists for both solvents in antidepressant drug.[106]

Wikstrom and his group in 2005 investigated in-line monitoring of transformation of theophylline anhydrous to theophylline monohydrate formation during wet granulation using Raman spectroscopy.[109]

Chen *et al* proposed advanced calibration strategy for the Raman intensity of suspension which depends on the analyte concentration, the physical properties of samples such as particle size, overall solid concentration, and homogeneity of the solid phase. It was observed that traditional multivariate linear calibration methods such as PLS could not effectively separate the Raman contributions due to the changes in analyte concentration from those caused by the variations of sample`s physical properties even *in situ* quantitative monitoring of phase transition and growth kinetics processes of four crystalline polymorphic forms of citric acid in suspensions using FT-Raman spectroscopy.[110]

Mazurek and Szostak developed a method for quantification of Atorvastatin calcium in tablets by FT-Raman spectroscopy using chemometric methods such as partial least square (PLS) and principal component regression (PCR).[111] The study confirms the high potential of FT-Raman spectroscopy combined with chemometric techniques in the quantitative analysis of pharmaceuticals with relatively low active ingradient content in commercial preparations.

Whiteside *et al* demonstrated the potential for detection and quantification of low levels of amorphous lactose in formulations using H / D exchange and FT-Raman spectroscopy. Deuterium exchange method has also been applied to the samples which contain a hydrophobic compound.[112]

Koleva and his group in 2008 developed quantitative Infrared and Raman spectroscopic approach for determination of Phenacetin and Salophen in binary solid mixtures with Caffeine : Phenacetin / Caffeine and Salophen / Caffeine.[113] These results together with recently reported applications to Phenacetin and aspirin polymorphs clearly demonstrate the applicability of these spectroscopic tools for quantitative determination of pharmaceutical constituents in solid state binary mixtures. The IR spectroscopy gave confidence of 98.9 % and 98.3 % for both systems. Raman spectroscopic data have shown minor improvement to 99.1 %. Linear

calibration range using IR and Raman method is confined within 0.013 - 0.8 and 0.012 - 0.9 mole fraction for IR and Raman methods, respectively.

Koleva *et al* also developed a quantitative method by polarized Infrared and Raman spectroscopic for the determination of antibiotic compounds of Cephalosporins such as Cefamandole, Cephalexin, Cefaloglycine and Cefalotin in six solid binary mixtures.[114] The correlation co-efficient (r^2) values within the 99.32 - 99.88 % and 99.0 - 95.54 % confidence are obtained by using the absorption ratios.

In 2008 Mazurek and Szostek performed FT-Raman spectroscopy for quantitative determination of Diclofenac sodium in tablets and capsules with the help of PLS, PCR and CP-ANN.[115] The proposed method is a fast and convenient alternative to the standard pharmacopoeia procedures of Diclofenac sodium quantification in commercial preparation of solid dosage forms.

Kontoyannis *et al* developed a simple, non-destructive methodology based on FT-Raman spectroscopy for the polymorphic quantitative analysis of Risperidone in commercially available film-coated tablets.[116]

Wikstorm and coworkers determined the hydrate transition temperature of several hydrate forming compounds namely Theophylline, Carbamazepine and Caffeine using transformation kinetics obtained by Raman spectroscopy.[117]

Nemet *et al* developed PXRD and Raman spectroscopic methods for the quantitative determination of Famotidine polymorphs.[118] Both PXRD and Raman spectroscopy are applicable for the quantitative measurement of Famtodine polymorphic forms in their mixtures. In the case of variable properties of the analyte such as particle size, crystal habit and orientations, Raman spectroscopy provides more accurate and precise results in comparison to PXRD. Raman spectroscopic method is expected to be less sensitive to sample preparation and is very robust.

In 2011 Buckley and Matousek studied recent advances in the application of transmission Raman spectroscopy to pharmaceutical analysis.[119] The transmission Raman spectroscopy provides highly chemical specific information, and has ability to obtain quantitative volumetric data from thick and highly turbid samples. The method provides rapid volumetric quantification of API, excipients and a polymorphs within intact tablets, capsules and powders.

Atef *et al* proposed Raman spectroscopy as a quick and reliable method to quantify the alpha, the gamma polymorphic forms of Indomethacin which is more precise and rugged compared to difficulty involved in using differential scanning calorimetry as a quantitative tool.[120]

Croker and coworkers proposed a comparative study of the use of powder X-ray diffraction, Raman and near infrared spectroscopy for quantitative analysis of binary powder mixtures of Form II and Form III of Piracetam.[121]

The present chapter deals with the synthesis and physico-chemical characterization of three polymorphic forms of Sertraline hydrochloride by using various analytical techniques. Further, it highlights the potential of the FT-Raman spectroscopy for quantitative determination of polymorphic impurity (Form I and Form III) present in Sertraline hydrochloride Form V.

5.4: Experimental:

Materials and reagents

5.4.1: Drug:

Sertraline hydrochloride was obtained as a gift sample from Sun Pharmaceutical Industries Limited, Vadodara, India. Sertraline hydrochloride (Zoloft®) is an antidepressant and anorectic drug of the non tricyclic class. Its chemical name is (1S, 4S)–*cis*-4-(3,4-dichlorophenyl)-1,2,3,4, tetrahydro–N-methyl-1-naphthalenamine hydrochloride(1), having molecular formula $C_{17}H_{17}NCl_2$.HCl, and molecular weight 342.73. Sertraline hydrochloride is a white to off white crystalline powder, has a pK_a of 9.16, is slightly soluble in water, isopropyl alcohol and sparingly soluble in ethanol.

Sertraline hydrochloride is useful as an antidepressant and anorectic agent, and is also useful in the treatment of chemical dependencies, anxiety-related disorders and Parkinson's disease and chemical dependencies. In year 1993, Robert Sysko and their group in U.S. Pat. No. 5,248,699 (Pfizer Inc.) reported that Sertraline hydrochloride can exist in different crystalline polymorphic forms as shown in Figure 5.1 which differ from each other in their stability, physical properties, spectral data and methods of preparation.[122]

Sertraline hydrochloride is a highly potent and selective inhibitor of serotonin (5HT) CNS neuronal reuptake in the brain (i.e. a serotonin-specific reuptake inhibitor (SSRI).

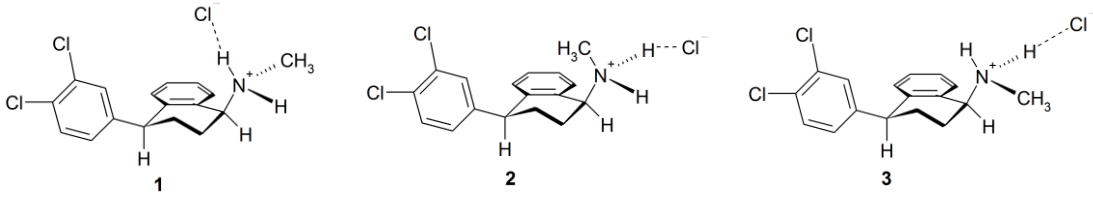

Figure 5.1: Conformational polymorphs of Sertraline hydrochloride (1) Form I, (2) Form III and (3) Form V

Solvents and reagents

Analytical Reagent Grade methanol, acetone, n-hexane, tetrahydrofuran and hydroquinone from Merck, India were used as received. Double distilled water (0.22 micron nylon filter) was used throughout the experiments.

5.4.2: Synthesis of Sertraline hydrochloride polymorphic Form I, III, V:

Method I:

Accurately weighed 15.0 g of Sertraline free base was dissolved in 100 mL of analytical grade isopropyl alcohol and 30 mL of concentrated hydrochloric acid was added to the solution and mixed thoroughly. The obtained slurry was heated to reflux to get a clear solution and then gradually cooled to room temperature at 25 ± 5°C. The slurry was filtered and dried under vacuum at 50 ± 2° C for 3 h which gave Sertraline hydrochloride as polymorphic Form I shown in scheme 5.1.

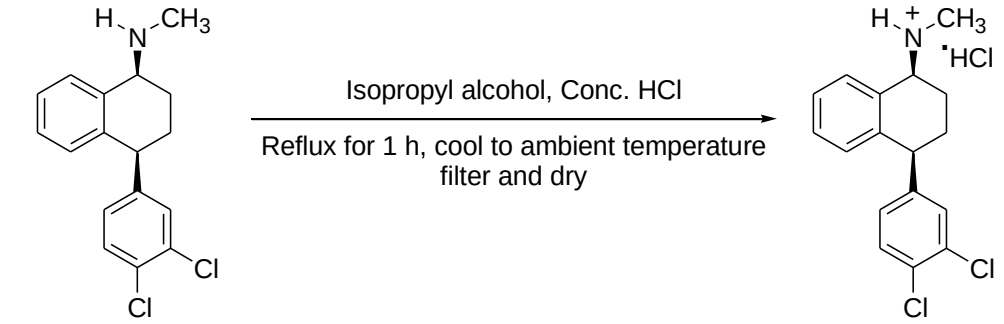

Sertraline (Free base)

Sertraline hydrochloride (Form I)

Scheme 5.1: Synthesis of Sertraline hydrochloride Form I

Method II:

Accurately weighed 6.0 g Sertraline hydrochloride Form I was dissolved in 30.0mL of (1 : 1) mixture of analytical grade isopropyl alcohol and water and heated upto 80 ± 2°C for 20 min and then gradually cooled to room temperature at 25 ± 5°C. The slurry was filtered and dried under vacuum at 50 ± 2°C for 3 h. This method resulted in complete polymorphic conversion from Sertraline hydrochloride Form-I to Form V shown in scheme 5.2.

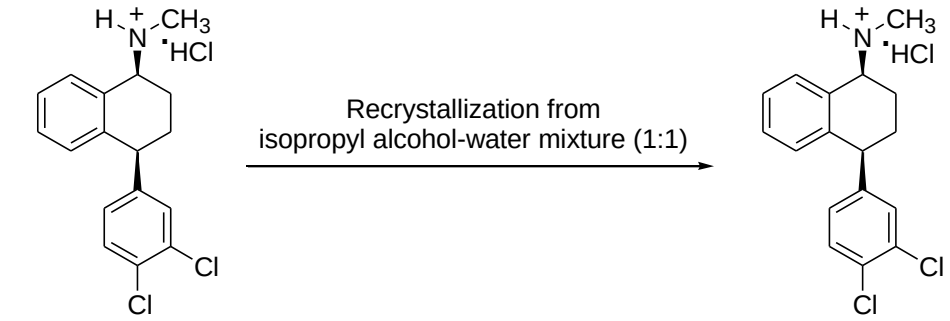

Sertraline hydrochloride (Form I)

Sertraline hydrochloride (Form V)

Scheme 5.2: Synthesis of Sertraline hydrochloride Form V from Form I

Method III

Similarly, exactly 4.0 g of Sertraline hydrochloride Form V was heated to 190 - 200°C for 30 min in a silicone oil bath in a glass assembly with cold condenser, Sertraline hydrochloride Form V sublimed and condensed on cold condenser, was collected as Sertraline hydrochloride Form III shown in scheme 5.3.

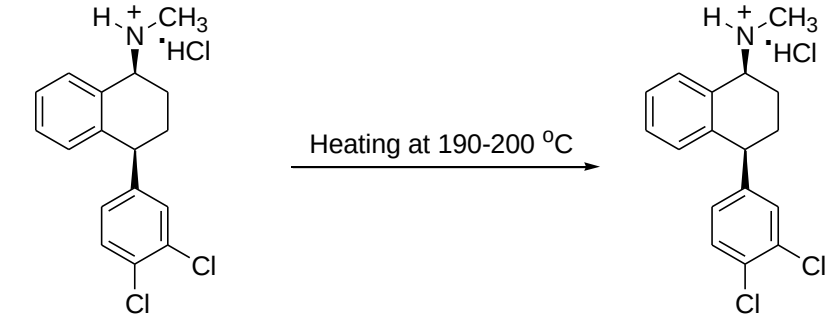

Sertraline hydrochloride (Form V)

Sertraline hydrochloride (Form III)

Scheme 5.3: Synthesis of Sertraline hydrochloride Form III from Form V

5.4.3: Polymorphic characterization:

Fourier transform infrared spectroscopy (FTIR)

The Infrared (FT-IR) spectra of purified and dried polymorphic drug of Sertraline hydrochloride of Form I, Form III and Form V were recorded in the range from 400 to 4000 cm^{-1} on a Perkin Elmer (Model-Spectrum One) FT-IR spectrophotometer. Approximately 2 mg of the sample was mixed thoroughly with 100 mg of KBr (dried) and then compressed to form discs using one cm diameter pellets, IR spectra was recorded with resolution of 4.00 cm^{-1} and 16 scans each for sample at room temperature.

Modulated Differential scanning calorimetry (MDSC)

Modulated Differential Scanning Calorimetric analysis was carried out by using a Model-DSC Q2000, TA instruments. The instrument temperature and heat capacity were calibrated using indium as standard and about 2.5 mg samples of purified polymorphic forms of Sertraline hydrochloride of Form-I, Form-III and Form-V were placed in standard aluminum pans sealed with lids. The crimped aluminum pans were heated from 160 to 350 °C, isothermal for 5 min, at a heating rate of 2 °C min^{-1} with modulated ± 1.0 °C every 60 s.

Nuclear magnetic resonance spectroscopy (NMR)

^{1}H NMR spectra of purified and dried polymorphic drug, Sertraline hydrochloride of Form I, Form III and Form V were recorded using NMR spectrometer (AV-III, Bruker BioSpin AG, Switzerland) operating at proton frequency at 500.13 MHz using 5 mm Broad Band Observe probe head at room temperature (~30 ± 2 ºC). The ^{1}H NMR spectra were obtained after accumulating 16 scans by using 1% sample in methanol-d_4 (Merck, Germany 99.9% of D). All data were processed using Bruker Biospin Topspin 2.1 version software.

Similarly proton decoupled ^{13}C-NMR spectra along with DEPT-90 and DEPT-135 were recorded by using 10 % sample in methanol-d_4 with spectrometer operating at ^{13}C-carbon frequency 125.76 MHz with same probe head.

^{13}C Solid State-NMR

The solid state ^{13}C NMR spectra of dried polymorphic drug substance of Sertraline hydrochloride of Form I, Form III and Form V were recorded on 500 MHz NMR spectrometer using a Bruker BioSpin 4 mm MAS BB/^{1}H solid state probe head by using zirconia rotor. The ^{13}C Solid State NMR spectrum utilized proton/carbon-13 cross-polarization magic angle spinning (CP-MAS) with variable amplitude cross-polarization. The sample was spun at 5 kHz and a total of 512 scans were collected with a recycle delay of 20 seconds at CP-MAS experiment. A line broadening of 40 Hz was applied to the spectrum before FT was performed. Chemical shifts were reported on the δ scale using the carbonyl ^{13}C-carbon of glycine standard at 176.03 ppm as a secondary reference.

Similarly, the solid state ^{13}C CP-MAS along with TOSS (Total Suppression of Spin Sideband) NMR spectrum was obtained on 500 MHz NMR spectrometer (AV-III, Bruker BioSpin) using a Bruker Biospin 4 mm MAS BB/^{1}H solid state probe head for the identifications of spin side bands with 160 scans at spinning rate of 5 kHz. All acquired time domain FID (free induction decay) data were processed using Bruker BioSpin Topspin 2.1 version software.

Powder X-ray diffraction (PXRD)

Powder X-ray diffraction pattern (PXRD) were recorded on a Philips X'Pert PRO, Netherlands, using a Ni-filter equipped with Cu Kα1 radiation (1.5405 A^{o}) source (Cu anode), Solid-state Germanium detector and spinning sample stage were used to record diffractograms of purified and dried polymorphic forms of Sertraline hydrochloride, *viz* Form I, Form III and Form V. Following experimental parameters were used for recording the diffractogram : Scan range (2-theta values): 4.0° to 40°, X-Ray tube (generator) setting: 45 kV, 40 mA, Step size: 0.05°, time per step:10 which is used primarily for phase analysis and determination of crystal pattern.

Scanning electron microscopy (SEM)

Surface morphology and shape of the purified and dried polymorphic drug of Sertraline hydrochloride of Form I, Form III and Form V were examined with scanning electron microscope (Model-Quanta-200, Make - FEI Company, The Netherlands). The samples were mounted with carbon tape on a double-sided

adhesive with spot size 5, an accelerated voltage of 15 kV and a current of 20 mA prior to observation. The SEM images of Sertraline hydrochloride Form I, III and V representative areas were captured with suitable magnifications.

Fourier Transform Raman spectroscopy (FT-Raman)

Raman spectra of purified and dried polymorphic drug, Sertraline hydrochloride of Form I, Form III and Form V were recorded by using a FT- Raman Spectrometer (Model: RFS 100/S, Bruker Optik) equipped with a 750 mW Nd : YAG laser source operating at 1064 nm having laser power 350 mW and liquid nitrogen cooled germanium detector, scanning range from (+) 4000 cm^{-1} to (–) 2000 cm^{-1} and number of scans fifty.

The three polymorphic forms of Sertraline hydrochloride used in this study have been identified and verified by FT-IR, XRD, ^{13}C Solid State-NMR, FT-Raman, SEM and DSC techniques. Raman spectrometric methods have been developed for quantitative measurement of the polymorphic forms of Sertraline hydrochloride in their mixtures. This study aims to deduce some useful conclusions regarding quantitative polymorph analysis which could also be utilized in API and solid state pharmaceutical products. Raman vibrational bands, which permit simple determination of their phases in their mixtures by applying relative intensity method, using a specific wave number for the quantification of Form I and Form III in Sertraline hydrochloride Form V active pharmaceutical ingredient as well as solid state pharmaceutical products.

Raman intensity for analytical method

$$Raman\ intensity\ (I) = Kv^4 \hat{J} C \qquad (5\text{-}1)$$

where, I = Intensity, ν = Frequency of scattered radiation, C = Concentration,

K = Constant includes laser power at the sample, $\hat{J}$ = Scattering coefficient of Raman line

FT-Raman Methodology for quantification of Sertraline hydrochloride Form I

$$Relative\ intensity\ (R_I) = \frac{I_b}{I_a + I_b} \qquad (5\text{-}2)$$

where, I_a = Intensity of Raman line at 179.0 cm^{-1},

I_b = Intensity of Raman line at 194.2 cm^{-1}

The quantitative Raman spectroscopic approach for determination of Setraline hydrochloride Form I and Form III in From V solid mixtures was carried out by applying corrected relative intensity method[113, 114] by using following equations,

$$Corrected\ intensity\ of\ Form\ I\ (Y_I) = R_I - R_V \quad (5\text{-}3)$$

where, R_V is the Relative intensity of Form V calculated with pure Sertraline hydrochloride Form V

$$Y_I = m_I X_I + C_I \quad (5\text{-}4)$$

where, X_I = % Concentration of Form I, C_I = Intercept, m_I = slope

FT-Raman methodology for quantification of Sertraline hydrochloride Form III

$$Relative\ intensity\ (R_{III}) = \frac{I_c}{I_c + I_b} \quad (5\text{-}5)$$

where, I_c = Intensity of Raman line at 489.06 cm^{-1}

I_b = Intensity of Raman line at 194.2 cm^{-1}

$$Corrected\ intensity\ (Y_{III}) = R_{III} - R_V \quad (5\text{-}6)$$

$$Y_{III} = m_{III} X_{III} + C_{III} \quad (5\text{-}7)$$

where, X_{III} = % Concentration, C_{III} = Intercept, m_{III} = slope of Form III.

5.5: Results and discussion:

5.5.1: Polymorphism identification:

IR Spectroscopy

FT-IR spectra for Form I, Form III and Form V of Sertraline hydrochloride are presented in Figure 5.2. The spectra of Form I, II and V show asymmetric and symmetric stretching of $-CH_2$ groups at 2690 - 2755 cm^{-1} and 2464 - 2483 cm^{-1} respectively due to the conformational changes in the cyclohexane ring C (2), C (3) methylene groups. The stretching frequency of N-methyl group for three different polymorphic Sertraline hydrochloride have distinct difference in the range of 1400-1500 cm^{-1} and the positional isomer can be differentiated in the bending region from 700 - 825 cm^{-1} presented in Table 5.4.

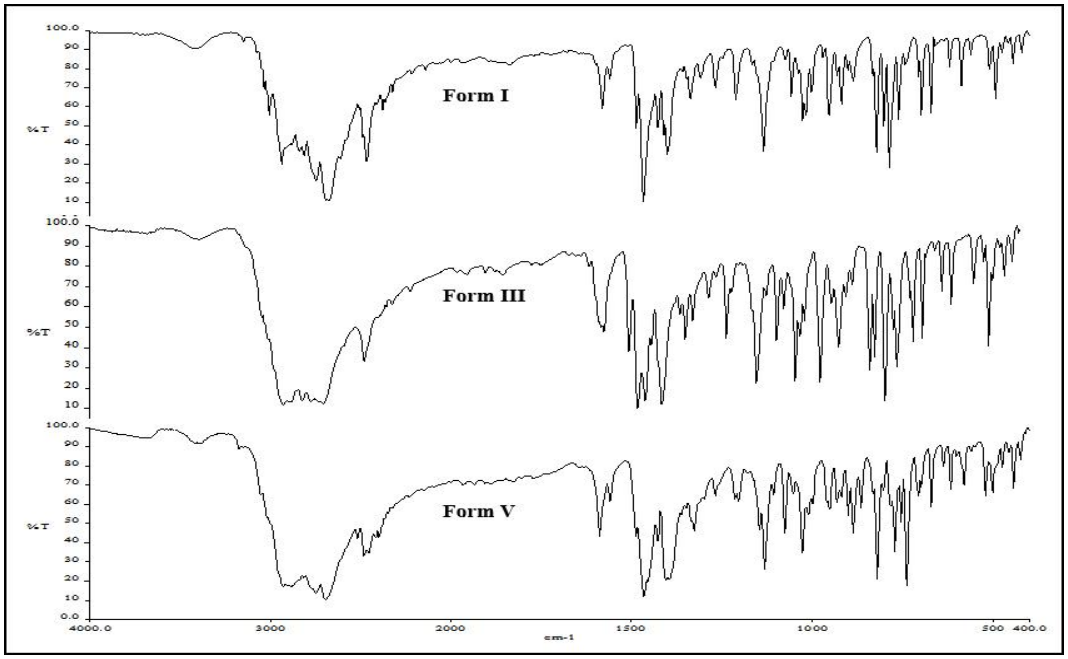

Figure 5.2: Comparative IR spectra of different Forms of Sertraline hydrochloride

Sr. No.	Wave number in cm^{-1} Form I	Wave number in cm^{-1} Form III	Wave number in cm^{-1} Form V
1	2696.51, 2748.88	2693.77	2696.37, 2751.37
2	2468.88	2464.77	2482.83
3	1403.58, 1469.49	1401.46, 1446.65,1468.67	1406.61, 1468.48
4	700.19, 764.01, 789.42, 825.20	745.09, 777.52, 819.97	741.12, 773.72, 822.66

Table 5.4: Interpretation of FT-IR spectra of different Forms of Sertraline hydrochloride

Raman Spectroscopy

As in the case of FTIR spectra, FT-Raman spectra (Fig.5.3) of three polymorphic forms of Sertraline hydrochloride I, III and V also have different distinct spectral pattern. Form I has a strong distinct signal at 194.0 cm^{-1} (Fig.5.4) where as Form III (Fig. 5.5) has a strong distinct signal at 489 cm^{-1}. On the other hand Form-V exhibits two distinct Raman lines at 194.0 $cm^{-1}$and 179.0 cm^{-1}.

The FT-Raman spectra of placebo, also scanned with similar parameters, does not show any of the above signals at those frequencies. Hence Raman technique can be easily applied for polymorphic identification as well as quantification for Sertraline hydrochloride API and its pharmaceutical solid dosage.

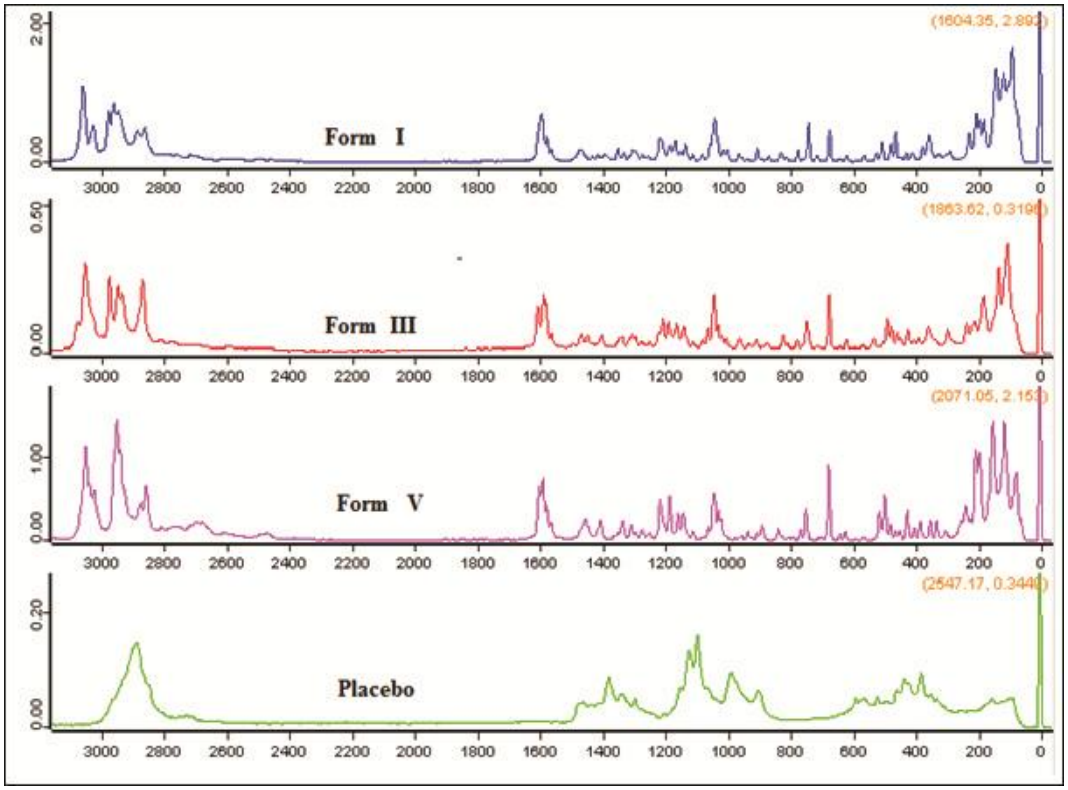

Figure 5.3: Comparative Raman spectra of three Forms of Sertraline hydrochloride along with placebo

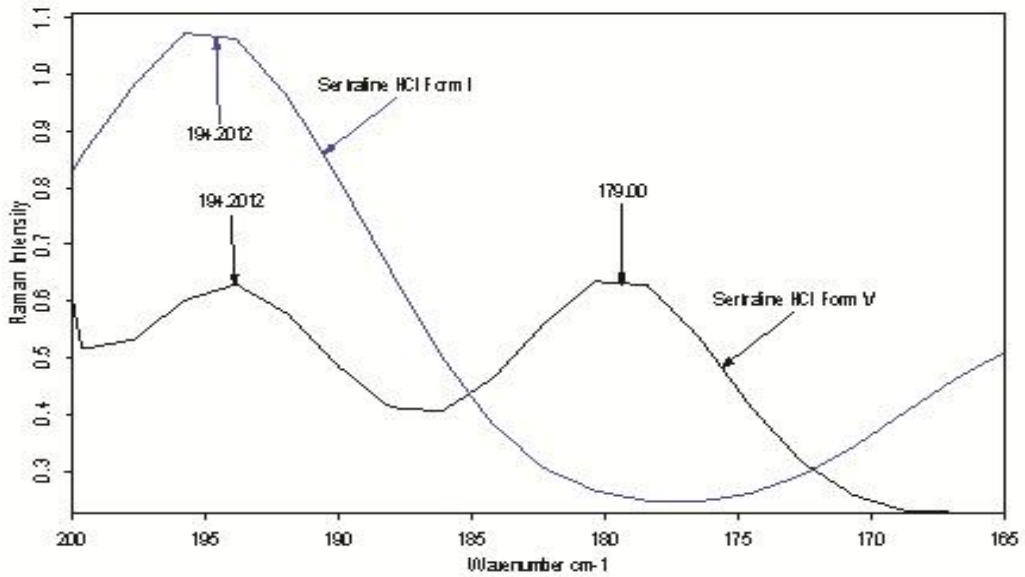

Figure 5.4: Expanded view of FT-Raman Spectra of Sertraline HCl of Form I and V

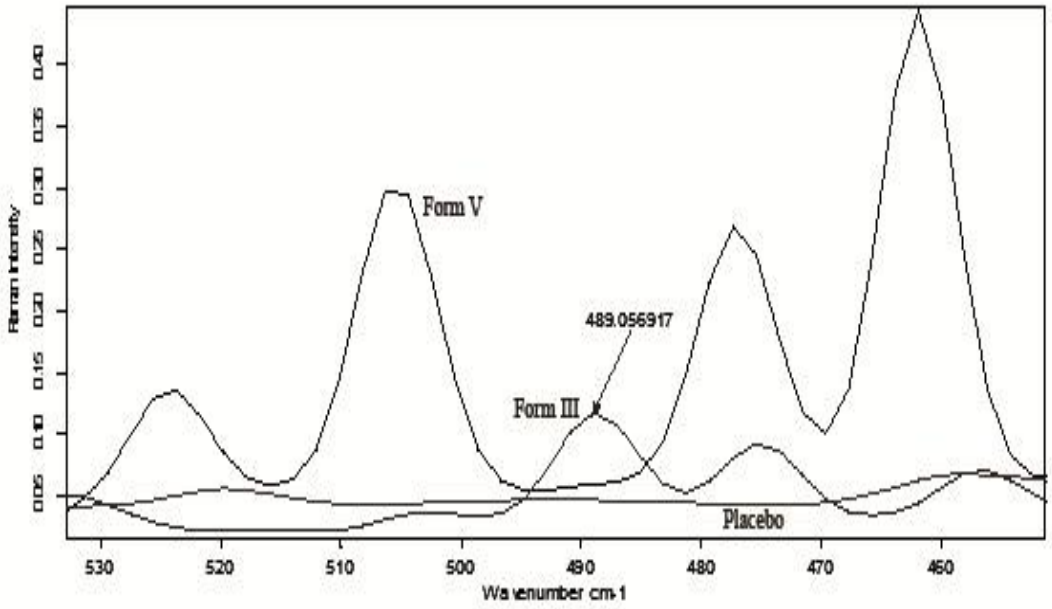

Figure 5.5: Raman spectra overlay of Form V with Form III along with placebo

Solution state NMR of Sertraline hydrochloride

^{1}H-NMR and proton decoupled ^{13}C-NMR spectra of all the polymorphic forms of Sertraline hydrochloride were recorded with methanol-d_4 with AV-III 500 MHz instrument with BBO probe head, and are given in Figure 5.6 and Figure 5.7. The spectra clearly show that in solution state all the polymorphic forms were chemically and structurally identical.

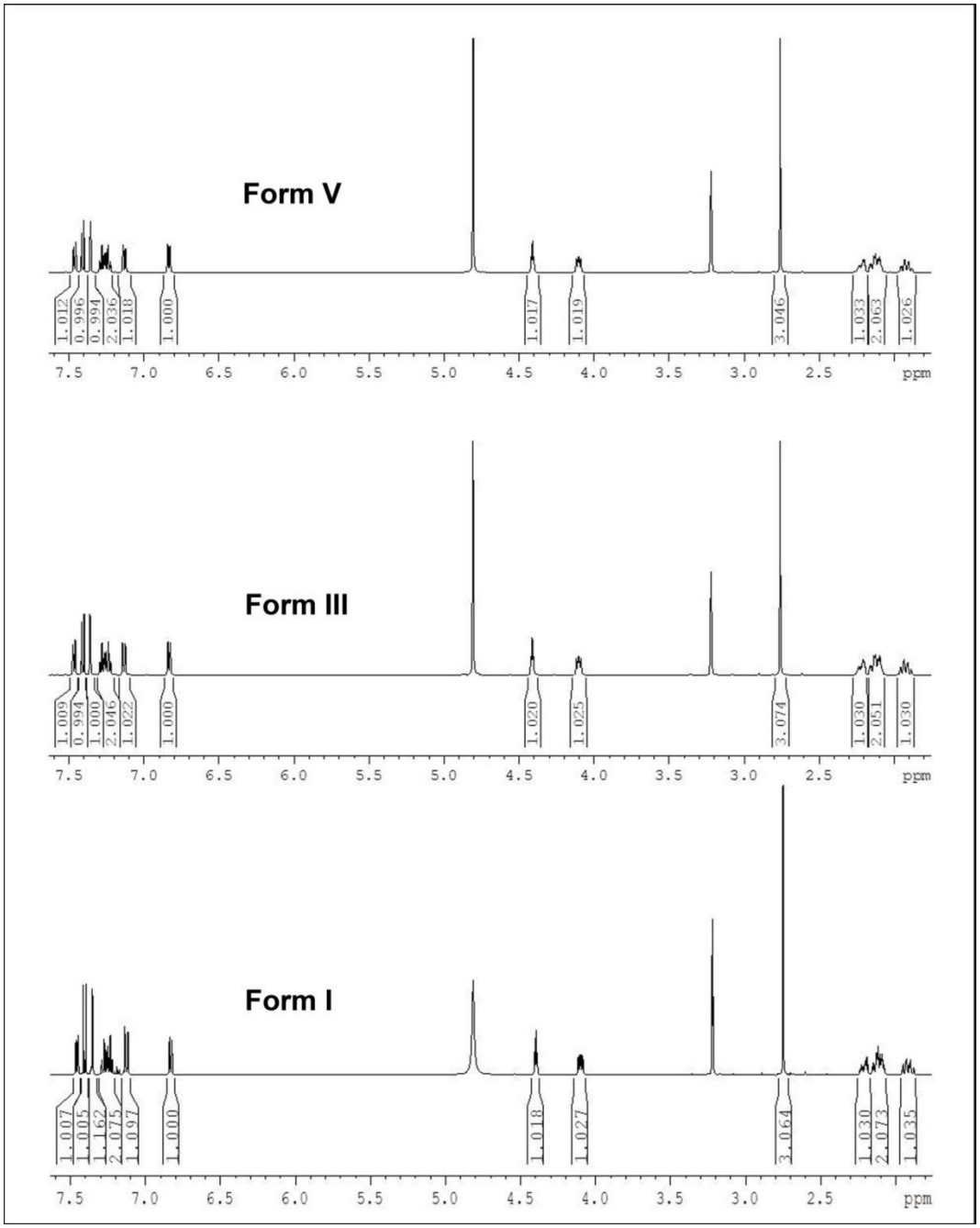

Figure 5.6: Comparative ^{1}H-NMR spectra of three Forms of Sertraline hydrochloride in methanol-d_4

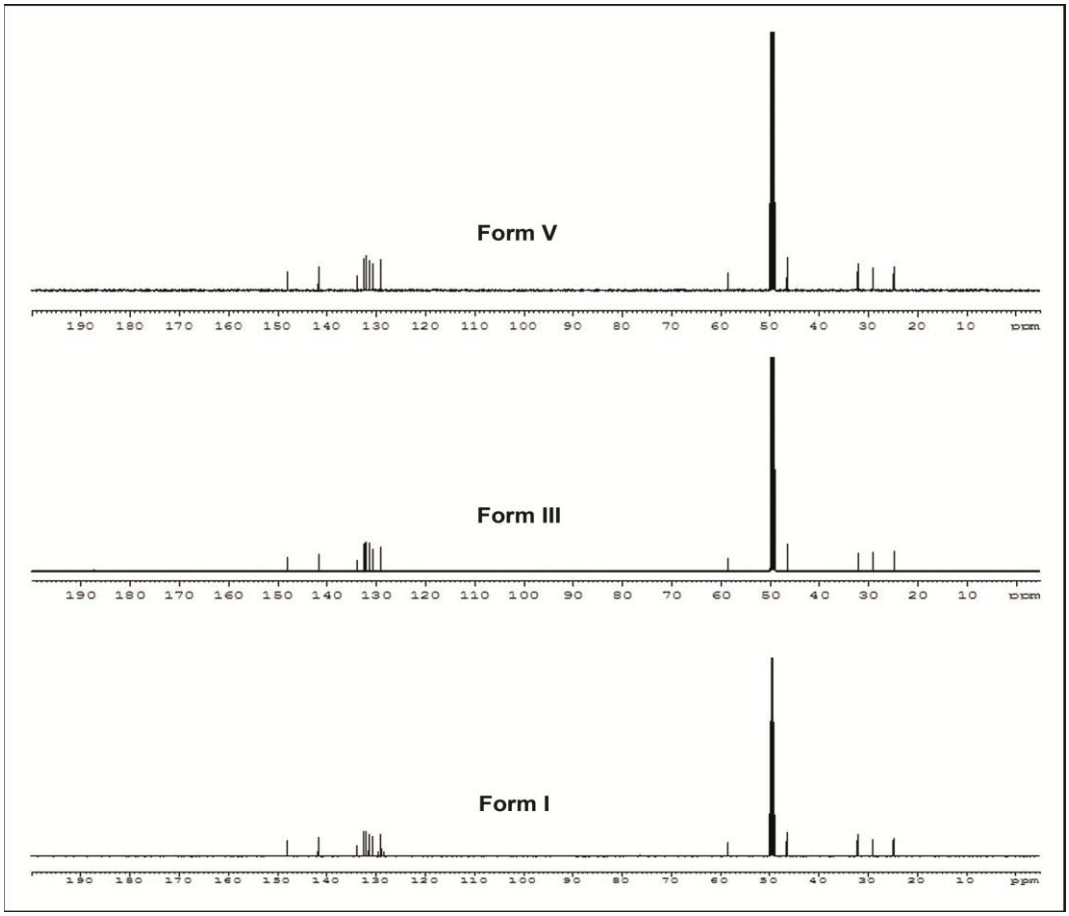

Figure 5.7: Proton decoupled ^{13}C-NMR spectra of three Forms of Sertraline hydrochloride in methanol-d_4

Solid State NMR (SS-NMR)

Robert Glaser *et al* reported the (C_2) isotropic chemical shift values in solid state CP/MAS with TOSS ^{13}C-NMR spectra of conformational polymorphs of (1S,4S)-Sertraline hydrochloride Form I (δ 28.5), Form III (δ 24.83) and Form V (δ 22.6) were correlated with a γ-gauche effect resulting from antiperiplanar and synclinal torsion angles as measured by X-Ray crystallography as shown in Figure 5.8. The following table (Table 5.5) indicates the difference in solid state signals of different Forms. The SS-NMR spectra support the fact that Form I, III and V exist in different three dimensional conformational polymorphs as shown in Figure 5.9.

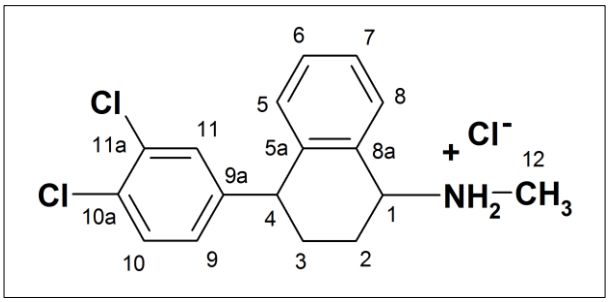

Figure 5.8: Planar structure of Sertraline hydrochloride

Assignment of carbon	Form I	Form III	Form V
	Chemical shift in ppm	Chemical shift in ppm	Chemical shift in ppm
C_1	58.39	56.70	58.59
C_2	28.27	24.83	22.66
C_3	28.27	28.75	26.41
C_4	47.24	47.33	47.20
C_{5a}	140.71	142.01	143.51
C_{9a}	144.57	148.30	146.52
$-CH_3$	31.68	31.89	35.26

Table 5.5: Chemical shift of different polymophs of Sertraline hydrochloride

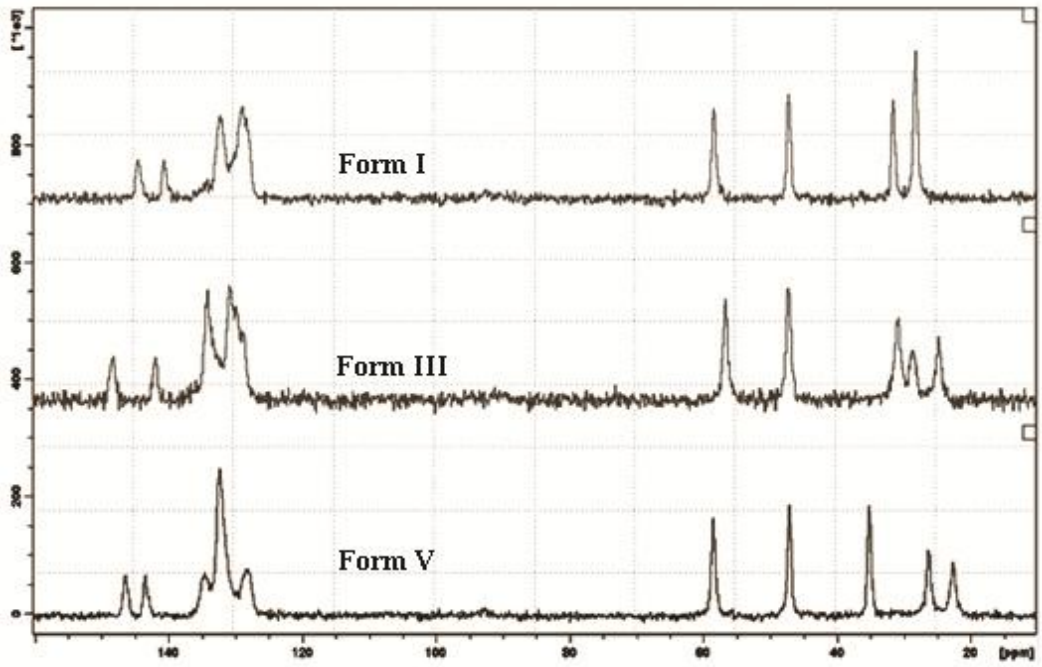

Figure 5.9: SS-NMR (CP-TOSS) spectra of three Forms of Sertraline hydrochloride

Powder XRD

All the polymorphic Forms I, III and V of the Sertraline HCl were subjected to XRPD analysis in the 2-theta range 3° to 40° which indicated that all are crystalline in nature. X-ray powder diffraction peak patterns of Forms I and III and V are unique and differentiable. It is clear from Figure 5.10 that the non-interfering characteristic intense 2-theta peaks for Form I are at 15.73° and 22.50°, for Form III at 21.55° and for Form V at 11.0°. Comparision of diffractogram of Form I and III with Form V is shown in Fig.5.11 and Fig.5.12 respectively.

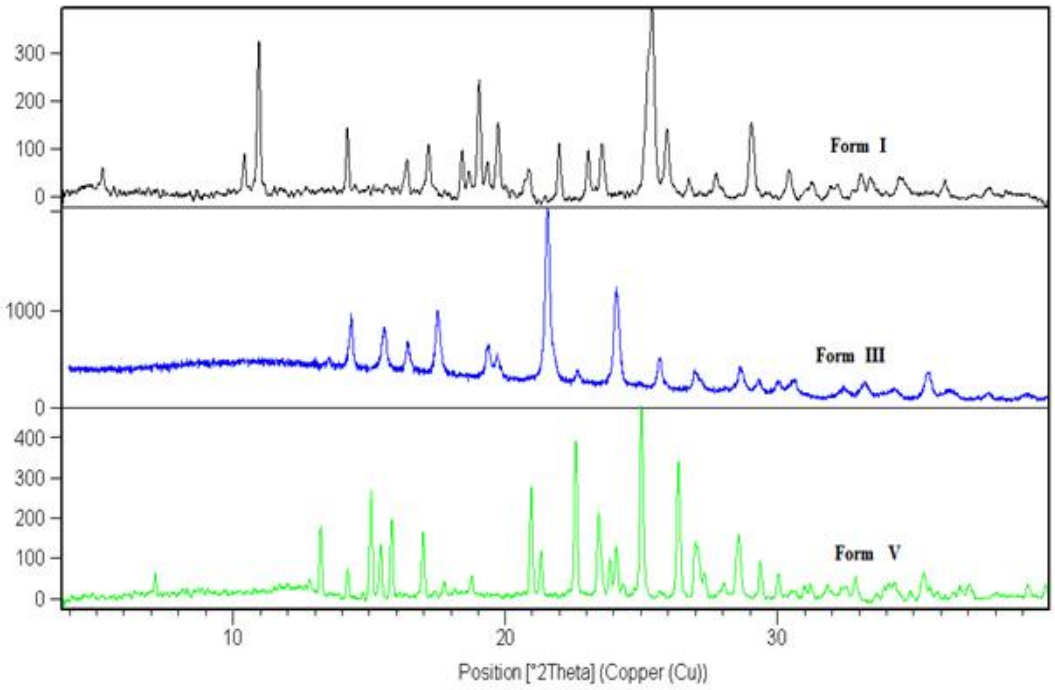

Figure 5.10: Comparative powder XRD pattern of three Forms of Sertraline hydrochloride

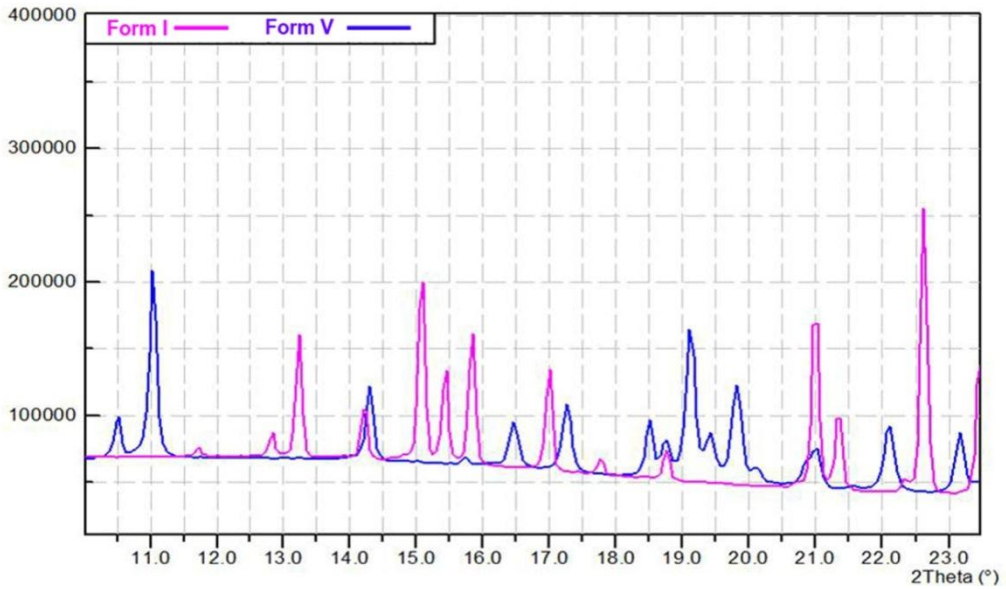

Figure 5.11: Powder XRD overlay of Form I and Form V

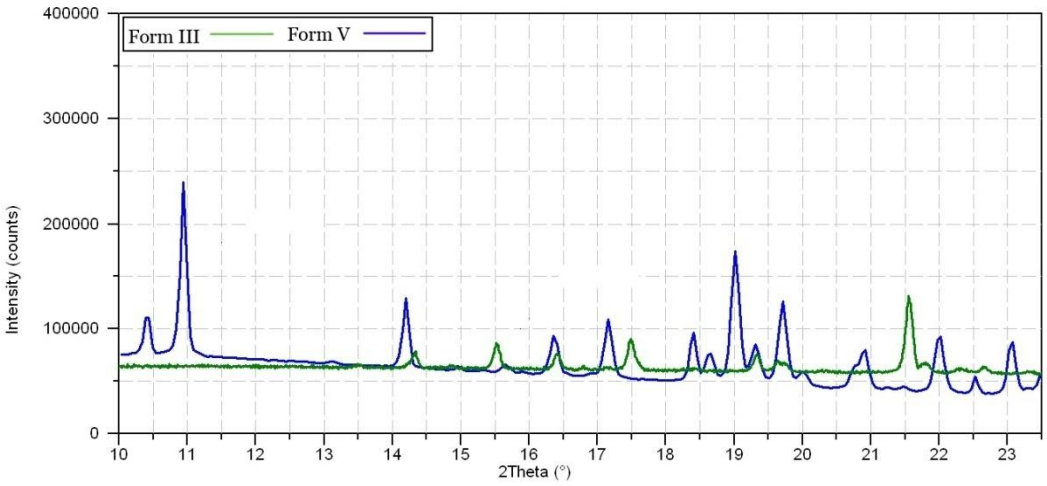

Figure 5.12: Powder XRD overlay of Form III and Form V

Modulated Differential Scanning Calorimetry (MDSC)

Similarly, polymorphic forms with distinct crystalline nature may show different thermal behavior due to their conformational changes. The three different polymorphic forms of Sertraline HCl were analyzed by modulated DSC, the thermograms show reasonably different endothermic peaks showing different amount of heat capacity.

The Modulated Differential Scanning Calorimetry (MDSC) thermogram of three polymorphic Forms of Sertraline hydrochloride exhibits different sharp endothermic peaks ranging from 220.87 ºC to 262.83 ºC. Comparison of thermograms of the three forms can be seen from Figure 5.13 and data is presented in Table 5.6.

Polymorphic Form	**Observed endothermic peak in °C**		
I	220.87	245.38	260.69
III	-	246.03	260.16
V	-	246.49	262.83

Table 5.6: DSC data of Sertraline hydrochloride Form I, Form III and Form V

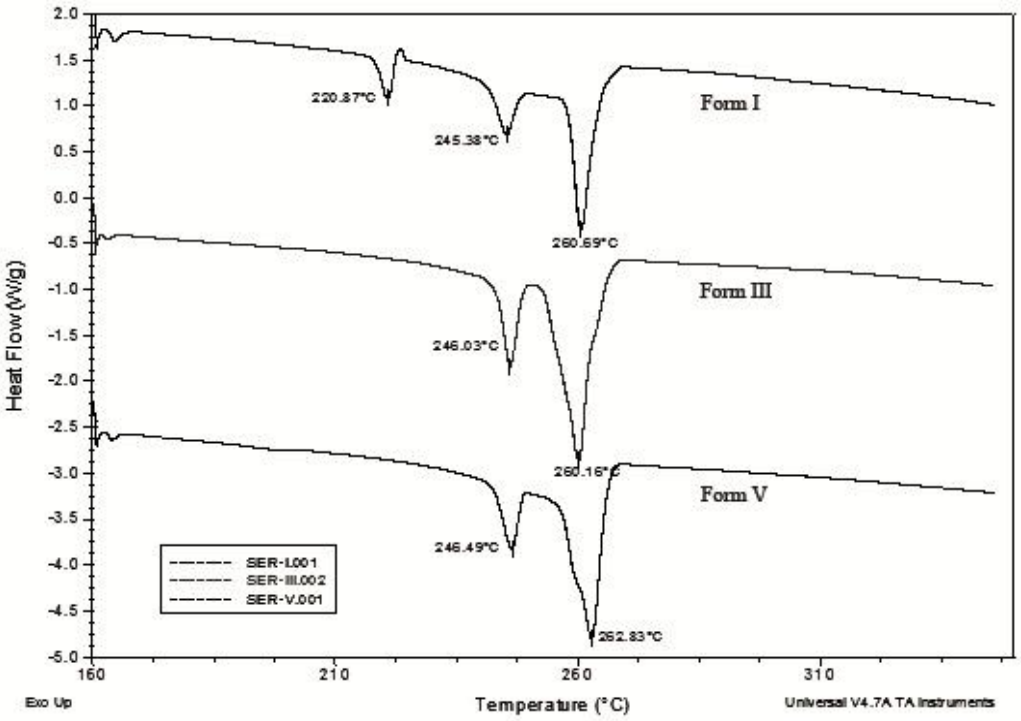

Figure 5.13: MDSC thermograms of three Forms of Sertraline hydrochloride

Scanning Electron Microscopy (SEM)

The morphology of the prepared polymorphic forms of Sertraline hydrochloride was studied by SEM and the micrographs taken at different magnifications are shown in Figure 5.14. SEM studies show that morphology of Form I, Form III and Form V can be easily differentiated at the surface. Form III looks like flakes and Form V has needle like morphology.

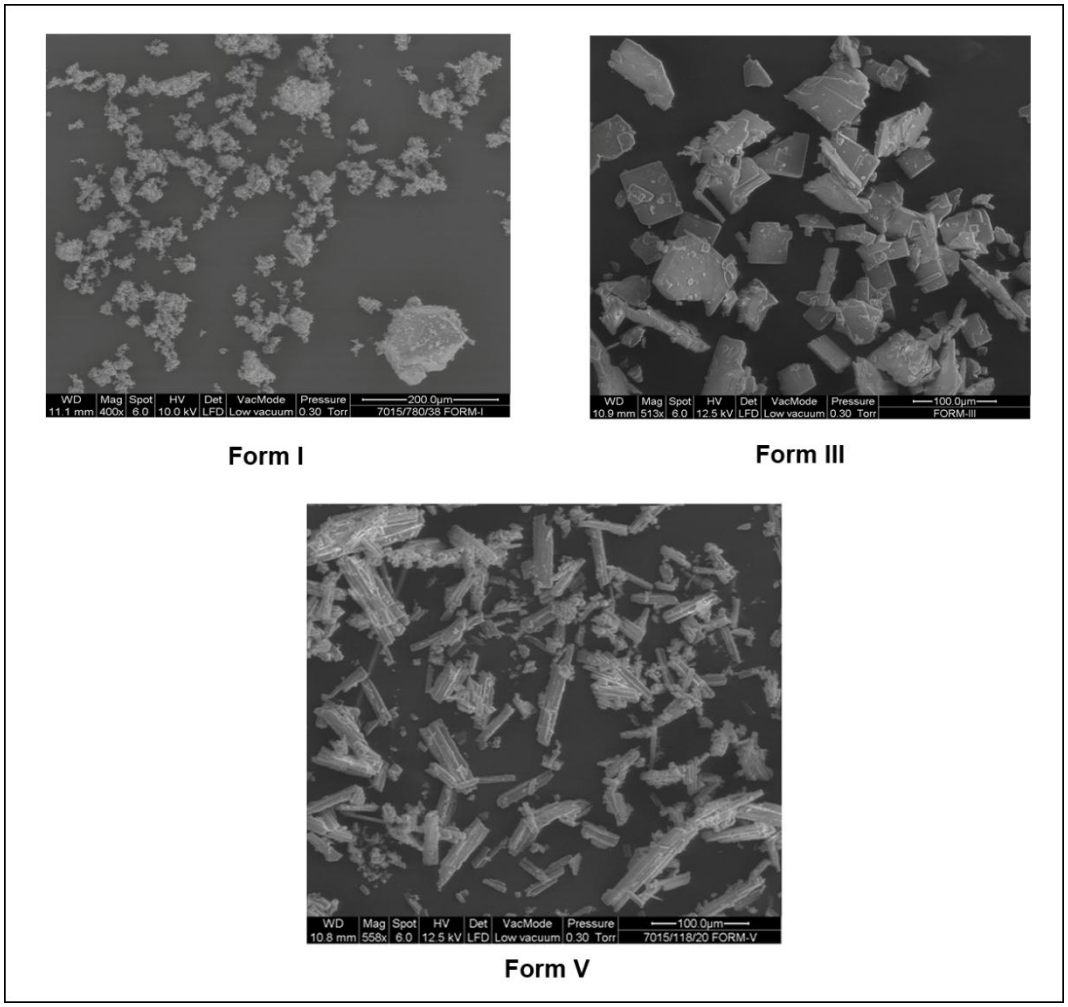

Figure 5.14: SEM images of three Forms of Sertraline hydrochloride

5.5.2: Polymorphic drug quantification by Raman spectroscopy:

5.5.2.1: Standard physical mixture preparation:

The standards were prepared by accurately weighing 5 mg of Form I, 100 mg of Form V and 195 mg of placebo, mixing them thoroughly in a homogenizer for 3 min for this study.

Sample analysis

Pre weighed 10 tablets of Sertraline hydrochloride were crushed using mortar and pestle to give a fine powder and 5 mg of this powder was taken in FT-Raman sample holder. The spectra were recorded in triplicate and relative intensity of three replicates were calculated. Finally, from the mean relative intensity, the amounts of Form I and Form III present in Form V of Sertraline hydrochloride were calculated from the Equation (5-4) and (5-7) respectively.

5.5.2.2: Quantification of Sertraline hydrochloride Form I present in Form V:

The intensity of Raman line at 179.0 cm^{-1} decreases as concentration of Form-V decreases whereas the intensity of the line at 194.2 cm^{-1} increases as concentration of Form I increases in the physical mixture of the polymorphic drug substance. The Raman spectra of both the test substance (physical mixture of Form I and Form V) and the pure Form V were recorded and the relative intensities of both the samples were calculated by dividing the intensity of Raman line at 194.2 cm^{-1} of the two samples by sum of intensities of Raman line at 194.20 cm^{-1} and 179.00 cm^{-1}. However, in the calculation of relative intensity, corrected intensity of the peak at 194.20 cm^{-1} was used by subtracting the contribution from pure Form V at this wave number as can be seen from the Fig. 5.4. The difference between relative intensity of test substance and pure Form V is nothing but the corrected intensity which is due to the presence of Form I in Form V.

5.5.2.3: Linearity:

Standard physical mixtures for linearity study were prepared by using pure polymorphic form of API Sertraline hydrochloride in which amount of Form I was varied from 1.0 mg to 20.0 mg level, the amount of Form V was kept constant at 100 mg and calculated amount of placebo was added to keep the final weight of the mixture same (300 mg) throughout. The details of the amount taken are given in Table 5.7.

Sr. No.	Form I (mg)	Form V (mg)	Placebo (mg)	Relative intensity	Corrected intensity
1	0	100	200	0.5980	NA
2	1	100	199	0.6066	0.0086
3	2	100	198	0.6151	0.0171
4	3	100	197	0.6160	0.0179
5	5	100	195	0.6203	0.0223
6	8	100	192	0.6249	0.0269
7	10	100	190	0.6309	0.0329
8	15	100	185	0.6380	0.0400
9	20	100	180	0.6493	0.0512

Table 5.7: Linearity study of Sertraline hydrochloride Form I by FT-Raman

The standard polymorphic physical mixture samples were thoroughly homogenized in a homogenizer for 3 min and the Raman spectra were recorded from -2000 cm^{-1} to 4000 cm^{-1} with laser power of 350 mV and fifty scans for each spectrum.

The relative intensities of the peak at 194.2 cm^{-1} in the mixtures (calculated as described above) showed a linear variation with the concentration of Form I present in the mixture. However, at lower concentrations (2% and below) deviation (Fig.5.15) from linearity is observed due to interference from high percentage of placebo and Form V.

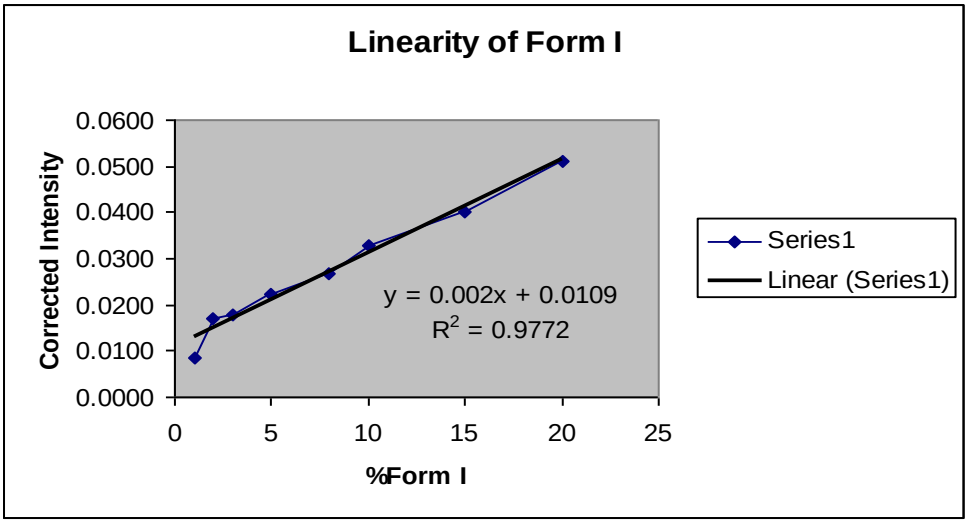

Figure 5.15: Linearity curve of Sertraline hydrochloride Form I

5.5.2.4: Method Precision:

To check the method precision, six samples containing accurately weighed amounts of Form I (5 mg) and Form V (100 mg) with placebo (195 mg) were mixed thoroughly in a homogenizer for 3 min and the Raman spectra of these samples were recorded, each three times, keeping the same instrumental parameters. The average values of the intensities of each sample are presented in Table 5.8. The intensity data of the six replicate samples show % RSD equal to 0.59 which conforms to the accepted limits of precision of the method.

Sr. No.	Relative intensity	Mean	%RSD
1	0.5972	0.6007	0.5883
2	0.6055		
3	0.6020		
4	0.5959		
5	0.6023		
6	0.6013		

Table 5.8: Method precision data of Sertraline hydrochloride Form I

5.5.2.5: Ruggedness:

Intermediate precision (Different Analyst)

Similarly different set of standard physical mixture containing 5% of Form I in Form V with placebo was prepared by a different analyst and was mixed thoroughly in homogenizer for 3 min. Raman spectra were recorded with above mentioned scanning parameters with six replicates. The observed data is presented in Table 5.9. The six replicate corrected intensity data indicates that the method is rugged with % RSD of 0.79 when a different analyst performed the analysis.

Sr. No.	Relative intensity	Mean	%RSD
1	0.6018	0.6003	0.7931
2	0.5949		
3	0.6012		
4	0.5941		
5	0.6046		
6	0.6052		

Table 5.9: Method ruggedness of Sertraline hydrochloride Form I (Different Analyst)

Variation in homogenization time

The three standard physical mixtures were prepared with the same composition, but with different homogenizing time, *viz:* 2 min, 4 min and 5 min. The spectra of these samples were recorded in triplicate. The average relative intensity of the peak at 194.2 cm^{-1} corresponding to Form I of the three samples studied agree

very well (Table 5.10) thereby proving the ruggedness of the method with respect to homogenization time.

Sr. No.	Homogenization time (min)	Relative intensity
1	2	0.5983
2	4	0.6056
3	5	0.6031

Table 5.10: Method ruggedness of Sertraline hydrochloride Form I (Variation in homogenization time)

5.5.2.6: Robustness:

Three sample mixtures were used in this study and the Raman spectra of each sample were recorded in triplicate by changing the FT-Raman instrumental scanning parameters like number of scans, laser power etc. and average values of the relative intensity are given in Table 5.11.

Sr. No.	Parameters	Relative intensity
1	ns = 30	0.5941
2	ns = 40	0.5986
3	ns = 50	0.6028
4	ns = 60	0.6010
5	Laser power = 330	0.6108
6	Laser power = 340	0.6006
7	Laser power = 360	0.6013

Table 5.11: Robustness study of Sertraline hydrochloride Form I

The observed relative intensity data indicates that there is no significant variation in the results and therefore, the proposed method is robust. The laser power of 350 mV and number of scans at 50 can be taken as optimum.

5.5.2.7: Recovery:

Standard physical mixtures for recovery study were prepared by using pure polymorphic form of API Sertraline hydrochloride Form I, Form V and placebo in the range of Form I form 2.5 mg, 5.0 mg and 7.5 mg level with variation of placebo concentration by keeping the constant weight of Form V. The physical mixture used

for recovery study were thus equivalent to 50 % level, 100 % level and 150 % level of Form I standard physical mixture preparation with respect to 5 mg limit.

The recovery results (Table 5.12) indicate that the proposed method is accurate with acceptable percentage of recovery for the quantification of Form I in Form V in the presence of placebo. As per the recovery data the Sertraline hydrochloride polymorphic Form I quantification in Form V is accurate only if the acceptable limit is not less than 2 % of label claim.

Sr. No.	Form I added (mg)	Relative intensity	Corrected intensity	Form I found (mg)	% Recovery
1	2.52	0.6140	0.0159	2.5104	99.62
2	5.06	0.6189	0.0209	4.9798	98.41
3	7.58	0.6237	0.0256	7.3710	97.24

Table 5.12: Recovery study of Sertraline hydrochloride Form I

5.5.3: Quantification of Sertraline hydrochloride Form III present in Form V:

The Raman spectra of both the test substance (physical mixture of Form III and Form V) and the pure Form V were recorded and the relative intensities of both the samples were calculated by dividing the intensity of Raman line at 489.06 cm^{-1} of the two samples by sum of intensities of Raman line at 194.20 cm^{-1} and 489.06 cm^{-1}. However, in the calculation of relative intensity, corrected intensity of the peak at 489.06 cm^{-1} was used by subtracting the contribution from pure Form V at this wave number as can be seen from the Figure 5.5. The difference between relative intensity of test substance and pure Form V is nothing but the corrected intensity which is due to the presence of Form III in Form V.

Standard physical mixture preparation

The standards were prepared by accurately weighing 5 mg of pure Form III, 100 mg of Form V and 195 mg of placebo, mixing thoroughly in a homogenizer for 3 min for this study.

5.5.3.1: Linearity:

Standard physical mixtures for linearity study were prepared by using pure polymorphic form of API Sertraline hydrochloride in which amount of Form III was

varied from 1.0 mg to 20.0 mg level, the amount of Form V was kept constant at 100 mg and calculated amount of placebo was added to keep the final weight of the mixture (300mg) throughout. The details of the amount taken are given in Table 5.13.

Sr. No.	Form III (mg)	Form V (mg)	Placebo (mg)	Relative intensity	Corrected intensity
1	0	100	200	0.3120	NA
2	1	100	199	0.3218	0.0099
3	2	100	198	0.3258	0.0138
4	5	100	195	0.3334	0.0215
5	8	100	192	0.3419	0.0299
6	10	100	190	0.3492	0.0372
7	15	100	185	0.3611	0.0491
8	20	100	180	0.3782	0.0662

Table 5.13: Linearity data of Sertraline hydrochloride Form III by FT-Raman

The standard polymorphic physical mixture samples were thoroughly homogenized in a homogenizer for 3 min and the Raman spectra were recorded from from 4000 cm^{-1} to -2000 cm^{-1} with laser power of 350 mV and fifty scans for each spectrum.

The relative intensities of the peak at 489.05 cm^{-1} in the mixtures (calculated as described above) showed a linear variation with the concentration of Form III present in the mixture as shown in Figure 5.16. It is observed that the intensity of Form III is linear from 1.0 mg onwards with respect to the concentration present in the mixture of From V and placebo. The regression equation for the linear curve is also shown in Figure 5.16.

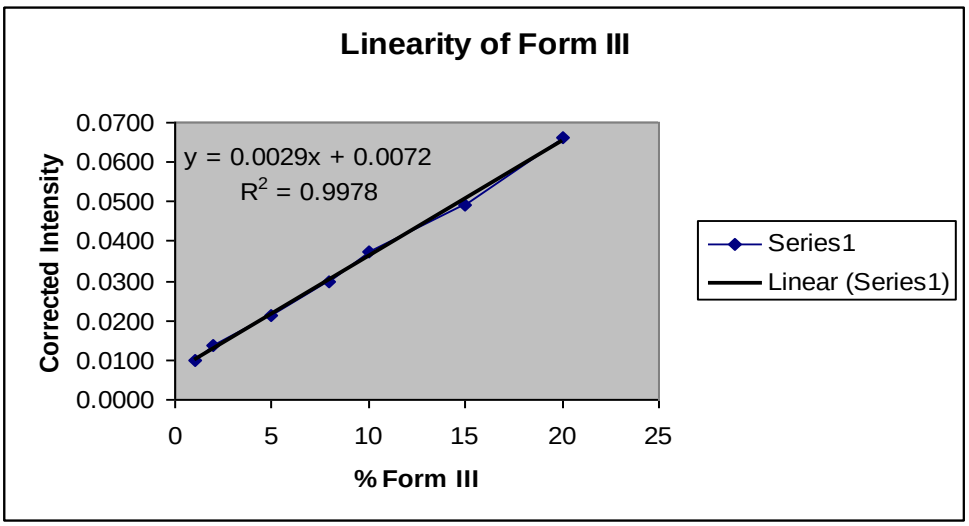

Figure 5.16: Linearity curve of Sertraline hydrochloride Form III

5.5.3.2: Method precision:

Similarly, six samples containing accurately weighed amounts of Form III (5 mg) and Form V (100 mg) with placebo (195 mg) was mixed thoroughly in a homogenizer for 3 min and the Raman spectra of these samples were recorded, each three times, keeping the same instrumental parameters. The average values of the intensities of each sample are presented in below Table 5.14. The intensity data of the six replicate samples shows % RSD equal to 0.79 which conforms to the accepted limits of precision of the method.

Sr. No.	Relative intensity	Mean intensity	%RSD
1	0.3453	0.3493	0.7900
2	0.3505		
3	0.3475		
4	0.3534		
5	0.3495		
6	0.3496		

Table 5.14: Method precision of Sertraline hydrochloride Form III

5.5.3.3: Ruggedness:

Intermediate precision (Different Analyst)

A different set of standard physical mixture containing 5 mg of Form III was prepared by a different analyst in presence of Form V with placebo and was mixed

thoroughly in homogenizer for 3 min. Raman spectra were recorded with above scanning parameters with six replicates. The six replicate corrected intensity data are provided in Table 5.15. The data indicates that the method is rugged as the % RSD is 1.92 when a different analyst carried out the experiments.

Sr. No.	Relative intensity	Mean intensity	% RSD
1	0.3489	0.3500	1.9190
2	0.3512		
3	0.3519		
4	0.3433		
5	0.3433		
6	0.3614		

Table 5.15: Method ruggedness of Sertraline hydrochloride Form III (Different Analyst)

Variation in homogenization time

The three standard physical mixtures were prepared with the same composition, but with different homogenizing time, *viz* 2 min, 4 min and 5 min. The spectra of these samples were recorded in triplicate. The average relative intensity of the peak at 489.05 cm^{-1} corresponding to Form III of the three samples studied agree very well (Table 5.16) thereby proving the ruggedness of the method with respect to homogenization time. From the above relative intensity results it is clear that homogenizing time of 2 min is optimum for quantification of Form III by the developed method.

Sr. No.	Homogenization time (min)	Relative intensity
1	2	0.3459
2	4	0.3485
3	5	0.3509

Table 5.16: Method ruggedness of Sertraline hydrochloride Form III (Variation in homogenization time)

5.5.3.4: Robustness:

Three sample mixtures were used in this study and the Raman spectra of each sample were recorded in triplicate by changing the FT-Raman instrumental scanning

parameters like number of scans, laser power etc. and average values of the relative intensity at 489.05 $cm^{-1}$are given in below Table 5.17.

Sr. No.	Parameter	Relative intensity
1	ns = 30	0.3500
2	ns = 40	0.3475
3	ns = 50	0.3480
4	ns = 60	0.3507
5	Laser power = 330	0.3489
6	Laser power = 340	0.3496
7	Laser power = 360	0.3489

Table 5.17: Robustness study of Sertraline hydrochloride Form III

The observed relative intensity data indicates that there is no significant variation in the results and therefore, the proposed method is robust. The laser power of 350 mV and number of scans at 50 can be taken as optimum for quantification of Form III.

5.5.3.5: Recovery:

Standard physical mixtures for recovery study were prepared by using pure polymorphic form of API Sertraline hydrochloride Form III, Form V and placebo in the range of Form III form 5.0 mg, 7.5 mg and 10.0 mg level with variation of placebo concentration by keeping the constant weight of Form V. The physical mixture prepared for the recovery study are equivalent to 100 % level, 125 % level and 150 % level of Form III standard physical mixture preparation containing 5.0 mg of Form III.

Sr. No.	Form III added (mg)	Relative intensity	Corrected intensity	Form III found (mg)	% Recovery
1	5.23	0.3409	0.0243	5.3647	102.58
2	7.31	0.3410	0.0289	6.9965	95.71
3	10.26	0.3511	0.0391	10.6474	103.78

Table 5.18: Recovery study of Sertraline hydrochloride Form III

The results given in Table 5.18 indicate that the proposed method is accurate with acceptable percentage of recovery for the quantification of Form III in Form V in the presence of placebo. As per the recovery data the Sertraline hydrochloride polymorphic Form III quantification in Form V is accurate only if the acceptable limit is not less than 5 % of label claim.

5.5.4: Commercial tablet analysis for polymorphic content:

Pre weighed 10 tablets of Sertraline hydrochloride, Zosert (50 mg and 100 mg Label claim) manufactured by Sun Pharmaceutical Industries Ltd, India and Setral (100 mg label claim) manufactured by Tripada Healthcare Pvt. Ltd. India, were crushed using mortar and pestle to give a fine uniform powder. 5 mg of this powder was taken in FT-Raman sample holder. The spectra were recorded in triplicate and relative intensity of the three replicates were calculated and are presented in Table 5.19 and Table 5.20. From the mean relative intensity the amount of Form I and III present in Form V of Sertraline hydrochloride tablet were calculated using Equation (5-4) and (5-7) respectively.

Sr. No.	Label claim	Relative intensity	Corrected intensity	% Form I found
1	Zosert 50	0.5475	-0.0505	Not detected
2		0.5453	-0.0527	
3		0.5477	-0.0504	
4	Zosert 100	0.5556	-0.0424	Not detected
5		0.5581	-0.0400	
6		0.5595	-0.0386	
7	Setral 100	0.6736	0.0756	33.96
8		0.6729	0.0748	
9		0.6842	0.0861	

Table 5.19: Quantitative determination of Sertraline hydrochloride Form I in drug products

Sr. No.	Label claim	Relative intensity	Corrected intensity	% Form III found
1	Zosert 50	0.3268	0.0148	4.3
2		0.3291	0.0171	
3		0.3441	0.0321	
4	Zosert 100	0.3150	0.0030	Not detected
5		0.3135	0.0015	
6		0.3196	0.0076	
7	Setral 100	0.3961	0.0842	27.16
8		0.3960	0.0840	
9		0.3999	0.0879	

Table 5.20: Quantitative determination of Sertraline hydrochloride Form III in drug products

From the above discussion it is evident that the proposed validated FT-Raman technique is fast, sensitive, precise and convenient method for quantification of Sertraline hydrochloride Form I and Form III present in Form V of solid dosages form of commercial pharmaceutical products.

Conclusion

Once the existence of polymorphism has been identified, the drug substance available must be evaluated before the formulations are developed to get desired solubility, stability and bioavailability at the same time minimize undesirable effects like toxicity of any polymorph that may be present. Therefore, it is important to develop methods to identify and quantify the polymorphic impurities.

In the present study, different polymorphic forms of Sertraline hydrochloride such as Form I, III and V were synthesized by different techniques. These polymorphs have been characterized by using various spectroscopic (IR, Raman, SS-NMR), XRD, thermoanalytical (MDSC) and morphology by SEM. There is discernible difference in the Raman frequencies of the polymorphs. Quantification of polymorphic impurities namely, Form I and Form III of Sertraline hydrchloride in Form V in their solid oral drug products (tablets) has been achieved by using FT-Raman spectroscopy. The method has been validated based on different aspects of performance such as linearity, precision and accuracy. The proposed method is simple, rapid, selective and sensitive when compared to other quantification methods.

References

1. Brittain, H. G. *Encyclopedia of Pharmaceutical Technology*, **2002**, 2239, Marcel Dekker Publication, New York.
2. (a) Dunitz J. D.; Bernstein, J. *Acc. Chem. Res.* **1995**, *28,* 193. (b) Bernstein, J.; Davey, R. J.; Henck, J. O. *Angew. Chem. Int. Ed.* **1999**, *38*, 3441.
3. Grant, D. J. W.; Brittain, H. G. *Polymorphism in Pharmaceutical Solids*, **1999**. 1, Marcel Dekker, New York.
4. Vippagunta, S. R.; Brittain, H. G.; Grant, D. J. W. *Adv. Drug Delivery Rev.* **2001**, *48*, 3.
5. (a) Aguiar, A. J.; Krc, J.; Kinkel, A. W.; Samyn, J. C. *J. Pharm. Sci.* **1967**, *56*, 847. (b) Aguiar, A.J.; Zelmer, J. E. *J. Pharm. Sci.* **1969**, *58*, 983.
6. Byrn, S. R.; Pfeiffer, R. R. Stephenson, G.; Grant, D. J. W.; Gleason, W. B. *Solid-State Chemistry of Drugs,* **1999**, 103, SSCI, West Lafayette.
7. Nangia, A.; Desiraju, G. R. *Chem. Commun.* **1999**, *7*, 605.
8. Brittain, H. G. *Polymorphism in Pharmaceutical Solids,* **2009,** 2nd ed. Informa Healthcare USA, New York.
9. Hilfiker, R. *Polymorphism in the Pharmaceutical Industry,* **2006**, Wiley-VCH, Verlag GmbH and Co. KGaA, Weinheim.
10. I C H Q6A Guideline*: Specifications for New Drug Substances and Products*, Chemical Substances, October **1999**.
11. Byrn, S.; Pfeiffer, R.; Ganey, M.; Hoiberg, C.; Poochikian, G. *Pharm. Res.* **1995**, *12*, 945.
12. (a) Yu, L. X.; Fumess, M. S.; Raw, A.; Woodland, K. P.; Nashed, N. E.; Ramos, E.; Miller, S. P. F.; Adams, R. C.; Fang, F.; Patel, R. M.; Holcombe, F. O. Jr.; Chiu, Y.; Hussain, A. S. *Pharm. Res.* **2003**, *20*, 531. (b) Yu, L. X. *Adv. Drug Delivery Rev.* **2001**, *48*, 27.
13. Rodriguez-Spong, B.; Price, C. P.; Jayasankar, A.; Matzger, A. J.; Rodriguez-Hornedo, N. *Adv. Drug Delivery Rev.* **2004**, *56*, 241.
14. Pudipeddi, M.; Serajuddin, A. T. *J. Pharm. Sci.* **2005**, *94*, 929.
15. Hancock, B. C.; Parks, M. *Pharm. Res.* **2000**, *17*, 397.
16. Miroshnyk, L.; Mirza, S.; Sandler, N. *Expert Opin. Drug Delivery*, **2009**, *6*, 333.
17. Stahly, G. *Cryst. Growth Des.* **2007**, *7*, 1007.

18. Heinz, A.; Strachan, C. J.; Gordon, K. C.; Rades, T. *J. Pharm. Pharmacol.* **2009**, *61*, 971.
19. Knapman, K. *Mod. Drug Discovery,* **2000**, *3*, 53.
20. Byrn, S.; Pfeiffer R.; Ganey, M.; Hoiberg, C.; Poochikian, G. *Pharm. Res.* **1995**, *12*, 945.
21. Buckton, G. D. P. *Int. J. Pharm.* **1999**, *179*, 141.
22. Taylor, L. S.; Zografi, G. *Pharm. Res.* **1997**, *14*, 1691.
23. Tong, P.; Zografi, G. *J. Pharm. Sci.* **2001**, *90*, 1991.
24. Hancock, B. C.; Zografi. G. *J. Pharm. Sci.* **1997**, *86*, 1.
25. Hancock, B. C.; Parks, M. *Pharm. Res.* **2000**, *17*, 397.
26. Verreck. G.; Six, K.; Van Den Mooter, G.; Baert, L.; Peeters. J.; Brewster, M. E. *Int. J. Pharm.* **2003**, *251*, 165.
27. Beten, D. B.; Gelbcke, M.; Diallo, B.; Moes, A. J. *Int. J. Pharm.* **1992**, *88*, 31.
28. Aceves, J. M.; Cruz, R.; Hernandez, E. *Int. J. Pharm.* **2000**, *195*, 45.
29. (a) Waterman, K. C.; Adami, R. C.; Alsante, K. M.; Hong, J.; Landis, M. S.; Lombardo, F.; Roberts, C. J. *Pharm. Dev. Technol.* **2002**, *7*, 1. (b) Waterman, K. C.; Adami, R. C.; Alsante, K. M.; Antipas, A. S.; Arenson, D. R.; Carrier, R.; Hong, J.; Landis, M. S.; Lombardo, F.; Shah, J. C.; Shalaev, E.; Smith, S. W.; Wang, H. *Pharm. Dev. Technol.* **2002**, *7*, 113.
30. Hovorka, S. W.; Schoneich, C. *J. Pharm. Sci.* **2001**, *90*, 253.
31. Yoshioka, S.; Stella, V. J. *Stability of Drugs and Dosage Forms*. **2000**, p. 61-66, Kluwer Academic Publishers/Plenum Publishers, New York.
32. Suleiman, M. S.; Najib, N. M. *Int. J. Pharm.* **1989**, *50*, 103.
33. Singhal, D.; Curatolo, W. *Adv. Drug Delivery Rev.* **2004**, *56*, 335.
34. Bernstein, J.; Desiraju, G. R. (Ed). *Conformational Polymorphism, Organic Solid State Chemistry.* **1979**, p. 471, Elsevier, Amsterdam.
35. Burger, A.; Ramberger, R. *Mikrochim. Acta,* **1979**, *2*, 259.
36. Frankenbach, G. M.; Etter, M. C. *Chem. Mater.* **1992**, *4*, 272.
37. Zhang, G. G. Z.; Gu, C. H.; Zell, M. T.; Burkhardt, R. T.; Munson, E. J.; Grant, D. J. W. *J. Pharm. Sci.* **2002**, *91*, 1089.
38. Gu, C. H.; Grant, D. J. W. *J. Pharm. Sci.* **2001**, *90*, 1277.
39. Grant, D. J. W.; Higuchi, T. *Techniques of Chemistry, Solubility Behavior of Organic Compounds*, **1947**, p. 21. Saunders, WH Jr. (Ed.) Doctoral Thesis John Wiley and Sons, New York.

40. Lippold, B. C.; Ohm, A. *Int. J. Pharm.* **1986**, *28*, 67.
41. Anon. *Pharm. J.* **1998**, *261*, 150.
42. Grant, D. J. W.; Higuchi T. *Solubility Behavior of Organic Compounds*, **1990**, *656*, 26, Wiley, New York.
43. Yalkowsky, S. *Solubility and Solubilization in Aqueous Media,* **1999,** American Chemical Society, Washington, DC.
44. Almarsson, O.; Gardner, C. R. *Novel Approaches to Issues of Develop Ability*, available from: http:// www. Currentdrugdiscovery.com, Jan-**2003**, 21-26.
45. (a) Sasaki, K.; Suzuki, H.; Nakagawa, H. *Chem. Pharm. Bull*. **1993**, *41*, 325. (b) Haleblian, J.; McCrone, W. *J. Pharm. Sci.* **1969**, *58*, 911. (c) Yen, K. C.; Woo, E. M.; Tashiro. *Polymer*, **2009**, *50*, 6312.
46. Chase, B. D.; Rabolt, J. F. *Fourier Transform Raman Spectroscopy*, **1994**, Academic Press, St. Louis, USA.
47. Hu, Y.; Wikstrom, H.; Byrn, S. R.; Taylor, L. S. *J. Pharm. Biomed. Anal.* **2007**, *45*, 546.
48. Lee, E. H.; Boerrigter, S. X. M.; Rumondor, A. C. F.; Chamarthy, S. P.; Byrn, S. R. *Cryst. Growth Des.* **2008**, *8*, 91.
49. Dharmayat, S.; Calderon De Anda, J.; Hammond, R. B.; Lai, X.; Roberts, K. J.; Wang, X. Z. *J. Cryst. Growth*. **2006**, *294*, 35.
50. Upadhya, P. C.; Nguyen, K. L.; Shen, Y. C.; Obradovic, J.; Fukushige, K.; Griffiths, R.; Gladden, L. F.; Davies, A. G.; Linfield, E. H. *Spectrosc. Lett.* **2006**, *39*, 215.
51. Brittain, H. G. *Physical Characterization of Pharmaceutical Solids*, **1995,** Marcel Dekker, Inc., New York.
52. Brittain, H. G. *Polymorphism in Pharmaceutical Solids,* **1999,** Marcel Dekker, Inc., New York.
53. Forster, A.; Gordon, K.; Schmierer, D.; Soper, N.; Wu, V.; Rades, T. *Internet J. Vib. Spectrosc.* **1998**, *2*. ed.2.
54. Bugay, D. E. *Adv. Drug Delivery Rev.* **2001**, *48*, 43.
55. Colthup, N. B.; Daly, L. H.; Wiberley, S. E. *Introduction to Infrared and Raman Spectroscopy*, **1990,** 3rd ed., Academic Press, San Diego**.**
56. Wartewig, S.; Neubert, R. H. H. *Adv. Drug Delivery Rev.* **2005**, *57*, 1144.
57. Chalmers, J. M.; Everall, N. J. *Trends Anal. Chem.* **1996**, *15*, 18.

58. Petty, C. J.; Bugay, D. E.; Findlay, W. P.; Rodriquez, C. *Spectroscopy*, **1996**, *11*, 41.
59. Mc-Goverin, C. M.; Rades, T.; Gordon, K. C. *J. Pharm. Sci.* **2008**, *97*, 4598.
60. Small, G. W. *Trends Anal. Chem.* **2006**, *25*, 1057.
61. Rasanen, E.; Sandler, N. *J. Pharm. Pharmacol.* **2006**, *59*, 147.
62. Reich, G. *Adv. Drug Delivery Rev.* **2005**, *57*, 1109.
63. Elizarova, T.; Shtyleva, S.; Pleteneva, T. *Pharm. Chem. J.* **2008**, *42*, 432.
64. Tishmack, P. A.; Bugay, D. A.; Byrn, S. R. *J. Pharm. Sci.* **2003**, *92*, 441.
65. Offerdahl, T. J. *Pharm. Technol.* **2004**, *28*, 554.
66. Berendt, R. T.; Sperger, D. M.; Munson, E. J.; Isbester, P. K. *Trends Anal. Chem.* **2006**, *25*, 977.
67. Taday, P. F. *Phys. Eng. Sci.* **2004**, *362*, 351.
68. Newnham, D. A.; Taday, P. F. *Appl. Spectrosc.* **2008**, *62*, 394.
69. Brugemann, L.; Gerndt, E. K. E. *Phys. Res. Sect.* **2004**, *531A*, 292.
70. Hemley, R. J.; Chiarotti, G. L.; Bernasconi, M.; Uloivi, L. **2002,** IOS press, Italy.
71. Harris, K. D. M. *Am. Pharm. Rev.* **2004**, *7*, 86.
72. Roe, R. J. *Methods of X-Ray and Neutron Scattering in Polymer Science,* **2000,** Oxford University Press, New York.
73. Chau, B.; Hsiao, B. S. *Chem. Rev.* **2001**, *101*, 1727.
74. Lehto, V. P.; Tenho, M.; Baha-Heikkila. K.; Harjunen, P.; Paallysaho, M.; Valisaari, J.; Niemela, P.; Jarvinen, K. *Power Technol.* **2006**, *167*, 85.
75. Cooke, D.; Gidley, M. J.; Hedges, N. D. *J. Thermal Anal.* **1996,** *47*, 1485.
76. Ford, J.; Timmins, P. *Ellis Horwood Limited,* **1989**, Chichester, West Susswex, England.
77. Craig, D. M. Q.; Royall, P. G. *Pharm. Res.* **1998**, *15*, 1152.
78. Verdonck, E.; Schaap, K.; Thomas, L. C. *Int. J. Pharm.* **1999**, *192*, 3.
79. Royall, P. G.; Craig, D. Q. M.; Doherty, C. *Int. J. Pharm.* **1999**, *192*, 39.
80. Han, J.; Suryanarayanan, R. *Thermochim. Acta*. **1999**, *329*, 163.
81. Galwey, A.; Craig, D. *Thermal Analysis of Pharmaceuticals*, **2007**, p.139-192, Taylor and Francis Group, CRC Press, Boca Raton, FL.
82. Willson, R.; Haines, P. J. (Ed.) *Royal Society of Chemistry*, **2002,** Cambridge, UK.
83. Kemp, R. *Elsevier Science* **1998**, *B.V.* Amsterden, The Netherlands,
84. Gao, D.; Rytting, J. H. *Int. J. Pharm.* **1997**, *151*,183.
85. Price, R.; Young, P. M.; *J. Pharm. Sci.* **2004**, *93*, 155.

86. Lu, J.; Rohani, S. *Org. Process Res. Dev.* **2009**, *13*, 1269.
87. Liu, J. *Pharm. Dev. Technol.* **2006**, *11*, 3.
88. May, J. C.; Grim, E.; Wheeler, R. M.; West, J. *J. Biol. Stand.* **1982**, *10*, 242.
89. Zhu, L.; Chen, Y.; Gao, Y. Y.; Wang, J. K. *Chin. J. Antibiot.* **2008**, *33*, 755.
90. Vippagunta, R. R.; Pan, C.; Vakil, R.; Meda, V.; Vivilecchia, R.; Motto, M. *Pharm. Dev. Technol.* **2009**, *14*, 492.
91. Lowell, S.; Shields, J. E. *Powder Surface Area and Porosity*, **1984,** 2nd ed. Chapman and Hall Ltd, London.
92. *The Merck Index*, **1996,** 12th ed. Merck and Co. Inc. Whitehouse Station, NJ, USA.
93. Brown, S. D.; Burgess, J.; Fawcett, J.; Parsons, S. A.; Rusells, D. R.; Waltham, E. *Acta. Cryst.* 1995, *C51*, 1335.
94. Acharya, K. R.; Juchele, K. N.; Kartha, G. *J. Crystallogr. Spectrosc. Res.* **1982**, *12*, 369.
95. Caira, M. R.; Mohamed, R. *Acta. Cryst.* **1992**, *B48*, 492.
96. Matsuda, Y.; Akazawa, R.; Teraoka, R.; Otsuka, M. *J. Pharm. Phamacol.* **1993**, *46*, 162.
97. Larsen, I. K.; Anderson, L. A. *Acta. Cryst.* **1992**, *C48*, 2009.
98. Piennar, E. W.; Caira, M. R.; Lotter, A. P. *J. Crystallogr. Spectrosc. Res.***1993**, *23*, 785.
99. Gerber, J. J.; Caira, M. R.; Lotter, A. P. *J. Crystallogr. Spectrosc. Res.* **1993**, *23*, 863.
100. Agafonov, V.; Legendre, B.; Rodier, N.; Wouessidejewe, D.; Cense, J.M. *J. Pharm. Sci.* **1991,** *80*, 181.
101. Hiramatsu, Y.; Suzuke, H.; Kuchiki, A.; Nakagawa, H.; Fuiji, S. *J. Pharm. Sci.* **1996**, *85*, 761.
102. Chen, X.; Morris, K. R.; Griesser, U. J.; Byrn, S. R.; Stowell, J. G. *J. Amer. Chem. Soc.* **2002**, *124*, 15012.
103. Stampa, D.; del Corral, A.; Bosch, L. J.; Molins, G. E.; Onrubia, M. M.; *Paroxetine maleate polymorph and pharmaceutical compositions containing it, PCT Patent* WO 00/ 01693, **2000**.
104. Eyjolfsson, R. *Pharmazie*, **2002**, *57*, 347.
105. Mollica, G.; Geppi, M.; Pignatello, R.; Veracini, C. *Pharm. Res.* **2006**, *23*, 2129.
106. Novoselsky, A.; Glaser, R. *Magn. Reson. Chem.* **2002**, *40*, 723.

107. Munshi, M. V. *Solid-State Studies of the Polymorphs of Methylprednisolone*, **1973**, Ph.D. Dissertation, University of Michigan.
108. Bell, S.; Burns, D.; Dennis, A.; Speers, J. *Analyst*, **2000**, *125*, 541.
109. Wikstrom, H.; Marsac, P.; Taylor, L. *J. Pharm. Sci.* **2005**, *94*, 209.
110. Chen, Z.; Fevotte, G.; Caillet, A.; Littlejohn, D.; Morris, J. *Anal. Chem.* **2008**, *80*, 6658.
111. Mazurek, S.; Szostak, R. *J. Pharm. Biomed. Anal.* **2009**, *49*, 168.
112. Whiteside, P.; Luk, S.; Madden-Smith, C.; Turner, P.; Patel, N.; George, M. *Pharm. Res.* **2008**, *25*, 2650.
113. Koleva, B.; Kolev, T.; Tsalev, D.; Spiteller, M. *J. Pharm. Biomed. Anal.* **2008**, *46*, 267.
114. Koleva, B.; Kolev, T.; Tsalev, D.; Spiteller, M. *J. Pharm. Biomed. Anal.* **2008**, *48*, 201.
115. Mazurek, S.; Szostek, R. *J. Pharm. Biomed. Anal.* **2008**, *48*, 814.
116. Orkoula, M.; Kontoyannis, C. *J. Pharm. Biomed. Anal.* **2008**, *47*, 631.
117. Wikstrom, H.; Kakidas, C.; Taylor, L. *J. Pharm. Biomed. Anal.* **2009**, *49*, 247.
118. Nemet, Z.; Csonka Kis, G.; Pokol, G.; Demeter, A. *J. Pharm. Biomed. Anal.* **2009**, *49*, 338.
119. Buckeley, K.; Matousek, P. *J. Pharm. Biomed. Anal.* **2011**, *55*, 645.
120. Atef, E.; Chauhan, H.; Prasad, D.; Kumari, D.; Pidgeon, C. ISRN *Chromatography*, **2012**,1.
121. Croker, D.; Hennigan, M.; Maher, A.; Hu, Y.; Ryder, A.; Hodnett, B. *J. Pharm. Biomed. Anal.* **2012**, *63*, 80.
122. Sysko, R. J.; Allen Douglas J. M. *Sertraline Polymorph, United States Patent Number* USP 5,248,699, **1993**.

List of Publications

1. **Oxidative Acetylation of Tetramethyl Bisphenol-F,** Pradeep T. Deota, Hemant Parmar, Vaibhav B. Valodkar, Piyush R. Upadhyay, S. P. Sahoo, ***Synthetic Communications,*** Issue: Volume 36, 2006, Pages 673-678. ***(Impact Factor* 1.062)**
2. **A Simple Method For Simultaneous Determination of Aspirin And Paracetamol in Treated Municipal Sewage Water In Vadodara,** P. B. Samnani, Koppula Santosh Kumar, S. P. Sahoo, N. R. Patel, ***Environmental Science An Indian Journal,*** Issue : ESAIJ, 2(3), 2007 [194-199].
3. **Azoester-based H-shaped symmetrical mesogenic dimers containing –CH_3/-OCH_3 terminal substituent,** A. K. Prajapati, M. C. Varia and S. P. Sahoo, ***Phase Transitions,*** Issue : Volume 84, Number 4/2011, Pages 325-342. ***(Impact Factor* 1.006)**
4. **H-shaped mesogenic dimers containing polar –NO_2/-Cl terminus,** A. K. Prajapati, M. C. Varia and S. P. Sahoo, ***Liquid Crystals,*** Issue : Volume 38, Number 7/2011, Pages 861-869. ***(Impact Factor* 1.858)**
5. **Synthesis of Chiral Helical 1, 3-Oxazines,** Harish R Talele, Sibaprasad Sahoo and Ashutosh V. Bedekar, ***Organic Letters,*** Issue : Volume 14, Number 12/2012, Pages 3166-3169. ***(Impact Factor* 5.862*)***
6. **Quantitative determination of N,N-Dimethylamine hydrochloride in Metformin hydrochloride using ^{1}H qNMR spectroscopic and derivatization HPLC methods,** Sibaprasad Sahoo, Nisarg Desai, Anil Bhatt, K. Shivramchandra, B. V. Kamath, (MS submitted to APPS PharmaSci Tech).
7. **Investigation of molecular interaction of Salmon Calcitonin and Benzethonium chloride by NMR and other techniques,** Sibaprasad Sahoo, Soumik Dhara, K. Shivramchandra, B. V. Kamath (MS under revision for Journal of Peptide Science)
8. **Synthesis and characterization of Iloperidone-Cholesteryl sulfate sodium complex and its microspheres for sustained drug release,** Sibaprasad Sahoo, Nisarg Desai, B. Mahanta, D. Dash, K. Shivramchandra, B. V. Kamath (MS under revision for Journal of Microencapsulation)

Publication abstracts

Synthetic Communications®, 36: 673–678, 2006

ISSN 0039-7911 print/1532-2432 online
DOI: 10.1080/00397910500408928

Taylor & Francis
Taylor & Francis Group

Oxidative Acetylation of Tetramethyl Bisphenol-F

Pradeep T. Deota and Hemant S. Parmar
Applied Chemistry Department, Faculty of Technology and Engineering, Maharaja Sayajirao University of Baroda, Vadodara, India

Vaibhav B. Valodkar and Piyush R. Upadhyay
Department of Chemistry, Faculty of Science, Maharaja Sayajirao University of Baroda, Vadodara, India

S. P. Sahoo
Sun Pharmaceutical Advance Research Centre, Vadodara, India

Abstract: Oxidative acetylation of tetramethyl bisphenol-F (**2**) using two different reagents is described. The reaction of (**2**) with $NaIO_4$ in acetic anhydride furnished a novel triacetate (**3**) and its reaction with lead tetraacetate (LTA) in dry benzene resulted in the formation of a novel bis-cyclohexadienone (**4**).

Keywords: Bis(3,5-dimethyl-4-hydroxyphenyl)methane, bis(3,5-dimethyl-3-acetoxy-4-oxocyclohexa-1,5-dienyl)methane, cyclohexa-2,4-dienones, oxidative acetylation

September 2007 Volume 2 Issue 3

Trade Science Inc.

Environmental Science

An Indian Journal

Current Research Paper

ESAIJ, 2(3), 2007 [194-199]

A Simple Method For Simultaneous Determination Of Aspirin And Paracetamol In Treated Municipal Sewage Water In Vadodara

P.B.Samnani[1]*, Koppula Santhosh Kumar[1], S.P.Sahoo[2], N.R.Patel[2]

[1]Department of Chemistry, Faculty of Science, The Maharaja Sayajirao University of Baroda, Vadodara-390002-(INDIA)

[2]Sun Pharma Advance Research Centre (SPARC), Tandalja, Vadodara-390002-(INDIA)

E-mail : sampbus@yahoo.com

Received: 15th June, 2007 ; Accepted: 21st June, 2007

ABSTRACT

A clean method for simultaneous determination of pharmaceutical compounds in treated sewage water has been developed based on UV-Vis spectrometry. This study is a part of larger work for determination of pharma products in water bodies in Vadodara, India. We report in this article data for determination of two drugs: aspirin and paracetamol. These drugs, used as model compounds, were separated from dilute aqueous solution by solid phase extraction(SPE). Macroporous beads of polystyrene divinyl benzene polymer or an anion exchanger were used for pre-concentration followed by spectrophotometric determination. Experimental parameters were optimized. The developed method was used for determination of the drugs in water sample collected from a sewage treatment facility. Presence of these drugs was not detected at the detection limits of the methods, viz. 0.1ppm. The drugs were also not detected in an HPLC method up to concentration of 0.039ppm.

KEYWORDS

Solid phase extraction;
Pre-concentration;
Aspirin;
Paracetamol;
UV-spectrometer;
HPLC.

Phase Transitions
Vol. 84, No. 4, April 2011, 325–342

Taylor & Francis
Taylor & Francis Group

Azoester-based H-shaped symmetrical mesogenic dimers containing – CH_3/–OCH_3 terminal substituent†

A.K. Prajapati[a]*, M.C. Varia[a] and S.P. Sahoo[b]

[a]*Department of Applied Chemistry, Faculty of Technology and Engineering, The M. S. University of Baroda, Vadodara 390001, Gujarat, India;*
[b]*Sun Pharma Advanced Research Company Ltd, Tandalja, Vadodara 390020, Gujarat, India*

(*Received 16 July 2010; final version received 1 November 2010*)

Two extensive homologous series of H-shaped symmetrical dimers were synthesized and their thermotropic properties studied by differential scanning calorimetry and on a hot-stage of a polarizing microscope. These compounds consist of two mesogenic units of azoester interconnected through flexible spacers ($n = 4$) resulting in the structure of 'H-shaped' dimeric compounds. The difference between the two series is in the structure of terminal substituents (–CH_3 for series I and –OCH_3 for series II) attached on the azoester mesogens at one terminus. All these compounds were found to be smectogenic. The effect of different terminal substituents on mesomorphism is discussed. The *trans*-azobenzene groups of the H-shaped dimeric compounds display a high-intensity π–π^* transition at about 365 nm and a low-intensity π–π^* transition at around 460 nm, therefore, photochromism can be achieved by the introduction of the azo linkage to the H-shaped dimeric compounds.

Keywords: azoester; H-shaped; symmetrical dimers; smectic C; DSC

Liquid Crystals,
Vol. 38, No. 7, July 2011, 861–869

Taylor & Francis
Taylor & Francis Group

H-shaped mesogenic dimers containing polar -NO_2/-Cl terminus

A.K. Prajapati[a]*, M.C. Varia[a] and S.P. Sahoo[b]

[a]*Applied Chemistry Department, Faculty of Technology and Engineering, The M.S. University of Baroda, Vadodara, Gujarat, India;* [b]*Sun Pharma Advanced Research Company Ltd, Tandalja, Vadodara, Gujarat, India*

(*Received 12 January 2011; final version received 26 April 2011*)

Two homologous series of H-shaped symmetrical dimers were synthesised and their thermotropic properties studied by differential scanning calorimetry and on the hot-stage of a polarising microscope. These compounds consist of two mesogenic units of azoester interconnected through flexible spacers ($n = 4$) resulting in the structure of 'H-shaped' dimeric compounds. The difference between the two series is in the structure of the terminal substituents (-NO_2 for series **I** and -Cl for series **II**) attached on the azoester mesogens at one terminus. All these compounds were found to be smectogenic. The effect of different terminal substituents on mesomorphism is discussed. The *trans*–azobenzene groups of the H-shaped dimeric compounds display a high-intensity π–π^* transition at about 370 nm and a low-intensity π–π^* transition at around 460 nm; therefore, photochromism can be achieved by the introduction of the azo linkage to these H-shaped dimeric compounds.

Keywords: azoester; H-shaped; smectic A; smectic C; symmetrical dimers

ORGANIC LETTERS

2012
Vol. 14, No. 12
3166–3169

Synthesis of Chiral Helical 1,3-Oxazines§

Harish R. Talele,† Sibaprasad Sahoo,‡ and Ashutosh V. Bedekar*,†

Department of Chemistry, Faculty of Science, M.S. University of Baroda, Vadodara 390 002, India, and Sun Pharma Advance Research Centre, Tandalja, Vadodara 390 020, India

avbedekar@yahoo.co.in

Received May 8, 2012

ABSTRACT

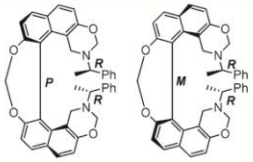

A series of novel 1,3-oxazines were prepared to construct a helical framework. The 1,3-oxazine attached to the phenanthrene unit showed a small bite angle θ (~12°), while the units attached to [4]helicene showed a larger θ (~35°) and exhibited helical isomers at ambient conditions. The diastereomers of the third type of helicene-like bis-oxazine attached to binaphthyl were easily separable and showed good thermal stability. All four diastereomers of bis-helicene were synthesized, and their absolute configuration was established.

Conferences and Presentations

1. Presented a oral entitled "**A simple quantitative NMR method and validation of DMA·HCl and DMF in Metformin hydrochloride",** Sibaprasad Sahoo, Nisarg Desai, Kishor Jadhav, K. Shivramchandra, B. V. Kamath, NMRS-2011 on Jan-2011 at the Department of Chemistry, Guru Nanak Dev University, Amritsar, Punjab.
2. Presented a poster entitled "**Molecular interaction/binding study of peptide, Calcitonin-Salmon and Benzethonium chloride as moniter by NMR",** Sibaprasad Sahoo, Soumik Dhara , Devesh Ajmeri, K. Shivramchandra, T. Rajamannar, B. V. Kamath, NMRS-2011 on Jan-2011 at the Department of Chemistry, Guru Nanak Dev University, Amritsar, Punjab.
3. Participated "**Symposium on Biomedical Magnetic Resonance and 8th NMRS"** at Centre of Biomedical Magnetic Resonance, Sanjay Gandhi Post Graduate Institute of Medical Sciences, Lucknow, held on 2002.
4. FT-NMR applications training on "**(Avance 1D/2D and Avance 3D**)" from Bruker BioSpin AG, at Fallanden, Switzerland, held on 2002.
5. Attended workshop on **"Solid State NMR"** at National Facility for High-Field NMR, TIFR, Mumbai, held on 2003.
6. Attended Indo-French workshop on "**New Solid State NMR Methods and Material Characterization"** at National Chemical Laboratory, Pune, held on 2005.
7. Attended workshop on "**Biomolecular NMR"** at National Facility for High-Field NMR, TIFR, Mumbai, held on 2006.
8. Attended advanced "**NMR and CP-MAS (Solid State-NMR)"** training courses from Bruker BioSpin GmbH, at Karlsruhe, Germany, held on 2008.
9. Participated "**Symposium on Magnetic Resonance and Biomolecular Mimetics"** at Indian Institute of Chemical Technology, Hyderabad, held on 2009.
10. Attended advanced "**Thermal Method of Analysis (DSC, TGA and MDSC)"** training courses from, TA Instruments at Delaware, USA, held on 2012.